NASA CR-72971
LMSC D159262

LIQUID PROPELLANT THERMAL CONDITIONING SYSTEM TEST PROGRAM

Final Report

by

B. R. Bullard

Prepared for

NATIONAL AERONAUTICS AND SPACE ADMINISTRATION
NASA LEWIS RESEARCH CENTER
CONTRACT NAS 3-12033
GORDON T. SMITH, PROJECT MANAGER

LOCKHEED MISSILES & SPACE COMPANY, INC.
A SUBSIDIARY OF LOCKHEED AIRCRAFT CORPORATION
SPACE SYSTEMS DIVISION - SUNNYVALE, CALIFORNIA

NASA CR-72971

FINAL REPORT
LIQUID PROPELLANT THERMAL CONDITIONING SYSTEM TEST PROGRAM

by

B. R. Bullard

Lockheed Missiles & Space Company
Sunnyvale, California

Prepared for

NATIONAL AERONAUTICS AND SPACE ADMINISTRATION

July 5, 1972

Contract NAS 3-12033

NASA Lewis Research Center
Cleveland, Ohio
G. T. Smith, Project Manager
Liquid Rocket Technology Branch

LOCKHEED MISSILES & SPACE COMPANY

FOREWORD

The Lockheed Missiles & Space Company (LMSC) is submitting this report in partial completion of the requirements of Contract NAS 3-12033. The test work described herein was performed at the LMSC Santa Cruz Test Base. The program was conducted under the management of Mr. G. T. Smith, Liquid Rocket Technology Branch, NASA-Lewis Research Center.

ABSTRACT

Results are presented from more than 1500 hours of testing on the liquid hydrogen thermal conditioning unit previously developed under Contract NAS 3-7942. Test parameters included: mixer and vent flowrates; tank size; ullage volume; pressurant gas; pressurant temperature; pressure level; and heat rate. Gaseous hydrogen and helium were used as pressurants. Analytical models are developed to correlate the test data and relate the performance to that anticipated in zero-gravity. Experimental and theoretical results are presented which relate the variables controlling vapor condensation at a moving interface. A recommended flight test is described for demonstrating the availability of cryogenic technology.

CONTENTS

ILLUSTRATIONS

TABLES

SUMMARY

The program described in this report was designed to thoroughly evaluate the performance of the zero-gravity venting system previously developed under Contract NAS 3-7942. This objective was satisfied through a combination of analysis and experimental tests that relate the effectiveness of the thermal conditioning unit (TCU) to various tankage and system variables. These variables include tank size, ullage volume, tank pressure level, pressurant gas, pressurant temperature, and system flowrates. Heat rate effect was determined by using ambient, and liquid nitrogen cold wall boundary conditions.

The program was divided into the following four tasks:

Task I - Thermal Conditioning Unit testing in 110-inch (2.8 m) Diameter Tan

Task II - Thermal Conditioning Unit testing in 41.5-inch (1.05 m) Diameter Tank

Task III - Condensation Investigation

Task IV - Analysis

The extent of the first two tasks is summarized in Table 1 which constitutes approximately 1500 hours of system operation. The 110-inch diameter tank tests included four different TCU installation configurations, each designed to change the configuration and location of the mixer jet relative to the liquid-vapor interface. The bottom mount configuration employed a central jet directed vertically towards the interface. The unit was also mounted at the side of the tank with the jet directed parallel to the surface. The third configuration employed a duct addition to the side mount which extended the jet discharge to the opposite side of the tank. Finally, a radial (relative to the jet centerline) nozzle was added to the crossover duct to create a wall bound jet of which part would intersect the interface and part would mix with the bulk propellant. Only the bottom and side mount configurations were evaluated for the 41.5-inch (1.05 m) diameter tank).

These system tests confirmed the validity of a complete therodynamic equilibrium model which relates the pressure response to the various operational parameters (i.e., vent rate, tank size, ullage volume, etc.), under conditions of adequate mixing. However, transient pressure decay following tank pressurization was distinctly faster with the bottom mounted configuration in the 110-inch (2.8 m) diameter tank, but no noticeable difference with orientation was detected in the 41.5-inch (1.05 m) diameter tank.

The condensation investigation (TASK III) was designed to experimentally correlate the variables that control vapor condensation on a moving liquid-vapor interface. The experiments seem to verify the parametric dependency described by the Sterbentz-Bullard theory, which was developed under NAS3-7942 and, which is independent of gravity level.

In Task IV, analytical models were developed for evaluating the test data and relating the results to anticipated flight performance. The forementioned equilibrium model relates the thermodynamic performance and all the scaling criteria.

Also, a theoretical model was developed which correlates the experimental data obtained at NASA/LeRC, on critical mixing requirements. This model uncovered two independent parameters not readily apparent from the experimental data and provides the basis for describing fluid circulation in zero-gravity. Finally, a test plan was developed for a flight demonstration test of five different cryogenic subsystems, including a thermal conditioning unit. This test plan describes the basic rationale, requirements, procedures, and test profile, for such a flight demonstration. It also contains an evaluation and selection from among potential launch vehicles, and a recommended test module design.

TABLE 1

TEST SUMMARY

LIQUID HYDROGEN THERMAL CONDITIONING SYSTEM

THERMAL CONDITIONING UNIT 110 INCH TANK

CONFIGURATION	NOMINAL ULLAGE (%)	MIXER FLOW (CFM) (1)	VENT FLOW LB/HR (2)	PRESSURANT CONDITIONS (3)	PRESSURE (PSIA) (4)	NO. TESTS
Bottom Mount Ambient Boundary (High Heat Leak)	5 to 80	0 to 5.5 (0 to 156)	0 to 3.0 (0 to 1.36)	140°R GH_2 530°R GH_2 140°R GHe 530°R GHe	17,28,36 (11.7, 19.3, 24.8)	209
Bottom Mount LN_2 Boundary (Low Heat Leak)	5 to 80	0 to 5.5 (0 to 156)	0 to 2.75 (0 to 1.25)	140°R GH_2	17, 28 (11.7, 19.3)	34
Side Mount (Ambient Boundary)	5 to 70	0 to 5.5 (0 to 156)	0 to 3 (0 to 1.36)	140°R GH_2 530°R GH_2 140°R GHe 530°R GHe	17, 28 (11.7, 19.3)	131
Side Mount with Duct	5	0 to 5.5	0 to 2.5	530°R GH_2	17, 28	30
Side Mount with Duct and Radial Nozzle	5, 29	0 to 5.5 (0 to 156)	0 to 2.4 (0 to 1.09)	530°R GH_2	17, 28 (11.7, 19.3)	74

TCU 41.5 INCH TANK

Bottom Mount	5 to 80	0 to 5.5 (C to 156)	0 to 3.5 (0 to 1.59)	140°R GH_2 530°R GH_2 140°R GHe 530°R GHe	17, 28 (11.7, 19.3)	183
Side Mount	5 to 80	0 to 5.5	0 to 3.4	Same as above	17, 28	71

(1) Numbers in parentheses are in liters per minute.

(2) Numbers in parentheses are in K_g per minute.

(3) 140°R ≈ 77°K; 530°R ≈ 294°K.

(4) Numbers in parentheses are in (Newtons per square meter) 10^{-4}.

INTRODUCTION

So effective h ve become the thermal protection systems for cryogenic space propulsion vehicles that nonvented storage of liquid hydrogen is now a practical consideration for Earth-orbital and planetary orbit injection missions. Even so, in all propellant tankage systems a pressure-relief system is mandatory for safety and system operational considerations. For example, tank venting may be desired for reduction of tank pressure after an engine firing so that repeated pressurization may be accomplished for successive engine firings without excessively increasing tank pressure. In this way, lower tank operating pressures and tank weights may be obtained and still provide the required net positive suction pressure to the engine.

Normally, a gas-vent relief valve might be considered for venting the hydrogen tank. In space flight. however, long periods of near-zero-gravity coast of the spacecraft occur. Space flight experience has shown that in zero gravity the location and movement of the liquid propellant in the tank are uncertain. Thus, under such conditions, pressure relief of the tank through an ordinary gas vent relief valve is unreliable and at best very inefficient because of the likely ingestion of large amounts of liquid hydrogen that would be vented directly overboard. Actual mission failures have occurred because of excessive propellant loss and consumption of attitude-control propellants to correct for large variations and unbalances in vehicle motions that were induced by the vent system.

Provision on the vehicle of propellant settling rockets to allow for positive location of the ullage bubble at the ordinary gas vent valve to eliminate liquid propellant venting is a possible solution. However, such a system can be very heavy and limited in its utility. For a spacecraft such as an Earth-Mars Kickstage vehicle, with a 110-inch (2.8 m) diameter hydrogen tank, a minimum of 55 separate vent cycles would be required to maintain the

hydrogen tank at 17 psia (117,000 N/m^2) ± 1/2 psia (3450 N/m^2) for the 220-days duration of the flight. A settling rocket system for these requirements would weigh about 560 lbs (245 Kg). Obviously, such a systen weight is exorbitant, although optimization of pressure control requirements may reduce the weight somewhat below 560 lbs (245 Kg).

The NASA-LeRC recognized these practical difficulties some time ago and awarded a contract to the Lockheed Missiles & Space Company (NAS 3-7942, Liquid Propellant Thermal Conditioning System, dated 26 January 1966) to identify a light weight pressure relief system concept that avoids these difficulties. The concept, referred to as a liquid propellant thermal conditioning system, maintains tank pressure control through extraction of either liquid or gaseous hydrogen and through utilization of the heat transport properties of this extracted fluid. By passing the extracted fluid through a high-pressure-drop valve, the resulting refrigerated vapor, when passed through a heat exchanger, can be used to efficiently absorb heat from the bulk propellant and ullage in the propellant tank. This chilling of the tank contents causes condensation of some of the ullage gas with a concomitant drop in tank pressure. Upon passing through the heat exchanger, the refrigerated vapor is converted to a saturated or superheated gas and is vented overboard. The system and vent fluid process is illustrated schematically in Fig. 1.

In this previous work, conducted under Contract NAS 3-7942, design data and analysis techniques were developed for evaluating liquid propellant thermal conditioning systems. These techniques, which are described in Ref. 1, were used to define an optimum design for the Earth-Mars vehicle. A prototype system, shown in Fig. 2, was fabricated for Lockheed, and a limited amount of testing was conducted to allow some comparison between theory and experiment. The primary test variables included liquid level, mixer input power, and mixer jet orientation (i.e., perpendicular to and parallel with the gravitational vector).

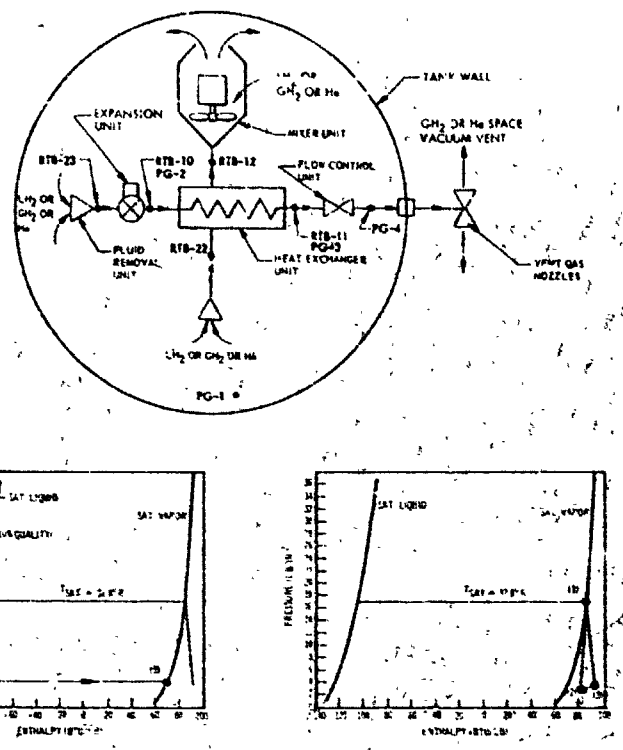

(a) Fluid Removal Unit Immersed in Liquid Hydrogen

(b) Fluid Removal Unit Immersed in Gaseous Hydrogen

Figure 1 Liquid Propellant Thermal Conditioning System Schematic

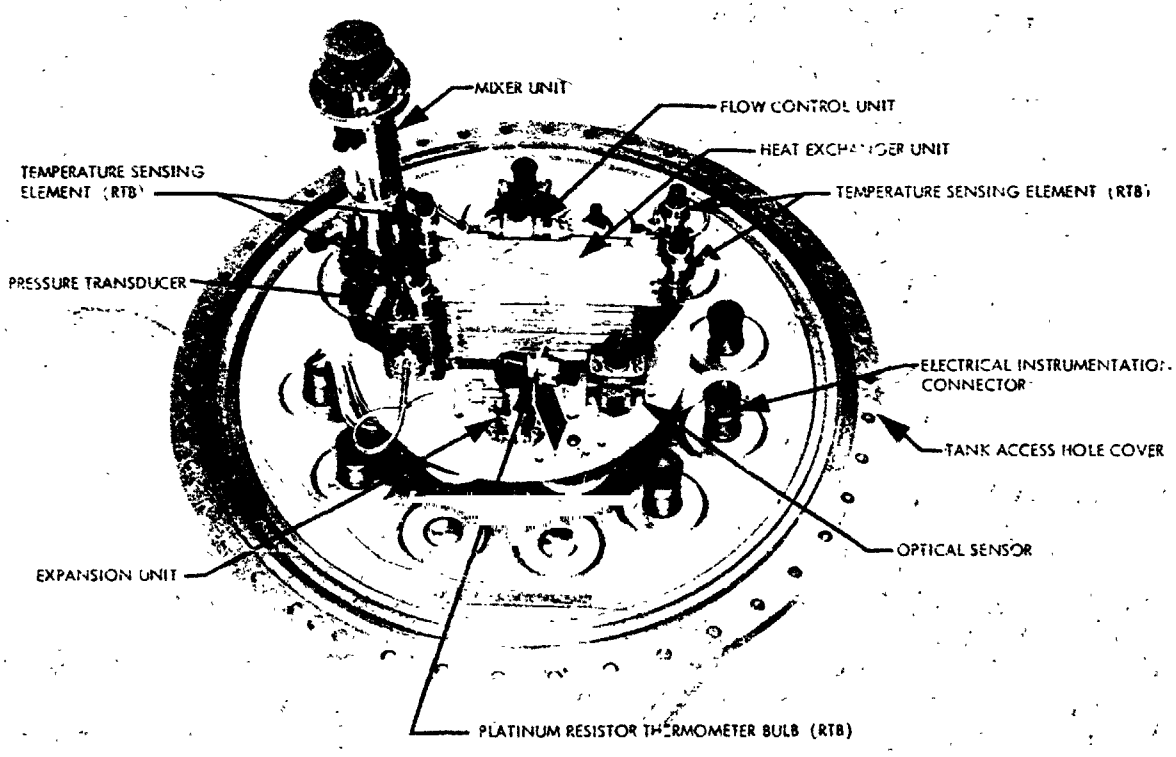

Figure 2 Thermal Conditioning System Mounted on Inside Surface of Access-Hole Cover

These tests generally demonstrated that the thermal conditioning system, as designed, and tested, will control the pressure level in a full scale liquid hydrogen tank, whether immersed in liquid or gaseous hydrogen. These also indicated no discernable difference in the unit performance with the two mixer discharge directions. Further, the tests in a one-gravity environment, although demonstrating the pressure control capability of the system, did show some divergence between the experimental response rates and those predicted by mixed model theory. Similar findings have been reported by other investigators (Ref. 2).

The objective of this program was to continue the investigation described above and to provide an evaluation of the effectiveness of liquid propellant venting systems. The program is both analytical and experimental in nature and is designed to measure the effectiveness of the thermal conditioning unit as it is affected by tank pressure level, helium concentration, and thermal conditioning unit variables, as well as confirm the preliminary findings from the previous work and provide some explanation for the discrepancy between mixed model predictions and experimental pressure response.

Specific objectives of the program which served to accomplish the foregoing broad objective were as follows:

1. Determine, experimentally, the pressure response effected by the TCU in both a 41.5 inch (1.05 m) diameter tank and a 110 inch (2.8 m) diameter tank, and the extent to which this response is affected by each operational variable.
2. Determine, experimentally, the variables controlling condensation on a moving liquid-vapor interface, and compare the results with the Sterbentz-Bullard theory developed under NAS 3-7942.
3. Develop analytical models to correlate the experimental results and provide the criteria for predicting performance under low-gravity flight conditions.

4. Using the experimental results and analyses, describe the system performance for an Earth-Mars kickstage.

5. Identify remaining areas of uncertainty, and any desirable changes in the system.

6. Develop a test plan for a flight demonstration of a thermal conditioning system.

The liquid hydrogen conditioning system that was evaluated in this program can be applied to a wide range of missions and vehicles as was shown in Refs. 1 and 3. However, the relevance of the specific technology developments contained in this report transends the usefulness of this specific system. The theoretical developments, evaluation criteria, and test techniques, as well as the design approaches described in Ref. 3, can be used to develop a system for the orbiting maneuvering stage of the Space Shuttle vehicle, and they are valid for other propellants as well as for hydrogen. Details of the program are described in the following sections of this report.

TEST SYSTEM CHARACTERISTICS

The detail design specifications of the prototype thermal conditioning system is described in Ref. 1. However, the operation of the system and the nominal requirements of each component are briefly reviewed herein. The actual characteristics, as determined from calibration tests on each component, are presented, and then interpreted in terms of the requirements.

The prototype thermal conditioning system was designed to satisfy, as nearly as practical, the operating requirements and conditions listed in Table 2 for the flight system. The system was comprised of the following elements.

- Expansion Unit
- Heat-exchanger unit
- Mixer unit
- Flow control unit
- Pressure switch

The expansion unit is a high pressure drop regulator, which expands the fluid to be vented to a lower pressure and temperature. This temperature drop provides the differential necessary for operation of the heat exchanger.

The heat exchanger is the unit where heat is transferred from the propellant in the tank to the refrigerated vent vapor coming from the expansion unit. In the process, the propellant in the tank is cooled and the refrigerated vent vapor is converted to a saturated or superheated vapor, which is then discharged from the propellant tank (State (3), Fig. 1).

The mixer unit induces flow of the tank propellant through the warm side of the heat exchanger; thus providing cooling of this fluid by forced convection rather than by pure conduction. However, a reduction in tank pres-

Table 2

SYSTEM DESIGN OPERATING CONDITIONS

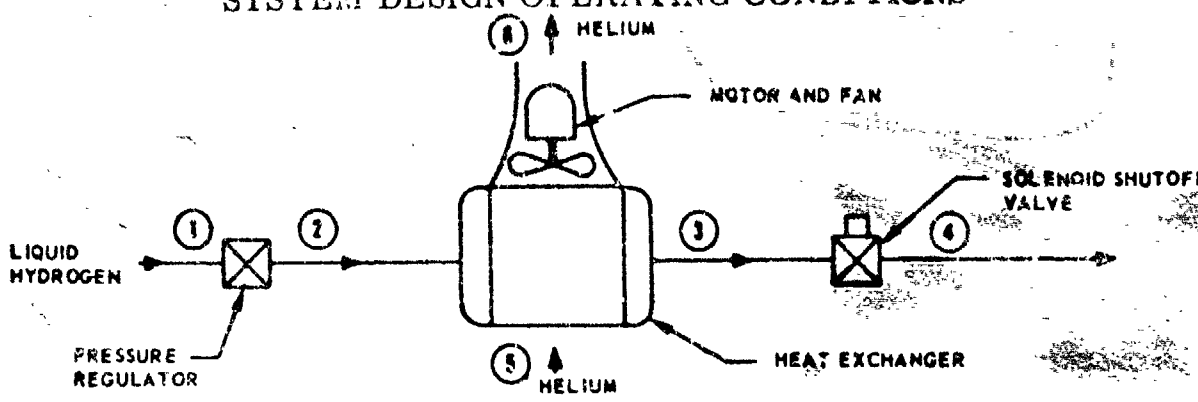

Station	Temperature (°R)	Pressure (psia)	Velocity (ft/sec)	Flow Rate (lb/hr)	Quality (lb vapor/lb fluid)	LH_2	Two-Phase Hydrogen	GH_2	GHe
			Conditions						
Cold-Side Fluid – LH_2, Warm-Side Fluid – LH_2									
1	37.4	17	0	1.4	0	X			
2	29.6	4	0.037	1.4	0.68		X		
3	29.6	4	0.5	1.4	1.00			X	
4	29.6	< 2	88.0	1.4	1.0			X	
5	37.4	17	2.7	1320	0	X			
6	37.4	17	5.0	1320	0	X			
Cold-Side Fluid – LH_2, Warm-Side Fluid – GHe									
1	37.4	17	0	1.4	0	X			
2	29.6	4	0.037	1.4	0.08		X		
3	29.6	4	0.50	1.4	1.0			X	
4	29.6	< 2	88.0	1.4	1.0			X	
5	37.4	17	2.7	57.4	1.0				X
6	34.1	17	5.0	57.4	1.0				X
Cold-Side Fluid – GH_2, Warm-Side Fluid – GH_2									
1	37.4	17	0	1.3	1.0			X	
2	37.0	4	0.56	1.3	1.0			X	
3	37.0	4	0.56	1.3	1.0			X	
4	37.0	< 2	105.0	1.3	1.0			X	
5	37.4	17	2.7	28.5	1.0			X	
6	37.4	17	5.0	28.5	1.0			X	
Cold-Side Fluid – LH_2, Warm-Side Fluid – GH_2									
1	37.4	17	0	1.4	0	X			
2	29.6	4	0.037	1.4	0.08		X		
3	29.6	4	0.5	1.4	1.0			X	
4	29.6	< 2	88	1.4	1.0			X	
5	37.4	17	2.7	28.5	1.0			X	
6	37.4	17	5.0	28.5	0.95		X		
Cold-Side Fluid – GH_2, Warm-Side Fluid – GHe									
1	37.4	17	0	1.3	1.0			X	
2	37.0	4	0.56	1.3	1.0			X	
3	37.0	4	0.56	1.3	1.0			X	
4	37.0	< 2	105.0	1.3	1.0			X	
5	37.4	17	2.7	57.4	1.0				X
6	37.4	17	5.0	57.4	1.0				X

sure is not achieved by cooling the bulk liquid unless the subcooled liquid can be used to induce vapor condensation. The analysis and experimental data presented in a later section shows that the condensation rate is related to the circulation velocity in the subcooled liquid at the interface. The mixer unit creates velocity gradients throughout the propellant tank which provide the mechanism for the vapor condensation and the associated positive pressure control.

The flow-control unit provides the system vent-flow shutoff function, as well as a fixed-orifice flow area. Because only gaseous hydrogen and/or helium will be present downstream on the heat exchanger cold side, a relatively constant vent flow rate will be attained during periods of tank venting. A solenoid-operated valve is used for flow control. In this prototype test system two valves were used to provide two nominal vent flow rates.

The pressure switch mounted outside the tank senses tank pressure. The aneroid with the pressure switch contracts as the tank pressure increases; an actuator then moves, causing the electrical switch element to close; and the solenoid of the flow control unit and the electric motor of the mixer units are activated as a preset pressure level. In a similar manner, these units are deactivated at a preset lower pressure level reached after tank venting.

Each component, its requirements and test results are discussed in the following paragraphs.

EXPANSION UNIT

This unit (Fig. 3) is basically a regulator designed to control the downstream pressure to 4 psia ± 0.2 (27,550 ± 1380 N/m^2), with either liquid or gaseous hydrogen, or helium at the inlet. When the pressure drops below 4 psia, the bellows expand pushing the stem upward and forcing the metering ball off the seat which permits flow to pass from the inlet through the outlet until the downstream pressure builds up sufficiently to reseat the metering valve.

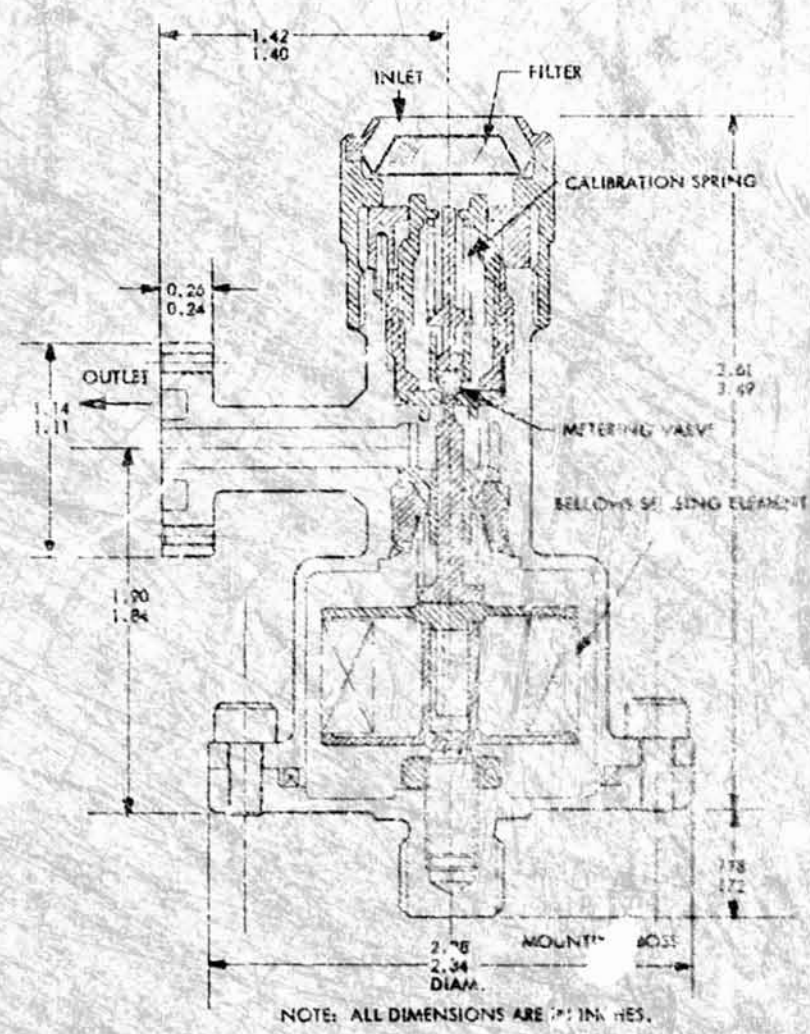

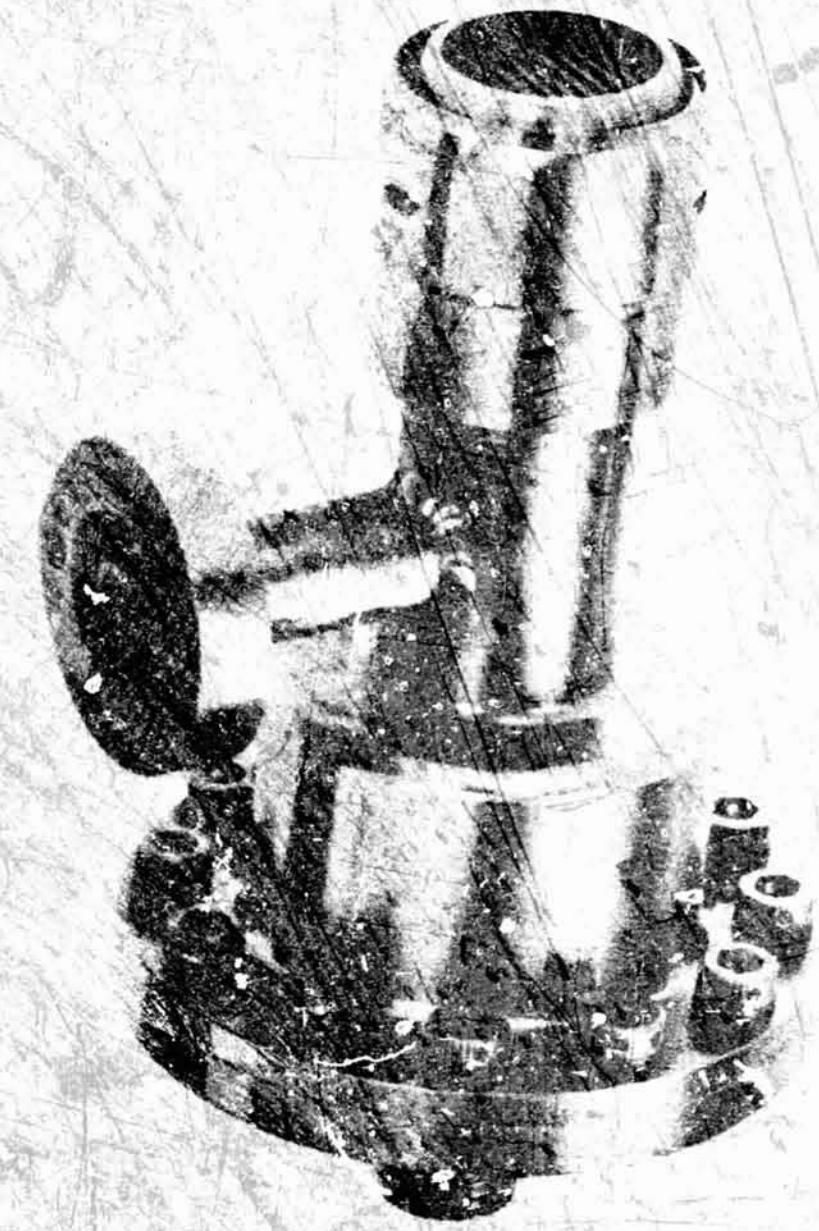

Figure 3 Expansion Unit

The expansion unit was calibrated in the test setup illustrated schematically in Fig. 4. Fig. 5 is a photograph showing the physical installation on the dewar lid before being lowered into the test dewar for the helium test. The copper tubing was removed for all tests with hydrogen. When conducting these tests, the back pressure control valve was throttled to give the desired flow rate through the system with the inlet pressure at either 16 or 29 psia (110,300 or 200,000 N/m^2). As a new inlet pressure was applied, the back pressure control valve was readjusted to hold the flow rate constant. For each flow rate, four discrete pressures were applied and the data was recorded.

The test results are shown in Table 3 for operating in liquid and gaseous hydrogen. It can be seen that neither inlet pressure nor flow rate had a significant effect on the regulated pressure. This is as it should be since the unit is a pressure regulator and not a flow control unit. From these tests it was concluded that the unit satisfied the requirement of regulating to 4 ± 0.2 psia (27,550 ± 1380 N/m^2).

FLOW CONTROL UNIT

The function of the solenoid valve is to limit the vent flow rate through the Thermal Conditioning Unit (TCU). This is accomplished by placing the valve downstream of the heat exchanger and sizing it to choke at the conditions of the vapor leaving the heat exchanger. A current limiter mounted external to the tank allows high current to flow to the valve for 300-500 msec. This pulls the solenoid in and allows the metering valve to move off the seat after which the valve is held open with a limited current of approximately 30 milliamps. Fig. 6 shows an outline drawing which gives the over-all dimensions of the flow control unit. Two of these units were calibrated. They are identical in operating mode and external dimensions. However, the orifice sizes are different by approximately 2:1. The smaller valve (No. 1) had been calibrated in the previous program, and the effective area was determined to be 0.0053 square inches ($3.4 \times 10^{-6} m^2$). At the design conditions of 4 psi and 30°R (27,550 N/m^2 and 16.7°K), the resulting choked flow should be 2.2 lbs (1 Kg) per hour.

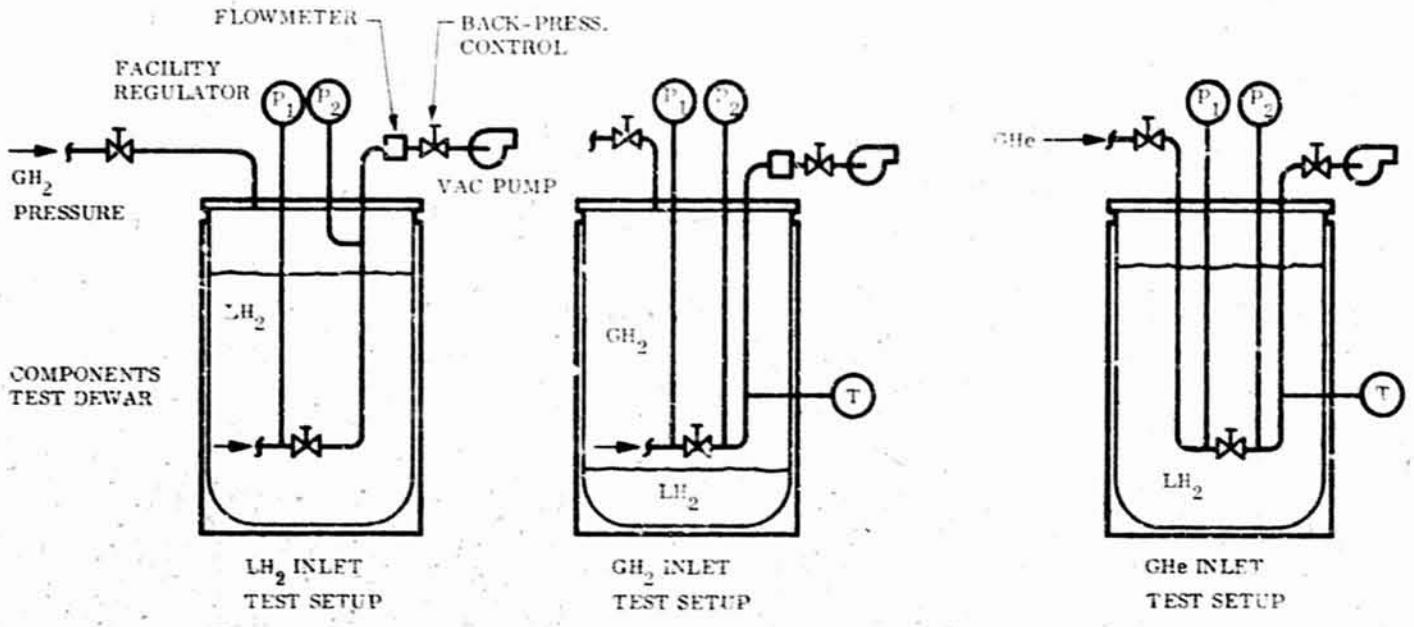

Figure 4 Expansion Unit Calibration Test Schematic

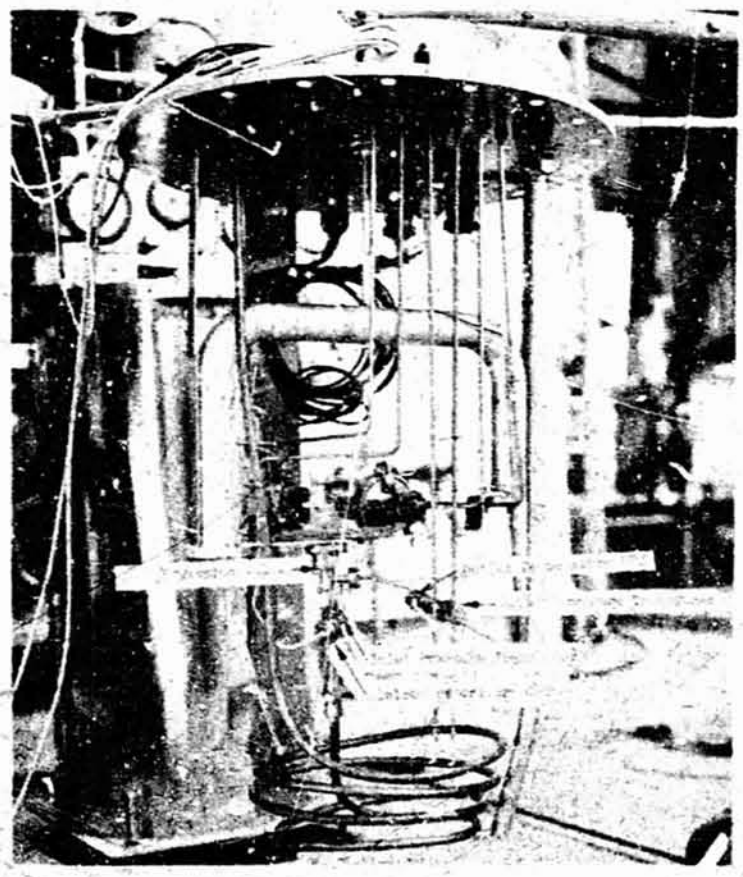

Figure 5 Expansion Unit Calibration Test Installation

TABLE 3

CALIBRATION TEST RESULTS - EXPANSION UNIT

FLOW RATE lbs/hr	(Kg/hr)	INLET PRESSURE psia	$(N/m^2)10^{-4}$	REGULATED PRESSURE psi	$(N/m^2)10^{-4}$	FLUID
0.5	(0.23)	16,19,25,29	(110,131,172,200)	4.1	(28.2)	Liquid Hydrogen
1.1	(0.50)	15,19,25,29	(103,131,172,200)	4.1	(28.2)	
2.1	(0.95)	15,19,25,29	(103,131,172,200)	4.2	(28.9)	
3.2	(1.45)	15,19,25,29	(103,131,172,200)	4.0	(27.6)	
4.0	(1.81	16	(110)	4.1	(28.2)	
3.9	(1.77)	19	(131)	4.0	(27.6)	
4.0	(1.81)	25	(172)	4.0	(27.6)	
4.0	(1.81)	29	(200)	3.95	(27.2)	Liquid Hydrogen
1.0	(0.45)	16,19,25,29	(110,131,172,200)	3.85	(26.5)	Hydrogen Vapor
2.0	(0.91)	15,19,25,29	(103,131,172,200)	4.2	(28.9)	
3.8	(1.73)	15,19,25,29	(103,131,172,200)	4.0	(27.6)	Hydrogen Vapor

The second valve (No. 2) was designed for 4 lbs (1.81 K_g) per hour at the same operating conditions.

Electrical tests as well as flow leakage tests were conducted on the high flow valve at the vendors. The pull in current varied between 0.5 and 0.59 amps which is consistent with the value of 0.55 amps that was previously measured on the original valve.

Flow Control Unit

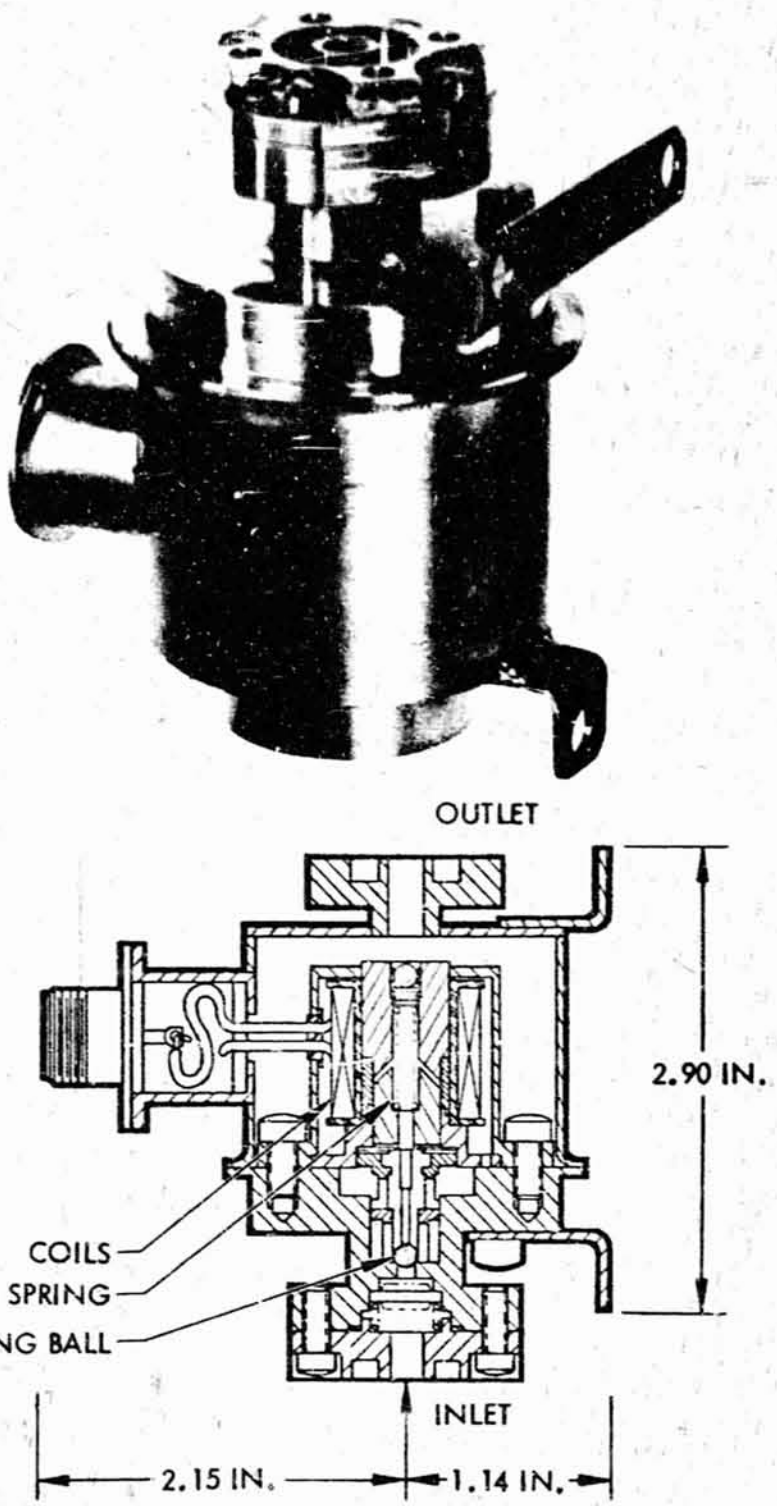

Figure 6 Flow Control Unit

Valve port leakage test results are given in Table 4. These do not satisfy requirements for a flight type unit but, even these were obtained after repeatedly lapping the valve seats. Further reduction will require a change in the design.

TABLE 4

LEAKAGE TEST RESULTS - FLOW CONTROL UNIT NO. 2

TEST NO.	GAS	TEMPERATURE °R	TEMPERATURE °K	LEAK RATE* $(Cfm)10^6$	LEAK RATE* $(\ell/m)10^4$	APPROXIMATE ACCUMULATIVE CYCLES
1	Helium	Ambient		4.14	1.16	3
2	Helium	Ambient		2.86	0.80	10
3	Nitrogen	Ambient		0.96	0.27	15
4	Helium	140	77	96.2	27.0	18
5	Helium	140	77	64.1	18.0	50
6	Helium	Ambient		15.0	4.20	50
7	Helium	Ambient		5.70	1.60	53

* Converted to standard conditions

Flow measurements at the vendor were made at both room and liquid nitrogen temperatures. The effective flow area for each test point were also calculated. The test results are tabulated in Table 5. At design conditions of 4 psia and 30°R (27,550 N/m^2 and 16.7°K) the required effective flow area was estimated to be 0.009 sq. inches ($5.7 \times 10^{-6} m^2$).

TABLE 5

VENDOR FLOW TEST RESULTS - FLOW CONTROL UNIT NO. 2

GAS	INLET CONDITIONS PRESSURE psig	INLET CONDITIONS PRESSURE N/m^2	INLET CONDITIONS TEMPERATURE °R	INLET CONDITIONS TEMPERATURE °K	GAS WEIGHT/FLOW lbs/hr	GAS WEIGHT/FLOW Kg/hr	EFFECTIVE ORIFICE AREA in^2	EFFECTIVE ORIFICE AREA $(m^2)10^6$
Helium	28	193,000	Ambient		16.8	7.62	0.0124	7.97
	30	206,500	Ambient		17.1	7.75	0.0120	7.71
	25	172,300	Ambient		15.0	6.80	0.0119	7.65
	20	138,000	Ambient		12.6	5.72	0.0114	7.34
Nitrogen	30	206,500	Ambient		46.2	20.9	0.0129	8.30
	25	206,500	Ambient		40.8	18.5	0.0128	8.24
	20	138,000	Ambient		35.4	16.0	0.0128	8.24
Helium	30	206,500	160	88.9	25.2	11.4	0.00962	6.20
	25	172,300	160	88.9	22.5	10.2	0.00968	6.24
	20	138,000	160	88.9	19.5	8.85	0.00962	6.20

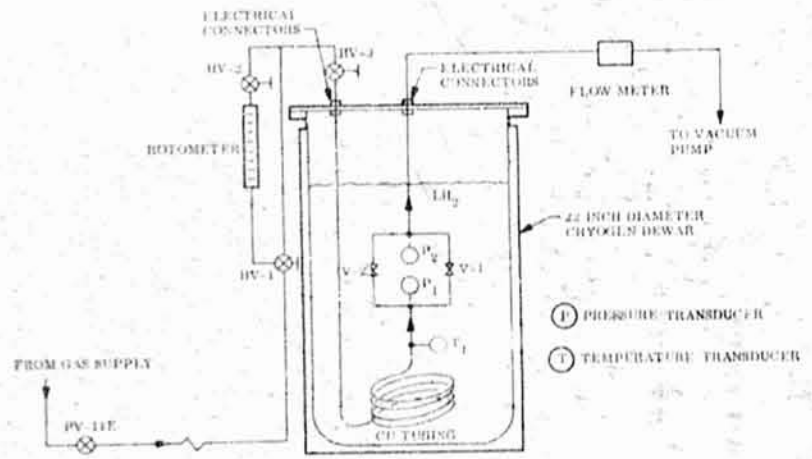

(a) Installation Schematic

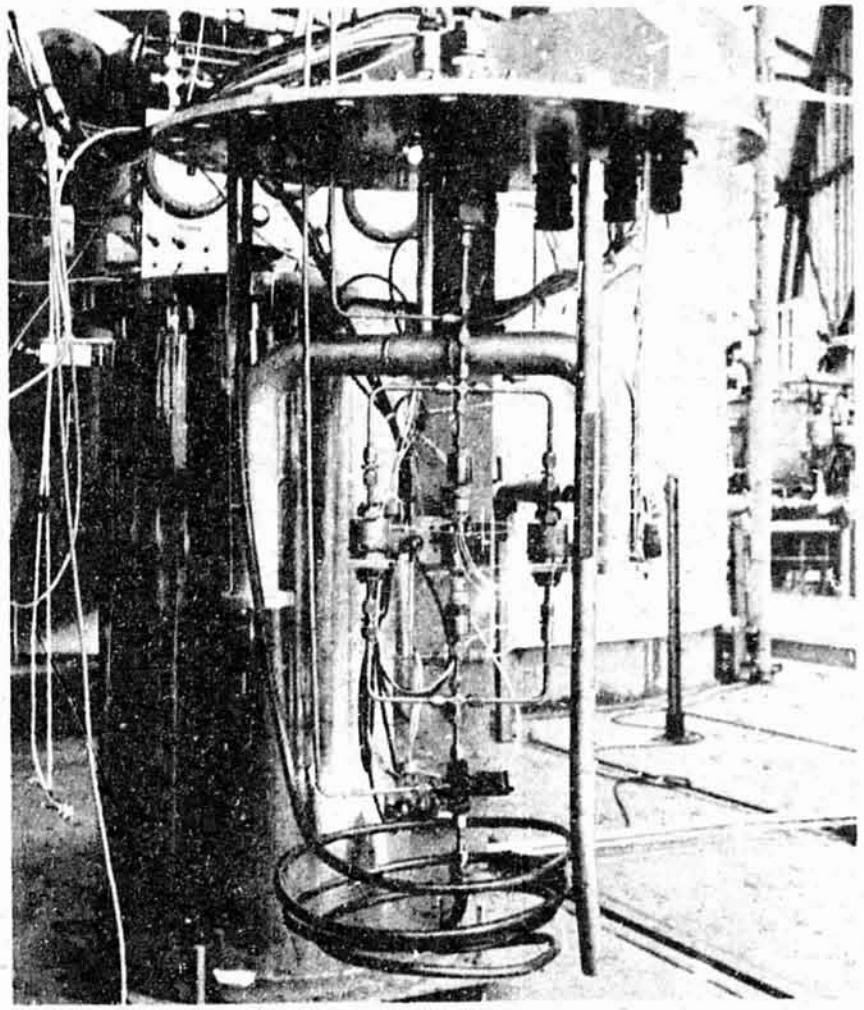

(b) Photograph as installed

Figure 7 Test Installation for Solenoid Valve Calibration

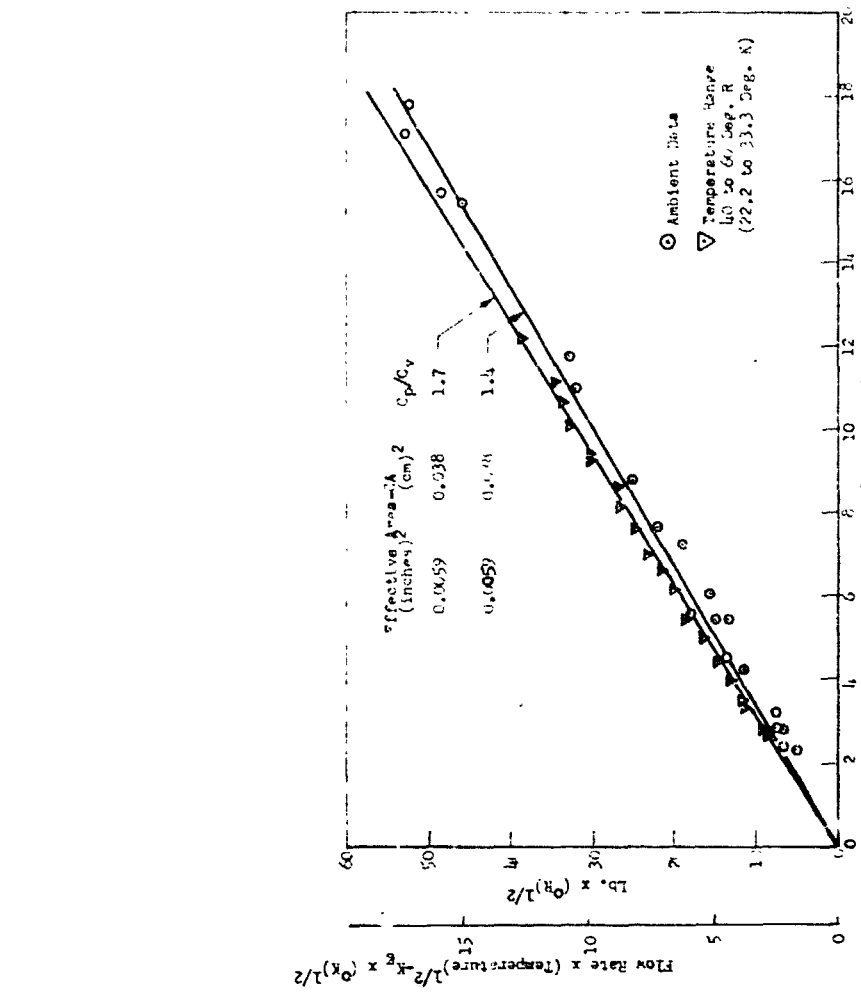

(b) High Flow Valve (No. 2)

(a) Low Flow Valve (No. 1)

Figure 8 Solenoid Valve Calibration Data

All previous calibration testing was performed at relatively high pressures, and at temperatures above 140°R (77°K). Lockheed used the test setup illustrated in Fig. 7 to extend this data down into the actual operating regime. Fig. 7 also contains a photograph showing the actual in tank arrangement. The resulting calibration data is presented in Fig. 8. There is a slight shift in the data between ambient and cryogenic temperature. However, this is a consequence of the increased specific heat ratio at the lower temperatures.

PRESSURE SWITCH

The function of the TCU pressure switch (Fig. 9) is to activate and deactivate the vent system in order to maintain the tank selected pressure within the range of 3 to 5 psig (20,650 to 34,500 N/m^2). Since this unit would be mounted outside the tank, it would always be subjected to the ambient rather than propellant temperatures. Therefore, calibration tests were conducted at ambient, dry ice, and LN_2 temperatures.

The test setup is illustrated in Fig. 10. The pressure at the sensing port was slowly increased by bleeding in helium from the supply bottle. When the pressure reached activation level, the switching element would make contact, allowing current to flow through the electrical continuity indicator. This pressure was recorded. The supply pressure was then closed off and a bleed valve opened to relieve the pressure at the sensing port until the switch would break, shutting off the current through the electrical continuity indicator. This pressure was recorded as the break pressure.

The pressure cycle was repeated 10 times at each temperature and the results are presented in Table 6.

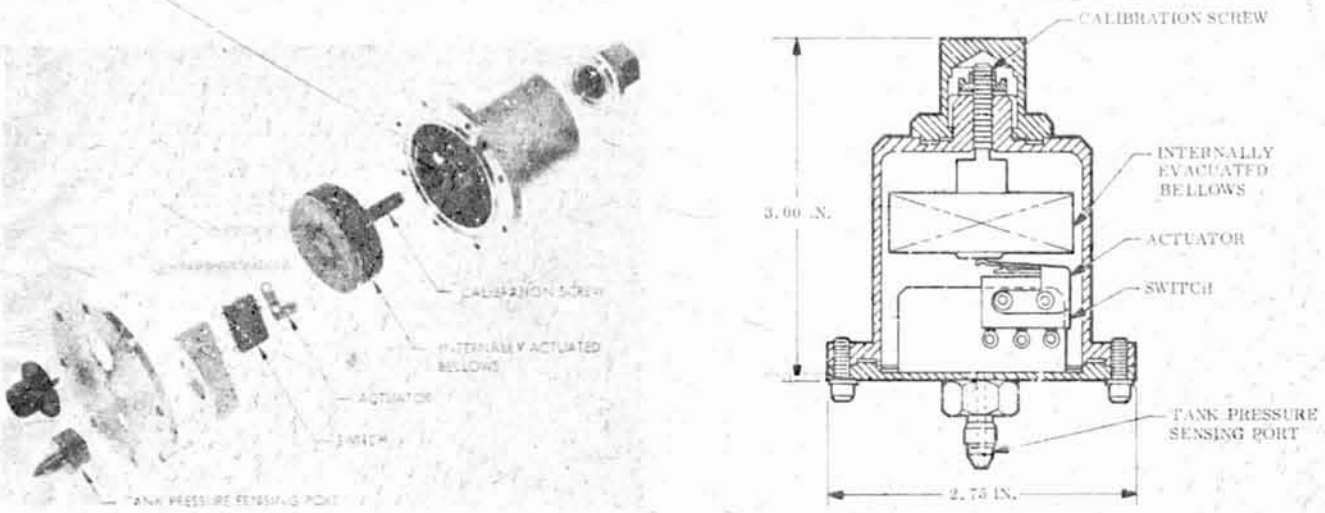

Figure 9 Pressure Switch

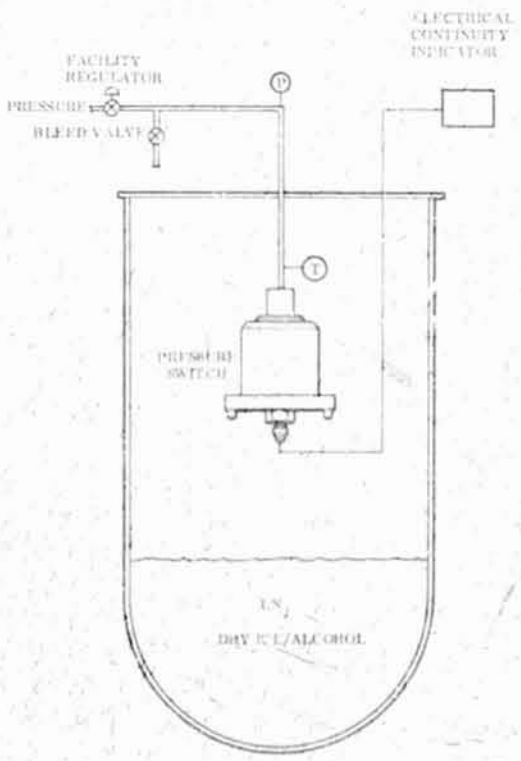

Figure 10 Pressure Switch Calibration Test Schematic

TABLE 6

CALIBRATION TEST RESULTS - PRESSURE SWITCH

TEST CYCLE NO.	500°R (278°K) Pressure - psig*		351°R (195°K) Pressure - psig		140°R (77°K) Pressure - psig		500°R (278°K) Pressure - psig	
	Make	Break	Make	Break	Make	Break	Make	Break
1	4.1 (28,200)	3.0 (20,670)	4.8 (33,100)	3.5 (24,100)	5.0 (34,450)	3.7 (25,500)	4.2 (28,950)	3.0 (20,670)
2		3.0 (20,670)				3.4 (24,100)		
3								
4								
5								
6								
7								
8								
9								
10	4.1 (28,200)	3.0 (20,670)	4.8 (33,100)	3.5 (24,100)	5.0 (34,450)	3.5 (24,100)	4.2 (28,950	3.0 (20,670)

* Numbers in parentheses are in Newtons per sq. meter

These tests indicated that the make and break pressures are very repeatable at any given temperature. However, the operating level tends to be higher when the switch is at sub-zero temperature, but for the temperature range evaluated in these tests, the operating limits were consistently within the prescribed control band of 3 - 5 psi (20,670 - 34,450 N/m^2).

MIXER UNIT

The mixer unit used in the prototype thermal conditioning system is shown in Fig. 11. It consists of a three-phase, six pole, ac induction motor and a single-stage, shrouded axial flow fan. This unit was available from a previous program and was used to avoid the development of a mixer unit specifically designed for TCU application. The unit is rated at 440 volts and 400 cycles. However, at these conditions, the head rise across the fan was approximately ten times that required for the TCU application. Therefore, a calibration test program was conducted to determine the operating characteristics of the unit at reduced frequencies and voltage.

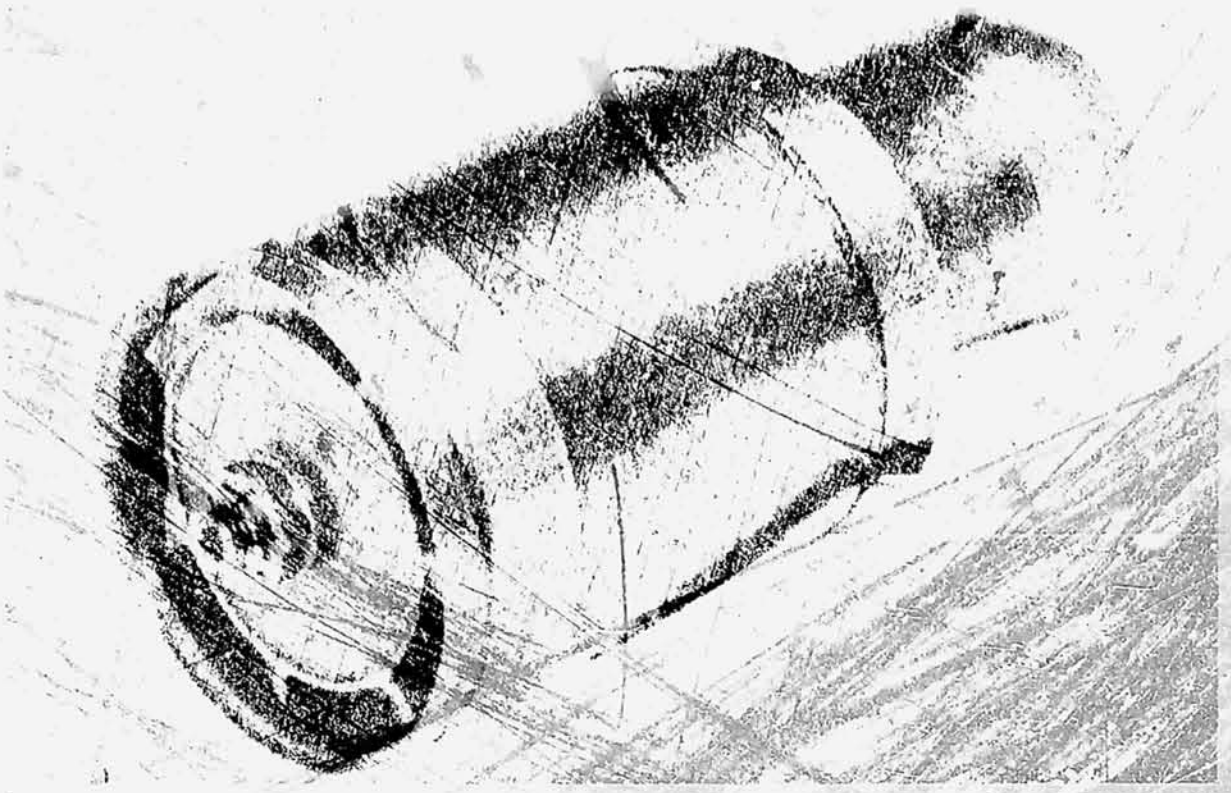

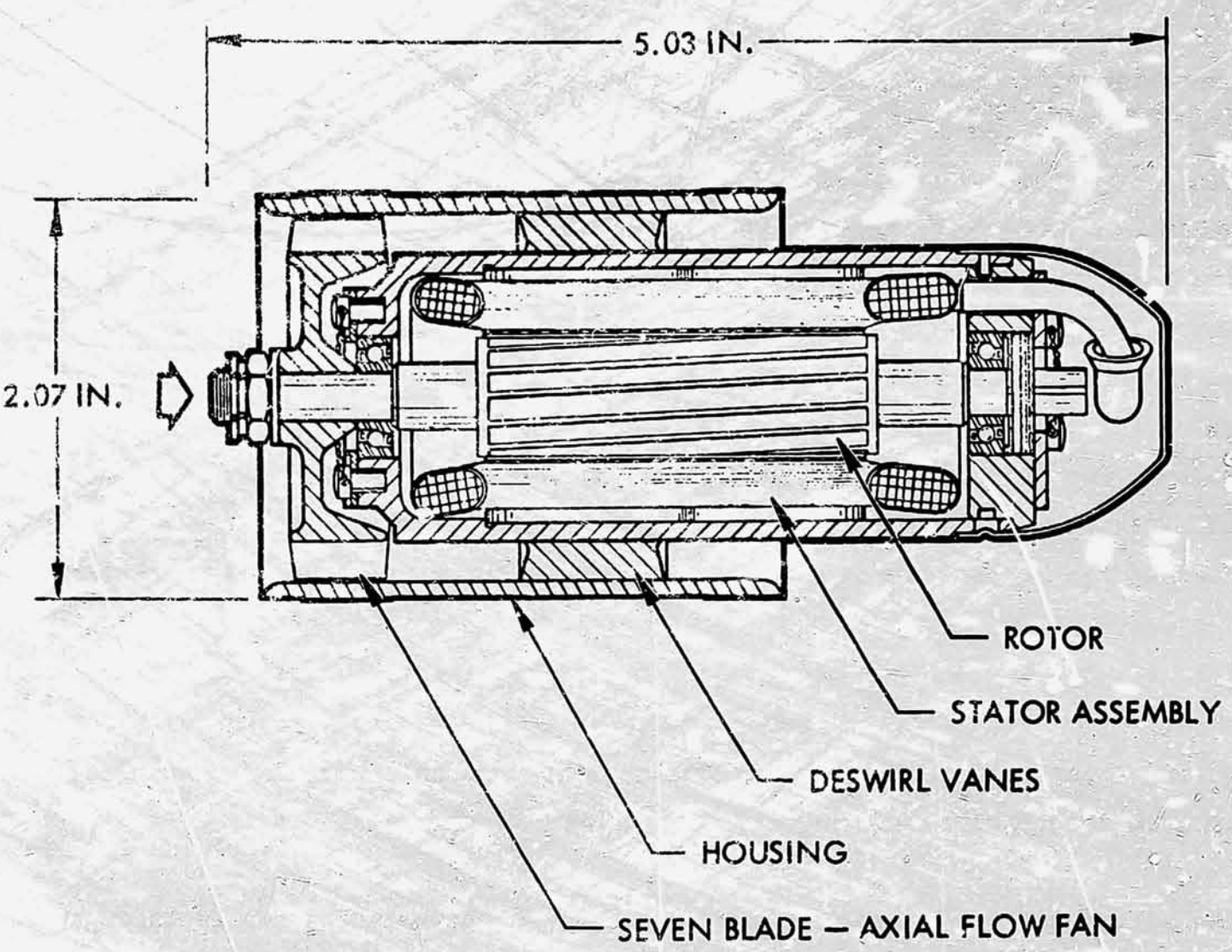

Figure 11 Sectional View and Photograph of Mixer

Fig 12 contains a schematic illustration of the mixer test set up for gas flow tests and a photograph showing the lower half of the flow loop removed. This was the only modification needed to run tests in liquid hydrogen. The tests were conducted by applying a fixed electrical frequency to the motor and varying the voltage in discrete steps to change the flow rate. The flow rate, fan head rise, fan speed, and motor power were measured at each point.

The speed measuring device was one developed for a turbine type flow meter to be used in liquid hydrogen. It employs a coil assembly mounted on the fan housing, and a power supply with a high frequency oscillator and preamplifier. The oscillator/preamplifier of this system transmits a high frequency carrier wave signal to the coil in the pickoff assembly. As the rotor blades pass through the field of the coil, the amplitude of the carrier signal is demodulated at a rate corresponding to the rotor speed, which is proportional to the flow rate. The modulated signal is subsequently detected, amplified and shaped in the preamplifier for retransmission of a constant amplitude pulse signal to the receiving instrument.

The speed measurement revealed that applied voltage and frequency to the motor is not sufficient to define the mixer operation. This is illustrated in the chart record shown in Fig. 13, which was obtained with the mixer unit operating in liquid hydrogen. The applied motor frequency was 170 cps. The voltage was increased in discrete steps with a resulting increase in speed and flow rate until the voltage reached 40 volts at which point the motor reached synchronous speed. Further increases in voltage increased neither the speed, flow, or head rise. However, once synchronous speed has been reached, the voltage can be reduced to approximately 20 volts without changing mixer output (but it does reduce the power to the motor). It was also found during these calibration tests that the mixer operation becomes unstable for applied frequencies below 160 cps and above 175 cps.

The mixer unit performance characteristics are shown in Figures 14 through 16 for liquid operation, with an applied frequency of 170 cps. Fig. 14 shows

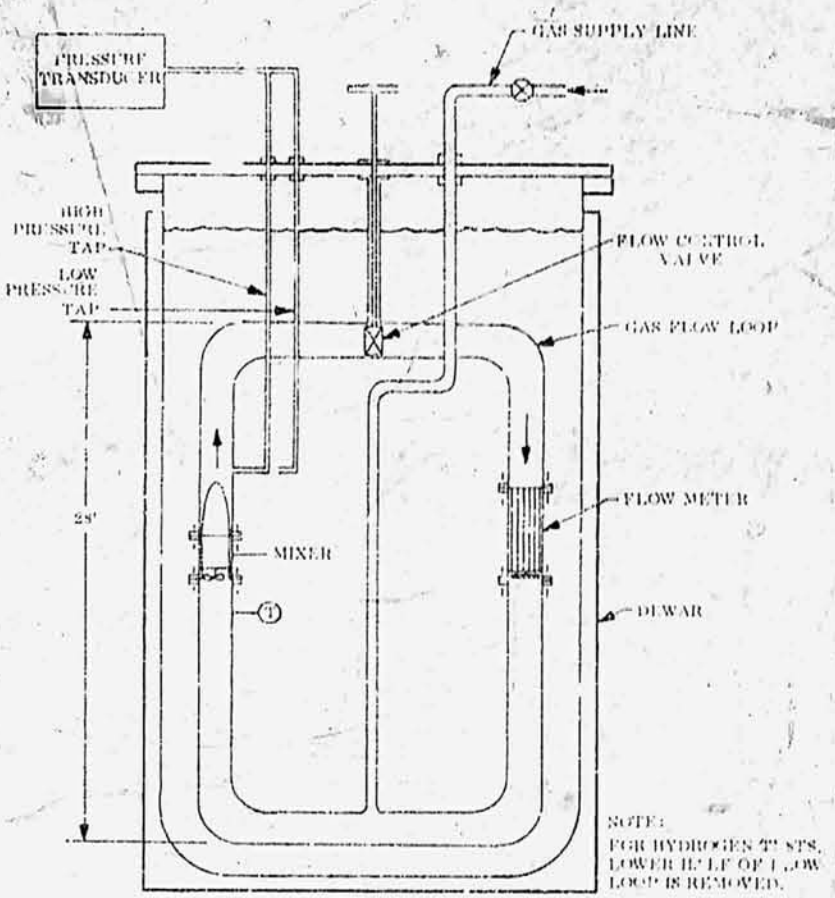

(a) Schematic for Calibration with Gas

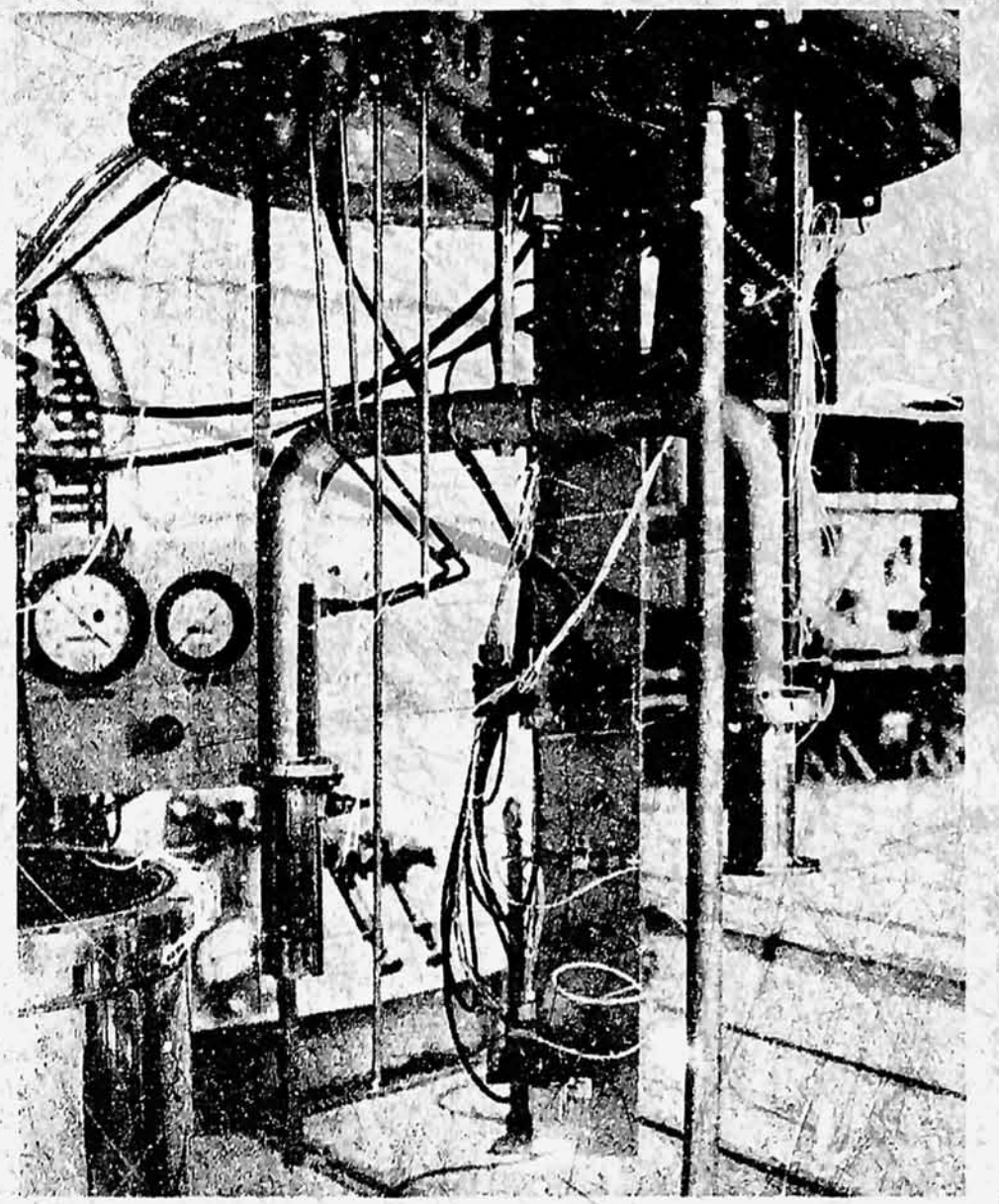

(b) Photograph of Flow Loop for Calibration in Liquid

Figure 12 Test Installation for Mixer Calibration

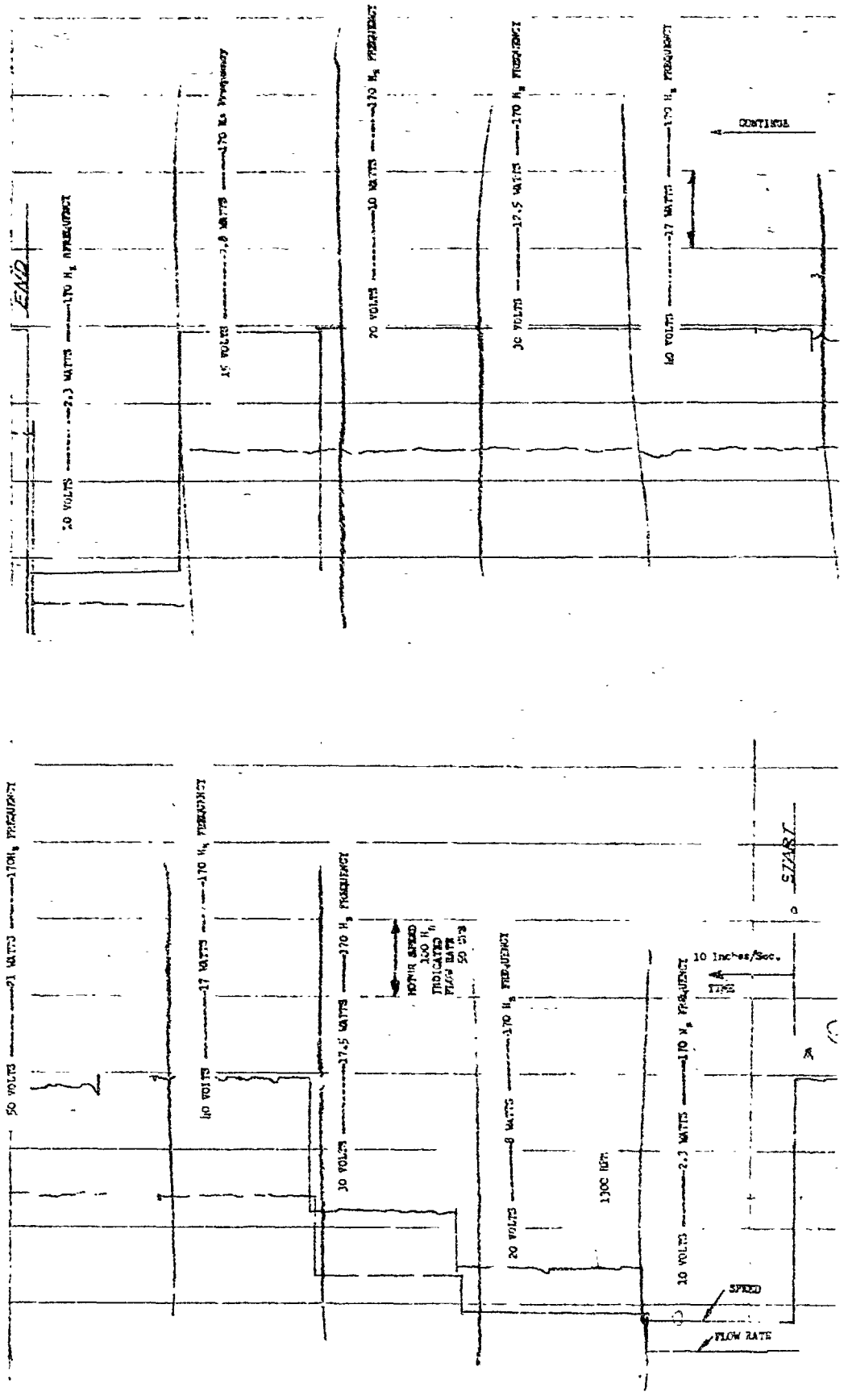

Figure 13 Strip Chart Record of Mixer Characteristics at 170 CPS Applied Frequency

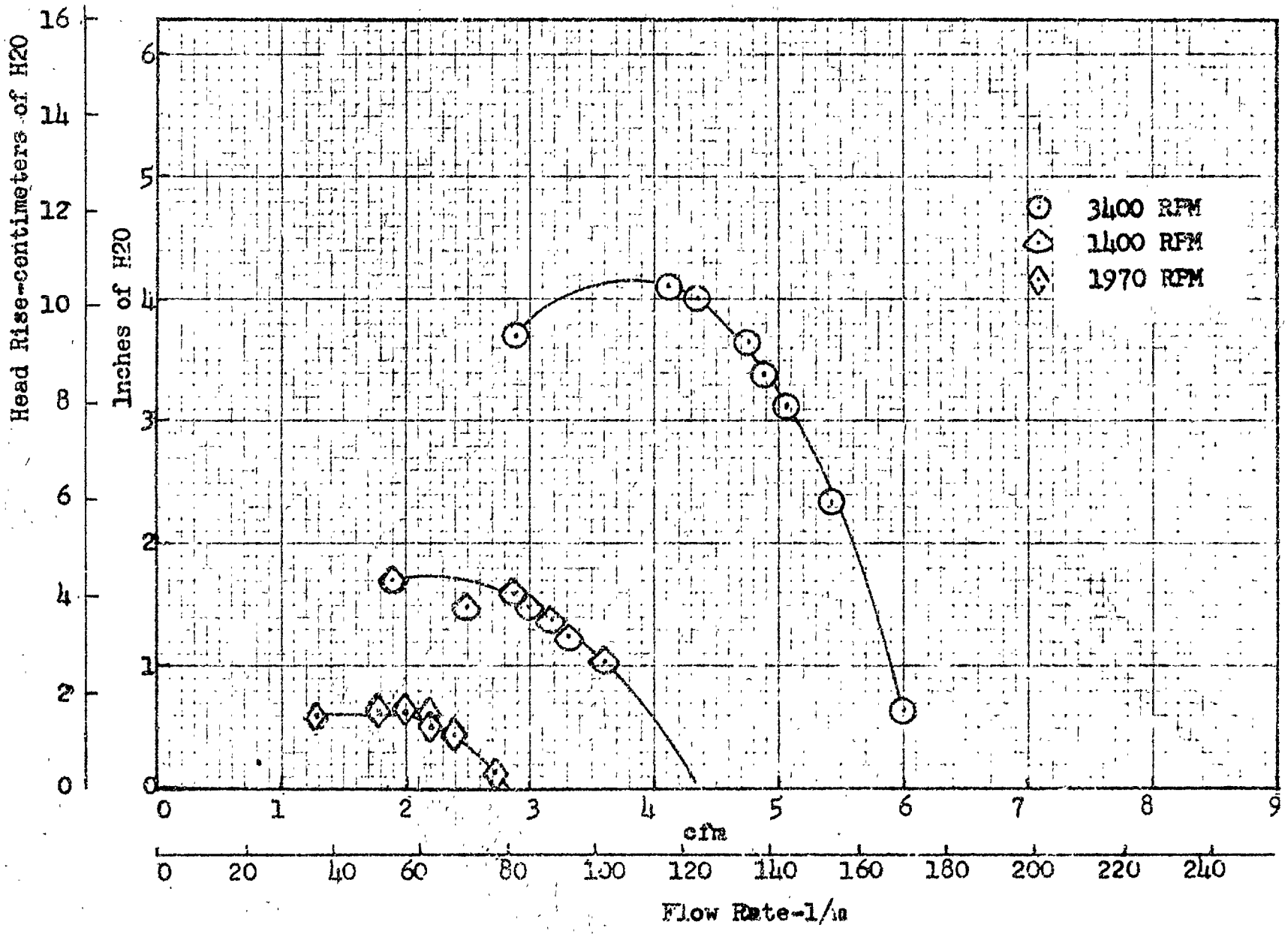

Figure 14 Mixer Unit Head-Capacity Curve in Liquid Hydrogen
Applied Frequency = 170 CPS

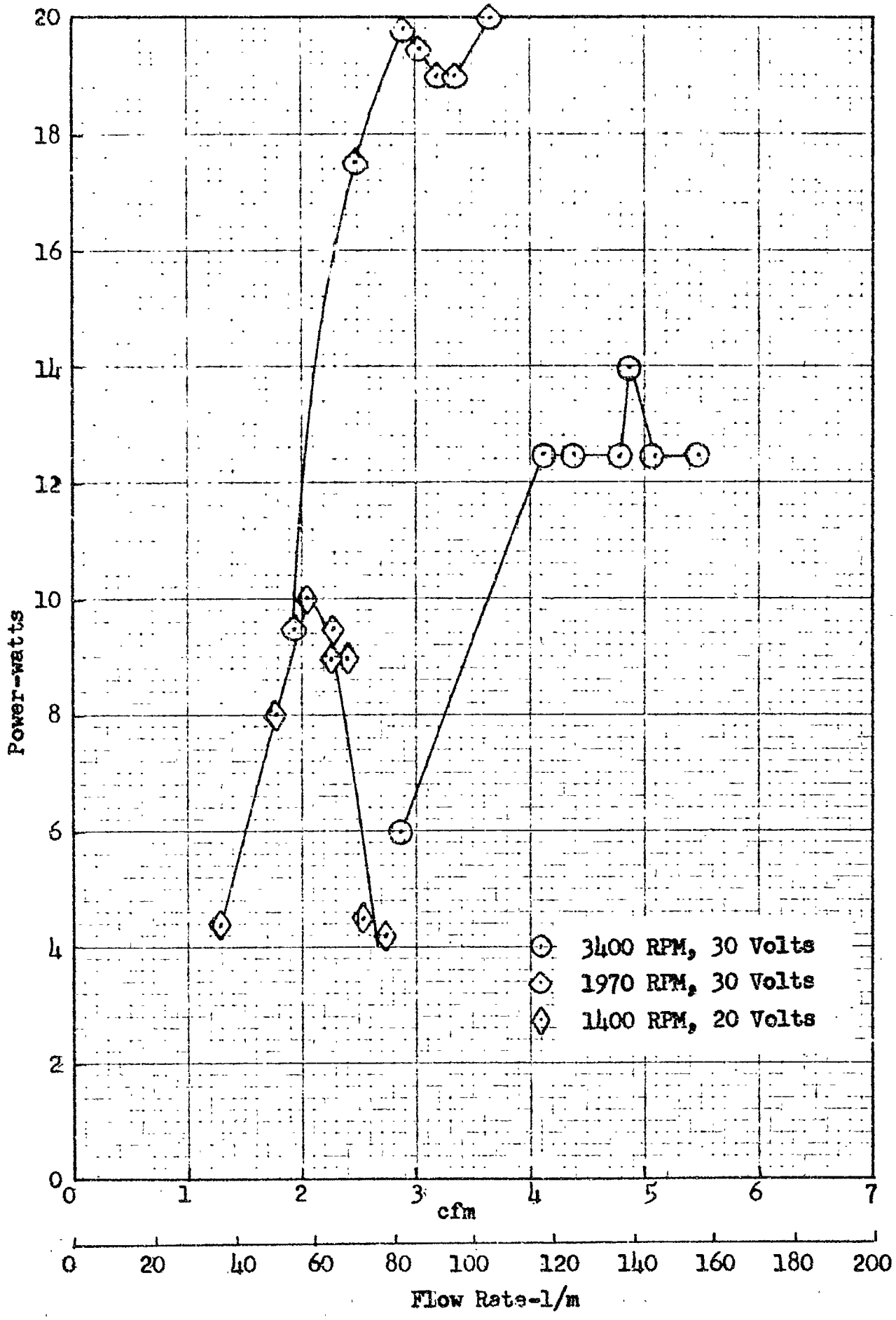

Figure 15 Mixer Motor Power Requirements in Liquid Hydrogen

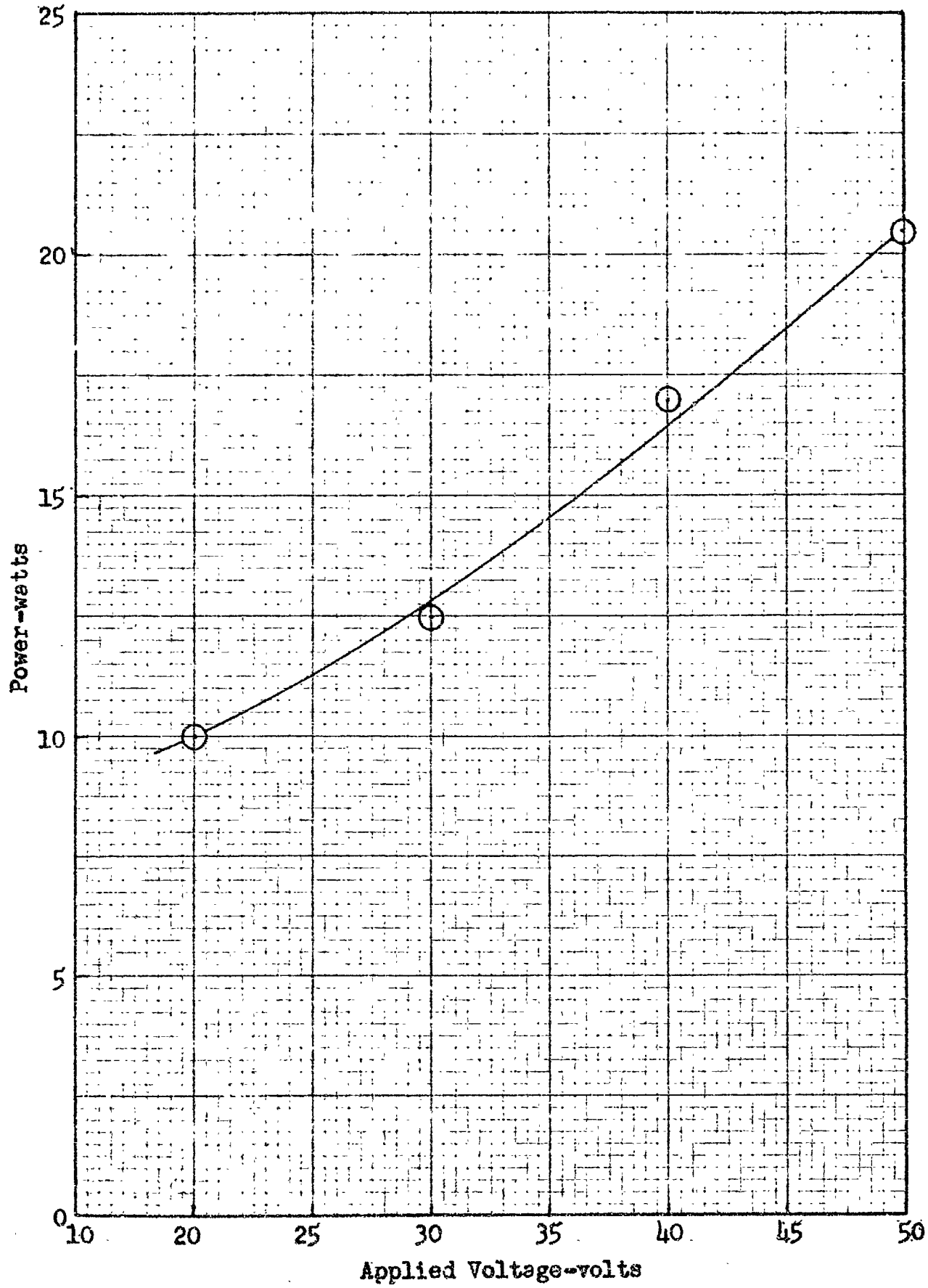

Figure 16 Power Characteristics at 3400 RPM in Liquid Hydrogen

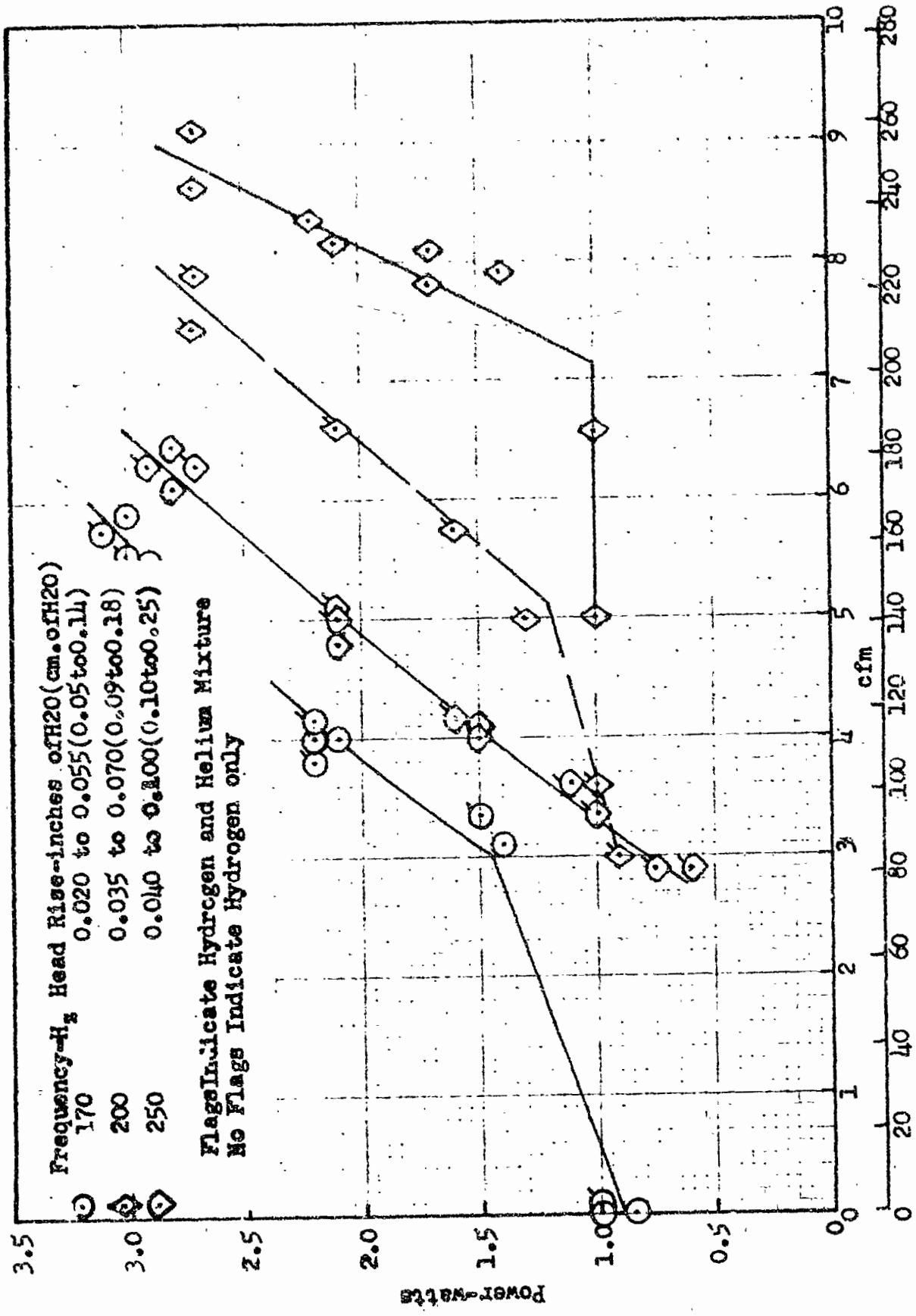

Figure 17 Mixer Unit Power Characteristics in Gas

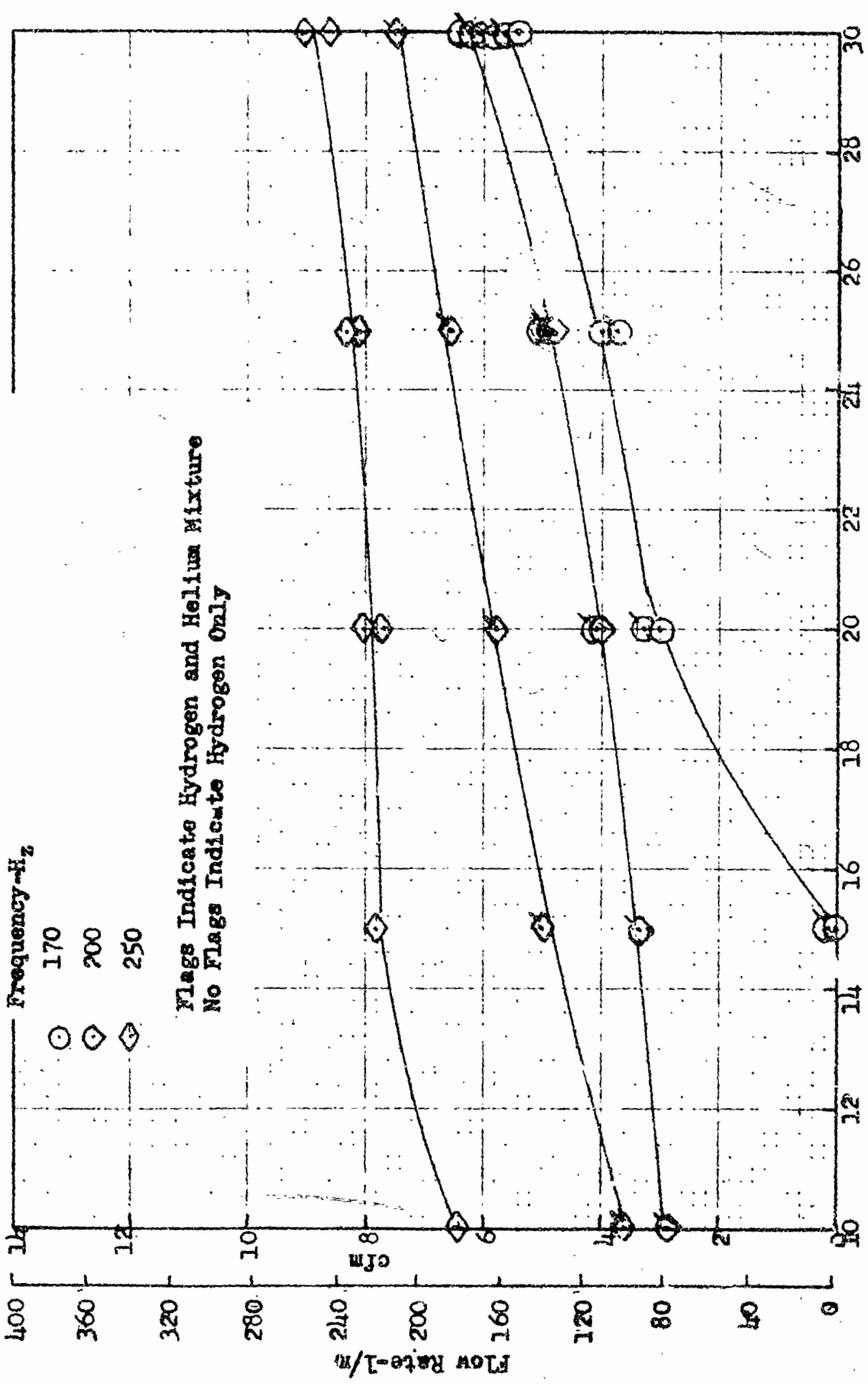

Figure 18 Mixer Unit Flow Rates in Gaseous Hydrogen and Mixtures of Helium and Hydrogen Gas

head capacity curves for three different nominal shaft speeds. The upper curve is for synchronous operation. For lower flow rates, the motor must be operated in the induction (or high slip) mode which is represented by the two lower curves on Fig. 14. Fig. 15 shows the power requirements corresponding to the three different speed curves, when applied voltage is held constant at 30 volts. Fig. 16 shows the effect of voltage on power requirements at synchronous speed, which indicates that the efficiency goes down with increasing voltage inasmuch as the fluid power does not change with voltage.

The mixer unit was also calibrated in hydrogen vapor, and a mixture of helium and hydrogen vapor. The results are shown in Figs. 17 and 18. It was found that flow rate increased with both voltage and frequency. Voltage did not affect the pressure rise across the fan which was governed primarily by the setting on the throttling valve that was placed downstream of the mixer unit. Also, at a fixed frequency, the power is primarily governed by flow rate, as shown on Fig. 18.

HEAT EXCHANGER

This unit provides the mechanism whereby the refrigerated vent fluid from the expansion unit can be vaporized by extracting the necessary heat from the bulk propellant. In the process, the bulk propellant becomes subcooled and causes a drop in tank pressure, providing the heat transfer rate in the heat exchanger exceeds that coming into the propellant from external and internal sources.

The counterflow plate-fin heat exchanger shown in Fig. 19 was designed and fabricated for the prototype thermal conditioning system. The prescribed requirements were that it be capable of vaporizing 1.4 lbs (0.635 K_g) of hydrogen per hour with helium on the warm side and a total temperature differential of 8 R° (4.45 K°).

Heat Exchanger Unit

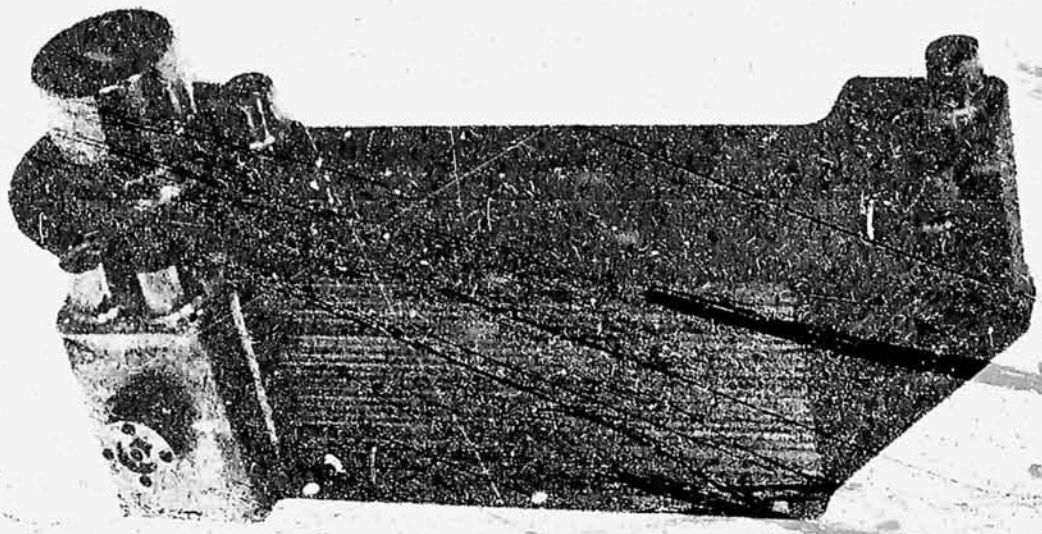

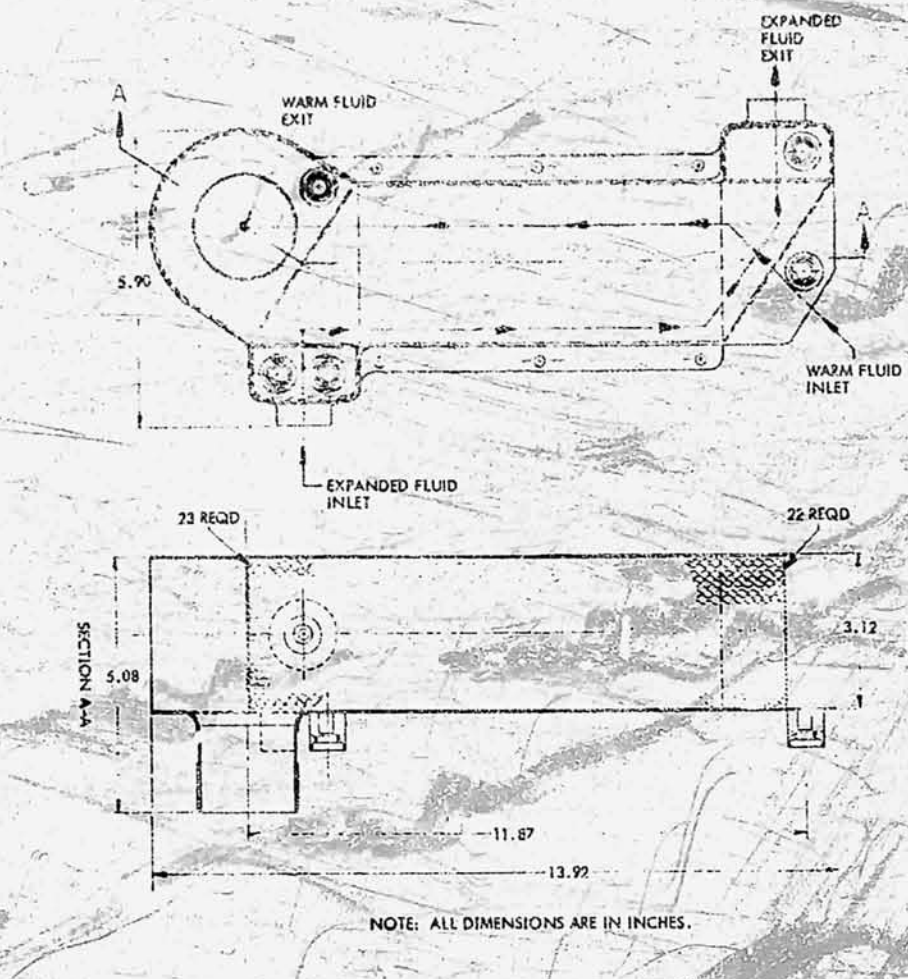

Figure 19 Heat Exchanger Unit

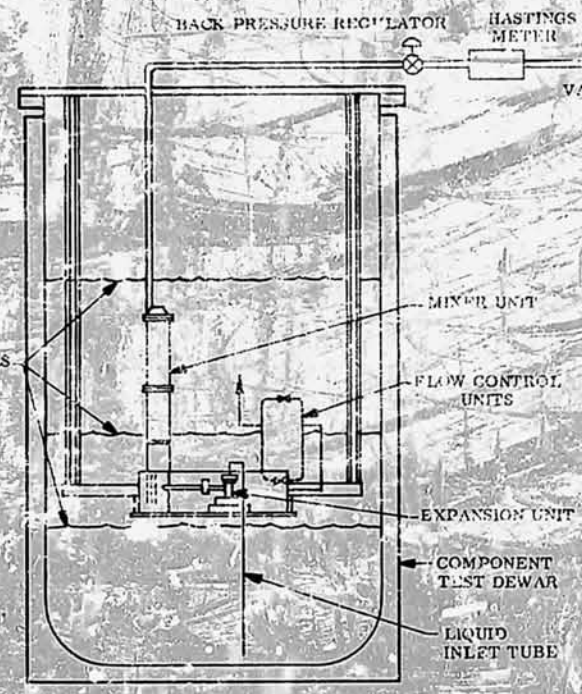

(a) Schematic

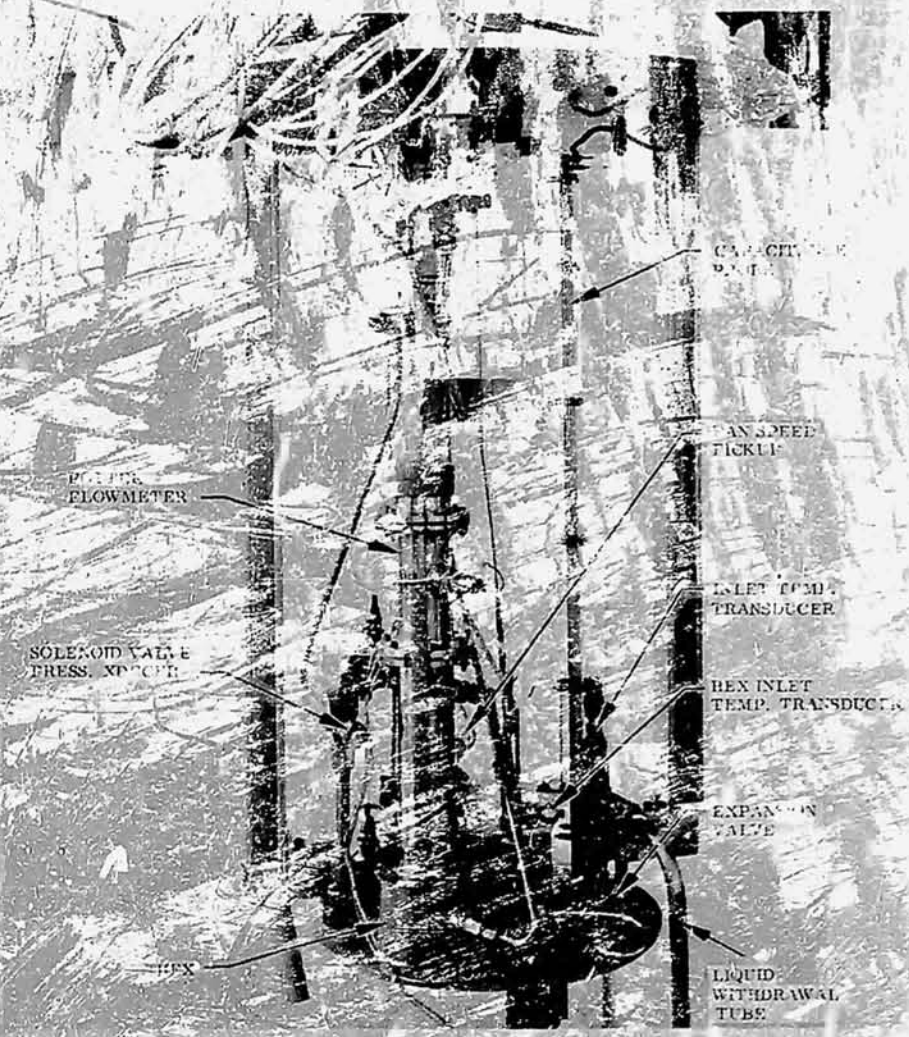

(b) Test Installation

Figure 20 Heat Exchanger and System Test Installation

The complete thermal conditioning system was set up in the 22 inch (0.56 m) test dewar as illustrated schematically on Fig. 20 to determine the performance of the heat exchanger and its matching characteristics with regard to the mixer unit. Also shown on Fig. 20 is a photograph of the illustration showing the manner in which it was suspended from the dewar lid. The maximum cold side flow rate was controlled by the selection of flow control valve No. 1 or No. 2. The facility throttling valve was used to back pressure the solenoid valve and reduce the flow as desired. The warm side flow was varied, while holding vent rate constant, by changing the mixer voltage and speed.

The test conditions and data for liquid hydrogen are presented in Table 7. The mixer was operated with flow rates ranging from 0.8 to 5.7 cfm (22.6 to 161 liters/min). Even the low mixer flow was sufficient to vaporize all the vent side fluid, and superheat the vapor. This is substantiated by the fact that the vent flow rate was nearly constant at 1.7 and 2.8 lbs/hr (0.77 and 1.27 K_g/hr) for valves 1 and 2, respectively. The superheat is illustrated on Fig. 21 which shows the heat exchanger effectiveness as a function of the flow ratio. This effectiveness should be zero for the condition where the warm side flow rate is just sufficient to vaporize the cold side flow and should approach 1 asymptotically. The fact that Fig. 21 shows many of the points above slightly 1 reflects small inaccuracies in the temperature measurement. However, it is clear that the mixer flows were more than adequate with liquid on both sides of the TCU. Some data was also taken with the mixer inoperative. The resulting high flow rates through the cold side of the heat exchanger indicate that two phase flow is passing through the flow control valves. The flow meter used to measure the mixer flow rates became erratic below 0.8 cfm (22.6 liters/min). Consequently, the intermediate flow rate between 0 and 0.8 cfm (22.6 ℓ/m) which would be just sufficient to vaporize the liquid on the cold side of the heat exchanger could not be determined.

The pressure drop measurements through the warm side of the heat exchanger were very erratic. However, they were estimated from the mixer speed and flow measurements. These are compared on Fig. 22 with previous predictions from air test data.

TABLE 7

SYSTEM CALIBRATION RESULTS IN LIQUID HYDROGEN

RUN NO.	MOTOR FREQ. (cps)	MOTOR VOLTS	MOTOR SPEED (rpm)	MOTOR POWER (watts)	MIXER FLOW (clm)	VENT VALVE	VENT FLOW (lb/hr)	REGULATED HEX PRESSURE (psia)	VENTED VAPOR TEMP. (°R)
7	170	30	3320	5.5	5.6 (158)	1	0.8 (0.36)	2.7 (18,600)	36.8 (20.4)
8	"	30	3360	4.7	5.6 (158)	2	2.0 (0.90)	2.6 (17,900)	37.2 (20.6)
9	"	30	1850	9.4	3.6 (102)	2	1.25(0.56)	2.6 (17,900)	37.0 (20.5)
10	"	30	1880	9.8	3.6 (102)	1	1.25(0.56)	2.6 (17,900)	37.1 (20.6)
11	"	30	3380	10.6	5.7 (161)	1	1.75(0.79)	3.7 (25,500)	37.5 (20.8)
12	"	28	1890	17.9	3.6 (102)	1	1.75(0.79)	3.7 (25,500)	37.8 (21.0)
13	"	30	3380	10.6	5.7 (161)	2	2.62(1.18)	3.6 (24,800)	37.7 (20.9)
14	170	28	2000	17.8	3.3 (93.5)	2	2.81(1.27)	3.6 (24,800)	37.5 (20.8)
19	0	-	-	-	0	2	4.0 (1.81)	3.7 (25,500)	31.6 (17.6)
20	"	"	"	"	"	2	5.1 (2.31)	3.6 (24,800)	30.5 (16.9)
21	"	"	"	"	"	1	3.2 (1.45)	3.7 (25,500)	30.4 (16.9)
22	"	"	"	"	"	1	4.0 (1.81)	3.7 (25,500)	30.1 (16.7)
23	"	"	"	"	"	1	4.6 (2.08)	3.7 (25,500)	30.1 (16.7)
24	0	-	-	-	0	2	3.9 (1.77)	3.6 (24,800)	31.7 (17.6)
25	170	30	3380	8.9	5.7 (161)	2	2.81(1.27)	3.7 (25,500)	37.1 (20.6)
26	170	28	1910	6.9	3.5 (99)	2	2.75(1.24)	3.7 (25,500)	37.1 (20.6)
27	0	-	-	-	-	2	4.25(1.92)	3.6 (24,800)	31.6 (17.6)
28	170	25	1560	5.5	2.3 (65.1)	2	2.8 (1.27)	3.7 (25,500)	37.0 (20.5)
29	0	-	-	-	-	1	4.1 (1.86)	3.6 (24,800)	30.3 (16.8)
30	170	17	860	2.4	1.6 (45.3)	1	1.75(0.79)	3.7 (25,500)	36.4 (20.2)
31	"	15	1050	1.9	0.8 (22.6)	1	1.7 (0.77)	3.8 (26,200)	36.6 (20.3)
32	"	28	1670	6.8	3.6 (102)	1	1.66(0.75)	3.8 (26,200)	37.8 (21.0)
33	"	30	3380	4.8	5.6 (158)	1	1.7 (0.77)	3.8 (26,200)	37.2 (20.6)
34	"	12	8255	1.2	1.4 (39.7)	2	2.8 (1.27)	3.6 (24,800)	36.3 (20.2)
35	170	8	480	0.5	0.9 (25.5)	2	2.8 (1.27)	3.7 (25,500)	35.5 (19.7)

Numbers in parentheses are SI Units: Mixer Flow - liters/min
Vent Flow - K_g/hr
Pressure - N/m^2
Temperature - °K

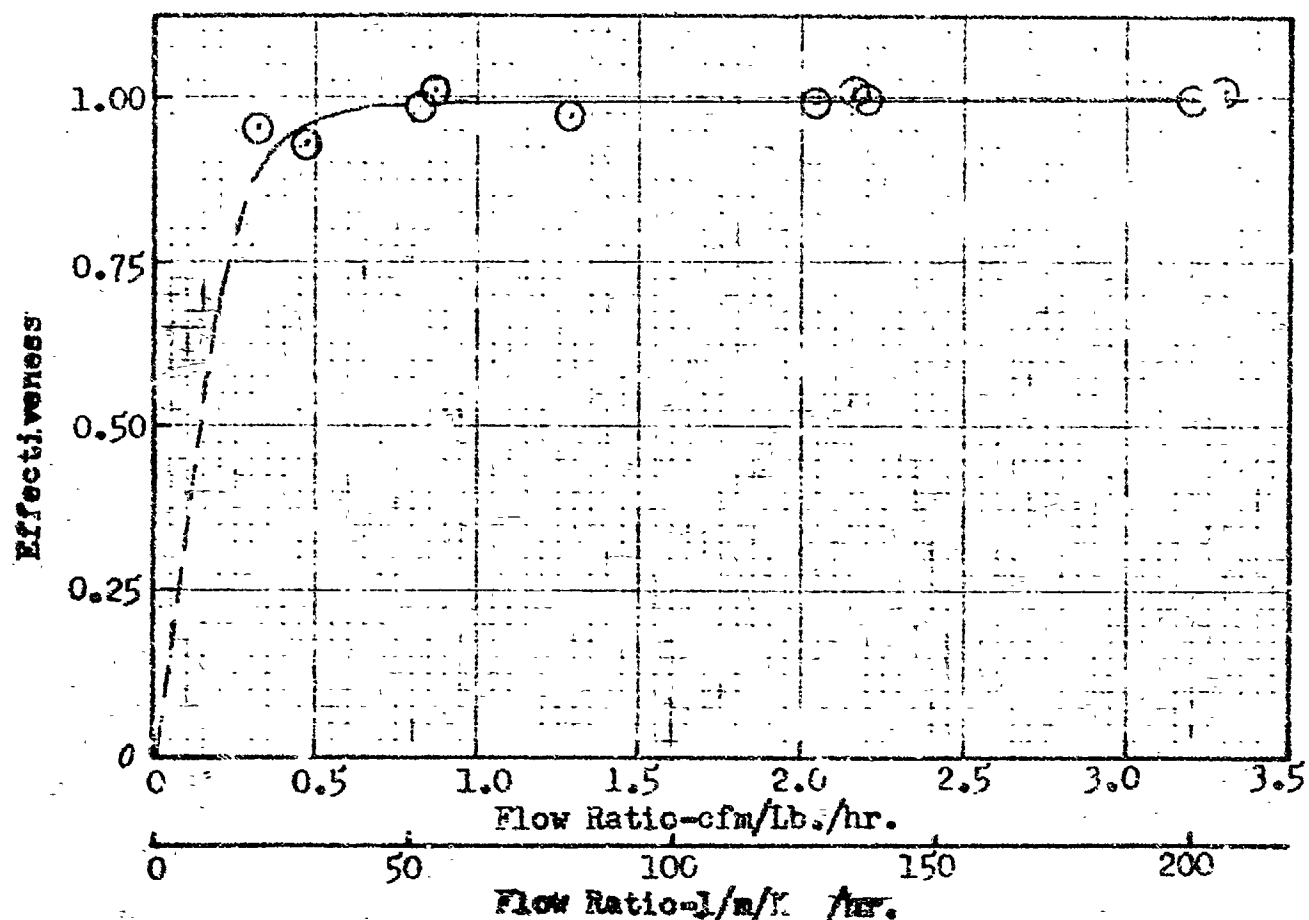

Figure 21 Heat Exchanger Effectiveness In Liquid Hydrogen

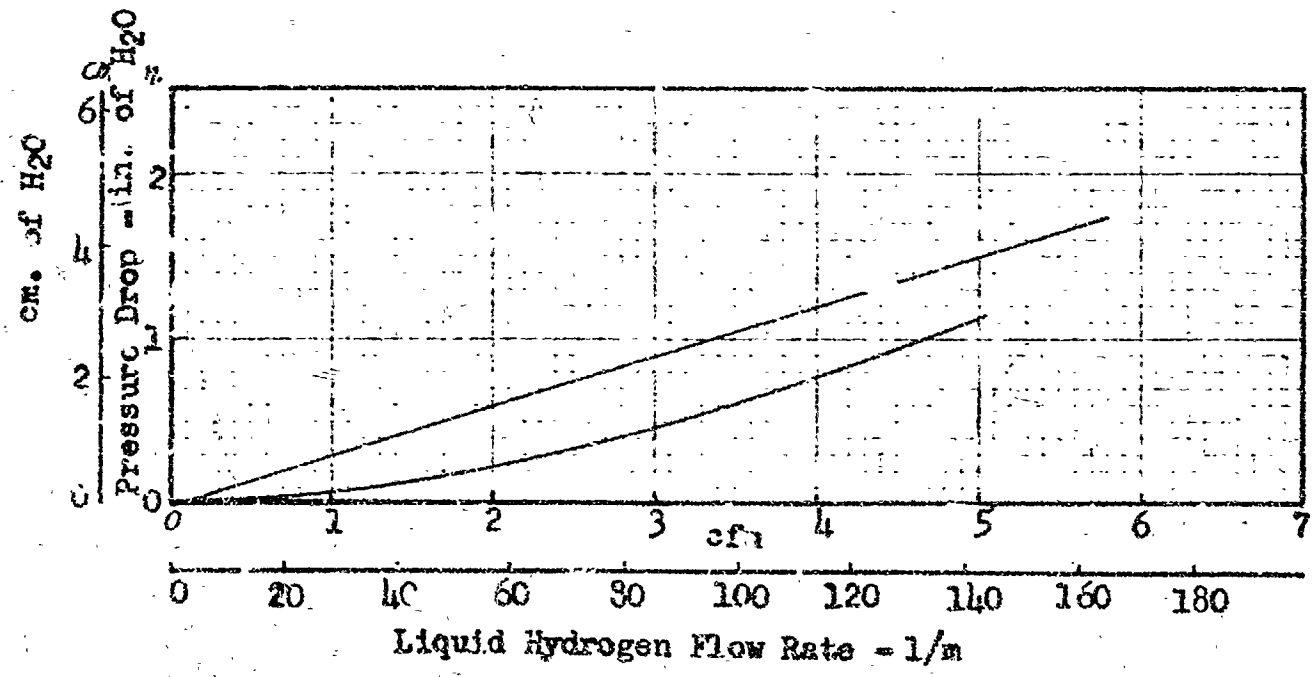

Figure 22 Warm Side Heat Exchanger Pressure Drop

The operating characteristics of the mixer are shown on Figs. 23 and 24 when the heat exchanger supplies the load. The speed variation with flow rate is approximately linear. However, power surge occurs at approximately 3.6 cfm (102 liters/min) and a speed of 2000 rpm, if the load is being increased.

A liquid withdrawal tube was attached to the expansion valve and extended to the bottom of the dewar approximately 6 inches (0.152 m) below the heat exchanger to allow operation with liquid on the vent side and gas on the warm side of the heat exchanger. However, when the liquid level was dropped below the heat exchanger, the surrounding vapor temperature rose so quickly because of high heat leak through the top of the dewar that the liquid was being vaporized in the inlet tube before passing through the expansion unit. Therefore, this test condition was established in the subsequent tests in the hydrogen tanks.

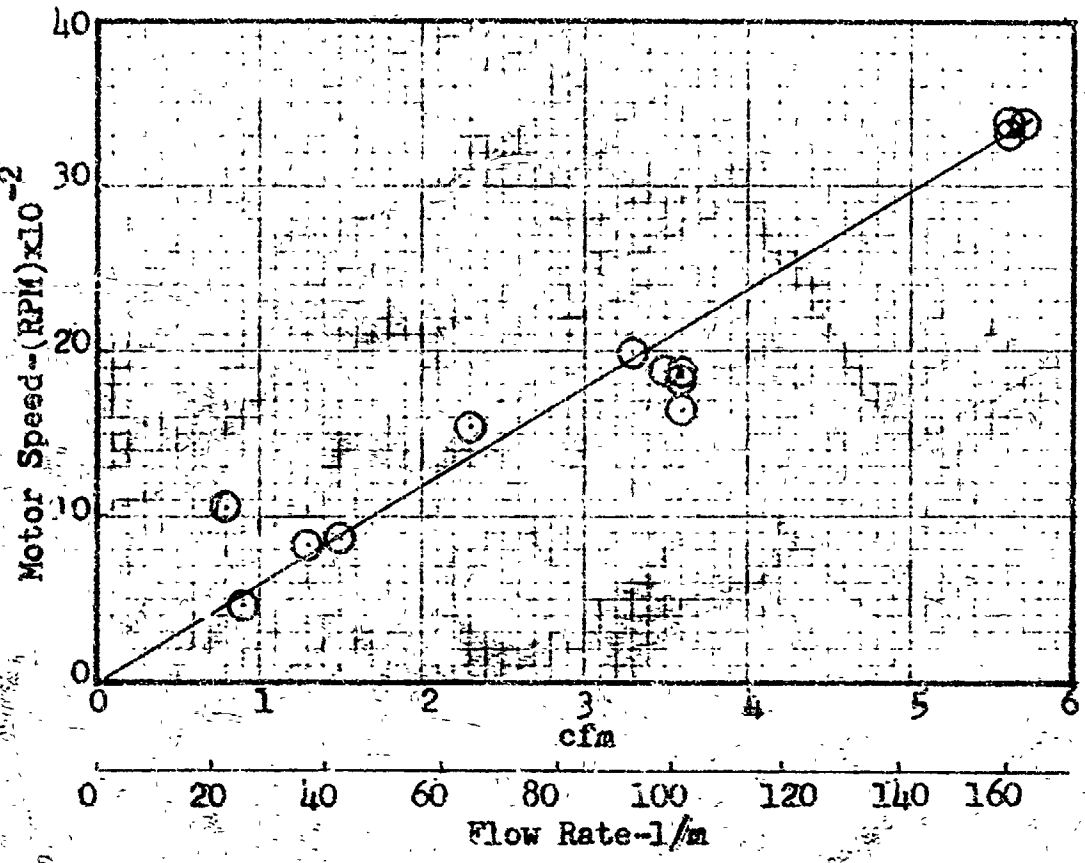

Figure 23 Effect of Mixer Speed on Heat Exchanger Flow

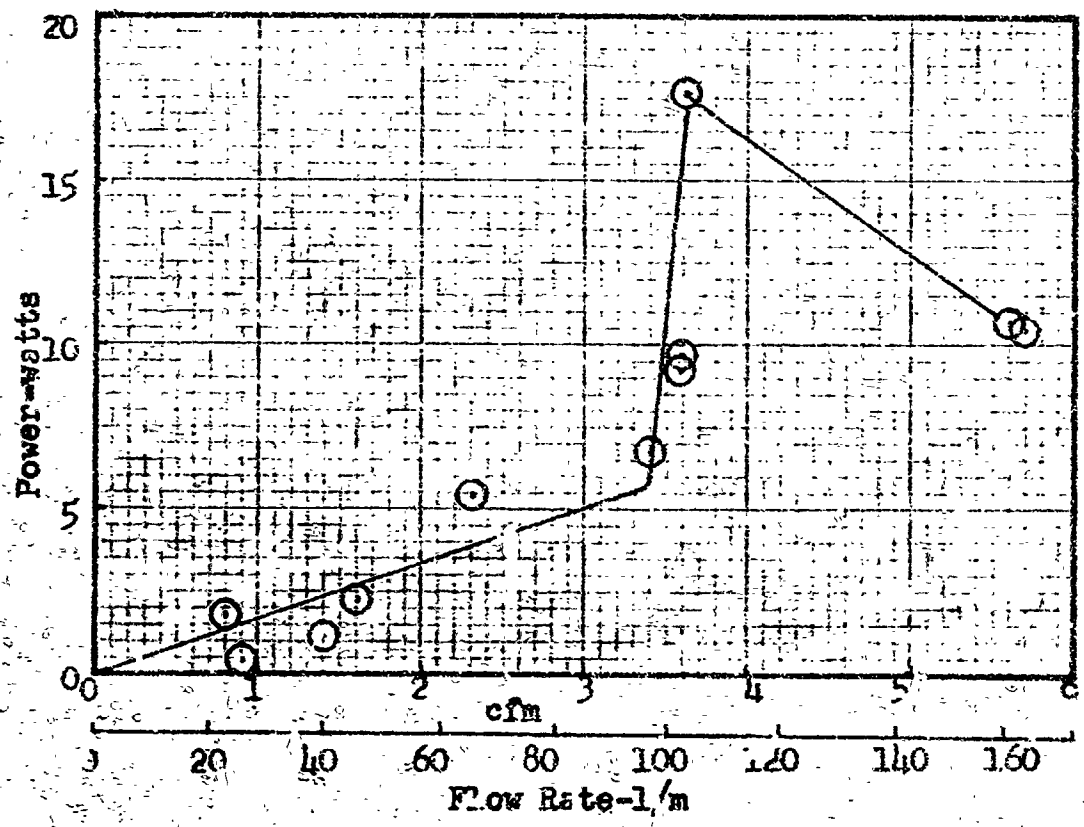

Figure 24 Effect of Heat Exchanger Flow Requirements on Mixer Power

THERMAL CONDITIONING SYSTEM TEST PROGRAM

This test program was designed to thoroughly establish the operating characteristics of the TCU for several mounting positions and configurations in liquid hydrogen tanks. The extent to which TCU performance is affected by tank size, tank pressure level, helium concentration, tank heating rate, and TCU variables such as mixer and vent rates, was to be determined.

Testing was performed at various ullage volumes, in both a 41.5 inch-diameter (1.05m) tank and a 110 inch-diameter (2.8m) tank to determine scaling effects. In each tank a test series was conducted with the TCU located in the bottom of the tank and the mixer jet directly vertically upward. A second series was conducted with the unit mounted on the side of the tank. Additionally, tests in the large tank included two series with special internal ducting designed to alter the propellant circulation characteristics in the tank in a manner which would simulate a low gravity pressure control situation. In addition to the systems performance testing, each component was individually calibrated to determine its performance characteristics. The test apparatus, instrumentation, test conditions, and procedures are described in this section. Data, test results, evaluations, and analyses of test data are presented in a subsequent section entitled: Results and Analysis.

TESTING IN A 41.5 INCH-DIAMETER (1.05 METER) LIQUID HYDROGEN TANK

Test Facility Descriptions

Bottom Mount Configuration

The thermal conditioning unit tested in this program is the same one previously evaluated under NAS 3-7942, and described in refs. 1 and 3, except for the addition of a second solenoid valve. This provided the capability for higher venting rates than were previously possible. Figure 25 is a schematic which illustrates the modified TCU package which accommodates the parallel installation of the two flow control units. Other than the TCU the major component of this test apparatus is a spherical, 41.5 inch-diameter (1.05m), liquid hydrogen tank, with an 18 inch-diameter (0.5m) access cover. The cover has nine penetrations to accommodate plumbing and electrical feedthrough fittings. The only penetration not through the cover is a vent line fitting located in the opposite pole of the tank.

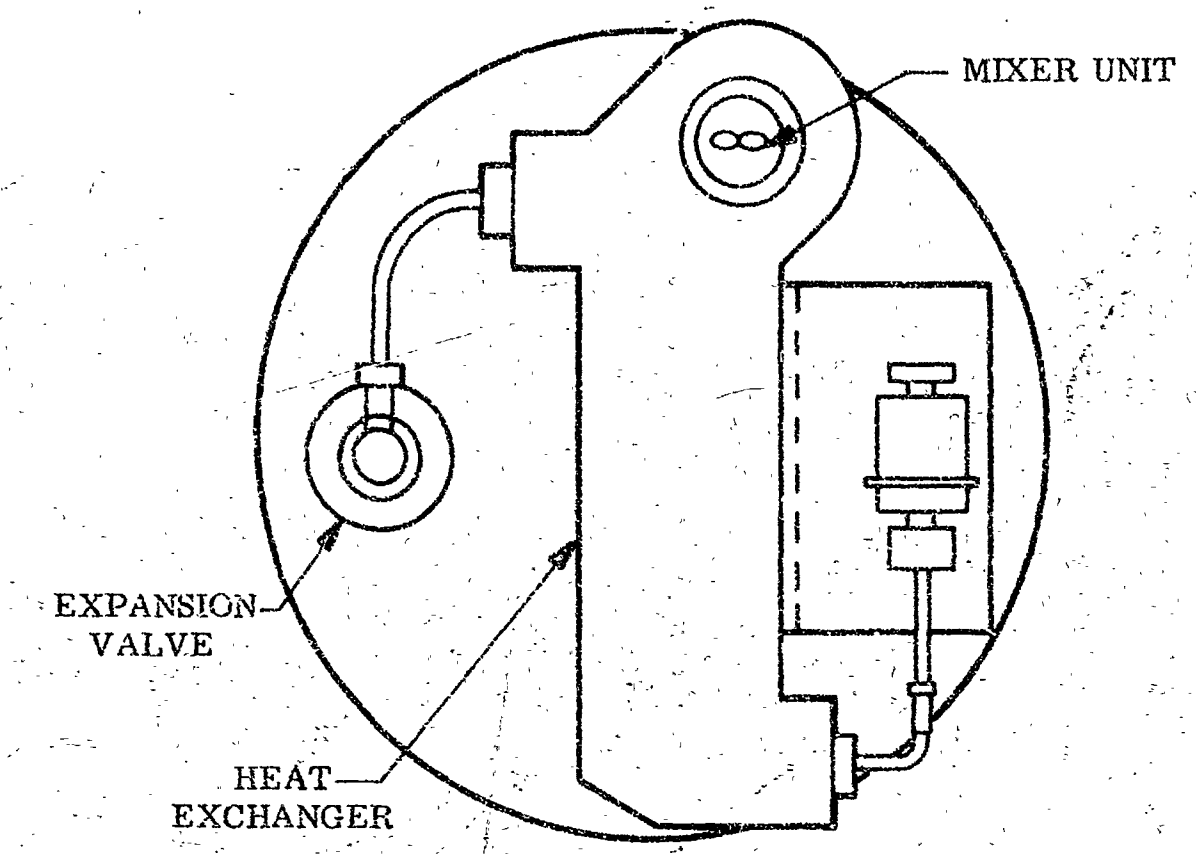

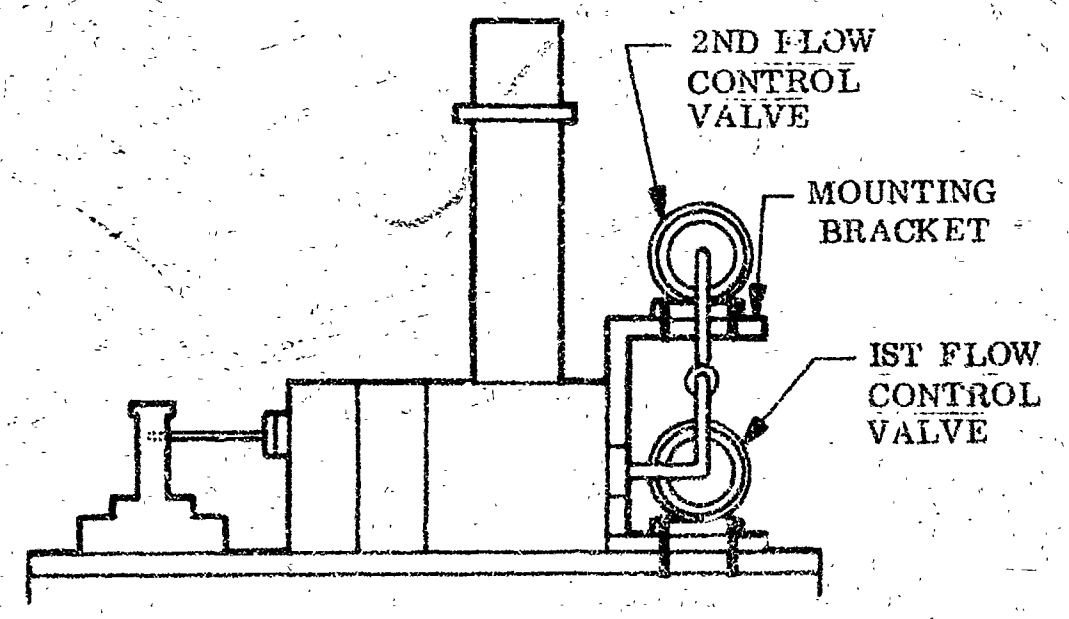

Figure 25 Schematic of Modified ECU Assembly

The support structure for this tank was designed to orient the tank with the access cover at the bottom. Thus, the interior surface of the cover, the lower tank plumbing fittings, the electrical feedthrough connectors and all associated Conoseal glands are submerged when the tank is filled with liquid hydrogen. The support system consists of three 1.5 inch (0.038m) diameter tubular stainless steel struts which connect to a flange that is attached directly to the access cover.

The thermal protection system for this 41.5-inch (1.05m) diameter test apparatus consists of 16 double aluminized Mylar radiation shields separated by 14 Tissuglas spacers. These were made up in two blankets which were prefabricated in oversize gores and a polar cap and then trimmed to fit with close tolerance butt joints during installation. Each blanket section is held together by molded Nylon retainers spaced 6 inches on center. The inner blanket is attached to the tank surface with Velcro Strip fasteners. The overlapping outer blanket sections were attached with Teflon tabs and aluminized Mylar tape at the butt joints.

The fill and drain line and the support struts were surrounded with a fiberglass penetration chamber for the first 18 inches (0.59m) below the tank. This penetration chamber was also insulated with 16 layers of MLI and its inner volume was loosely packed with fiberglass batting to eliminate radiation between penetrations, chamber walls, and the tank.

Internally, the tank is fitted with stiffened ring anti-slosh baffle at the tank equator, and a pressurant diffuser baffle located approximately 1-3/4 inches (0.044m) below the venting and pressurizing port, in the polar region of the tank.

The TCU was mounted in the bottom of the tank with the mixer discharge directed vertically upward, as shown schematically on Fig. 26. The TCU was supported from the lid on three legs that bolted to the TCU base-plate. The base plate was 5 inches above the lid, and when the flow meter was attached to the mixer discharge duct, the exit was 2.25 inches (0.057m) above the tank center line. Fig. 27 is a series of photographs showing different views of this installation including one with the tank being lowered onto the tank lid.

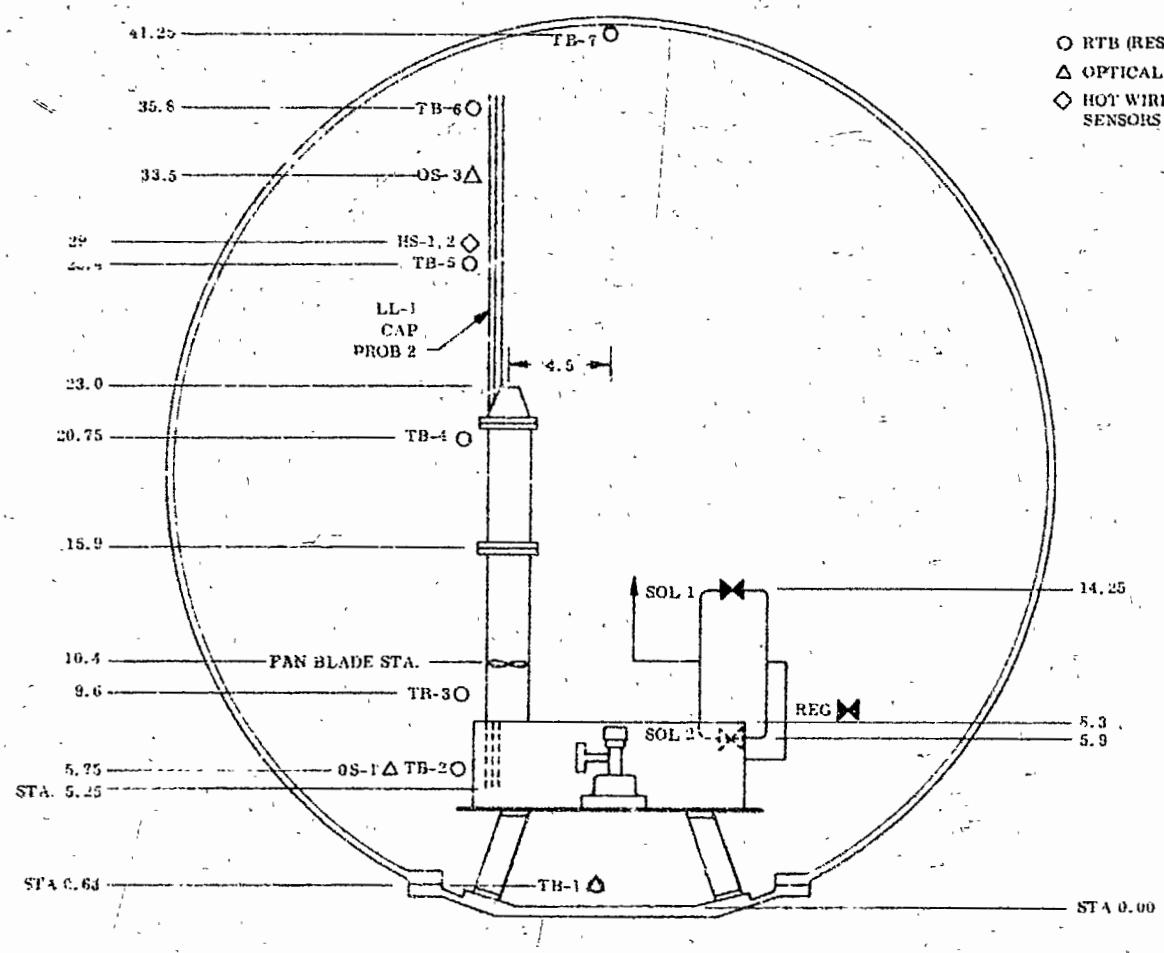

Figure 26. Bottom Mount Test Configuration - 41.5 inch (1.05 m) Tank

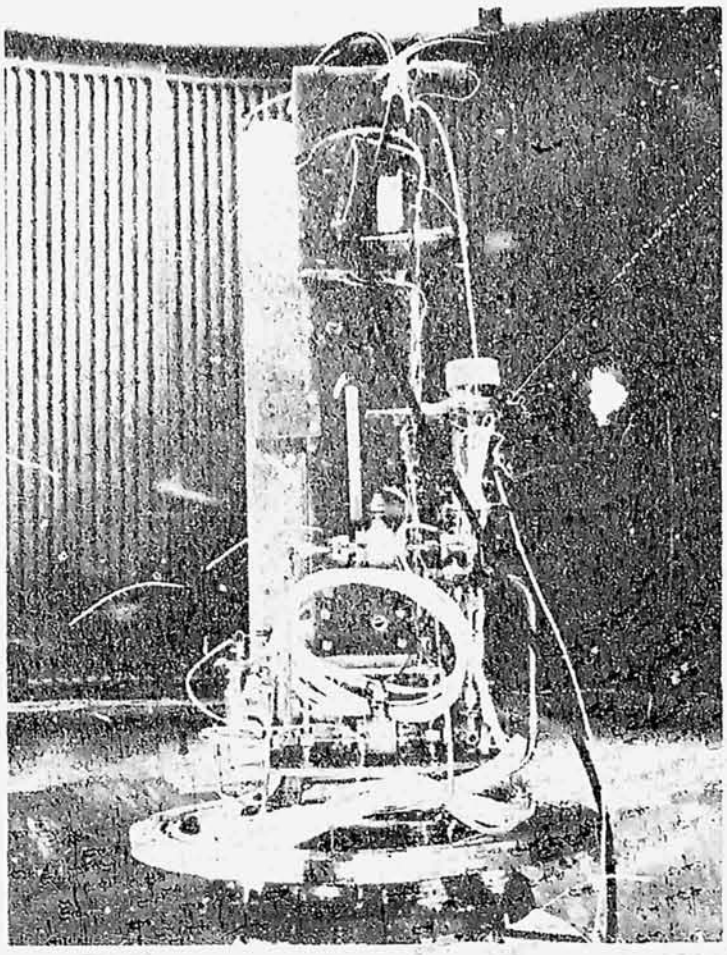

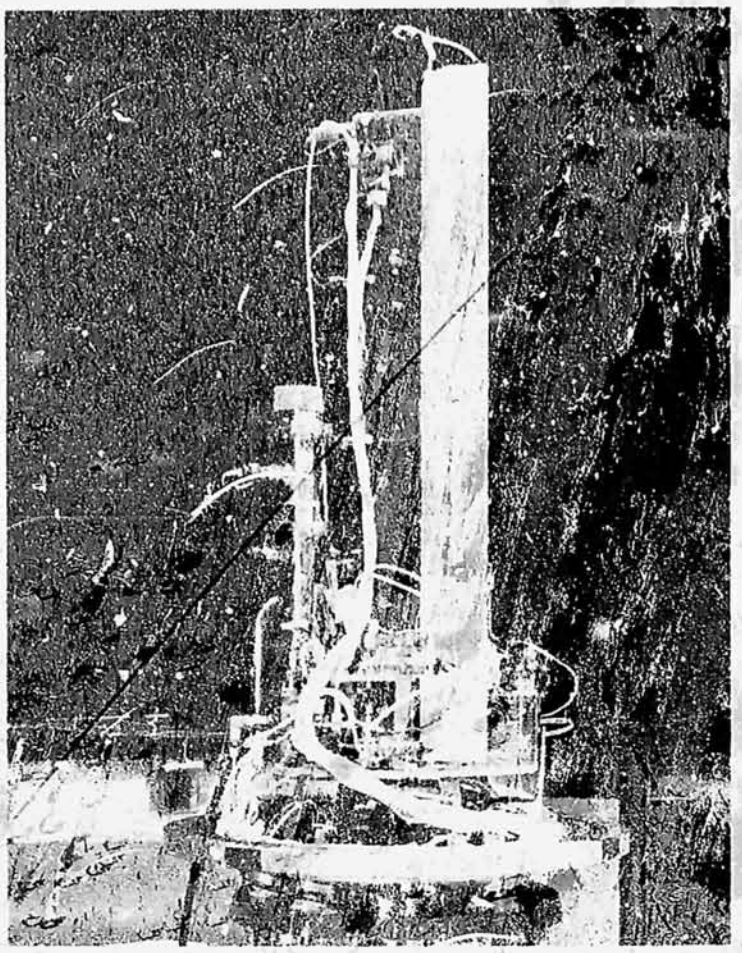

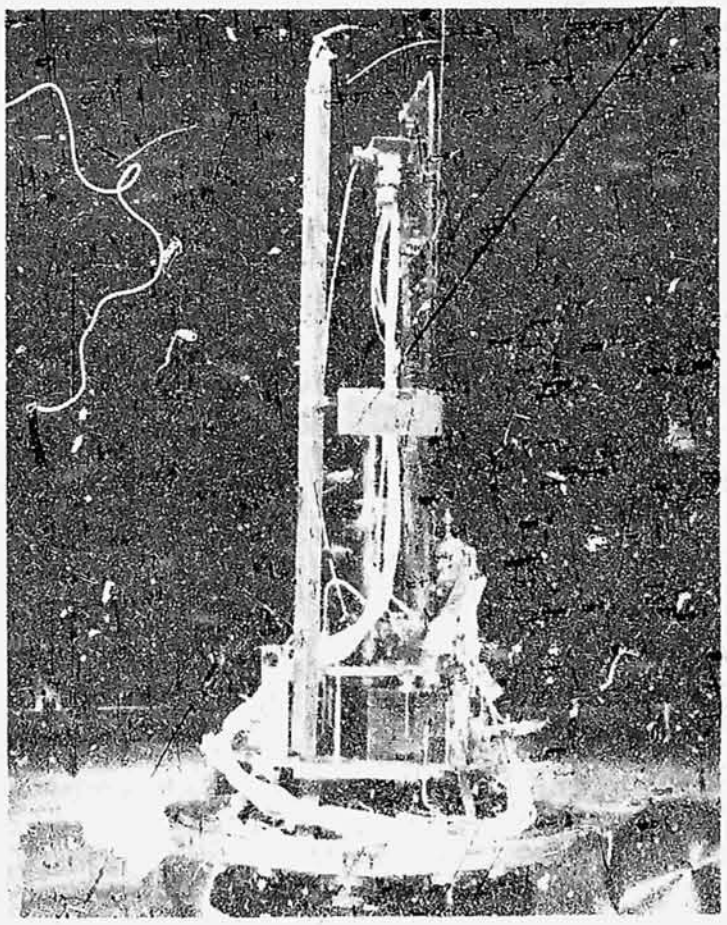

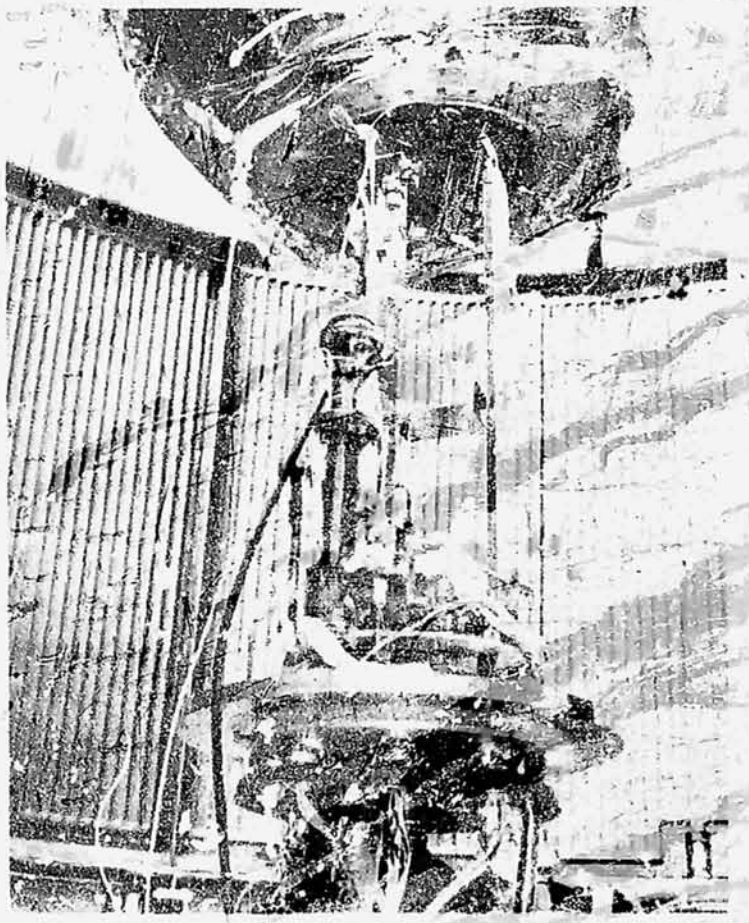

Figure 27 Photographs of TCU on 41.5" Dia. Tank Lid - Bottom Mount Configuration

The test apparatus was installed in the cryogenic flight simulator as illustrated in Fig. 28. The TCU vent system, downstream of the flow control units, was evacuated with a large vacuum pump having a capacity of 2000 cfm (56,600 liters/min) with an inlet absolute pressure of 0.5 psi (34,400 N/m^2).

Tank venting for boiloff tests was accomplished through a separate ullage vent port and plumbing system which also served as part of the pressurization plumbing. The line was double jacketed from the tank lid, through the chamber wall to an LN heat exchanger which provided the capability for pressurizing with gas (hydrogen or helium) at 140°R (77°K). For ambient pressurant tests, the heat exchanger loop was eliminated with isolation valves.

Power was supplied to the mixer and the two solenoid valves through an electrical connector in the tank access cover. Each valve was equipped with a current limiter that was mounted outside the tank. The current limiter allows high current (0.5a) to pass through the solenoid valves from 300 to 500 msec causing the solenoid to pull in, after which the current is automatically limited to 30 ma which is sufficient to hold the valve open. A manually controlled switching circuit was provided to permit flow through either of the two flow control valves, as desired. The speed and flow rate through the mixer unit was varied with a variable voltage power supply for the mixer motor having a frequency and voltage range of 0-400 HZ and 0-100 volts, respectively. A manually controlled, on-off switch was wired in parallel with the pressure switch so that the mixer unit could be operated independent of the rest of the TCU.

Instrumentation for the test was selected to take advantage of conventional cryogenic instrumentation of proven accuracy and repeatability. Thirty-six measurements were made at each sampling. Thirteen of these were used to measure specific parameters and conditions within the TCU. The remainder were used to track liquid level and temperature data within the propellant, as well as tank pressure. Table 8 identifies the instrumentation and Fig. 26 shows the location of the in-tank sensors. This schedule provides for redundancy on critical measurements such as tank pressure, vent fluid pressure, liquid level, etc.

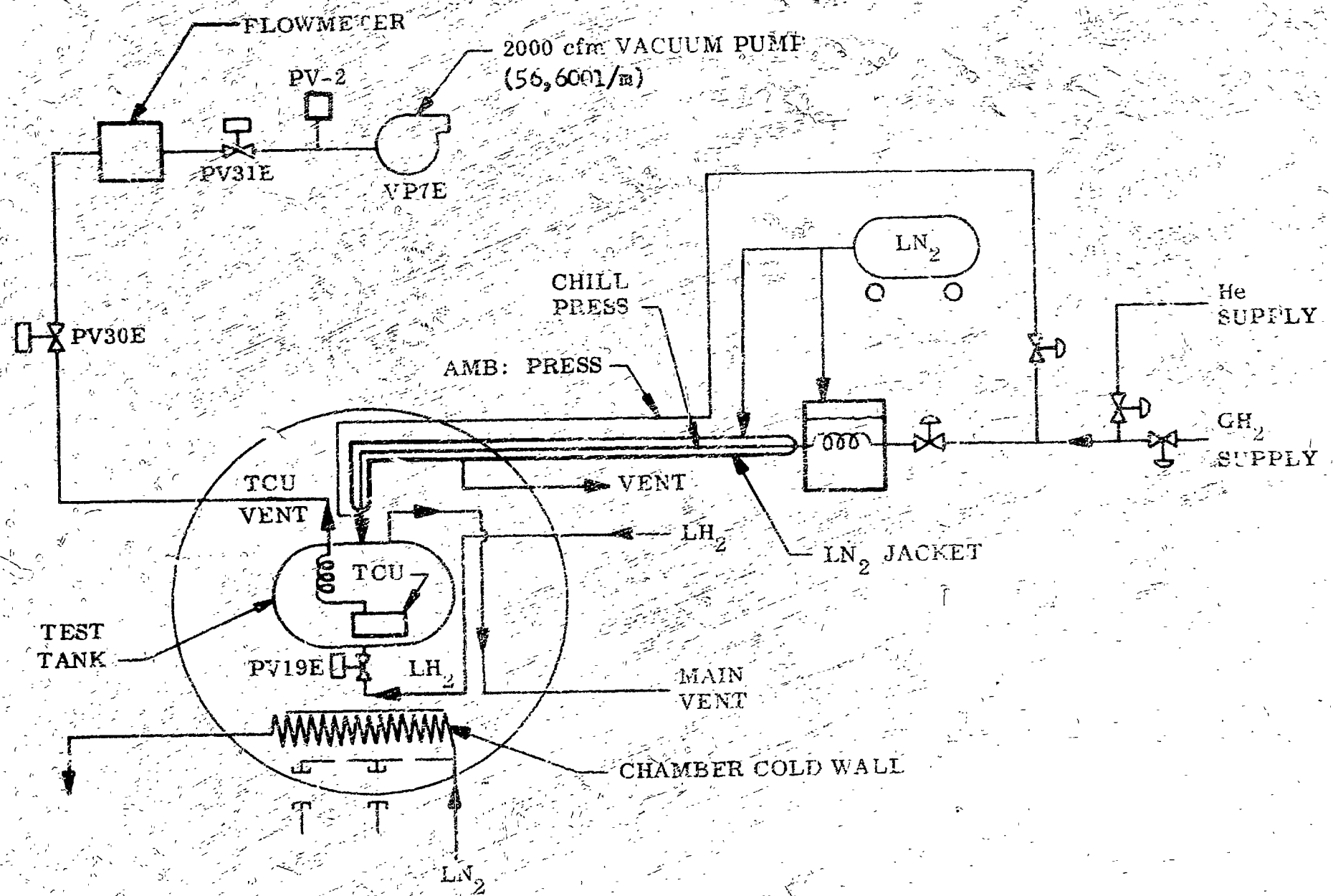

Figure 28 Test Facility Schematic

TABLE 8

INSTRUMENTATION SCHEDULE
41.5 inch (1.05 m) DIAMETER TANK

TABLE 8

INSTRUMENTATION SCHEDULE -

41.5 INCH (1.05 METER) DIA[illegible] TANK

Press. Tank Ullage #2	PTU-2	142	5-2	Transducer [illegible]	GP54F-502	1584	0 - 50 PSIG	
Press. Coldside Inlet	PCi	143		Statham	[illegible]	1991	0 - 25 PSIA	
Press. Solenoid Valve Vent #1	PV-1	144		Statham	PA2031Ch 15-350	1600	0 - 15 PSIA	
Press. Solenoid Valve Vent #2	PV-2	145	6-1	Statham	PA2031C 25-350	2365	0 - 10 PSIA	±0.5 PSIA
Press. Warmside	PW	147		C.C.C.	416P 14A	1861	0 - 0.4 PSID	
Press. Vacuum Chamber	PC (TC)	148		Fredricks	3A	2365		
Boiloff Flow	FB	149		Rosemount	124AD-101B5	92	0 - 1.2#/hr.	±0.05#/hr.
Flow Rate Warmside	FW	150	7-1	Potter	2" 66101A	LK-2-17		±0.3 CFM
Flow Rate Coldside	FC	151	2	Hastings	AHL-25X	11		±0.3#/hr.
Fan Speed	NF	152	4-1	Fisher-Porter	9667B 016VQ1			
Motor Power	MP	153		Scientific Columbus	1382B	798		Unknown
Press. Switch Trace	PS	154						
Solenoid Valve #1 Volts	SE-1	155					1 - 20 VDC	
Solenoid Valve #2 Volts	SE-2	156					1 - 20 VDC	
Solenoid Valve #1 Current	SI-1	157					0 - 1.0 Amp	
Solenoid Valve #2 Current	SI-2	158					0 - 1.0 Amp	
RF Liquid Level Sensor	RFS-1	159						
Optical Level Sensor #1	OS-1	160		Bendix GL-103				0.06"
Optical Level Sensor #3	OS-3	161		Bendix GL-103				
Hot Wire Level Sensor #1	HS-1	162		United Control	2641-1			
Hot Wire Level Sensor #2	HS-2	163		United Control	2641-1			0.06"
Press. Vacuum Chamber	PC (ION)	164		Fredricks				
Temp. Coldside Inlet	TCi	165		Cryo Cal Inc.	CR2500L 14-100	1306	30°R to 60°R	0.1°R @ LH_2 Temp.
Temp. Coldside Outlet	TCo	166				1267		
Temp. Warmside Inlet	TWi	167				1325		
Temp. Warmside Outlet	TWo	168		Cryo Cal Inc.	CR2500L 14-100	1411	30°R to 60°R	0.1°R @ LH_2 Temp.
GRT's Excitation	VE	169						
Temp. Bulk #1	TB-1	170		Rosemount	150MA10	7658	30°R to 490°R	±0.6°R @ LH_2 Temp.
Temp. Bulk #2	TB-2	171				7650		
Temp. Bulk #3 & Reg. Input	TB-3	172				7656		
Temp. Bulk #4	TB-4	173				7653		
Temp. Bulk #5	TB-5	174				7652		
Temp. Bulk #6	TB-6	175				7654		±0.6°R @ LH_2 Temp.
Temp. Bulk #7	TB-7	176		Winsco	2448	146		Unknown
LH_2 Bleed Temp.	LH_2 BT	177				151		
Temp. Downstream Ullage	T.D.U.	178		Winsco	24[illegible]	150	30°R to 650°R	Unknown

A Dymec digital recorder was used to record all data on magnetic tape for subsequent engineering evaluation. Additionally, certain selected control variables were recorded on strip charts as an operational aid to obtain immediate data trends and early detection of any problems that might develop.

Side Mount Configuration

Fig. 29 illustrates the side mounted installation. Two tubular struts were used to support the system from a bracket that was also used to support the instrument rack off the tank lid. This installation positioned the mixer discharge in the equatorial plane perpendicular to the gravitational vector as illustrated in Fig. 29. The inlet and discharge were nearly equidistant from the vertical centerline. Fig. 30 is a series of photographs showing different views of this installation before the tank was lowered onto the lid. All other features and facility requirements were the same as those for the bottom mount configuration.

Test Operations

Bottom Mount Series

The test procedures actually cover pre-test activity, test sequencing, and post test activity. The pre-test preparations were as follows:

- The TCU was installed on the tank lid and all plumbing connections were made.
- A bench leak check of all connections was made with a mass spectrometer.
- All electrical connections were made and the fan was checked for proper rotational direction.
- The 42.5 inch (1.05m) diameter tank was then lowered over the TCU (See Fig. 27) and mounted onto the tank lid.
- After making the vent/pressurization system connections the entire system was again helium leak checked.
- After the flight simulator was closed up, instrumentation precalibrations were performed, and chamber pump down was initiated.
- The tank and plumbing lines were purged with nitrogen gas until gas samples indicated all oxygen was removed from the system.

- o The flow control valves were then opened, and the TCU components and tank were purged with nitrogen gas an additional 15 minutes.
- o The nitrogen purge sequence was repeated with hydrogen gas until all nitrogen was removed from the system. This purge was continued for 30 minutes.
- o All TCU components, instrumentation and facility functions were checked for the last time before initiating hydrogen fill.

Prior to initiating the TCU tests, the tank was filled to the 5 percent ullage level where a soak period and boiloff stabilization test was conducted. This took approximately 6 hours, of which the last three indicated steady boiloff and pressure.

The TCU test procedures can best be described in reference to the test sequence and conditions. One hundred and eighty-three runs were conducted with the bottom mounted configuration. These are delineated in Table 9.

The indicated nominal ullage volumes were allowed to vary 5 percent before the liquid level was readjusted, and the pressure was allowed to vary 1 psi (6895 N/m^2). With these qualifications, a typical procedural sequence for conducting a test was as follows:

- o Adjust liquid and pressure level if below the prescribed lower limit for the upcoming test.
- o Adjust applied motor voltage to give the prescribed mixer flow rate for the upcoming test.
- o Set Dymec recorder for continuous printout for tests with pressurization.
- o Turn TCU off, Dymec on, and pressurize with appropriate gas, as required.
- o Cease pressurization when strip chart recorder indicates the maximum pressure has been attained.
- o Simultaneously turn on mixer and open the appropriate solenoid valve.
- o Continue the test until data indicates a constant rate of change has been obtained.
- o Vent the tank down to the nominal tank pressure and repeat the sequence for the next test.

C2

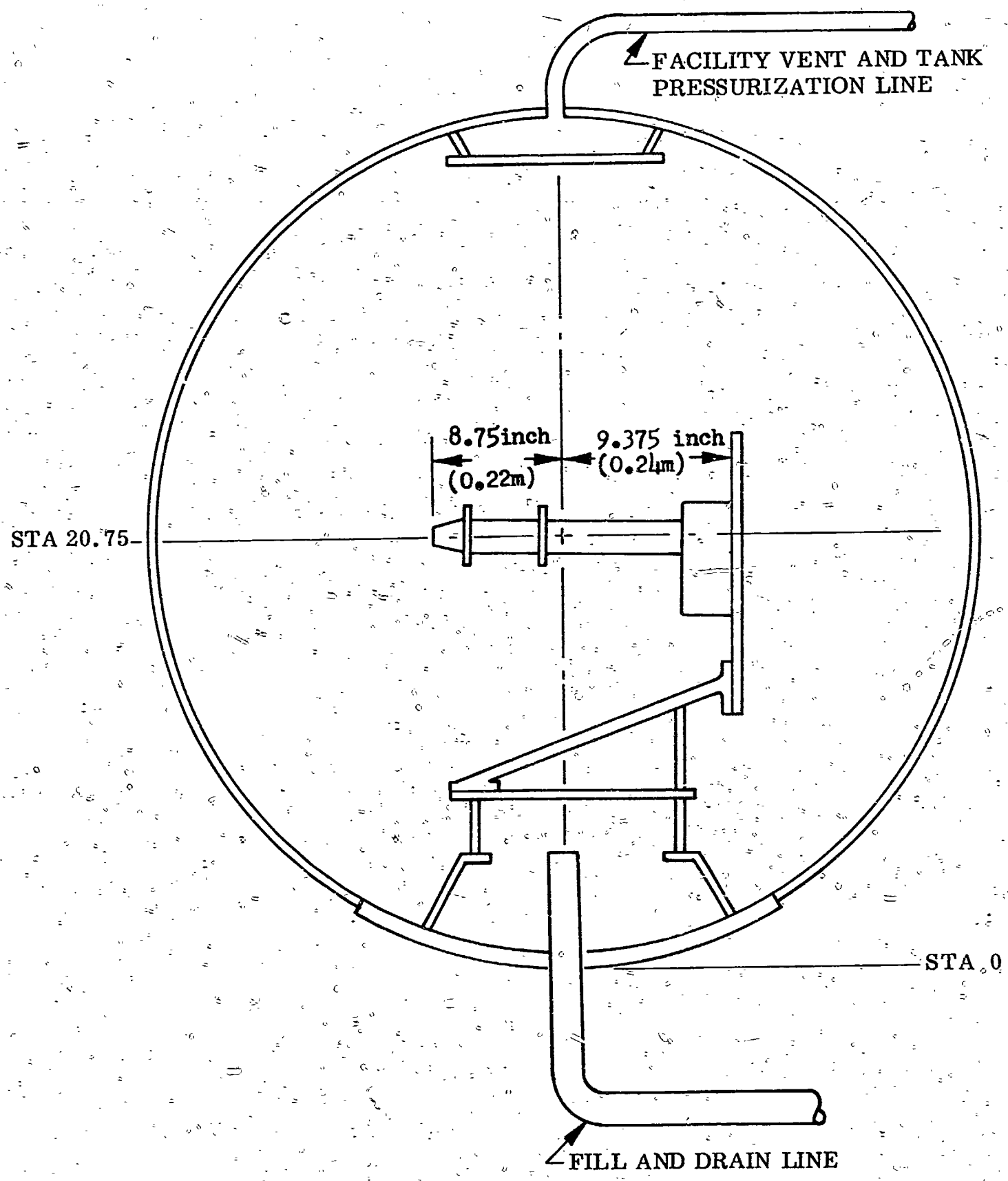

Figure 29 Side Mount Test Configuration - 41.5 inch(1.05m) Tank

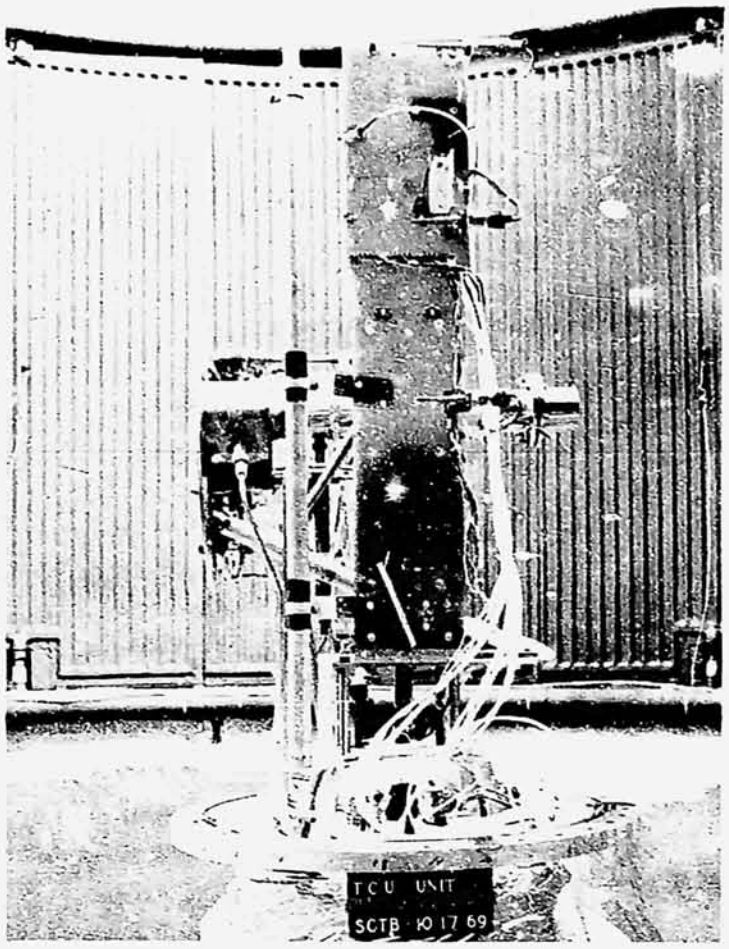

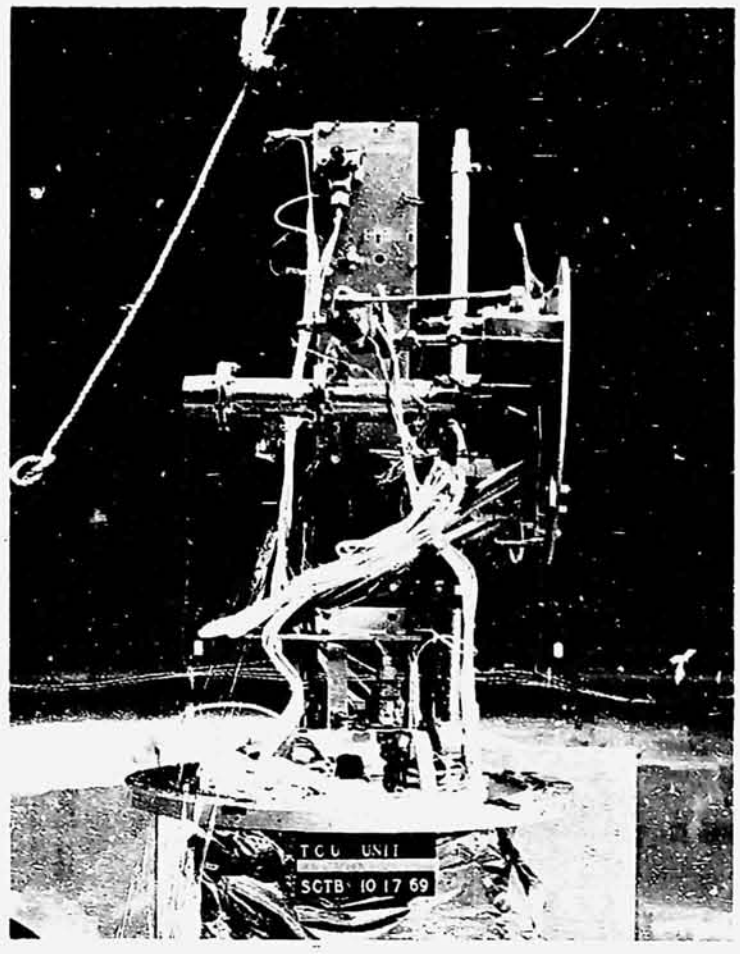

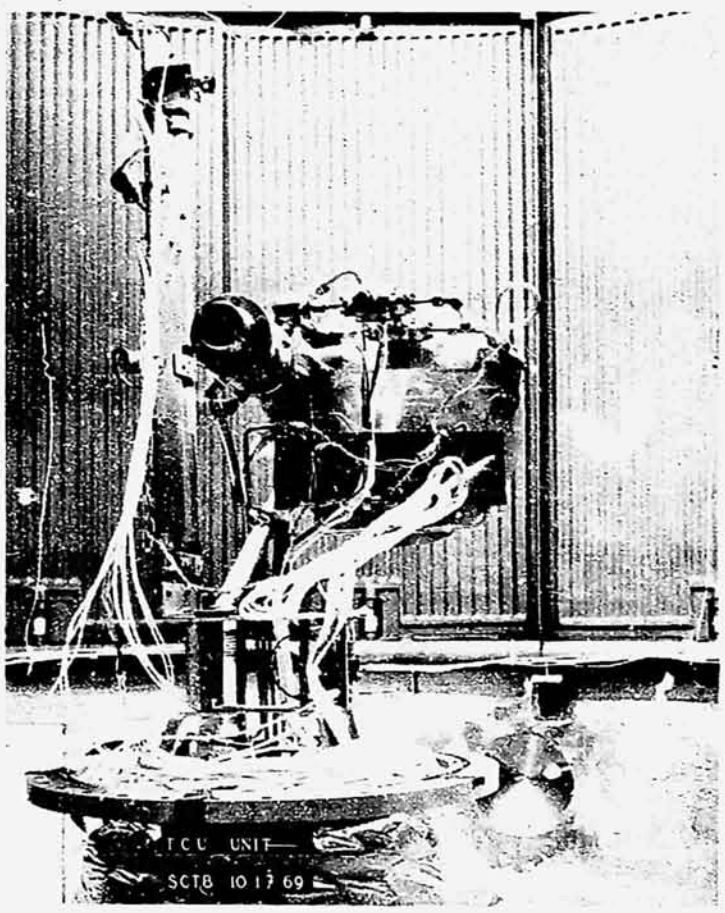

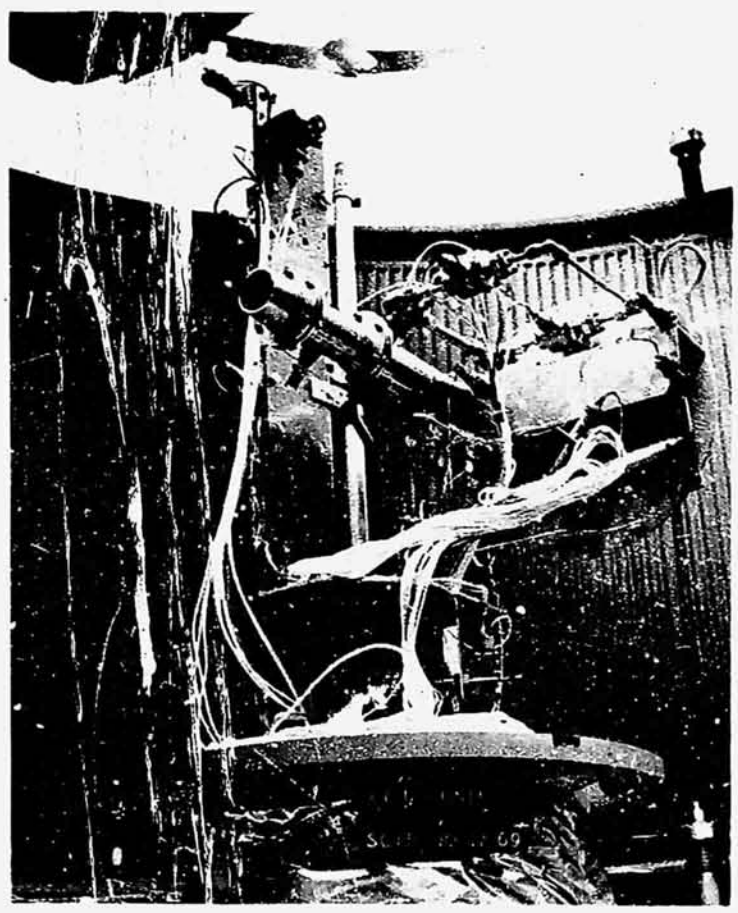

Figure 30 TCU on 41.5inch (1.05 m) Tank Lid - Side Mount Configuration

TABLE 9

41.5 INCH (1.05m) TANK-BOTTOM MOUNT TEST CONDITIONS

Run No.	Nominal Vent Flow(3)	Nominal Ullage Volume(1)	Nominal Mixer Flow(2)	Nominal Tank Pressure psia (N/m^2)10^{-4}	Comments
1	-	1	-	17 (11.7)	Establish equilibrium conditions, at 17 psia (11.7x10^4 N/m^2) and determine dp/dθ
2	1	1	1	17	Operate TCU after equilibrium at 17 psia is established. Run time shall be of sufficient duration to establish decay rate at each condition.
3	2	1	1	17	
4	1	1	2	17	
5	2	1	2	17	
6	1	1	3	17	
7	2	1	3	17	
8	-	1	-	17-28 (11.7-19.3)	Establish tank equilibrium at 17 psia. Pressurize to 28 psia (19.3x10^4 N/m^2) with GH_2 at 140°R (77°K) and establish pressure-time relation untill dp/dθ 0
9	-	1	1	17-28	Vent from final pressure of run 8 to 17 psia and equalize tank conditions. Then pressurize to 28 psia with GH_2 at 140°R and establish pressure-time relation with mixer on until dp/dθ = 0.
10	-	1	2	17-28	Repeat run 9 with mixer speed 2.
11	-	1	3	17-28	Repeat run 9 with mixer speed 3.
12	1	1	1	17-28	Vent from final pressure on run 11 to 17 psia and equalize tank. Pressurize to 28 psia with GH_2 at 140°R and operate TCU to establish decay rate at each condition.
13	2	1	1	17-28	
14	1	1	2	17-28	
15	2	1	2	17-28	
16	1	1	3	17-28	
17	2	1	3	17-28	

TABLE 9 (Cont'd.)

Run No.	Nominal Vent Flow(3)	Nominal Ullage Volume(1)	Nominal Mixer Flow(2)	Nominal Tank Pressure psia (N/m^2)	Comments
18	-	1	-	17-28 (11.7-19.3)	**Establish equilibrium at 17 psia. Pressurize to 28 psia (19.3×10^4 N/m^2) with GH_2 at 530°R (294°K) and establish pressure-time relation until dp/dθ 0**
19	-	1	1	17-28	Vent from final pressure of run 18 to 17 psia and equalize tank conditions. Then pressurize to 28 psia with 530°R GH_2 and establish pressure-time relation with mixer on until dp/dθ = 0. Mixer speed 1.
20	-	1	2	17-28	Repeat data pt 19 with mixer speed 2.
21	-	1	3	17-28	Repeat data pt 19 with mixer speed 3.
22	1	1	1	17-28	Vent from final pressure on run 21 to 17 psia and equalize tank. Pressurize to 28 psia with GH_2 at 530°R and operate TCU to establish decay rate.
23	2	1	1	17-28	
24	1	1	2	17-28	
25	2	1	2	17-28	
26	1	1	3	17-28	
27	2	1	3	17-28	
28	-	1	0	17 (11.7)	Establish equilibrium at 17 psia. Place TCU on automatic operation. Hold tank at 17 psia and demonstrate cycling capability. Coldside valve position and mixer speed to be selected.

TABLE 9 (Cont'd.)

Run No.	Nominal Vent Flow(3)	Nominal Ullage Volume(1)	Nominal Mixer Flow(2)	Nominal Tank Pressure psia (N/m^2)	
29-48	-	1	-	17-28	Repeat data 8-27 using He as pressurant.
49	-	1	-	17-28 (11.7-19.3)	Establish equilibrium at 17 psia. Pressurize to 28 psia with He at 140°R. Place TCU on automatic operation for tank pressure of 17 psia. Operate TCU and demonstrate cycling. Cold-side valve position and mixer speed to be selected.
50-69	-	1	-	17-36 (11.7-24.8)	Repeat runs 18-27 and 40-49 at tank pressure of 36 psia.
70-96	-	2	-	17-28	Repeat run 1-27 with liquid level No. 2
97-116	-	2	-	17-28	Repeat runs 8-27 using He as pressurant.
117-183	-	3	-	-	Repeat runs 1-27, 29-48, and 50-69 with liquid level No. 3.

(1)Nominal Ullage Volume: 1 -5 Percent
2 -2½ Percent
3- 70 Percent

(2)Nominal Mixer Flow: 1 -3.5 cfm (100 l/m)
2 -5.6 cfm (160 l/m)
3 -2.5 cfm (71 l/m)

(3)Nominal Vent Flow: 1 -1.5 lb./hr. (682 gr./hr)
2 -2.7 lb./hr. (1230 gr./hr)

Two of the tests (Nos. 28, 49) were included to demonstrate the automatic control characteristics of the TCU. For Test No. 28, equilibrium was established at approximately 17 psia (117,000 N/m^2) and the system was placed on automatic control for two complete cycles. This test simulated an intermittent vent period during long coast flight. For Test No. 49, the tank was pressurized to 28 psi (193,000 N/m^2) with cold ($140^oR = 77^oK$) helium and the system was again placed on automatic control for two complete cycles. This simulated system pressure control followed an engine firing.

Side Mount Series

When the bottom mounted test series was completed, the TCU was reoriented and the 71 tests delineated in Table 10 were conducted. The intent was to duplicate the bottom mount series. However, two regulator failures were encountered forcing an early conclusion, after obtaining data at two liquid levels.

The first unit failed at the start of the side mounted TCU tests. When the TCU was activated, the vent rate was unusually high at 6 lbs per hour (2.7 Kg/hr) and the regulated pressure was 8.2 psia (56,500 N/m^2). Both started to drop off, however, and in a few minutes the vent flow dropped to zero and the heat exchanger pressure dropped to less than 1 psia (6900 N/m^2).

A second regulator was available. Its regulation with air was checked and was 3.3 psia (22,750 N/m^2) to 3.6 psia (24,800 N/m^2). This unit was installed for test in the 41.5 inch (1.05m) tank. It operated satisfactorily through the first two liquid levels. However, when attempting to run the TCU tests at level #3 a no-flow condition of the regulator was observed. An attempt was made to backflow the regulator by pressurizing the downstream side of the regulator through the instrumentation port. This was unsuccessful, and the tests were concluded. Subsequent tests revealed a manufacturing defect in the bellows on this second unit.

TESTING IN A 110 INCH-DIAMETER (2.8 METER) HYDROGEN TANK

Test Facility Descriptions

The major component of the test apparatus is an elliptical liquid hydrogen tank having major and minor diameters of 110 inch (2.8m) and 77.5 inch (1.97m) re-

Table 10

41.5 INCH (1.05 M) TANK-SIDE MOUNT TEST CONDITIONS

Run No.	Nominal Vent Flow(3)	Nominal Ullage Volume(1)	Nominal Mixer Flow(2)	Nominal Tank Pressure psia (N/m^2)	Comments
1	-	1	-	17 (11.7)	Establish equilibrium conditions, at 17 psia and determine dp/dθ.
2	1	1	1	17	Operate TCU after equilibrium at 17 psia is established. Run time shall be of sufficient duration to establish decay rate at each condition.
3	2	1	1	17	
4	1	1	2	17	
5	2	1	2	17	
6	1	1	3	17	
7	2	1	3	17	
8	-	1	-	17-28 (11.7-19.3)	Establish tank equilibrium at 17 psia. Pressurize to 28 psia with GH_2 at 140 R and establish pressure-time relation until dp/dθ 0.
9	-	1	2	17-28	Vent from final pressure of run 8 to 17 psia and equalize tank conditions. Then pressurize to 28 psia with GH_2 at 140 R and establish pressure-time relation with mixer on until dp/dθ 0.
10	-	1	3	17-28	Repeat run 9 with mixer speed 3.
11	1	1	2	17-28	Vent from final pressure on run 10 to 17 psia and equalize tank. Pressurize to 28 psia with GH_2 at 140 R and operate TCU to establish decay rate at each condition.
12	2	1	2	17-28	
13	1	1	3	17-28	
14	2	1	3	17-28	

Table 10(Cont'd.)

Run No.	Nominal Vent Flow(3)	Nominal Ullage Volume(1)	Nominal Mixer Flow(2)	Nominal Tank Pressure psia (N/m^2)	Comments
15	-	1	-	17-28 (11.7-19.3)	Establish equilibrium at 17 psia. Pressurize to 28 psia with 530 R GH_2 and establish pressure-time relation until dp/dθ 0.
16	-	1	1	17-28	Vent from final pressure of run 16 to 17 psia and equalize tank conditions. Then pressurize to 28 psia with 530 R GH_2 and establish pressure-time relation with mixer on until dp/dθ 0. Mixer speed 1.
17	-	1	2	17-28	Repeat data pt 19 with mixer speed 2.
18	-	1	3	17-28	Repeat data pt 19 with mixer speed 3.
19	1	1	1	17-28	Vent from final pressure on run 21 to 17 psia and equalize tank. Pressurize to 28 psia with GH_2 at 530 R and operate TCU to establish decay rate.
20	2	1	1	17-28	
21	1	1	2	17-28	
22	2	1	2	17-28	
23	1	1	3	17-28	
24	2	1	3	17-28	
25	2	1	2	17	Establish equilibrium at 17 psia. Place TCU on automatic operation. Hold tank at 17 psia and demonstrate cycling capability. Coldside valve position and mixer speed to be selected.

Table 10(Cont'd.)

Run No.	Nominal Vent Flow (3)	Nominal Ullage Volume (1)	Nominal Mixer Flow (2)	Nominal Tank Pressure psia (N/m^2)	Comments
26-35	-	1	-	17-28 (11.7-19.3)10^4	Repeat data 15-24 using He as pressurant
36-69	-	2	-	-	Repeat runs 1-35 with liquid level No. 2

(1) Nominal Ullage Volume: 1 - 5 percent
2- 25 percent

(2) Nominal Mixer Flow: 1 - 3.5 cfm (100 l/m)
2 - 5.3 cfm (150 l/m)
3 - 2.5 cfm (71 l/m)

(3) Nominal Vent Flow: 1 - 1.2 lb./hr. (525 gr./hr.)
2 - 2.5 lb./hr. (1130 gr./hr.)

spectively. The tank is supported within a box frame (Fig. 31) by eight fiberglass struts attached to the tank Y-ring at four locations. All penetrations, with the exception of a 3-inch (.076m) diameter fill and drain line, go through a 24-inch (0.79m) access lid at the top of the tank.

The tank is insulated with 100 layers of double aluminized Mylar separated with Tissuglass spacers. To facilitate entry into the tank and minimize turnaround time between tests, a fiberglass bubble was placed over the access cover to support the top portion of the insulation which is separated from the rest of the tank insulation with a butt joint. Thus, the bubble and tank access cover can be removed without disturbing the major portion of the thermal protection system. Internally, the tank is equipped with 3 ring baffles; one is located at the tank equator, the other two are located 16 inches (0.4m) below and 11 inches (0.28m) above the equatorial baffle. A plate baffle is located over the fill and drain port which is offset 6.75 inches (0.171m) and oriented 5 degrees to the tank centerline.

Test plans for the tank included provision for television coverage of the fluid circulation in the tank. Figure 31 indicates the camera installation that was used to minimize heat input to the propellant and freezing of the camera. A hole was cut in the fiberglass dome cover and an inverted cone was installed between the cover and the camera port to serve as a well for the camera. This inverted cone was insulated in the manner illustrated in Fig. 31, which exposed the large lateral surface of the camera to the warm ambient environment rather than to the cold hydrogen tank. The camera was suspended from a beam attached to the tank support structure, so as not to contact the tank and provide a direct conduction heat path. The camera port was designed with a double O-ring seal between the glass window and the Conoseal flange. The Kel-F81 O-rings were sandwiched between two layers of indium-foil. This "sandwich" concept was found to provide excellent sealing characteristics at cryogenic temperatures. A lens train was assembled internally to the port to increase the camera field of view. This is also shown in Fig. 31. Light sources were placed at several positions in the tank to provide redundancy, and maximum flexibility. Two twelve volt incandescent lamps were placed on opposite sides of the tank just below the center baffle. An additional lamp, with a reflective backing shield, was positioned on the inside of the tank lid. Also, a lighting port was designed

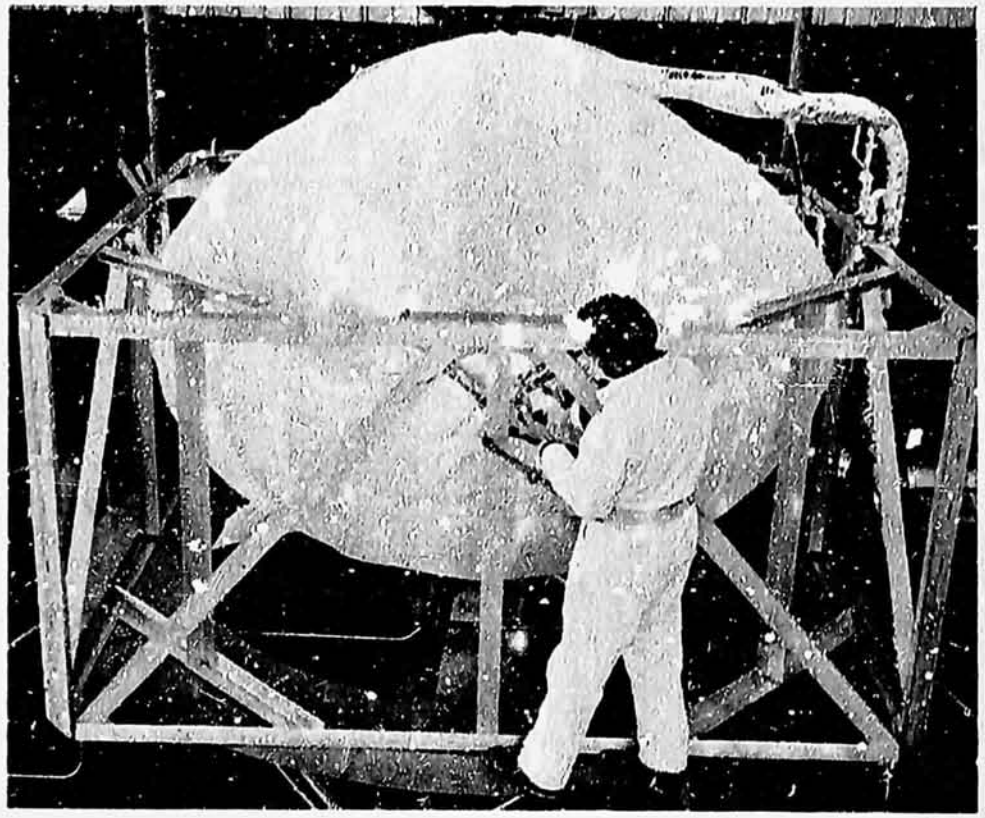

(a) Tank & Support Structure

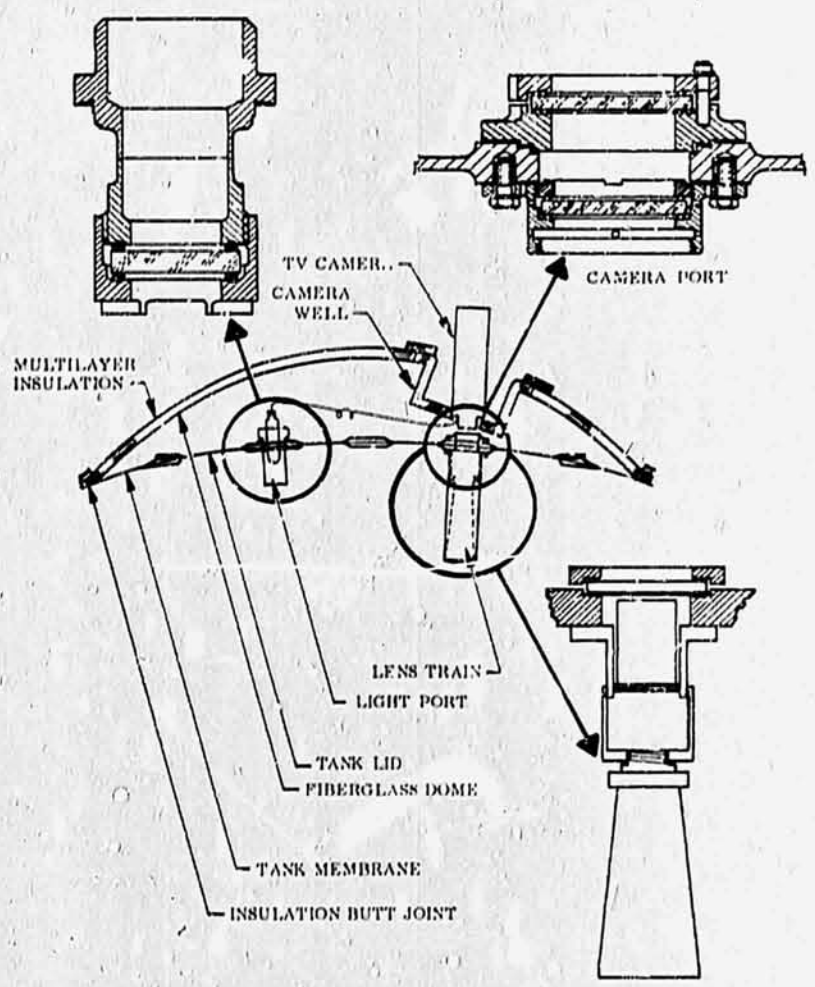

(b) Dome Modification for

Figure 31 - 110 Inch-Diameter (2.8 Meter) Liquid Hydrogen Tank Test Apparatus

to fit in one of the connector ports in the tank lid, and provide for an external light source. A 250 watt Sylvania Sun Gun lamp, which sets down in the well of the light port, was intended as the primary light source.

The instrumentation previously used in the 41.5 inch-diameter (1.05m) tank was also used in the 110 inch (2.8m) tank program. However, because of the size, and the peculiarities of the extra installation configurations, some additional instruments were employed. Table 11 identifies the instrumentation and Fig. 32 shows the locations within the tank.

In the upper portion of the tank, liquid level was indicated with either an optical or hot wire sensor. One of each was also used under the vapor traps to assure that vapor was contained when desired. In the lower part of the tank, hot wire sensors were used at the test liquid levels. These were backed up with a capacitance probe to provide a continuous liquid level indication, whereas the sensors were point indicators. The continuous measurement was desirable in the lower portion of the tank because the pressure response is much more sensitive to incremental changes in liquid level.

Propellant temperatures were measured with 6 platinum resistance thermometers (RTB's) and 8 Cu-Cn thermocouples. The latter were referenced to RTB-1, which is the platinum thermometer nearest the bottom of the tank.

Bottom Mount Configuration

For the first series of tests in the 110 inch (2.8m) tank, the TCU was supported off the fill baffle as illustrated schematically in Fig. 32. The angle of the fill baffle and its displacement from the centerline was offset by cutting three tubular spacers to different lengths and mitering the ends. The TCU base plate and the fill baffle were bolted together through these spacers. The mixer discharge was located approximately 8 inches (0.2m) below the tank mid-plane and 36 inches (0.91m) below the maximum liquid level. It was directed vertically towards the top of the tank. The expansion unit was removed from the TCU base plate and placed on the fill baffle, approximately 5 inches (0.13m) below the heat exchanger. This was to accommodate test conditions requiring liquid on the vent side at the expansion unit inlet with the heat exchanger immersed in gas. Fig. 33 is a photograph of this installation as seen looking down through the tank lid.

TABLE 11

INSTRUMENTATION SCHEDULE
110 inch (2.8 m) DIAMETER TANK

INSTRUMENTATION SCHEDULE

110 INCH (2.8 METER) DIAMETER TANK

SET-UP		DATA ACQUISITION		SENSOR				
Function	Code	Dynec Channel No.	Strip Chart No.	Manufacturing	Mode	S/N	Range	Accuracy
Press. Tank Ullage #1	PTU-1	141	1-1	C.E.C.	4-356-0138	T4077	0 - 50 PSIA	±0.5 PSIA
Press. Tank Ullage #2	PTU-2	142	1-2	Statham	PA285TC	25265	0 - 50 PSIA	±0.5 PSIA
Press. Coldside Inlet	PCi	143	2-1	C.E.C.	4-356-0138	T4076	0 - 20 PSIA	±0.5 PSIA
Press. Solenoid Valve Vent #1	PV-1	144	2-2	C.E.C.	4-356-0138	T3683	0 - 20 PSIA	±0.5 PSIA
Press. Solenoid Valve Vent #2	PV-2	145		Statham	PA203TC	1991	0 - 25 PSIA	±0.5 PSIA
Boiloff Flow	FB	146	3-1	Rosemount	12AAD-1018S	92	0 - 1.2#/hr.	±0.05#/hr.
Flow Rate Warmside	FW	147	4-1	Potter	2" 66101A	LX-2-17	0 - 25 CFM	±0.3 CFM
Flow Rate Coldside	FC	148	4-2	Hastings	AHL-25X	11	0 - 7#/hr.	±0.3#/hr.
Fan Speed	NF	149	3-2	Fisher & Porter	9667B 016V01			
Motor Power	MP	150		Scientific Columbus	1332B	798		Unknown
Press. Switch Trace	PS	151						
Solenoid Valve #1 Volts	SE-1	152	5-1				0 - 20 VDC	
Solenoid Valve #2 Volts	SE-2	153	6-1				0 - 20 VDC	
Solenoid Valve #1 Current	SI-1	154	5-2				0 - 1.0 Amps	
Solenoid Valve #2 Current	SI-2	155	6-2				0 - 1.0 Amps	
Optical Level Sensor #1	OS-1	156		Bendix	GL-103			0.06"
Optical Level Sensor #2	OS-2	157		Bendix	GL-103			0.06"
Hot Wire Level Sensor #1	HS-1	158		United Control	2641-1-1			0.06"
Hot Wire Level Sensor #2	HS-2	159		United Control	2641-1-1			0.06"
Hot Wire Level Sensor #3	HS-3	160		United Control	2641-1-1			0.06"
Hot Wire Level Sensor #4	HS-4	161		United Control	2641-1-1			0.06"
Temp. Coldside Inlet	TCi	162		Cryo. Cal Inc.	CR2500L 14-100	1306	36°R to 60°R	0.1°R @ LH_2 Temp.
Temp. Coldside Outlet	TCo	163		Cryo. Cal Inc.	CR2500L 14-100	1267	36°R to 60°R	0.1°R @ LH_2 Temp.
Temp. Warmside Inlet	TWi	164		Cryo. Cal Inc.	CR2500L 14-100	1325	36°R to 60°R	0.1°R @ LH_2 Temp.
Temp. Warmside Outlet	TWo	165		Cryo. Cal Inc.	CR2500L 14-100	1411	36°R to 60°R	0.1°R @ LH_2 Temp.
GRT's Excitation	VE	166						
Temp. Bulk #1 (RTB)	TB-1	167		Rosemount	150MA10	7653	30°R to 490°R	±0.6°R @ LH_2 Temp.
Temp. Bulk #2 (T/C)	TB-2	168			Cu/Cn		30°R to 490°R	±2°R
Temp. Bulk #3 (RTB)	TB-3	169		Rosemount	150MA10	7654	30°R to 490°R	±0.6°R @ LH_2 Temp.
Temp. Bulk #4 (T/C)	TB-4	170			Cu/Cn		30°R to 490°R	±2°R
Temp. Bulk #5 (T/C)	TB-5	171			Cu/Cn		30°R to 490°R	±2°R
Temp. Bulk #6 (RTB)	TB-6	172		Rosemount	150MA10	7655	30°R to 490°R	±0.6°R @ LH_2 Temp.
Temp. Bulk #7 (T/C)	TB-7	173			Cu/Cn		30°R to 490°R	±2°R
Temp. Bulk #8 (T/C	TB-8	174			Cu/Cn		30°R to 490°R	±2°R
Temp. Bulk #9 (RTB)	TB-9	175		Rosemount	150MA10	7656	30°R to 490°R	±0.6°R @ LH_2 Temp.
Temp. Bulk #10 (T/C)	TB-10	176			Cu/Cn		30°R to 490°R	±2°R
Temp. Bulk #11 (T/C)	TB-11	177			Cu/Cn		30°R to 490°R	±2°R
Temp. Bulk #12 (RTB)	TB-12	178		Rosemount	150MA10	7657	30°R to 490°R	±0.6°R @ LH_2 Temp.
Temp. Bulk #13 (T/C)	TB-13	179			Cu/Cn		30°R to 490°R	±2°R
Temp. Bulk #14 (RTB)	TB-14	180		Rosemount	150MA10	7658	30°R to 490°R	±0.6°R @ LH_2 Temp
Temp. Bulk Reference	TBR	181			Cu/Cn		30°R to 490°R	±2°R
Temp. LH_2 Bleed	TLH_2E	182		Winsco	2448	146	30°R to 490°R	Unknown
Press. Coldside Inlet	PCi-1	183		C.E.C.	4-354-0131	T3682	0 - 20 PSIA	±0.5 PSIA
Press. Vacuum Chamber	PC (T/C)	184		Fredricks	3A	2365	10^{-6} to 10^{-3} torr	
Press. Vacuum Chamber	PC (Ion)	185		Fredricks	3A	2365	10^{-6} to 10^{-3} torr	
Capacitance Level Sensor	CS-1	186		Lockheed				

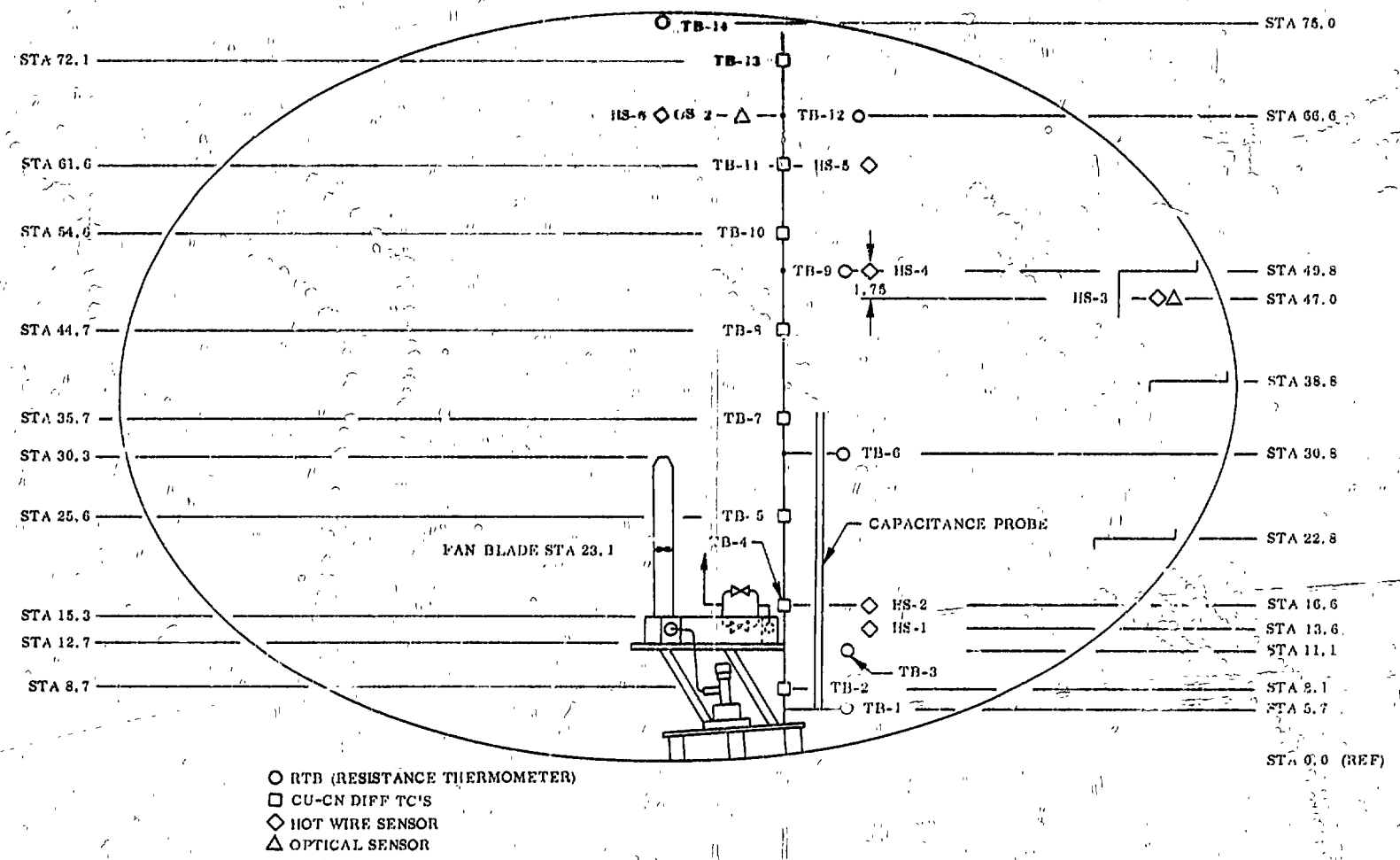

Figure 32 Installation Configuration and Instrumentation Locations for Bottom Mount Tests - 110 inch (2.8m) Diameter Tank

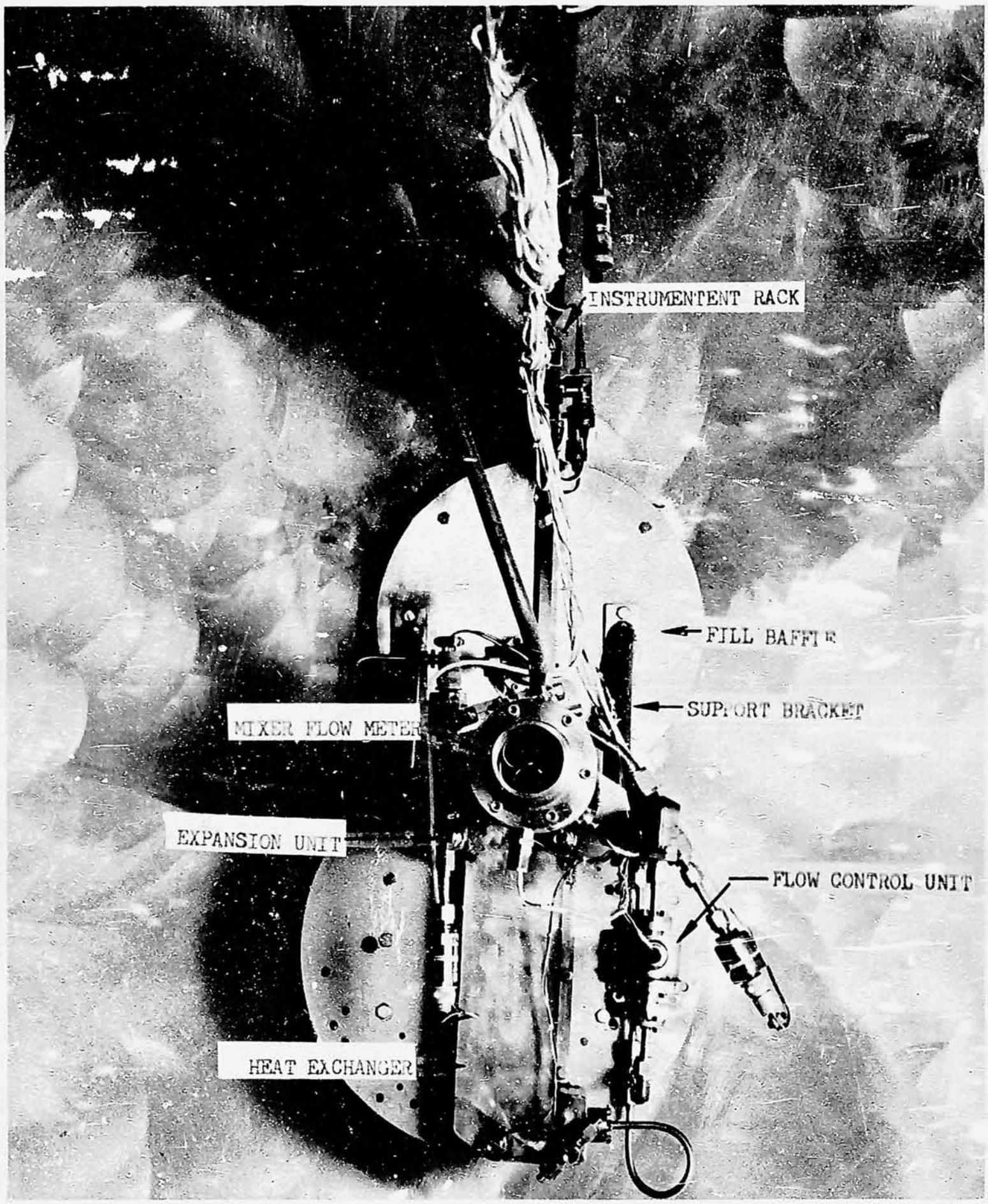

Figure 33 - Bottom Mount Installation As Viewed Through The Access Opening of the 110 Inch-Diameter (2.8 Meter) Tank

Side Mount Configuration

For the side mount test series, the TCU was supported off the center and upper baffles and the mixer discharges parallel with, and 5 inches (0.13m) above the equatorial plane. The nozzle was approximately 24 inches (0.61m) from the center of the tank, and 22 inches (0.56m) below the maximum liquid level. This is the same position that was used in NAS 3-7942 and is illustrated in Fig. 34 Fig. 35 is a photograph taken in the tank.

Side Mount - Configuration B

The tests with this and the subsequent configuration required the capability to trap vapor underneath the top baffle to simulate the condition of an ullage bubble trapped in the vicinity of the liquid discharge from the TCU mixer. This cooled liquid would then circulate past the ullage bubble extracting heat and thereby controlling the tank pressure. The vapor trap configuration is illustrated in Fig. 36. A series of 12 separate boxes were attached to the upper ring baffle. The boxes were welded from 6061 aluminum sheet to form a sealed unit except for the one open face. These individual traps were manifolded together so the liquid-gas interface would be at a uniform level.

A bleed line from the manifold was brought out of the tank so the baffle region could be exhausted of vapor for those tests not requiring that it be trapped. This same line was used to pressurize the tank for a few tests to compare rates when the tank is pressurized through the liquid with those obtained by pressurizing the ullage.

The TCU location was the same as for the side mounted tests. However, the mixer inlet and outlet were modified to place the suction and discharge near the tank wall at diametrically opposite points, under the vapor traps. The intent was to induce more complete circumferential circulation, particularly in the baffle region. The opposite ends of this installation are shown in the photographs of Fig. 37a and 37b. Fig. 38 is a schematic illustrating the hood used to modify the inlet.

Side Mount - Configuration C

This installation involved only one modification to Configuration B. A radial flow (relative to the mixer discharge tube) nozzle was added to the end of the

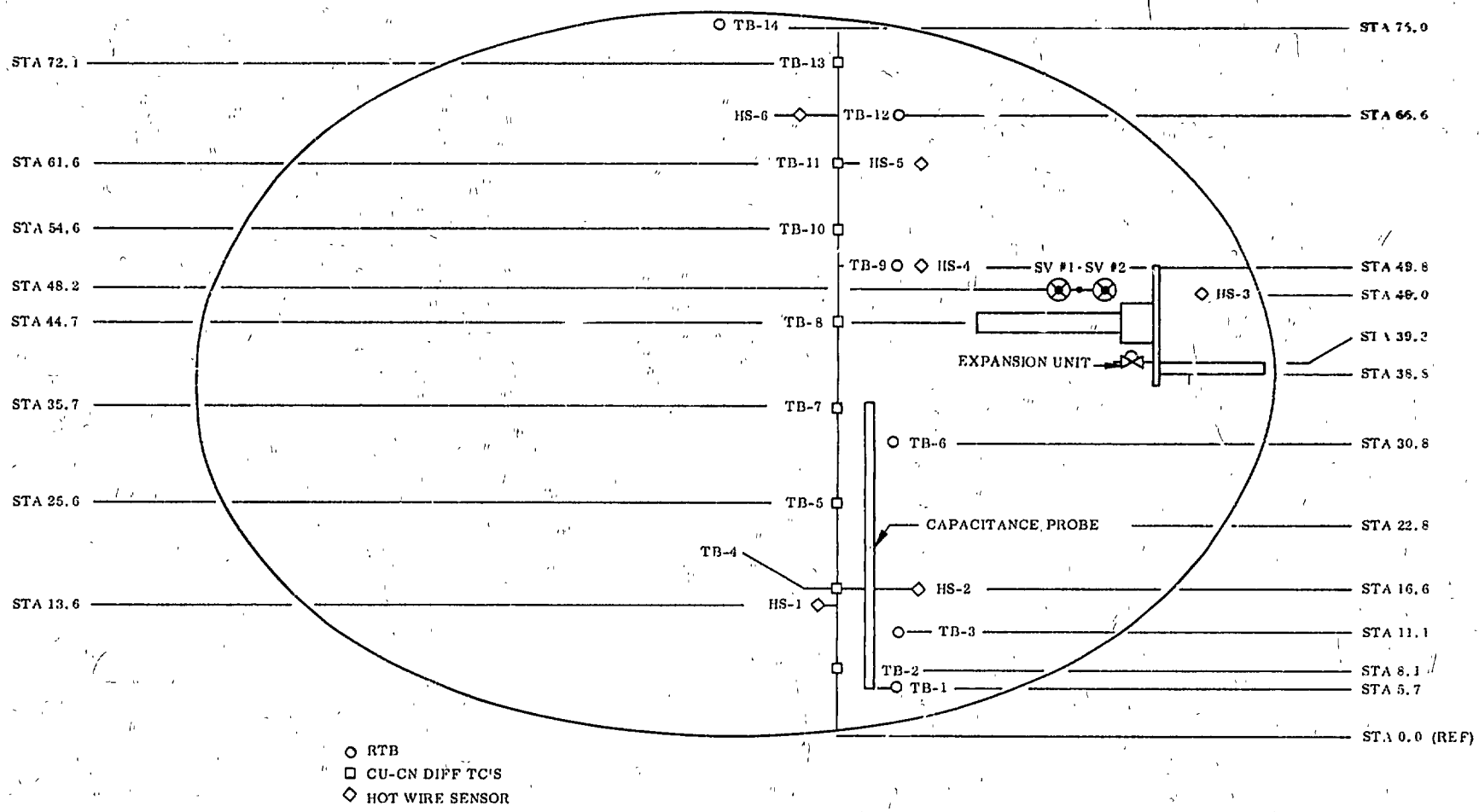

Figure 34 Installation Schematic For Side Mount Tests - 110 inch (2.8m) Tank

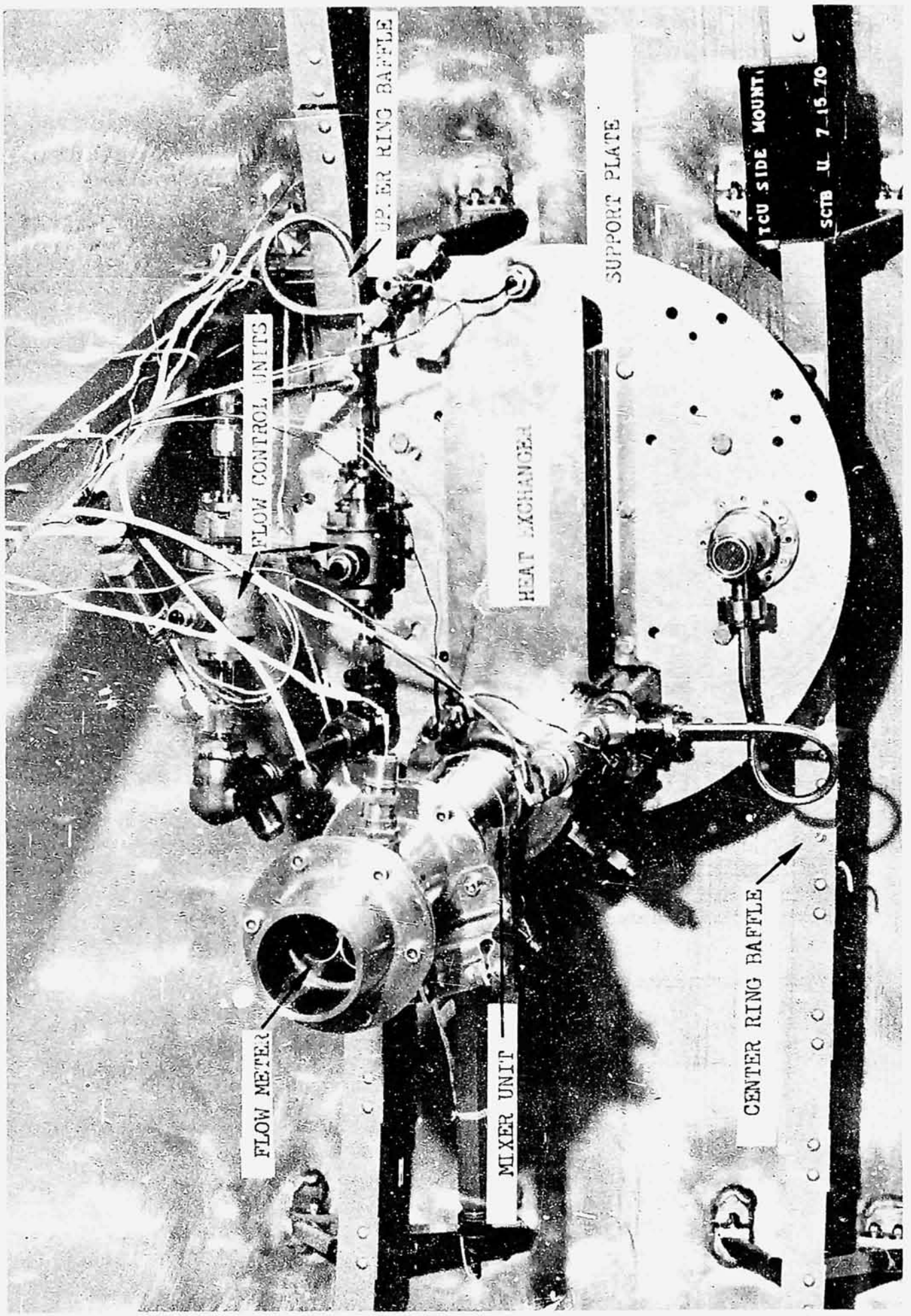

Figure 35 - Side Mounted Configuration A In The 110 Inch-Diameter (2.8 Meter) Tank

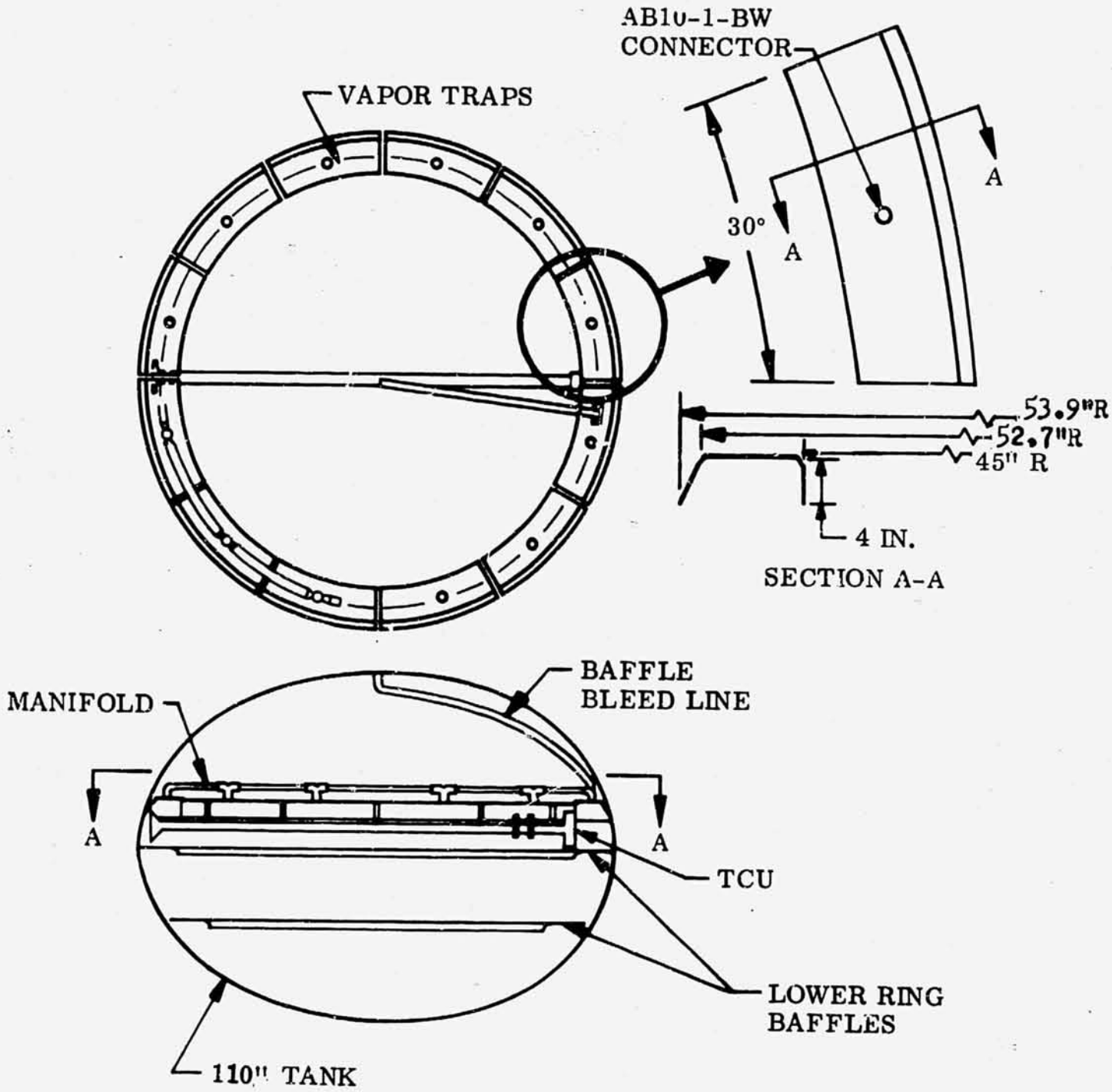

Figure 36 Vapor Trap Configuration for The 110 inch (2.8m) Tank

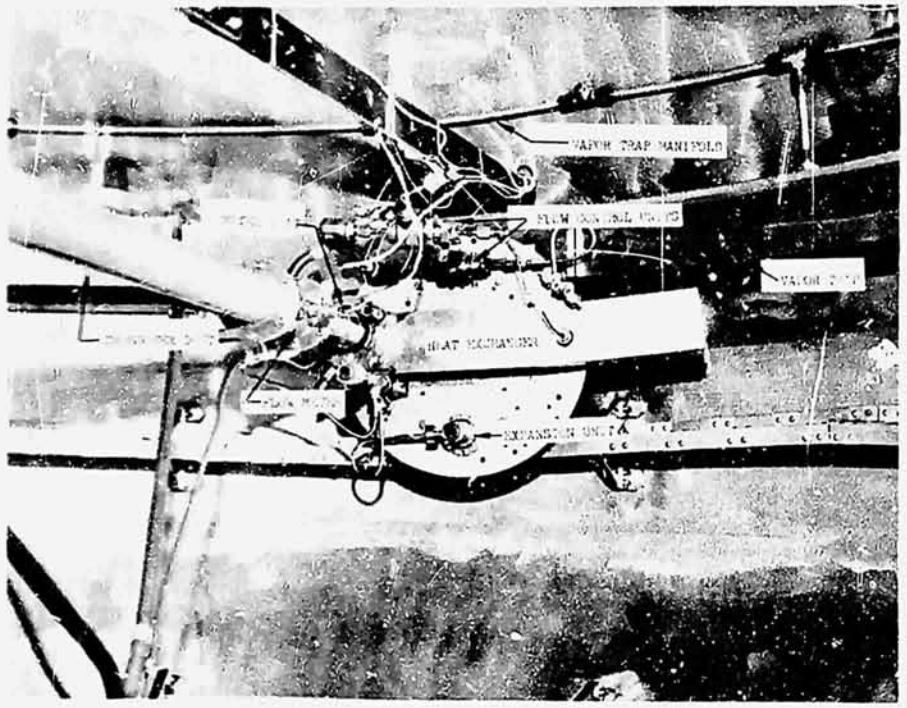

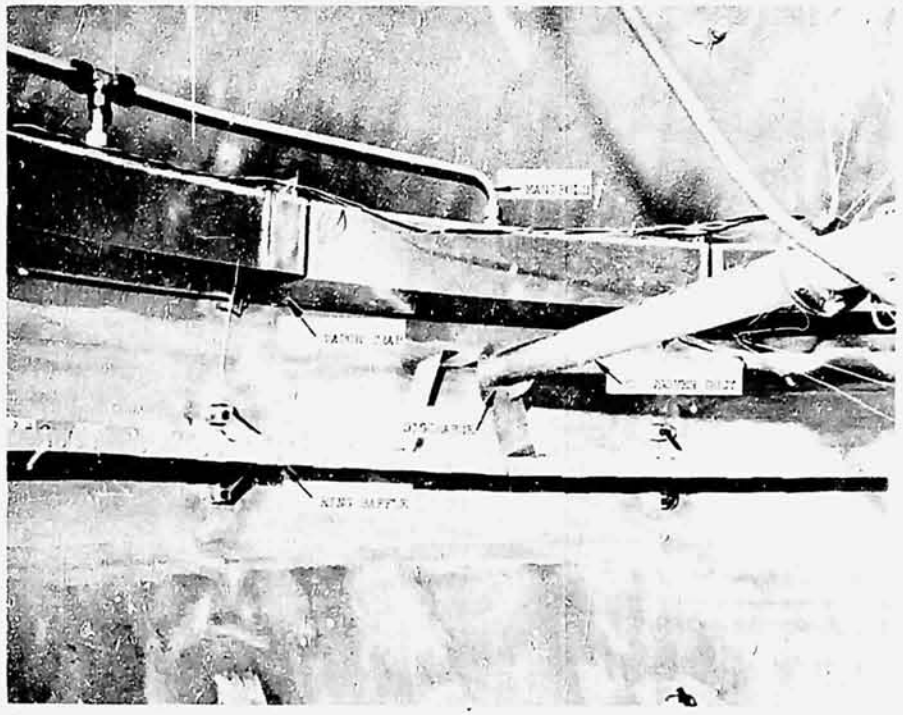

Figure 37 - Side Mount Configuration B as Viewed From Inside Tank
(a) Inlet (b) Discharge

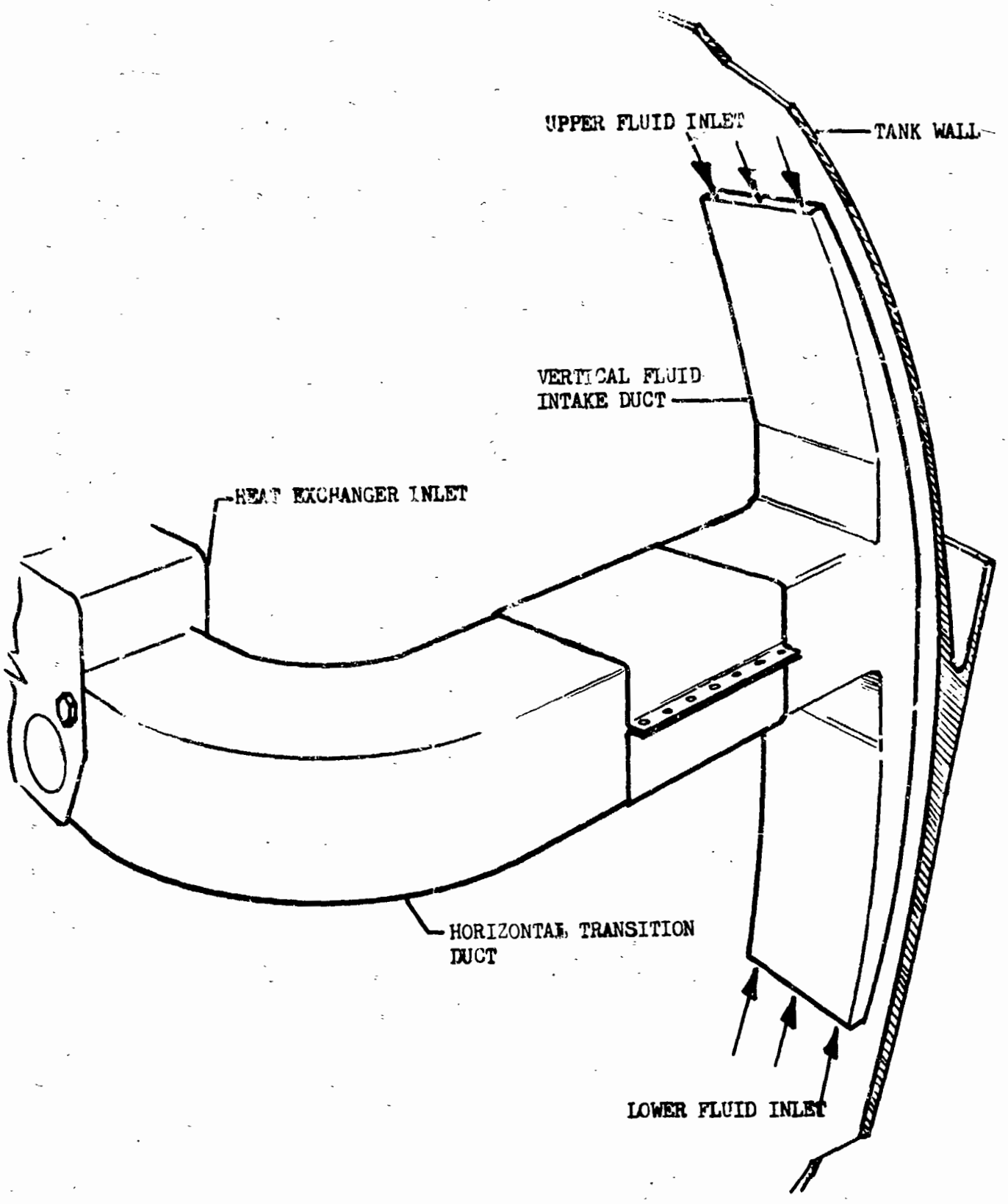

Figure 38 Heat Exchanger Inlet Adapter For Configuration C

crossover duct which was designed to create a wall bound jet tangent to the tank wall in all directions. The flow area was the same as for the 1.75 inch (0.044m) diameter nozzle used in all previous tests. Fig. 39 illustrates this installation as well as the additional instrumentation under the traps for configurations B and C.

TEST OPERATIONS

Bottom Mount Configuration

The pretest activities and the operational sequence for any particular test was the same as previously described for the 41.5 inch (1.05m) tank. The test conditions are delineated in Tables 12 and 13, which includes 196 tests with an ambient boundary and 31 tests with the space simulator's liquid nitrogen cold wall in operation to determine the influence propellant heating rate has on the system performance.

The first 36 tests were successfully completed, although it was noted that both the vent side flow rate and heat exchanger pressure (expansion unit discharge pressure) were lower for runs 34-36. The tank pressure response appeared to be satisfactory, and in accordance with the reduced flow rates. However, when the thermal conditioning system was turned on to start Run No. 37, the vent side flow rate surged and then fell quickly to zero, indicating that the expansion unit had apparently failed in the closed position. After the liquid hydrogen was drained, and the tank warmed up a few degrees, the TCU was activated and the expansion unit appeared to be working properly. Enough liquid was returned to the tank to immerse the unit and it was again activated. Again, the expansion unit failed to regulate, but this time it appeared to fail open as indicated by the high flow rates (9 lbs/hr 4 Kg/hr). A replacement bellows which had been ordered previously for the expansion unit was enroute from the vendor. However, rather than shut down prematurely and wait for the new bellows, it was decided to complete those tests requiring only mixing, or no mixing at all, as called for in Table 12 (i.e., runs 39-42, 50-53, 60-63, 77-80, 87-90, 97-100, 107-110, 124-127, 134-137, 144-147, 154-157, 164-167, 174-177).

At the conclusion of the self-pressurization and mixing tests, the tank was opened up and the expansion unit was removed with the intention of replacing the bellows. However, the replacement bellows would not function when checked

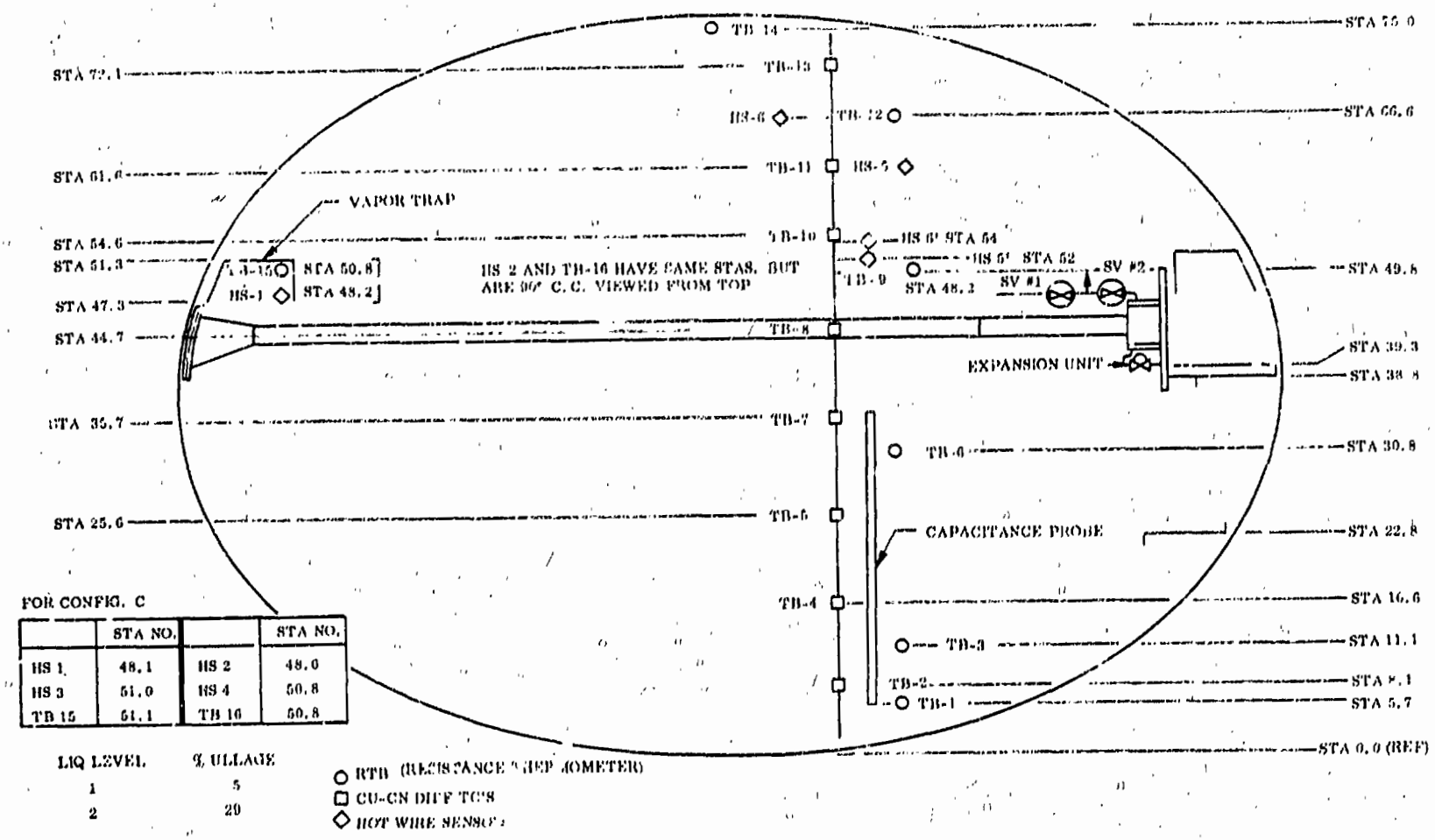

Figure 39 Installation Configuration and Instrumentation Locations for Side Mount Tests - Configuration C

TABLE 12

110-INCH DIAMETER (2.8m) TANK BOTTOM MOUNT CONFIGURATION AMBIENT BOUNDARY CONDITIONS

Run No.	Nominal Vent Flow(3)	Nominal Ullage Volume(1)	Nominal Mixer Flow(2)	Nominal Tank Pressure psia*	Comments
1	-	1	-	17 (11.7)	Establish equilibrium conditions, at 17 psia and determine dp/dΘ.
2	1	1	1	17	Operate TCU after equilibrium at 17 psia is established. Run time shall be of sufficient duration to establish decay rate at each condition.
3	2	1	1	17	
4	1	1	2	17	
5	2	1	2	17	
6	1	1	3	17	
7	2	1	3	17	
8	-	1	-	17-28 (11.7-19.3)	Establish tank equilibrium at 17 psia. Pressurize to 28 psia with GH_2 at 140°R and establish pressure-time relation until dp/dΘ = 0.
9	-	1	1	17-28 (11.7-19.3)	Vent from final pressure of run 8 to 17 psia and equalize tank conditions. Then pressurize to 28 psia with GH_2 at 140°R and establish pressure-time relation with mixer on until dp/dΘ = 0.
10	-	1	2	17-28	Repeat run 9 with mixer speed 2.
11	-	1	3	17-28	Repeat run 9 with mixer speed 3.

* Numbers in parentheses are $(N/m^2) \times 10^{-4}$

Table 12 (Cont.)

Run No.	Nominal Vent Flow(3)	Nominal Ullage Volume(1)	Nominal Mixer Flow(2)	Nominal Tank Pressure psia	Comments
12	1	1	1	17-28	Vent from final pressure on run 11 to 17 psia and equalize tank. Pressurize to 28 psia with GH_2 at $140^\circ R$ and operate TCU to establish decay rate at each condition.
13	2	1	1	17-28	
14	1	1	2	17-28	
15	2	1	2	17-28	
16	1	1	3	17-28	
17	2	1	3	17-28	
18	-	1	-	17-28 (11.7-19.3)	Establish equilibrium at 17 psia. Pressurize to 28 psia with $530^\circ R$ GH_2 and establish pressure-time relation until $dp/d\theta = 0$.
19	-	1	1	17-28	Vent from final pressure of run 18 to 17 psia and equalize tank conditions. Then pressurize to 28 psia with $530^\circ R$ GH_2 and establish pressure-time relation with mixer on until $dp/d\theta$ 0. Mixer speed 1.
20	-	1	2	17-28	Repeat data pt 19 with mixer speed 2.
21	-	1	3	17-28	Repeat data pt 19 with mixer speed 3.
22	1	1	1	17-28	Vent from final pressure on run 21 to 17 psia and equalize tank. Pressurize to 28 psia with GH_2 at $530^\circ R$ and operate TCU to establish decay rate.
23	2	1	1	17-28	
24	1	1	2	17-28	
25	2	1	2	17-28	
26	1	1	3	17-28	
27	2	1	3	17-28	

Table 12 (Cont.)

Run No.	Nominal Vent Flow(3)	Nominal Ullage Volume(1)	Nominal Mixer Flow(2)	Nominal Tank Pressure psia	Comments
28	-	1	0	17	Establish equilibrium at 17 psia. Place TCU on automatic operation. Hold tank at 17 psia and demonstrate cycling capability. Coldside valve position and mixer speed to be selected.
29-48	-	1	-	17-28	Repeat data 8-27 using He as pressurant.
49	-	1	-	17-28 (11.7-19.3)	Establish equilibrium at 17 psia. Pressurize to 28 psia with He at 140° R Place TCU on automatic operation for tank pressure of 17 psia. Operate TCU and demonstrate cycling. Cold-side valve position and mixer speed to be selected.
50-69	-	1	-	17-36 (11.7-24.8)	Repeat runs 18-27 and 40-49 at tank pressure of 36 psia.
70-96	-	2	-	17-28 (11.7-19.3	Repeat run 1-27 with liquid level No. 2
97-116	-	2	-	17-28	Repeat runs 8-27 using He as pressurant.
117-183	-	3	-	-	Repeat runs 1-27, 29-48, and 50-69 with liquid level No. 3.

Table 12 (Cont.)

Run No.	Nominal Vent Flow(3)	Nominal Ullage Volume(1)	Nominal Mixer Flow(2)	Nominal Tank Pressure psia	
184	1	4	1	28	Drain tanks to uncover warm side inlet. Pressurize to 28 psia with GH_2 at 140 R Operate TCU.
185	2	4	1	28	
186	1	4	2	28	
187	2	4	2	28	
188	1	4	3	28	
189	2	4	3	28	
190 196	-	1	-	36 (24.8)	Fill to liquid level No. 1 and establish equilibrium at 36 psia. Repeat runs 1-7

(1) Nominal Ullage Volume: 1 - 5 percent
2 - 29 percent
3 - 70 percent
4 - 85 percent

(2) Nominal Mixer Flow: 1 - 5.3 cfm (150 ℓ/m)
2 - 3.5 cfm (100 ℓ/m)
3 - 2.5 cfm (71 ℓ/m)

(3) Nominal Vent Flow: 1 - 1.5 lb/hr. (682 gr/hr.)
2 - 2.5 lb/hr. (1130 gr/hr.)

Table 13

110-INCH-DIAMETER (2.8 METER) TANK-BOTTOM MOUNT CONFIGURATION-
LIQUID NITROGEN BOUNDARY CONDITIONS

Run No.	Nominal Vent(3) Flow	Nominal Ullage Volume (1)	Nominal Mixer Flow(2)	Nominal Tank Pressure psia*	Comments
2	—	1	—	17 (11.7)	Establish equilibrium conditions at 17 psia and determine $dp/d\theta$.
2	1	1	1	17	Establish equilibrium at 17 psia. Operate TCU to establish decay rate at each condition.
3	2	1	1	17	
4	1	1	2	17	
5	2	1	2	17	
6	1	1	3	17	
7	2	1	3	17	
8	—	2	—	17	Establish equilibrium conditions
9	1	2	1	17	Operate TCU after equilibrium is established at 17 psia.
10	2	2	1	17	
11	1	2	2	17	
12	2	2	2	17	
13	1	2	3	17	
14	2	2	3	17	
15	—	3	—	17	Establish equilibrium at 17 psia and determine $dp/d\theta$.
16	1	3	1	17	Operate TCU after equilibrium is established at 17 psia.
17	2	3	1	17	
18	1	3	2	17	
19	2	3	2	17	
20	1	3	3	17	
21	2	3	3	17	

* Numbers in parentheses are $(N/m^2)\ 10^{-4}$

Table 13(Cont.)

Run No.	Nominal Vent Flow Position	Nominal Ullage Volume	Nominal Mixer Flow	Nominal Tank Pressure psia	Comments
22	–	3	–	17-28 (11.7-19.3)	Pressurize to 28 psia with GH_2 at 140°R and establish $dp/d\theta$.
23	–	3	1	17-28	Vent to 17 psia and establish equilibrium. Pressurize to 28 psia with GH_2 at 140°R and establish $dp/d\theta$ at mixer speed 1.
24	–	3	2	17-28	Repeat run 23 with mixer speed 2.
25	–	3	3	17-28	Repeat run 23 with mixer speed 3.
26	1	3	1	17-28	Establish equilibrium at 17 psia. Pressurize to 28 psia with GH_2 at 140°R and operate TCU.
27	2	3	1	17-28	
28	1	3	2	17-28	
29	2	3	2	17-28	
30	1	3	3	17-28	
31	2	3	3	17-28	

(1) Same As Table 12
(2) Same As Table 12
(3) Same As Table 12

in liquid nitrogen. Deflection tests were conducted on the bellows that had been removed from the 110 inch diameter (2.8m) tank. These revealed no change in the characteristics from those obtained prior to its use in the TCU. Also, when the regulator was installed in the component test dewar it performed as well as it had earlier during the TCU tests. In fact, it was possible to induce a failure only by completely icing up the inlet to the regulator. Therefore, the regulator was reinstalled and the tests were continued. Only one other unscheduled shutdown occurred and that was due to helium that had an excess of air. Almost immediately after starting a series of runs utilizing helium pressurization, the vent flow rate dropped to zero, as though the regulator had failed closed. However, after warming up the facility, the unit appeared to regulate properly, and continued to so when liquid hydrogen was again introduced. A helium sample was taker from the pressurant supply for chemical analysis. The result showed air in excess of 0.5 percent where specification called for less than 0.05 percent. Therefore, it was concluded that the port iced up. Although the helium pressurant was out of spec. this does reflect the sensitivity of the system to contamination.

The contaminated supply was replaced with pressurizing helium which has a specification limiting air content to less than 0.005 percent. No further problems were encountered. In retrospect, it appears that one previous shutdown during the 41.5 inch (1.05m) tank program, attributed to the regulator irregularities was probably caused by helium contamination, as also was a temporary failure in the mixer speed sensor.

The tests were sequenced so that those groups utilizing helium pressurant came at the end of a given liquid level series. When liquid level was to be changed, the ullage was purged of helium by overfilling the tank until the liquid was detected in the vent stack. The tank was then drained back and adjusted at the proper liquid level. This procedure eliminated the possibility of distorting the comparison between GHe and GH_2 pressurization.

The bottom mount series with the ambient boundary temperature spanned a period of six work weeks. At the end of each week a partial shutdown procedure was

followed, wherein the tank was drained and purged with the warm gaseous hydrogen. The tank was left in a vented condition and the flight simulator was left in a pumped down condition. Each Monday morning, the tank and TCU were purged. Then the tank was filled and a boiloff test was conducted.

Side Mount Configuration

The test conditions for the side mounted series were delineated in Table 14 which includes 76 tests. The first eleven tests were conducted following the same procedures, as for the bottom mounted series. At the higher mixer speeds the data appeared to be consistent with that from the bottom mount. However, when the mixer flow was reduced to the intermediate flow (run 4), the tank pressure response became very sluggish. When the mixer flow was further reduced (e.g., run 6), there was no pressure control and the pressure continued to rise for seven hours. Runs 7A, 7B, 7C were then inserted into the test schedule, as repeats of runs 3, 5, and 7, but in reverse order, to confirm that the tank contents were not being sufficiently mixed at the lowest speeds.

Runs 9-11 were tests with mixing only, after pressurizing with hydrogen at 140°R (77°K). The tank was vented down to saturation conditions between each run. These tests further substantiated the lack of mixing and pressure control at low speeds and resulted in modification to the test program which originally was to duplicate the bottom mount series.

The test sequencing was altered so that all of the high mixer flow tests were conducted in order. After these were completed, some of the remaining tests with intermediate and low speeds were conducted with minor modification to the test procedures. Rather than vent down after each run, two tests were run after each pressurization, by simply switching vent rates (e.g., switching from one solenoid valve to the other). At the end of the second test, the mixer speed was increased to maximum flow to demonstrate mixing, before the tank was vented down to start the next sequence.

Side Mount - Configuration B

The intent of this test series was to simulate a possible low gravity condition where a vapor bubble is formed (or trapped) at a hot spot on the tank wall, and

to evaluate the ability of the TCU to control tank pressure under this simulated condition. To achieve this objective, a series of 34 tests was formulated. These are delineated in Table 15. For runs 1-17, hydrogen gas was bled into the traps until they were filled, as indicated by a sudden drop in the voltage output from the hot wire sensors (which extinguished visual indicators on the test console). Simultaneously, the ullage was vented, as required, to maintain the starting pressure in the range of 17-19 psia ($11.7\text{-}13.01 \times 10^4$ N/m^2). Thus, for these tests, there were two liquid vapor interfaces on which the circulating liquid could operate to control tank pressure. Runs 18-34 were intended to repeat runs 1-17 except that the vapor trap was bled down until it filled with liquid, thus providing only the primary ullage interface for pressure control. However, tests 21, 22, and 23 showed the same lack of mixing and pressure control, experienced with the other side mounted tests. Therefore, the remaining intermediate and low mixing speed tests were eliminated, and two additional ones (8A, 9A) were added. Test 8A was an attempt to compare the effect of pressurizing the tank through the vapor trap rather than through the top of the tank. There was no obviously significant effect; consequently, all pressurizing was done through the ullage to be consistent with all the other test configurations. In run 9A, ambient helium, rather than hydrogen gas, was bled into the vapor trap before the tank was pressurized.

Side Mount - Configuration C

The test profile for this configuration consisted of the 69 tests delineated in Table 16. The first 34 tests were identical to those for Configuration B, being conducted at 5 percent ullage. The next 34 repeated these with the ullage volume increased to 29 percent, which placed the liquid level approximately 2 inches (0.058m) above the radial nozzle. The last test was an automatic control test conducted with the high vent flow and the highest mixer flow rate.

Table 14

110-INCH DIAMETER (2.8m) TANK SIDE MOUNT CONFIGURATION
AMBIENT BOUNDARY CONDITIONS

Run No.	Nominal Vent(3) Flow	Nominal Ullage(1) Volume	Nominal Mixer(2) Flow	Nominal* Tank Pressure	Comments
1	-	1	-	17 (11.7)	Establish equilibrium conditions, at 17 psia and determine $dp/d\theta$.
2	1	1	1	17	Operate TCU after equilibrium at 17 psia is established. Run time shall be of sufficient duration to establish decay rate at each condition.
3	2	1	1	17	
4	1	1	2	17	
5	2	1	2	17	
6	1	1	3	17	
7	2	1	3	17	
7A	2	1	3	17	Repeat run 7
7B	2	1	2	17	Repeat run 5
7C	2	1	1	17	Repeat run 3
8	-	1	-	17-28 (11.7-19.3)	Establish tank equilibrium at 17 psia. Pressurize to 23 psia with GH_2 at 140°R and establish pressure-time relation until $dp/d\theta = 0$.
9	-	1	1	17-28 (11.7-19.3)	Vent from final pressure of run 8 to 17 psia and equalize tank conditions. Then pressurize to 28 psia with GH_2 at 140°R and establish pressure-time relation with mixer on until $dp/d\theta = 0$.
10	-	1	2	17-28	Repeat run 9 with mixer speed 2.

* Numbers in parentheses are in (Newtons per sq. meter) 10^{-4}

Table 14 (Cont'd)

Run No.	Nominal Vent(3) Flow	Nominal Ullage(1) Volume	Nominal Mixer(2) Flow	Nominal Tank Pressure	Comments
11	-	1	3	17-28 (11.7-19.3)	Repeat run 9 with mixer speed 3.
12	1	1	1	17-28	Vent from final pressure on run 11 to 17 psia and equalize tank. Pressurize to 28 psia with GH_2 at 140°R and operate TCU to establish decay rate at each condition.
13	2	1	1	17-28	
18	-	1	-	17-28 (11.7-19.3)	Establish equilibrium at 17 psia. Pressurize to 28 psia with 530°R GH_2 and establish pressure-time relation until $dp/d\theta = 0$.
19	-	1	1	17-28	Vent from final pressure of run 18 to 17 psia and equalize tank conditions. Then pressurize to 28 psia with 530°R GH_2 and establish pressure-time relation with mixer on until $dp/d\theta = 0$. Mixer speed 1.
20	-	1	2	17-28	Do after No. 21 without repressurizing.
21	-	1	3	17-28	Repeat data pt 19 with mixer speed 3.
22	1	1	1	17-28	Vent from final pressure on run 21 to 17 psia and equalize tank. Pressurize to
23	2	1	1	17-28	
24	1	1	2	17-28	

Table 14 (Cont'd)

Run No.	Nominal Vent(3) Flow	Nominal Ullage(1) Volume	Nominal Mixer(2) Flow	Nominal Tank Pressure psia	Comments
25	2	1	2	17-28	28 psia with GH_2 at $530^{\circ}R$ and operate TCU to establish decay rate. Tests 25, 27 follow 24 and 26 without repressurizing.
26	1	1	3	17-28	
27	2	1	3	17-28	
28	2	1	1	17	Establish equilibrium at 17 psia. Place TCU on automatic operation. Hold tank at 17 psia and demonstrate cycling capability. Set for maximum vent and mixer flow rates.
29	-	1	-	17-28 (11.7-19.3)	Establish tank equilibrium at 17 psia. Pressurize to 28 psia with GH_e at $140^{\circ}R$ and establish pressure-time relation until $dp/d\theta = 0$.
30	-	1	1	17-28	Vent from final pressure of run 8 to 17 psia and equalize tank conditions. Then pressurize to 28 psia with GH_e at $140^{\circ}R$ and establish pressure-time relation with mixer on until $dp/d\theta = 0$.
33	1	1	1	17-28	Vent from final pressure on run 11 to 17 psia and equalize tank. Pressurize to 28 psia with GH_2 at
34	2	1	1	17-28	

Table 14 (Cont'd)

Run No.	Nominal Vent(3) Flow	Nominal Ullage(1) Volume	Nominal Mixer(2) Flow	Nominal Tank Pressure psia	Comments
					140°R and operate TCU to establish decay rate at each condition.
39	-	1	-	17-28	Repeat 29, 30, 33, 34 using ambient GH_e.
40	-	1	1	17-28	
43	1	1	1	17-28	
44	2	1	1	17-28	
49	2	1	1	17-28 (11.7-19.3)	Establish equilibrium at 17 psia. Pressurize to 28 psia with He at 140°R Place TCU on automatic operation for tank pressure of 17 psia. Operate TCU and demonstrate cycling. Set for maximum vent and mixer flows.
50	-	1	-	17-36 (11.7-25)10^4	Establish equilibrium at 17 psia. Pressurize to 36 psia with 530°R GH_2 and establish pressure-time relation until $dp/d\theta = 0$.
51	-	1	1	17-36	Vent from final pressure of run 50 to 17 psia and equalize tank conditions. Then pressurize to 36 psia with 530°R GH_2 and establish pressure-time relation with mixer on until $dp/d\theta = 0$. Mixer speed 1.

Table 14 (Cont'd)

Run No.	Nominal Vent(3) Flow	Nominal Ullage(1) Volume	Nominal Mixer(2) Flow	Nominal Tank Pressure psia	Comments
54	1	1	1	17-36	Vent from final pressure on run 21 to 17 psia and equalize tank. Pressurize to 28 psia with GH_2 at 530°R and operate TCU to establish decay rate.
55	2	1	1	17-36 (11.7-29)	
60	-	1	-	17-36	Repeat 50, 51 using 530°R GHe.
61	-	1	1	17-36	
64	1	1	1	17-36	Vent from final pressure on run 61 to 17 psia. Then pressurize to 36 psia with 530°R GHe and operate TCU to establish decay rate. Switch directly from vent 1 to vent 2. Repressurize for 66 and 68.
65	2	1	1	17-36	
66	1	1	2	17-36	
67	2	1	2	17-36	
68	1	1	3	17-36	
69	2	1	3	17-36	
70-76	-	2	-	17	Repeat run 1-7 with liquid level No. 2.
71-80	-	2	-	17-28	Repeat runs 8-11 using with liquid level No. 2.
87-96	-	2	-	-	Repeat runs 18-27 with liquid level No. 2.
107	-	2	-	17-28 (11.7-19.3)	Establish equilibrium at 17 psia. Pressurize to 28 psia with 530°R GHe and establish pressure-time relation until $dp/d\theta = 0$.

Table 15

110-INCH DIAMETER (2.8m) TANK SIDE MOUNT CONFIGURATION B TEST CONDITION

No.	Nominal Vent Flow(3)	Nominal Ullage Volume (1)	Nominal Mixer Flow(2)	Nominal Tank Pressure psia *	Comment
1	-	1	-	17 (11.7)	Fill vapor trap with 530°R GH_2. Establish equilibrium and determine rate of pressure rise
2	1	1	1	17	Fill vapor trap with 530°R GH_2 while maintaining tank pressure at nominal value by venting ullage. Determine Pressure decay rate.
3	2	1	1	17	
4	1	1	2	17	
5	2	1	2	17	
6	1	1	3	17	
7	2	1	3	17	
8	-	1	-	17-28 (11.7-19.3)	Fill vapor trap as above. Pressurize ullage to 28 psia and determine rate of pressure decay.
8A	-	1	-	17-28	Repeat No. 8 except pressurize through trap.
9	-	1	1	17-28	Vent to nominal pressure and repeat No. 8 with mixer speed No. 1
10	-	1	2	17-28	Repeat No. 9 with mixer speed No. 2
11	-	1	3	17-28	Repeat No. 9 with mixer speed No. 3
12	1	1	1	17-28	Vent to nominal ullage pressure and fill trap with vapor. Pressurize ullage and determine pressure decay rate.
13	2	1	1	17-28	
14	1	1	2	17-28	
15	2	1	2	17-28	
16	1	1	3	17-28	
17	2	1	3	17-28	
9A	-	1	1	17-28	Repeat No. 9 except pressurize with 530°R GH_e
18-34	-	1	-	-	Repeat Tests Nos. 1-17 with no vapor in the trap

* Numbers in parentheses are $(N/m^2) \times 10^{-4}$

Table 16

110-INCH DIAMETER (2.8m) TANK SIDE MOUNT CONFIGURATION B TEST CONDITION

Run No.	Nominal Vent Flow(3)	Nominal Ullage Volume(1)	Nominal Mixer Flow(2)	Nominal Tank Pressure psia *	Comment
1	-	1	-	17 (11.7)	Fill vapor trap with 530°R GH2 while maintaining tank pressure at nominal value by venting ullage. Establish equilibrium and determine rate of pressure rise.
2	1	1	1	17	Vent down from previous run until bulk boiling fills the vapor trap. If tank pressure falls below nominal pressurize and mix until equilibrium is established. Determine equilibrium rate of pressure decay.
3	2	1	1	17	
4	1	1	2	17	
5	2	1	2	17	
6	1	1	3	17	
7	2	1	3	17	
8	-	1	-	17-28 (11.7-19.3)	Vent tank until equilibrium is established with vapor in the trap. Pressurize to 28 psia and determine rate of pressure decay
9	-	1	1	17-28	Repeat No. 8 with mixer speed No. 1
10	-	1	2	17-28	Repeat No. 9 with mixer speed No. 2
11	-	1	3	17-28	Repeat No. 9 with mixer speed No. 3
12	1	1	1	17-28	Vent down to obtain vapor in trap as per No. 8. Pressurize to 28 psia and determine rate of pressure decay
13	2	1	1	17-28	
14	1	1	2	17-28	
15	2	1	2	17-28	

* Numbers in parentheses are (Newtons per Sq. meters)10^{-4}

Table 16(con't.)

Run No.	Nominal Vent Flow(3)	Nominal Ullage Volume(1)	Nominal Mixer Flow(2)	Nominal Tank Pressure psia	Comment
16	1	1	3	17-28	See 12-14
17	2	1	3	17-28	
18-34	-	1	-	-	Bleed vapor from trap and repeat runs 1-17 with liquid in trap
35 - 68	-	2	-	-	Repeat runs 1-34 at liquid level No. 2
69	2	2	1	17 (11.7)	Establish equilibrium at 17 psia. Place TCU on automatic and demonstrate automatic control

(1) Nominal Ullage Volume: 1 - 5Percent
2 - 29 Percent

(2) Nominal Mixer Flow: 1 - 5.3 cfm (150 ℓ/m)
2 - 3.5 cfm (100 ℓ/m)
3 - 2.5 cfm (71 ℓ/m)

(3) Nominal Vent Flow: 1 - 1.3 lb./hr. (547 gr./hr.)
2 - 2.2 lb./hr. (995 gr./hr.)

RESULTS AND ANALYSIS

The data obtained from the tests in the 41.5 inch (1.05m) and 110 inch (2.8m) diameter tanks are presented in this section. The results are compared with the oretical predictions. The performance of the complete thermal conditioning system, as well as each individual component has been evaluated and the results are presented herein.

TEST RESULTS - 41.5 INCH (1.05m) DIAMETER TANK

In a given tank and thermal environment, the operational variables include: (1) mixer flow rate; (2) vent flow rate; (3) pressure level and temperature; (4) pressurant gas; (5) ullage volume. In this section, typical runs have been grouped together, and pressure and propellant temperatures are presented in a manner so as to allow comparison for each individual parameter. For convenience, in the following discussion the bottom mount and side mount test numbers are designated with the letter A and B, respectively.

Figures 40-42 compare the pressure response to various mixer flow rates, following an ullage pressurization to approximately 28 psi ($193 \times 10^4 n/m^2$). Also shown on each figure is a comparison of temperature histories at several points in the liquid and ullage, for the lowest and highest mixer flow rate.

Each consecutive test at five percent ullage (Fig. 40) was started at a slightly higher pressure which accounts for the difference in final pressure level. However, it is significant that the minimum pressure following collapse is approximately 0.7 psi ($5.5 \times 10^3 n/m^2$) above starting pressure for all tests with mixing but the difference is 1.5 psi ($10.3 n/m^2$) with no mixing. Mixing the liquid significantly increases the pressure collapse rate, and the time it takes to reach minimum pressure decreases proportionaltely to an increase in mixer flow. The pressure reaches a minimum when 20-30 percent of the liquid has been circulated. It then starts to increase at a constant rate which is proportional to the rate of total heat input. The heating from external sources was determined, with a boiloff test conducted prior to the TCU tests, to be 124 BTu/hr (36.4w). The heat input to the mixer motor added an additional heat rate from 16 to 25 BTU/hr (4.8 - 7.3w); the lowest value corresponding to the lowest

mixer flow (Run 21). This variation is small compared to the total rate and therefore is not detectable in the equilibrium rates of rise. The temperatures on Fig. 40 are presented so that the response at each location can be assessed in terms of the mixer flow rate. The temperature uniformity at any time during a specific test can be seen from comparison of each temperature indication at that point in time (Fig. 43). It can be seen that the initial depressurization period is characterized by rapid adjustments, particularly that the higher liquid levels. Thereafter, the temperature rises fairly uniformly at all levels, which indicates good mixing. It is noted that the temperature (TB-6) just above the five percent ullage line is in phase with the tank pressure for the higher mixer flow, but still shows superheat at the end of the test; for the low flow rate. The temperature (TB-7) in the top of the ullage lags the pressure for both tests, although it did eventually reach equilibrium for test No. 20.

The temperatures in the ullage invariably continue to decrease after the pressure reached a minimum. They do, however, show a marked reduction in the rate of decay when the pressure reverses. At this point in time, the energy into the ullage from external sources is exactly balanced by the energy being transferred from the ullage to the liquid by conduction and mass exchange. During the depressurization period, either condensation or evaporization may occur, depending upon the relative magnitude of the conduction terms to the ullage and from the ullage to the liquid. By the time the pressure reaches a minimum, however, surface evaporation is the dominating process and thereafter the energy input to the ullage by mass addition must exceed any further sensible energy given up by the gas. This can be seen from the following expression which results from a mass and energy balance on the ullage.

$$\left(\frac{VC_v}{R}\right)\dot{p} = (MC_v)_L \dot{\bar{T}}u + M_g \bar{U}_g$$

In the absence of venting, an energy balance on the entire tank contents results in the following expression.

$$Q_o = (MC_v)_L \dot{\bar{T}}_L + \frac{u_L}{u_u}(MC_v)_u \dot{\bar{T}}u + \frac{(VC_v)u}{R}\dot{P}\left(1 - \frac{u_L}{u_u}\right)$$

For total thermodynamic equilibrium, the liquid and gas temperatures are equal and uniform throughout. With five percent ullage, the sensible energy term for the gas is less than one percent of that for liquid. For runs 20 and 21, the liquid temperatures are fairly uniform, but the gas still exhibits some superheat. However, the energy term for the gas is still less than two percent of that for the liquid. Therefore, it exhibits characteristics of a mixed system.

Figures 41 and 42 present a similar comparison for 25 and 70 percent ullage respectively. The temperature adjustment corresponding to the initial mixing gets progressively larger with ullage volume because of the increased energy required to pressurize, and the reduced quantity of liquid available to absorb this energy.

The effect of vent flow rate is shown on Figures 44-46. These data show that the large and rapid initial depressurization is caused by mixing and is essentially independent of vent flow rate. Once the initial depressurization occurs an apparent equilibrium rate of decay starts which is proportional to the vent rate. The differences in final pressure levels on Figure 44 reflect the difference in starting equilibrium pressure, rather than vent rate. Test No. A-15, which involved no pressurization can be compared with A-25 which was begun by first pressurizing from 14 to 29 psi (96.500 to 200,000 N/m^2) with ambient temperature hydrogen. The steady state decay rates are nearly identical.

Figure 45 also compares temperature responses at three different locations in the liquid. The temperatures initially increases during the rapid depressurization reflecting the high rate at which energy is being absorbed from the ullage. At the time corresponding to a completely mixed condition, the temperatures reverse and start down at a rate proportional to the vent flow rate, or if there is no venting, the rate of rise in termperature is reduced to an apparent equilibrium value.

In comparing the pressure responses, it can be seen that steady state rate of pressure change increases with volume, for a given vent rate. Figures 47-49

FOLDOUT FRAME 1

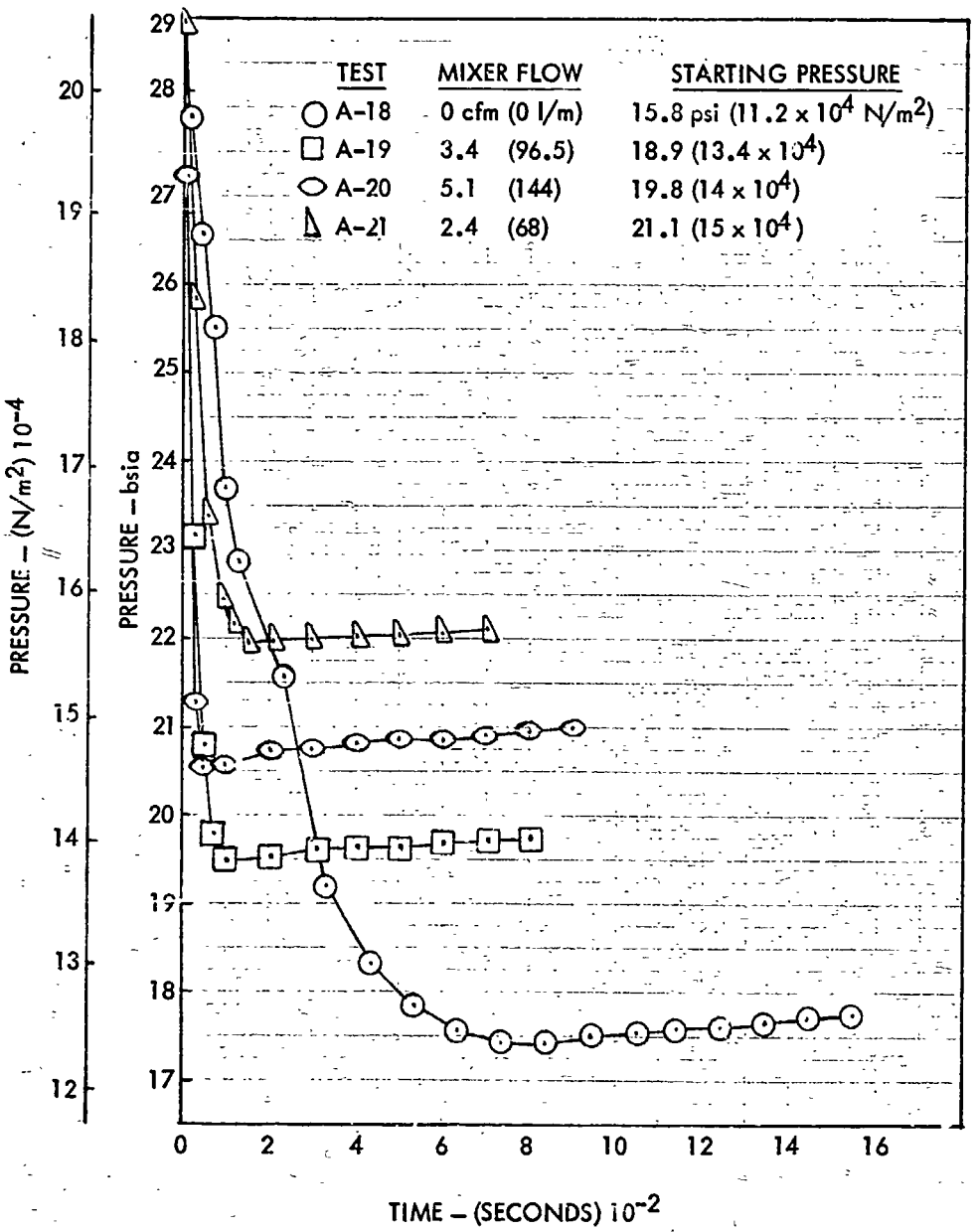

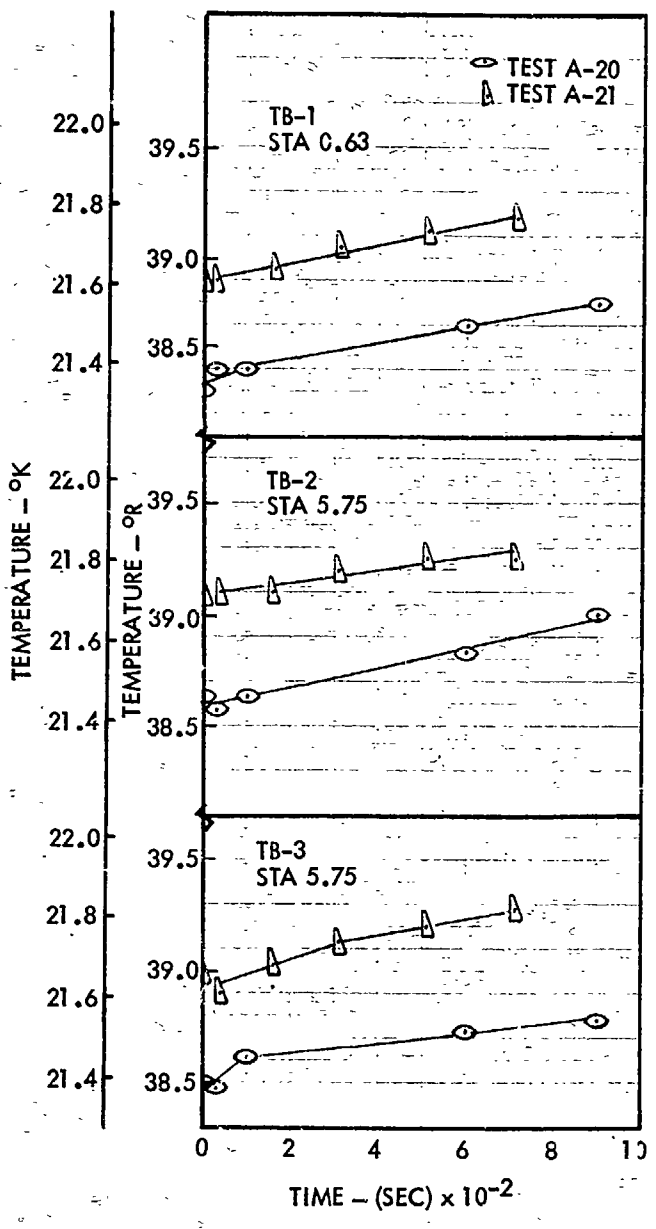

(b) Liquid Tempe

FOLDOUT FRAME 2

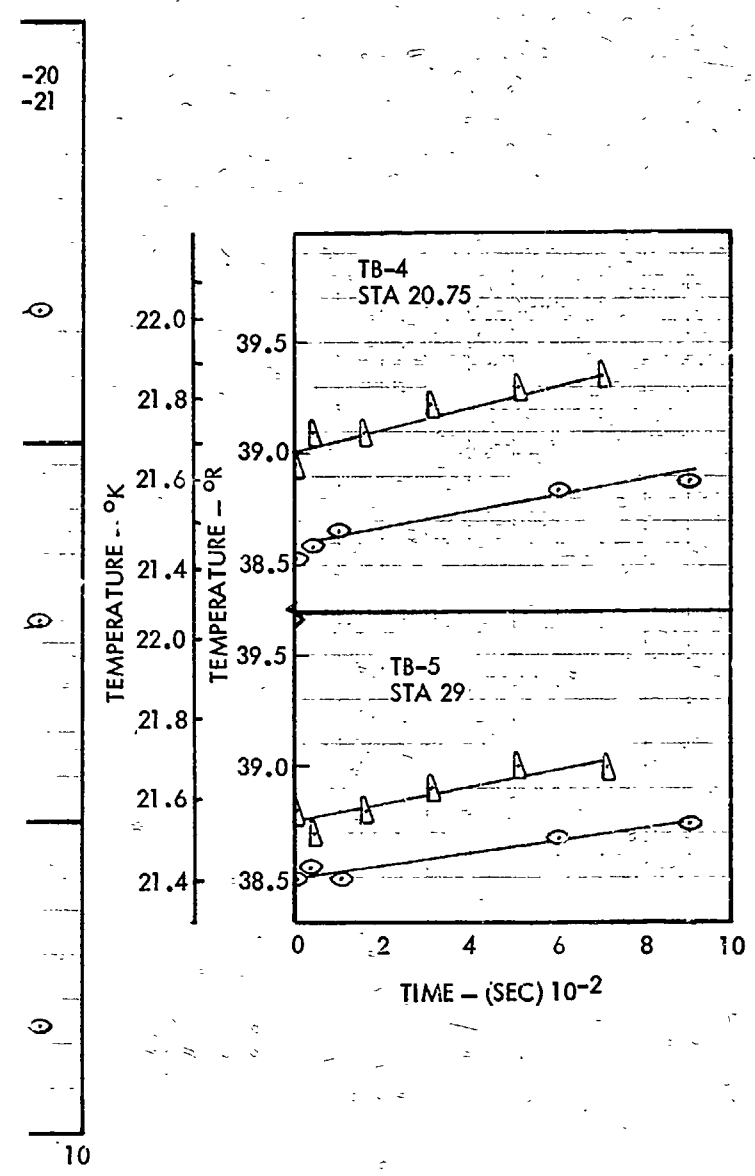

Liquid Temperature

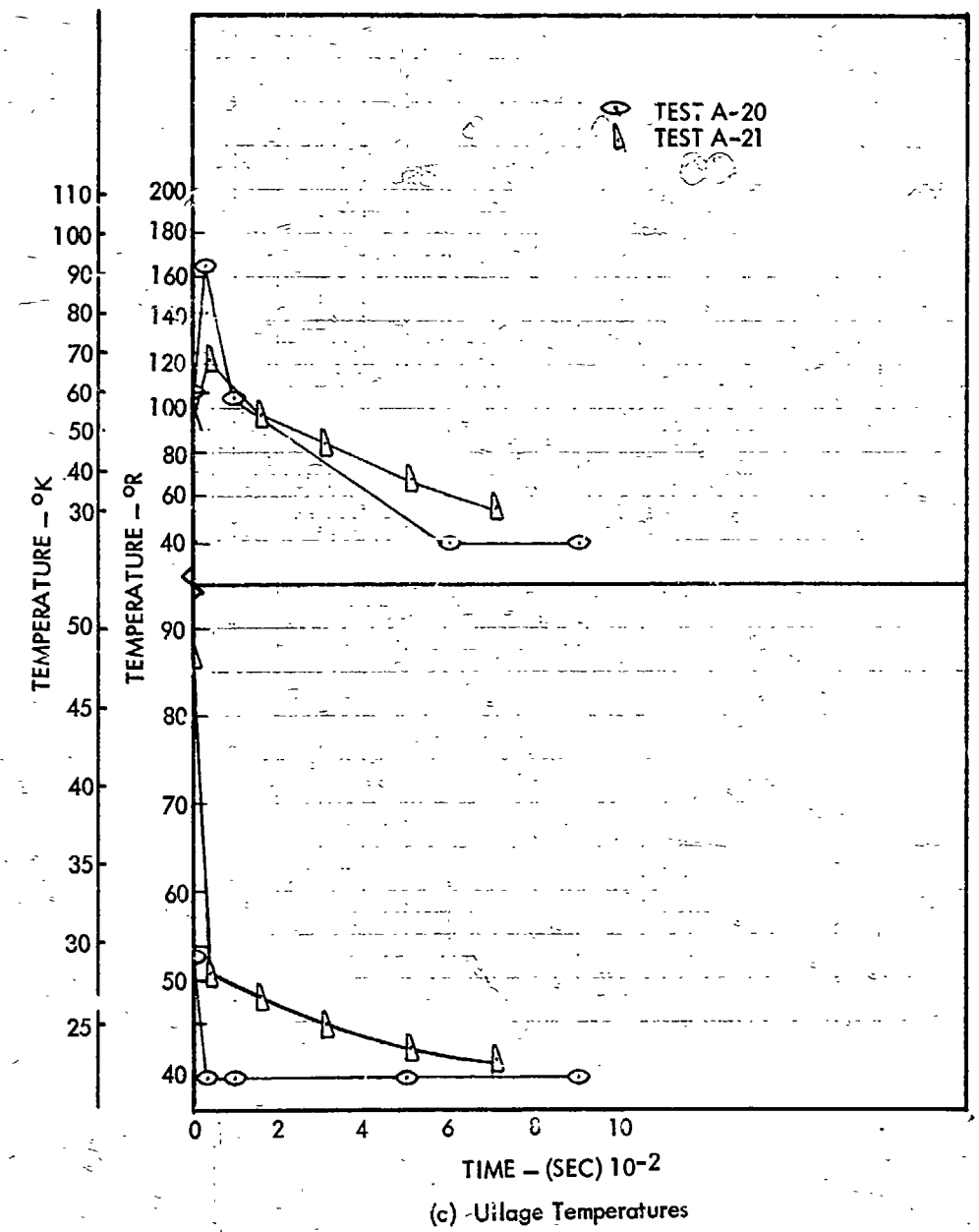

(c) Ullage Temperatures

Fig. 40 – Effect of Mixer Below Rate at 5 Percent Ullage – 41.5 Inch (1.05M) Tank – Bottom Mount

FOLDOUT FRAME 1

PRECEDING PAGE BLANK NOT FILMED

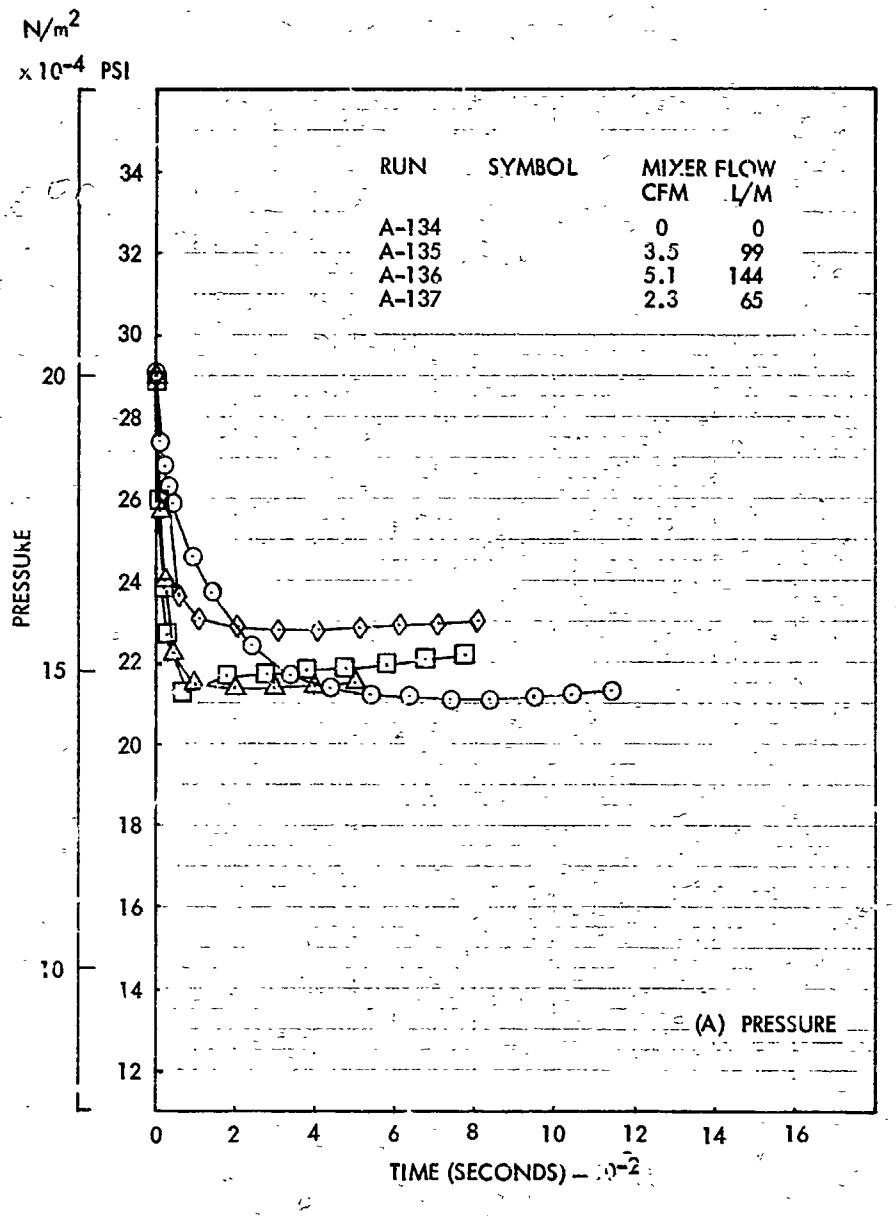

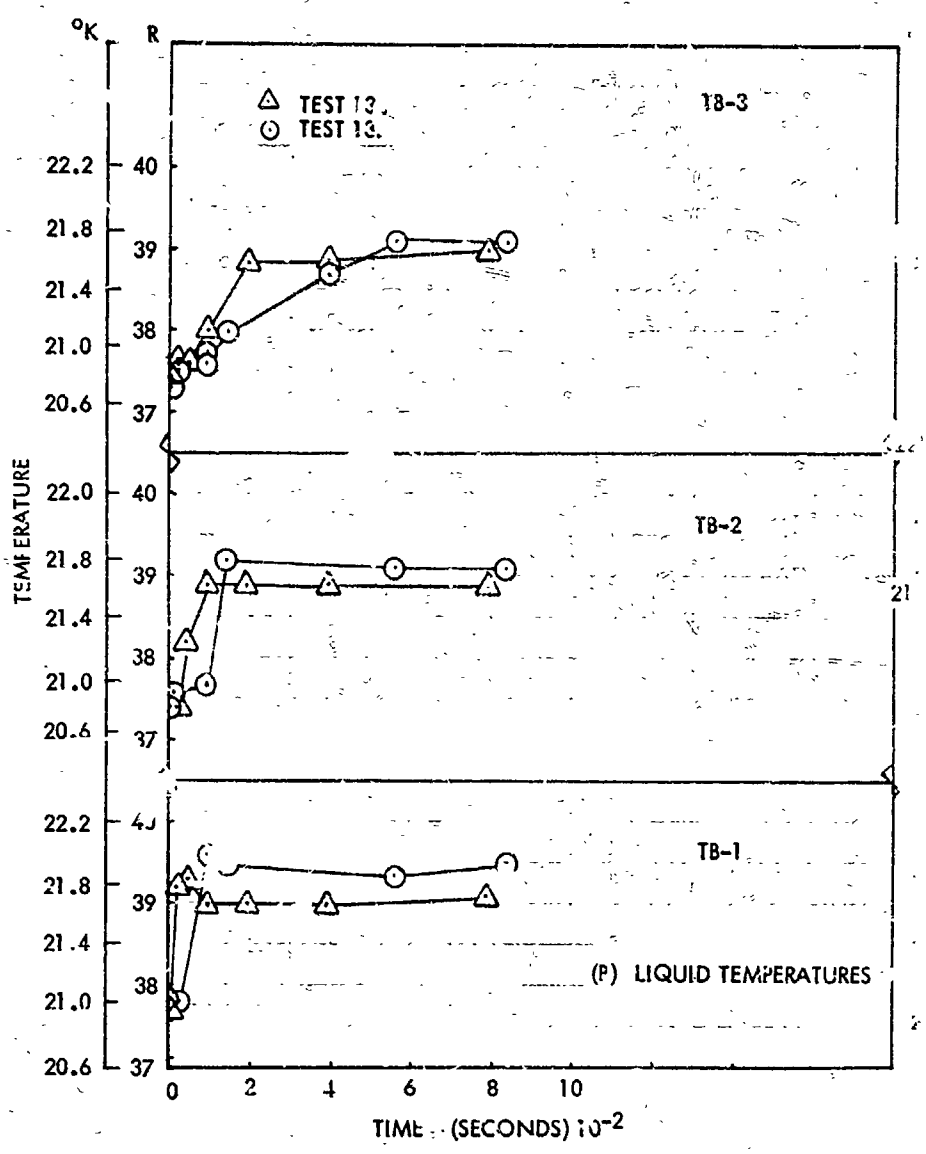

FOLDOUT FRAME 2

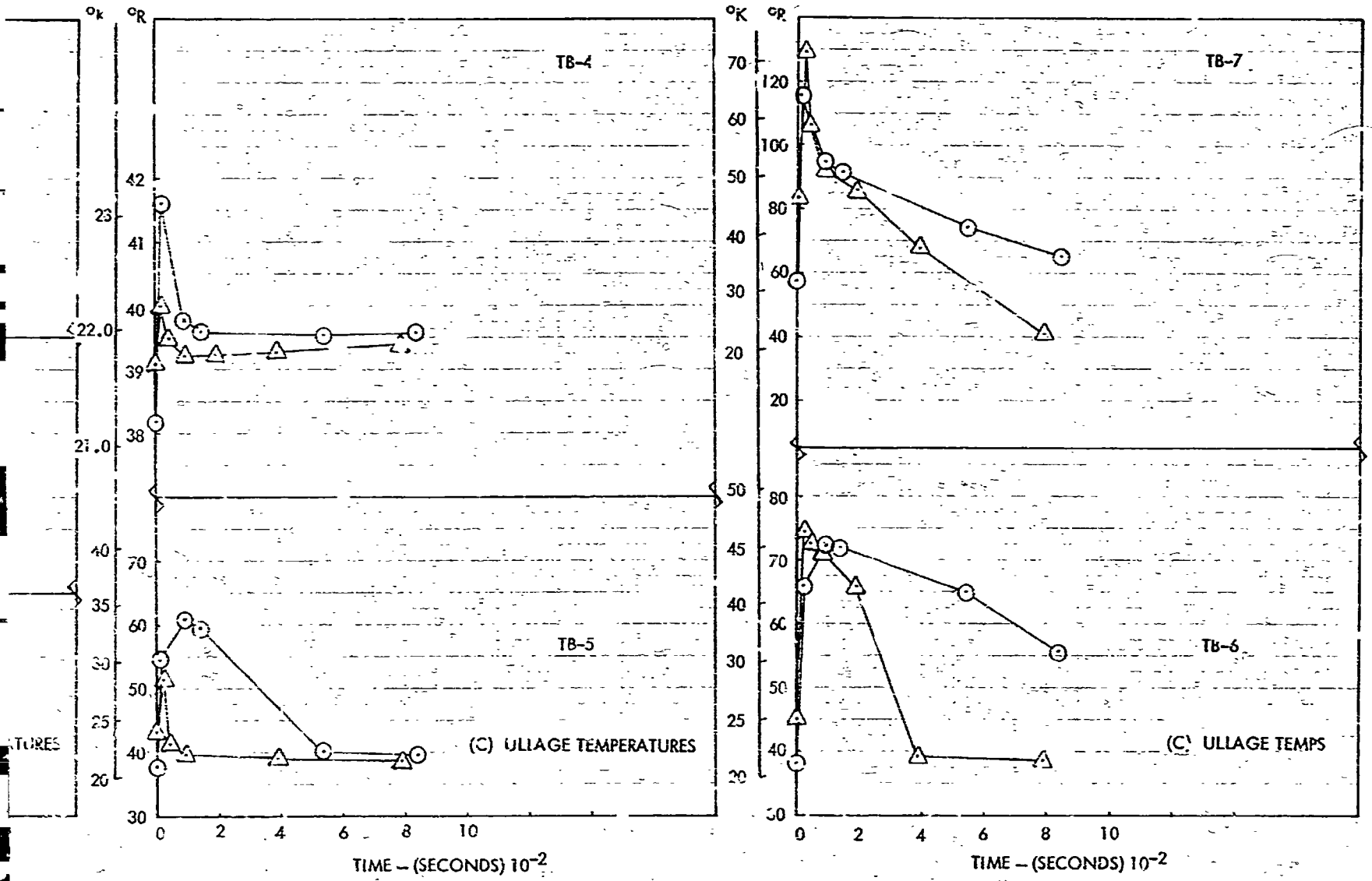

Fig 41 – Effect of Mixer Below Rate at 20 Percent Ullage – 41.5 Inch (1.05M) Tank – Bottom Mount

PRECEDING PAGE BLANK NOT FILMED

FOLDOUT FRAME 1

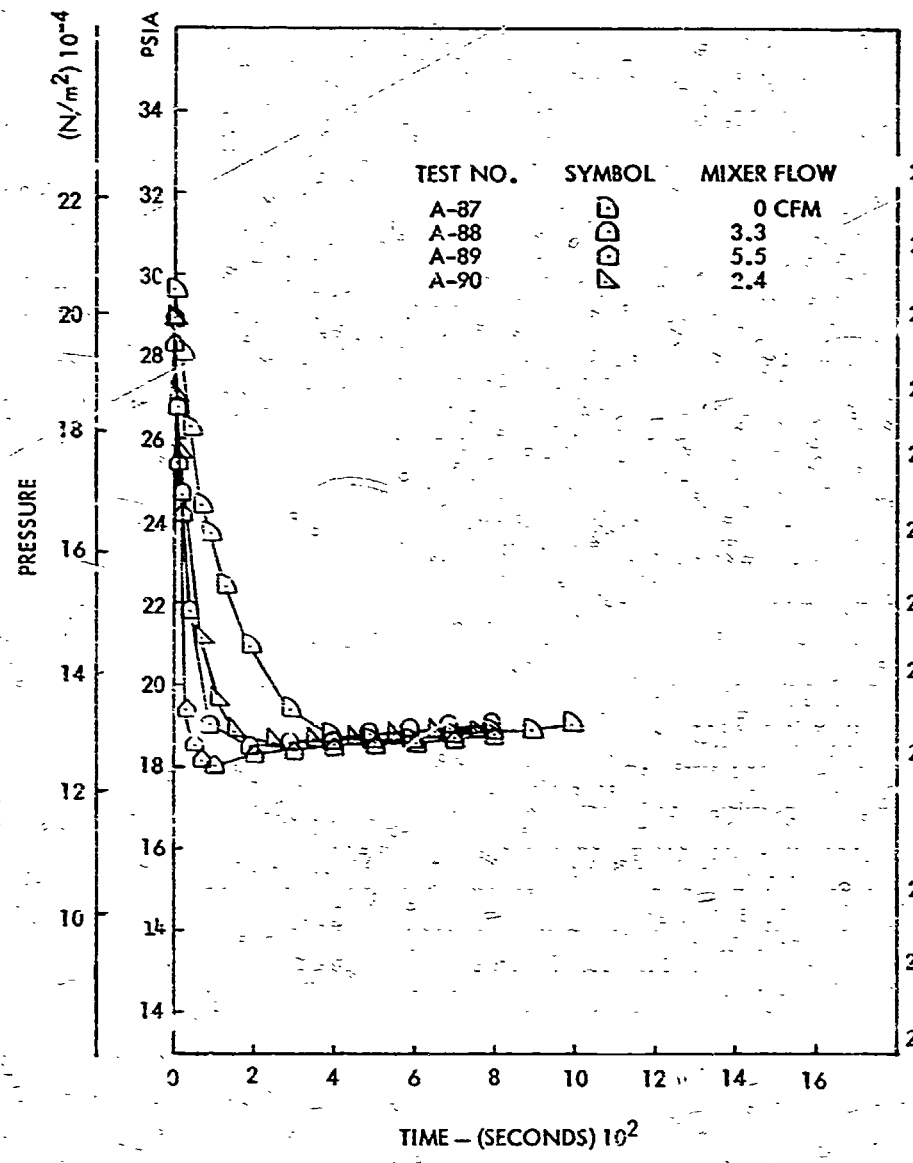

(A) PRESSURE

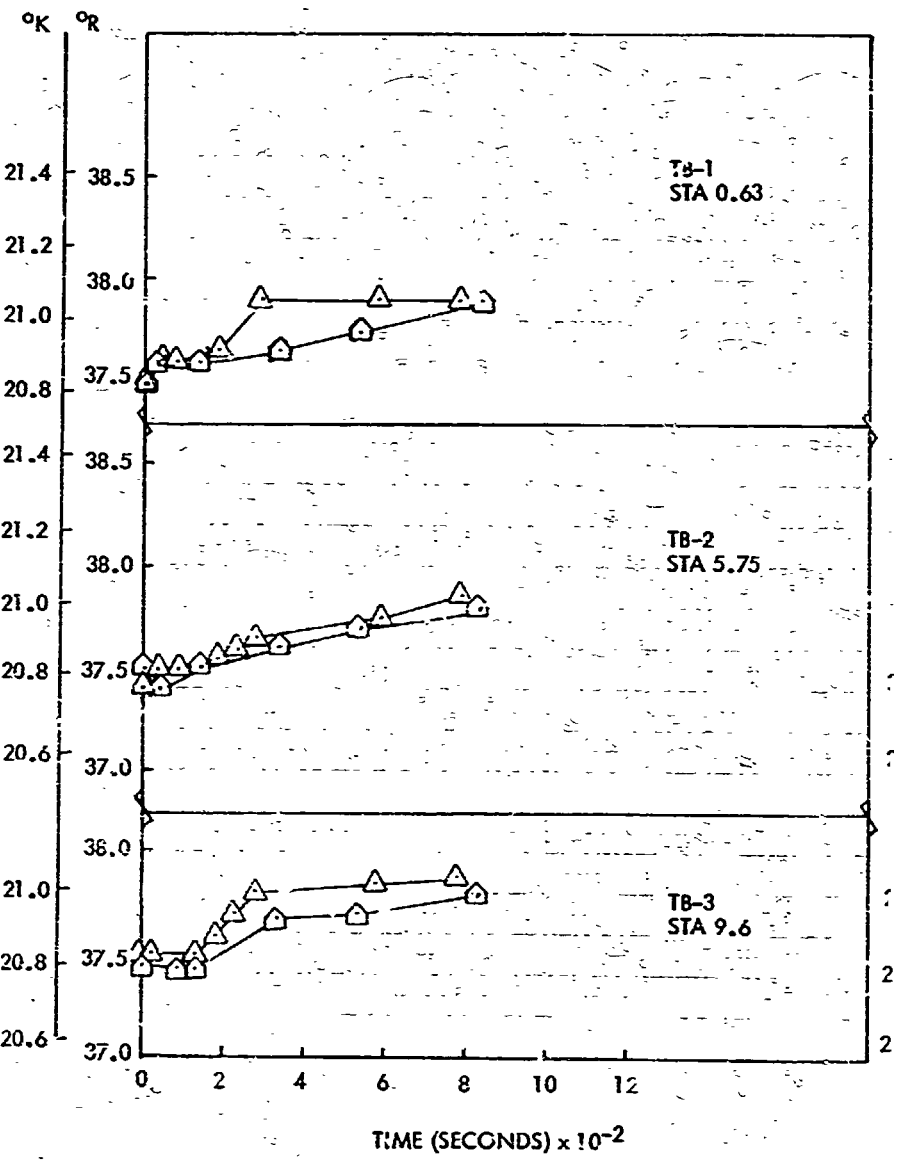

(B) LIQUID

FOLDOUT FRAME 2

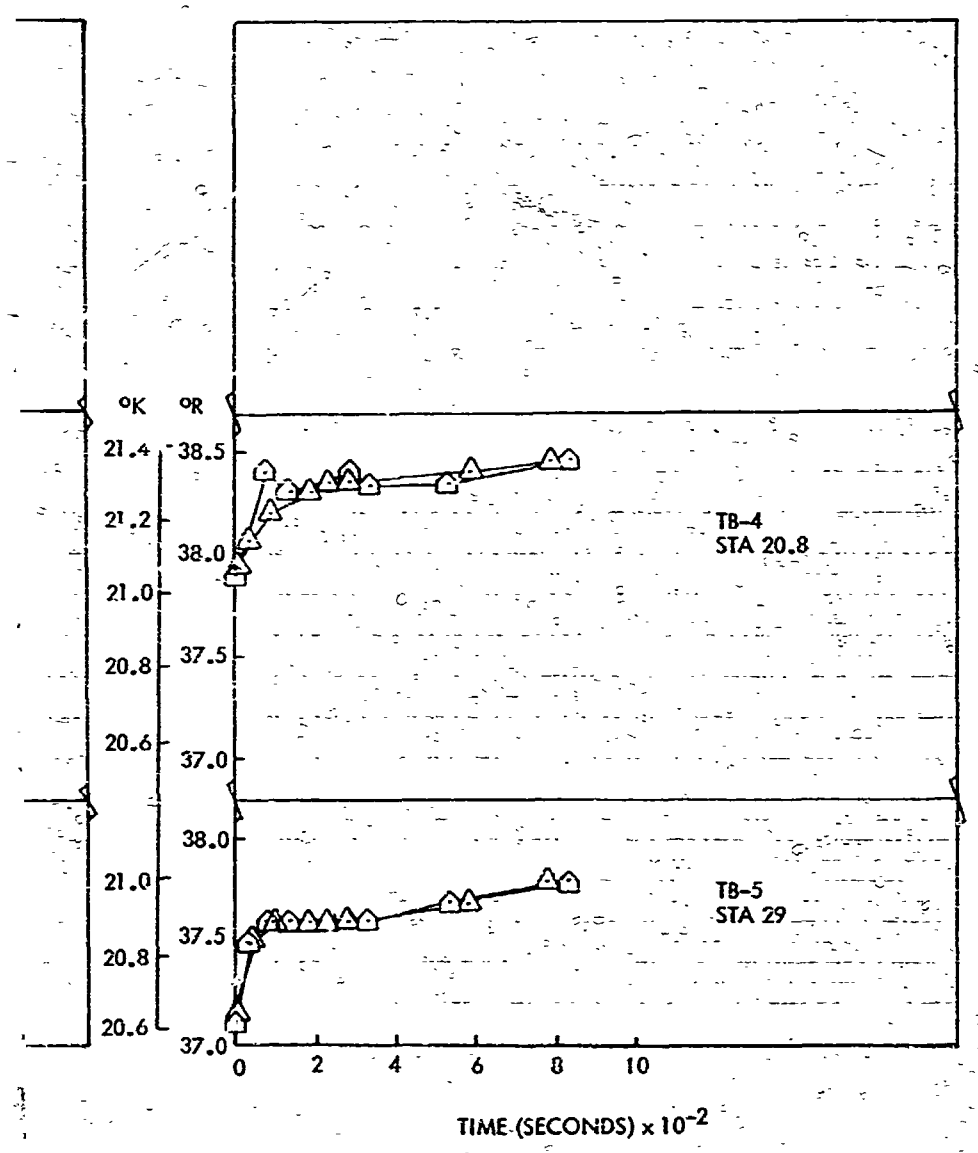

LIQUID TEMPERATURES (TESTS 89, 90)

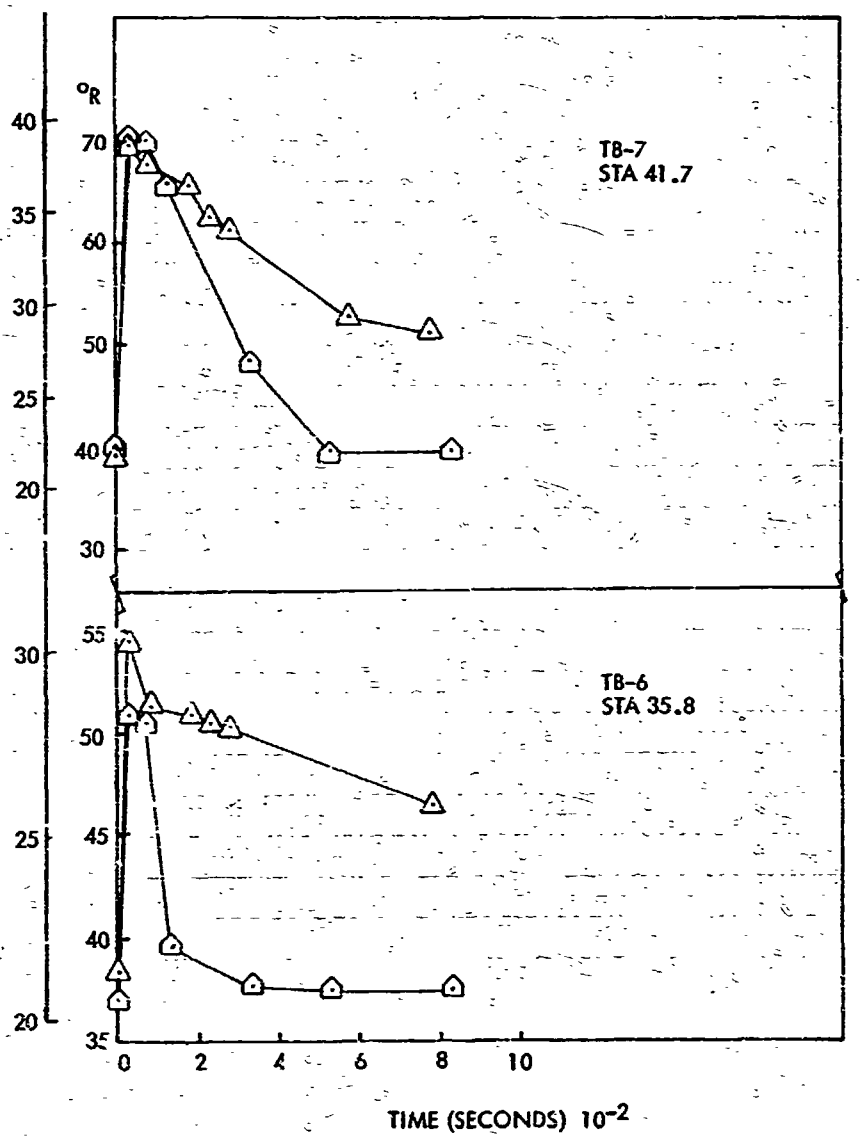

(C) ULLAGE TEMPERATURES (TESTS 89, 90)

Fig. 42 – Effect of Mixer Below Rate at 70 Percent Ullage – 41.5 Inch (1.05M) Tank – Bottom Mount

FOLDOUT FRAME 1

PRECEDING PAGE BLANK NOT FILMED

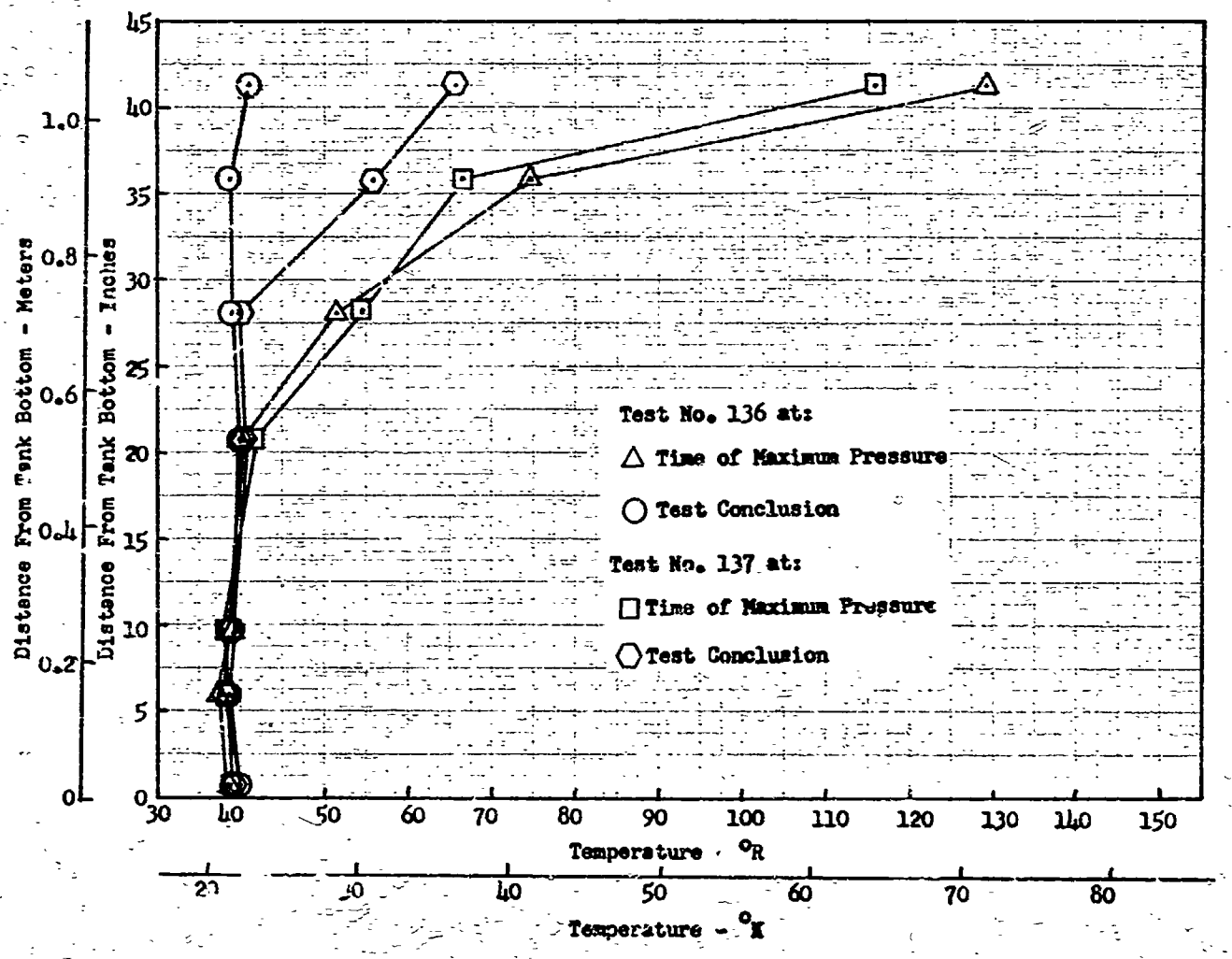

(a) 5 Percent Ullage

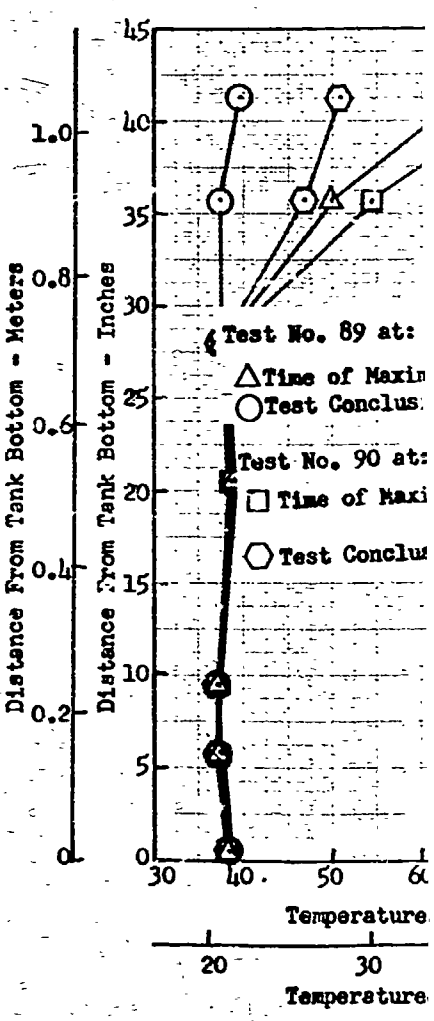

(b) 25 Percent U

FOLDOUT FRAME 2

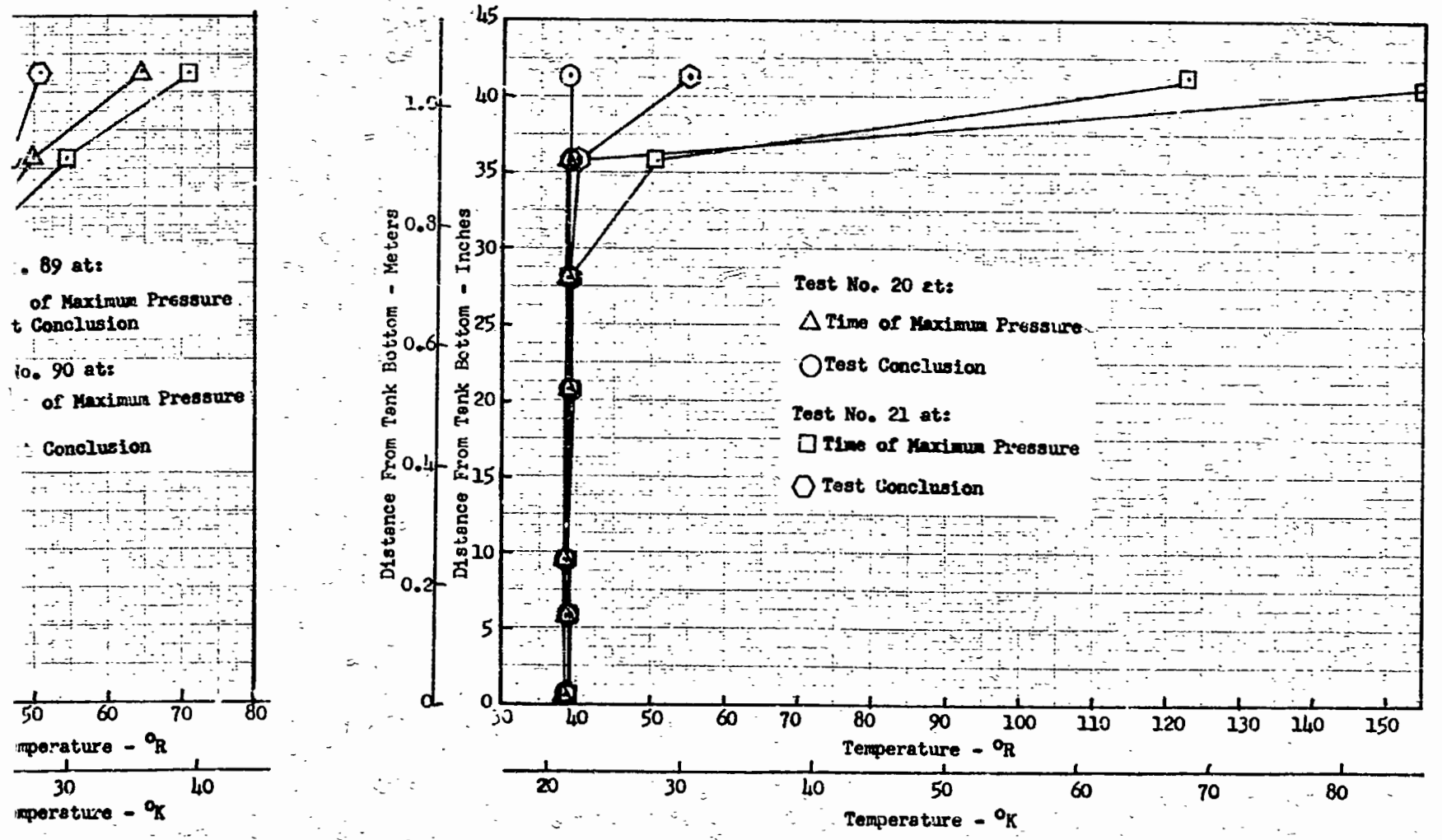

cent Ullage

(c) 70 Percent Ullage

Figure 43 Typical Temperature Profile Variations - 41.5 Inch (1.05 m) Tank - Bottom Mount

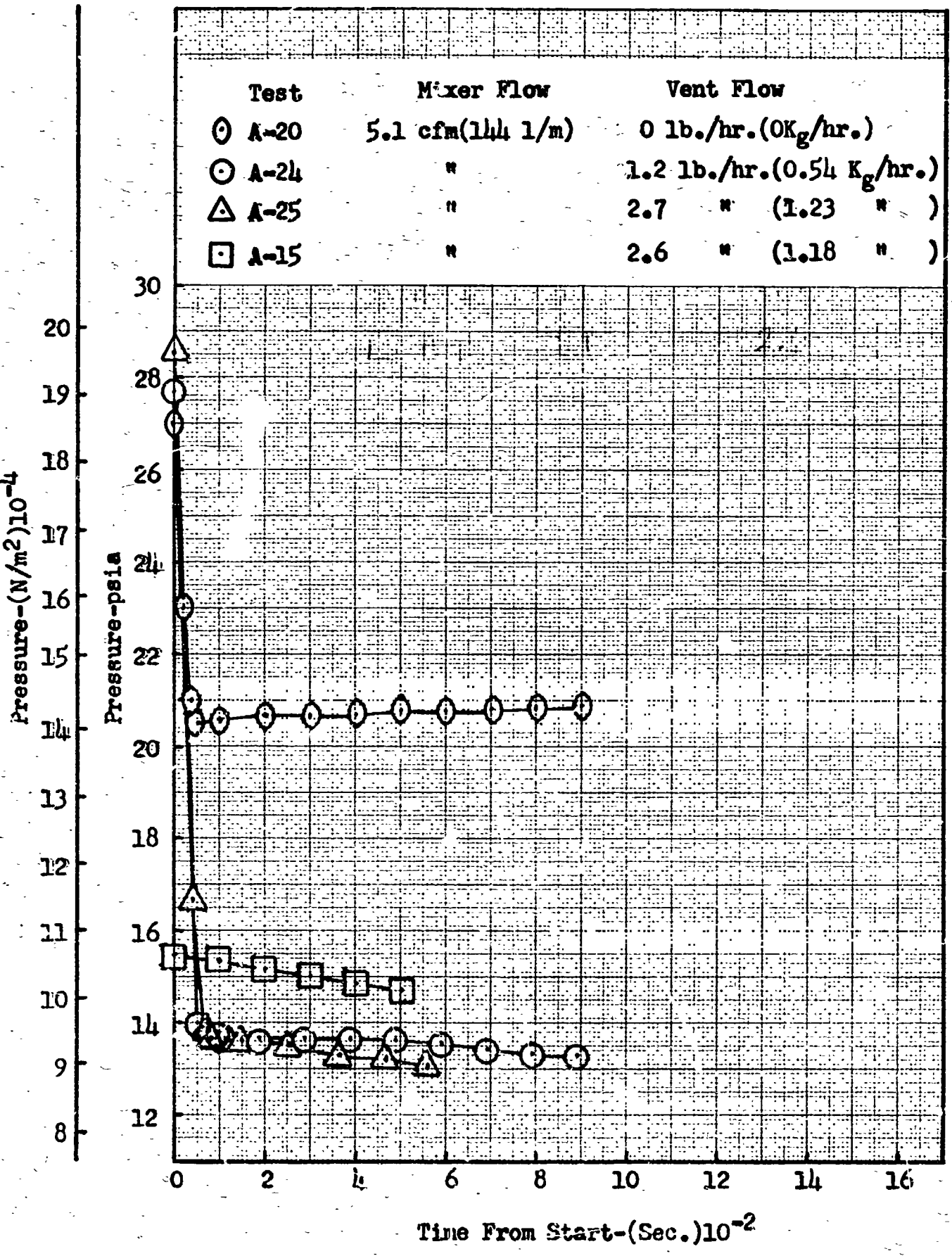

Figure 44 Comparative Effect of Vent Rate on Pressure Response at 5 Percent Ullage - 41.5 inch(1.05 m) Tank - Bottom Mount

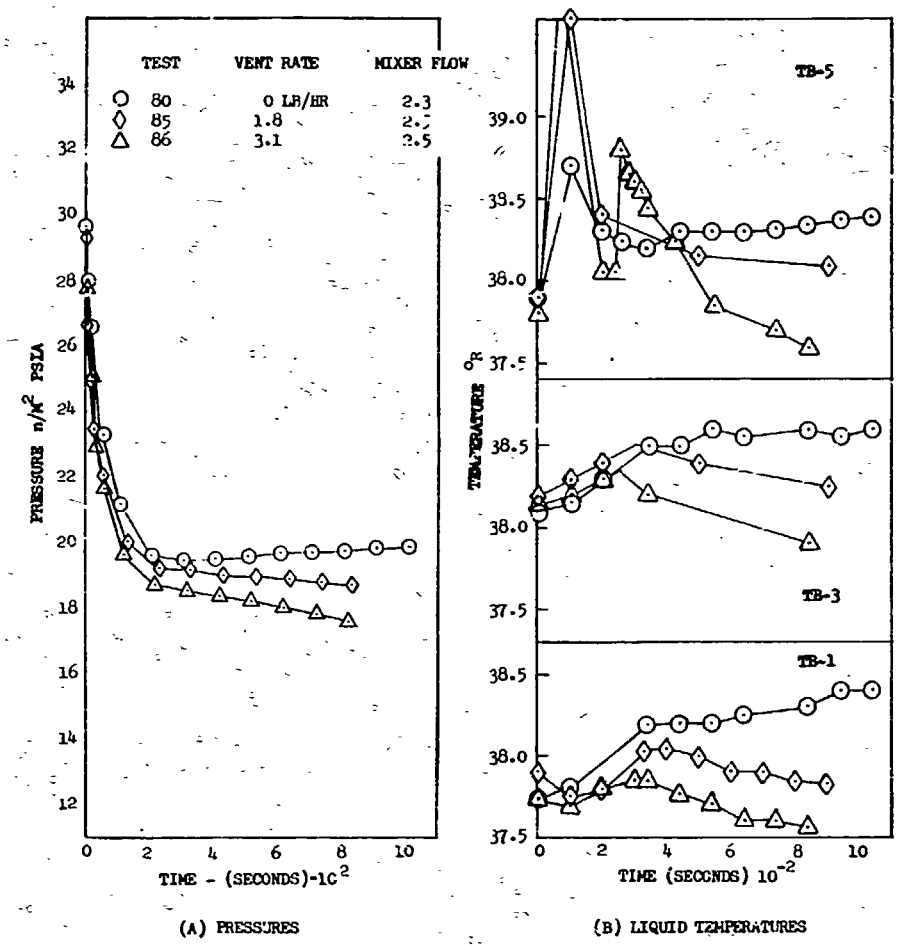

(A) PRESSURES

(B) LIQUID TEMPERATURES

Figure 45 Comparative Effect of Vent Rate on Pressure and Temperature Response at 25 Percent Ullage - 41.5 inch(1.05m) Tank - Bottom Mount

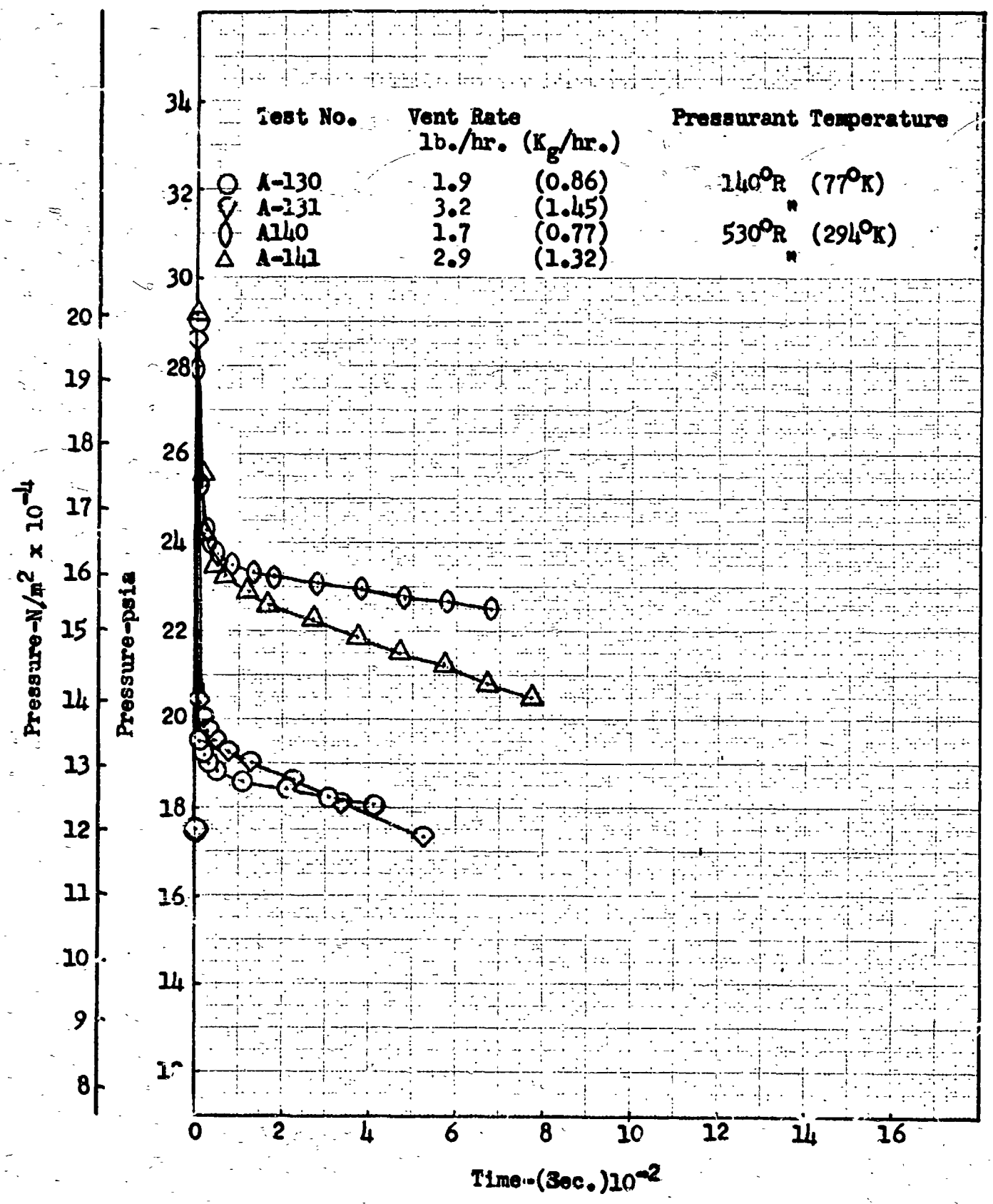

Figure 46 Comparative Effect of Pressurant Temperature on Pressure Response at 70 Percent Ullage - 41.5 inch(1.05m) Tank - Bottom Mount

show the comparative effects of various pressurant conditions. In general, it was found that increasing the pressurant temperature or pressure level had no effect on the final steady state pressure decay rate. However, at the higher ullage conditions, the difference between final and beginning equilibrium pressures tended to increase. This is due to the increased energy from the pressurant gas and the smaller heat sink in the liquid.

Throughout this program it was found that pressurizing with helium caused a significant increase in the mixing time and in the minimum pressure attained after mixing. However, no obvious effect is detected on the final, steady state rate of pressure change. This can be seen at all ullage volumes.

Figures 50 and 51 show one complete cycle where the TCU was controlling tank pressure automatically. For the helium test (Figure 50), the tank was pressurized to approximately 28 psi (193,000 N/m^2) before activating the TCU. It required approximately one hour before the system shut off. However, once the initial depressurization has occurred, and tank contents have been cooled to a new equilibrium value, the control cycle is nearly identical to that from test No. A-28, for which no pressurant was used. Good mixing is evidenced by the uniform changes in temperature at all levels, and in particular by the response of TB-6 which was approximately 1/4 inch (0.062 m) above the liquid surface at the end of the test.

The purpose of conducting tests in the side mounted configuration was to establish any influence this orientation might have on pressure control. This would be primarily indicative of the mixing characteristics as compared to the bottom mount configuration.

Figures 52 and 54 are typical of the findings from these tests which generally confirmed the parametric influence established from the bottom tests. Comparison of Figures 52 and 41 indicate that it takes a little longer to reach minimum pressure with the TCU mounted in the side position. In fact, approximately 80-90 percent of the tank volume passes through the mixer before minimum pressure occurs as compared to approximately 20 percent for the bottom mounted tests. Part of this may be due to a higher heat leak for this series of tests. The repeated handling of the tank insulation had caused deterioration and as a result the

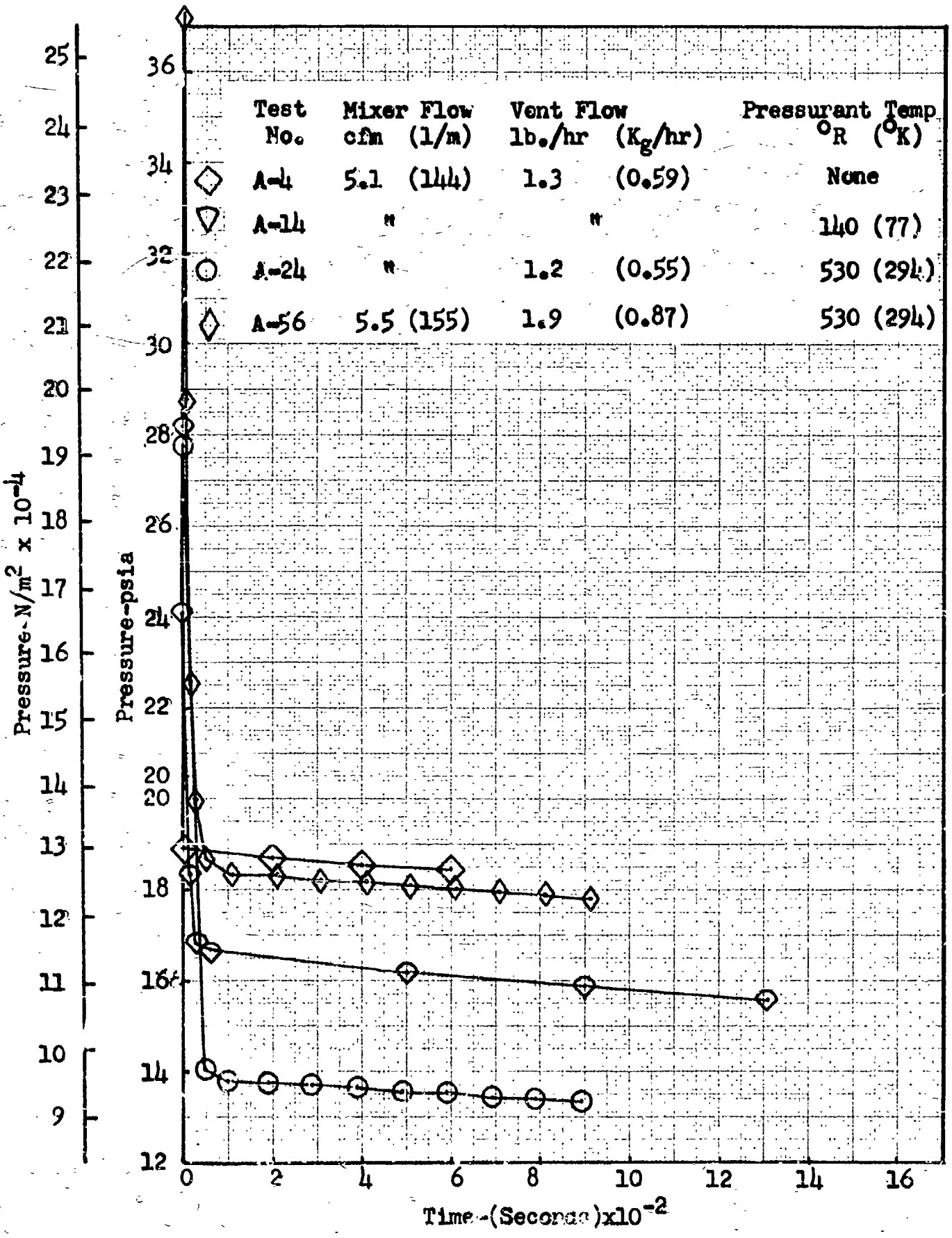

Figure 47 Comparative Effect of Pressurant Temperature And Level on Pressure Response at 5 Percent Ullage

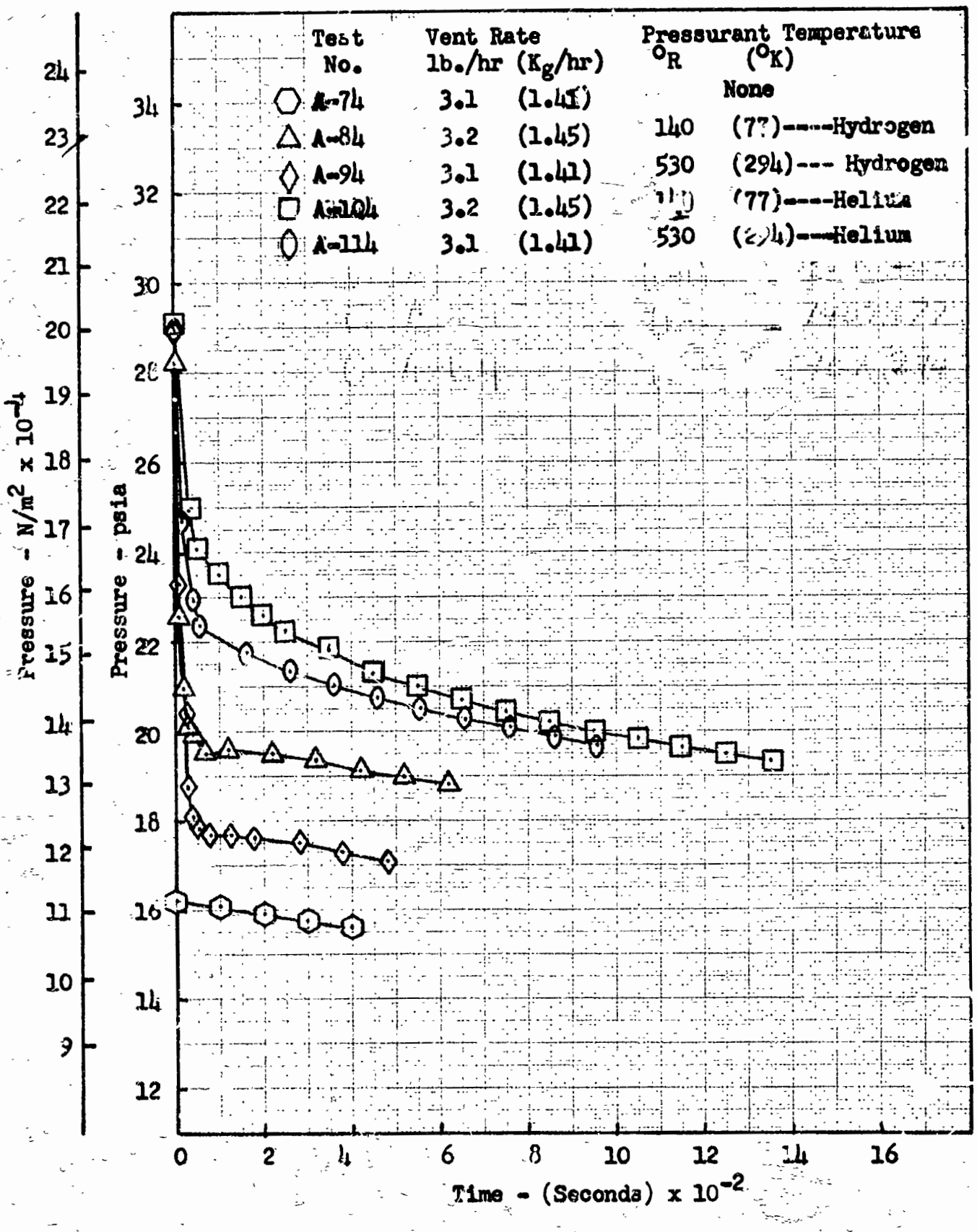

Figure 48 Comparative Effect of Pressurant on Tank Pressure Response at 25 Percent Ullage

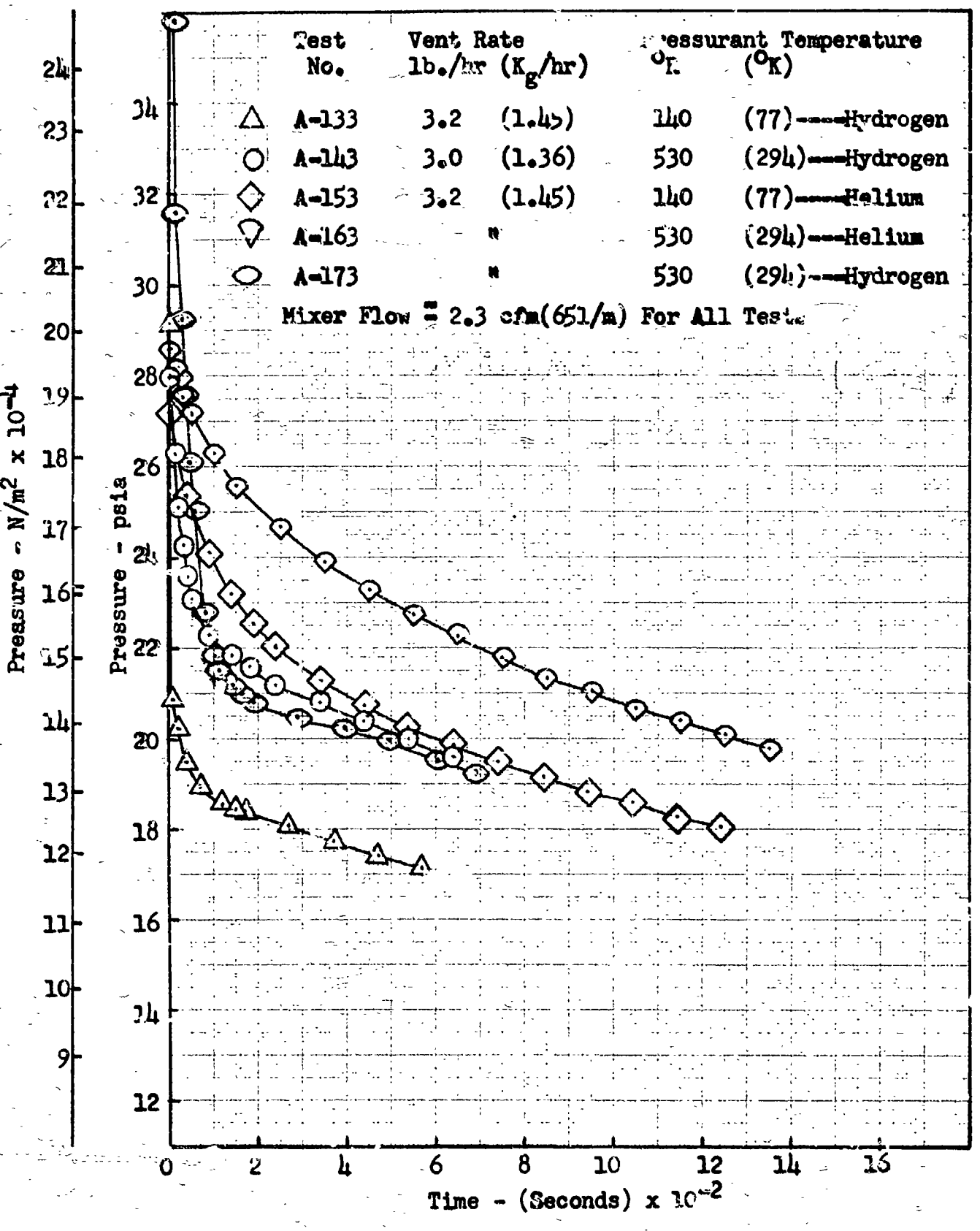

Figure 49 Comparative Effect of Pressurant on Tank Pressure Response at 70 Percent Ullage - 41.5 inch(1.05m) Tank

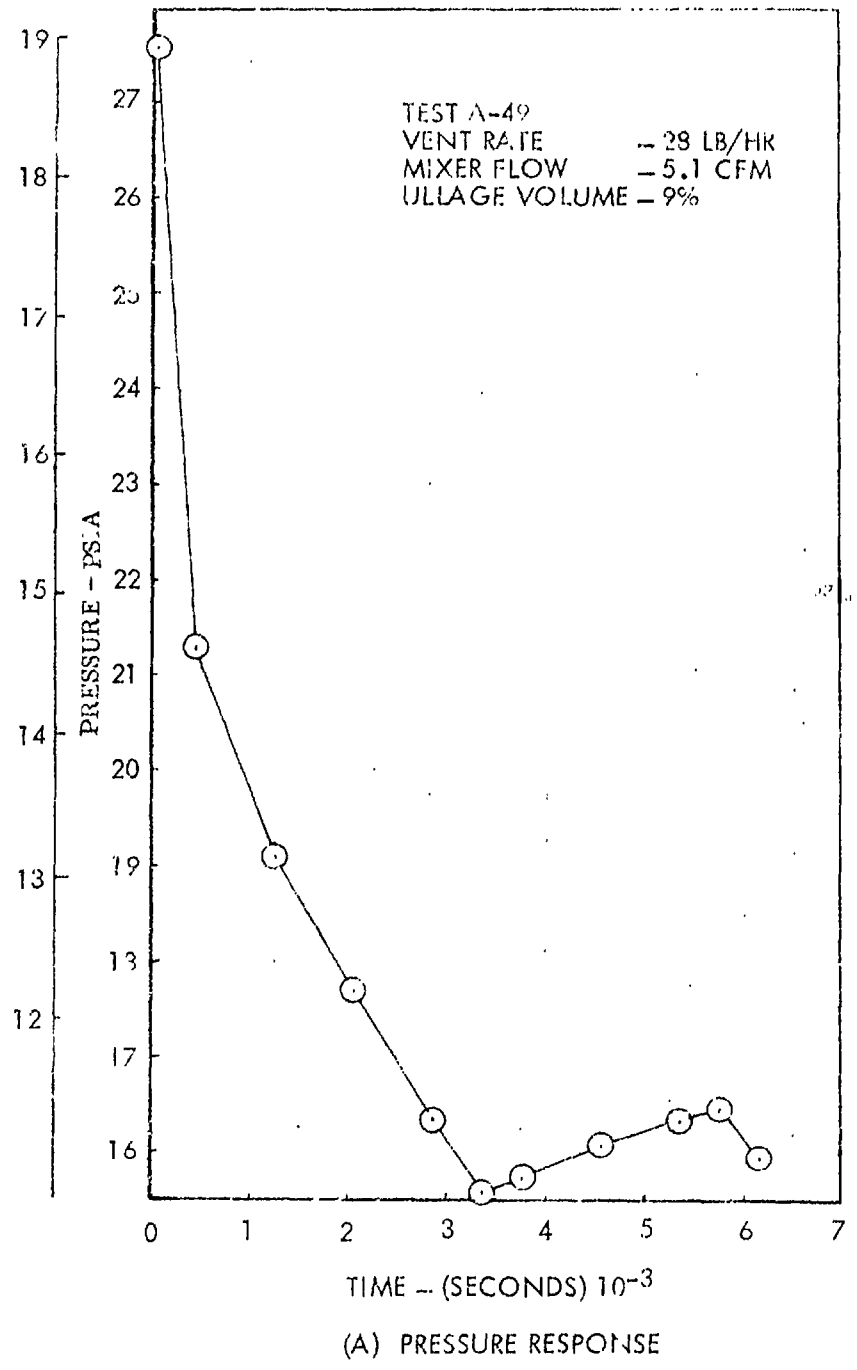

(A) PRESSURE RESPONSE

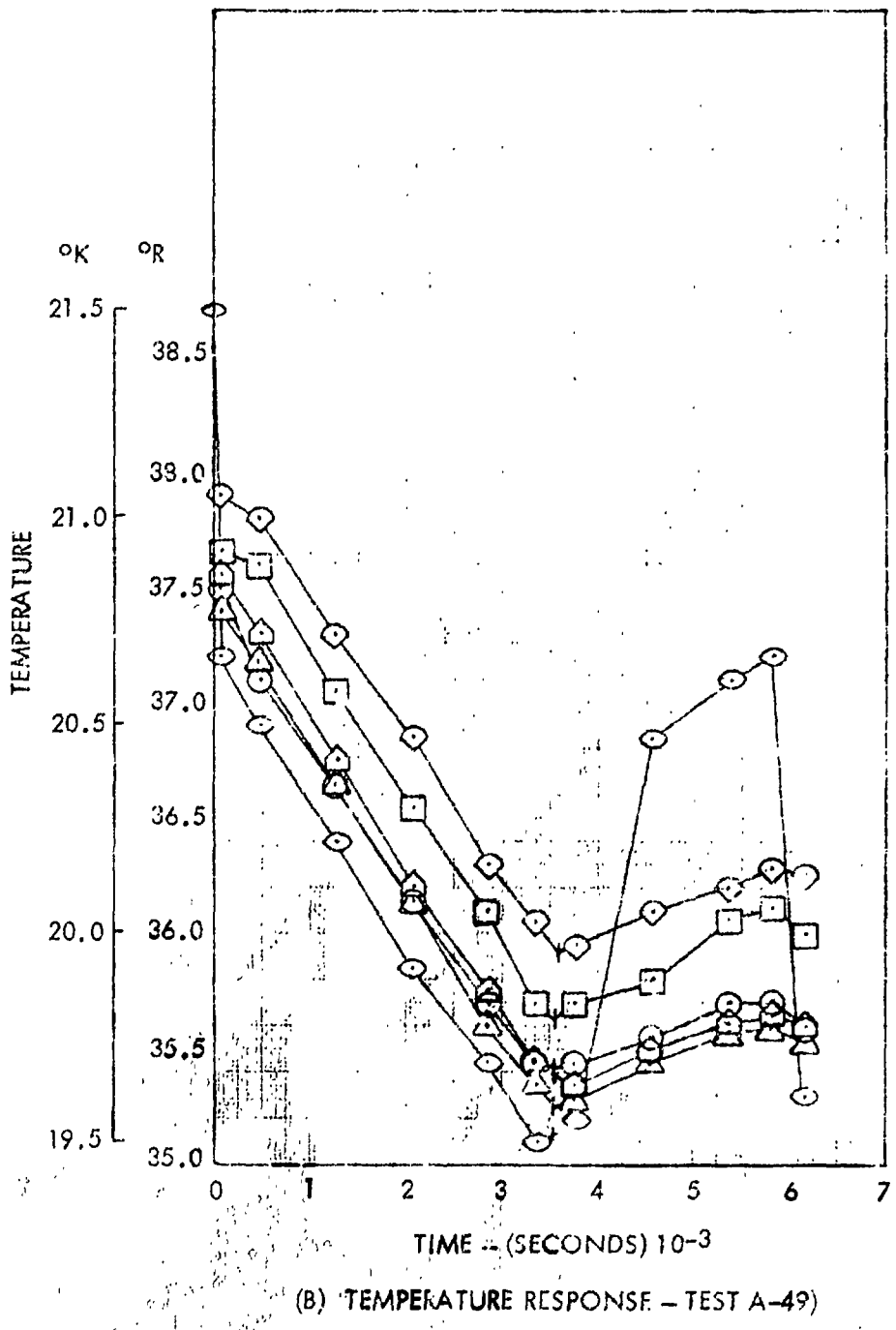

(B) TEMPERATURE RESPONSE – TEST A-49)

Figure 50 Automatic Control Characteristics Following Pressurization with Helium - 41.5 inch(1.05m) Tank

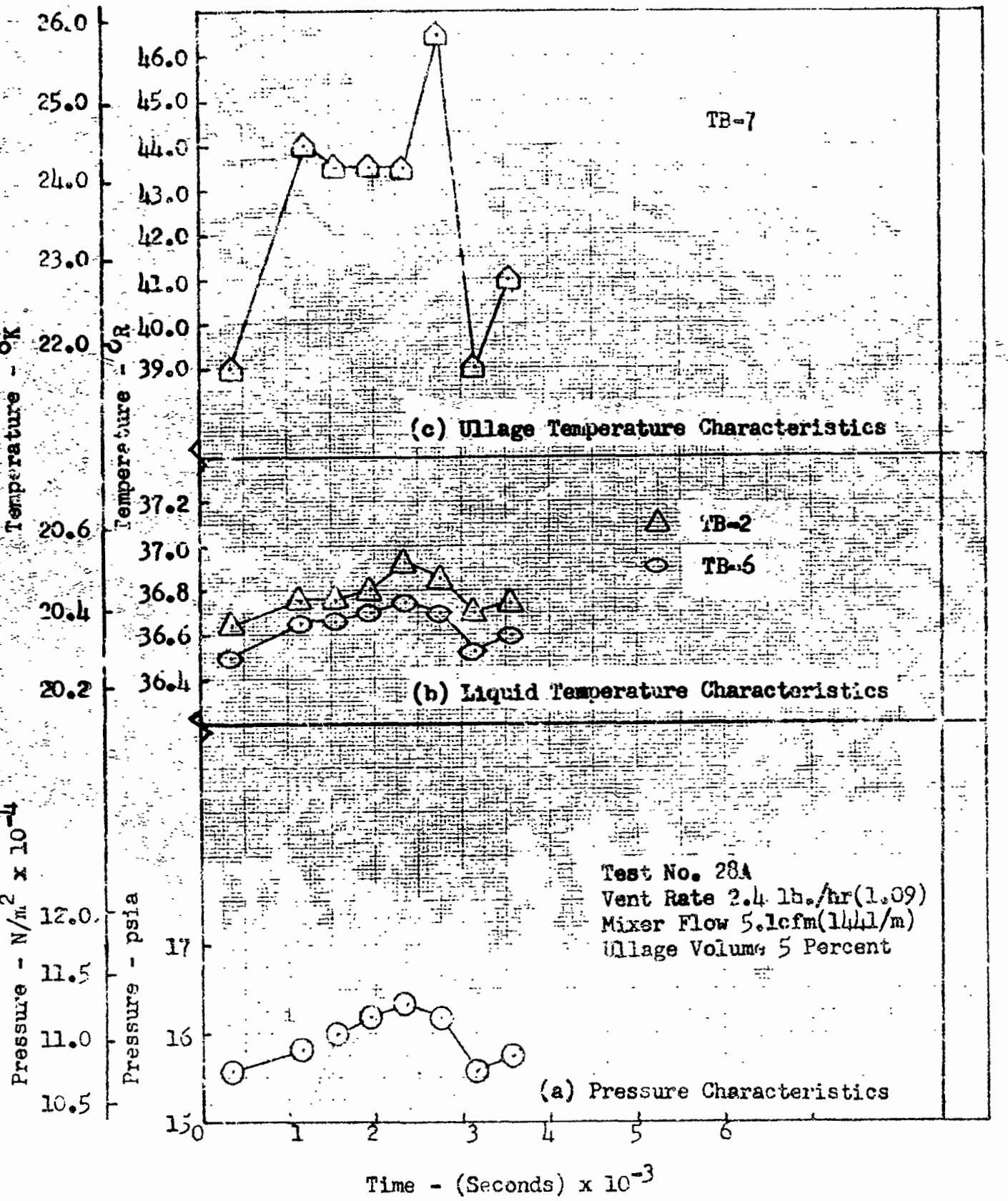

Figure 51 Automatic Control Characteristics without Helium Present

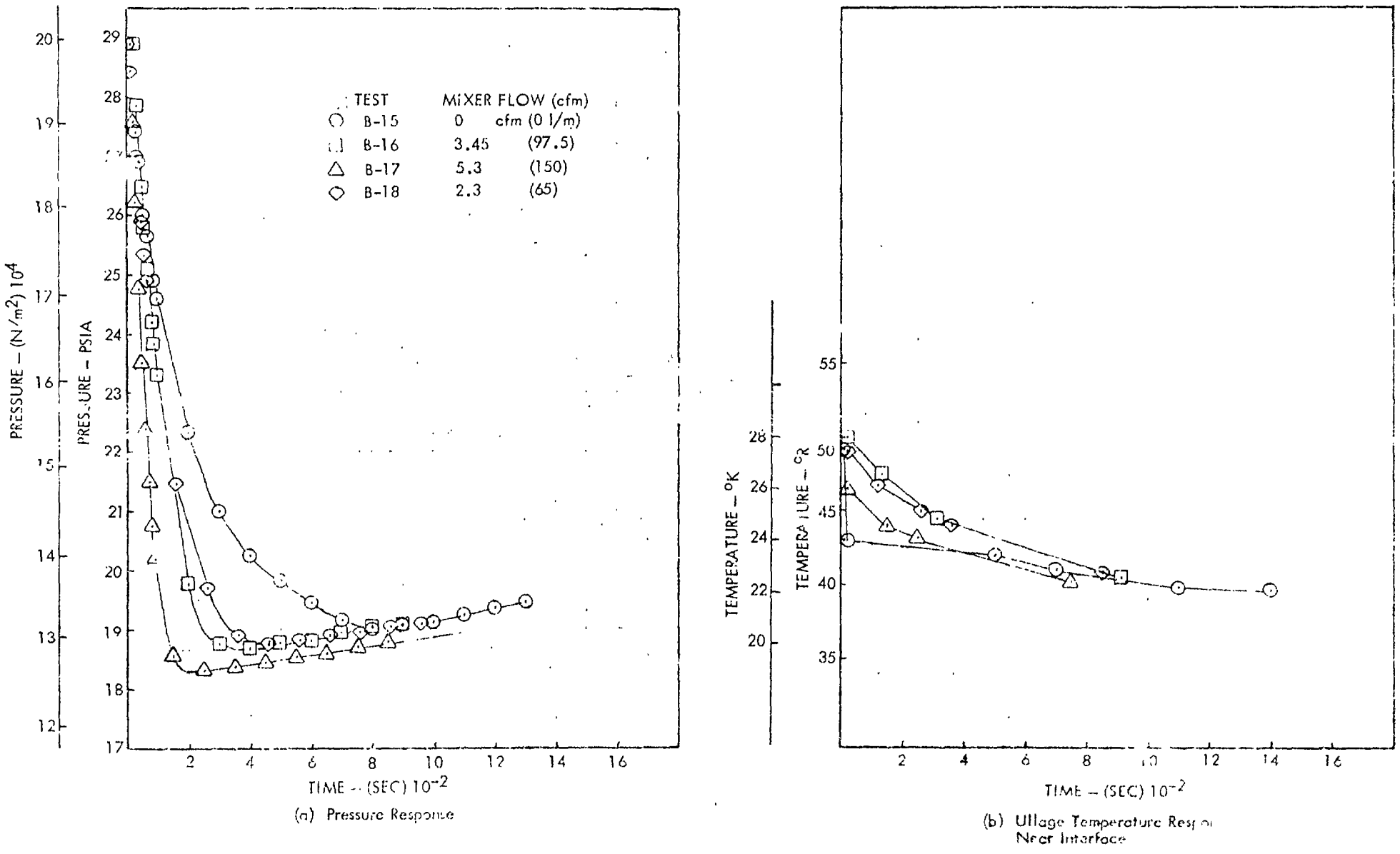

Figure 52 Effect of Mixer Flow at 5 Percent Ullage – Side Mount – 41.5 Inch (1.05 M) Diameter Tank

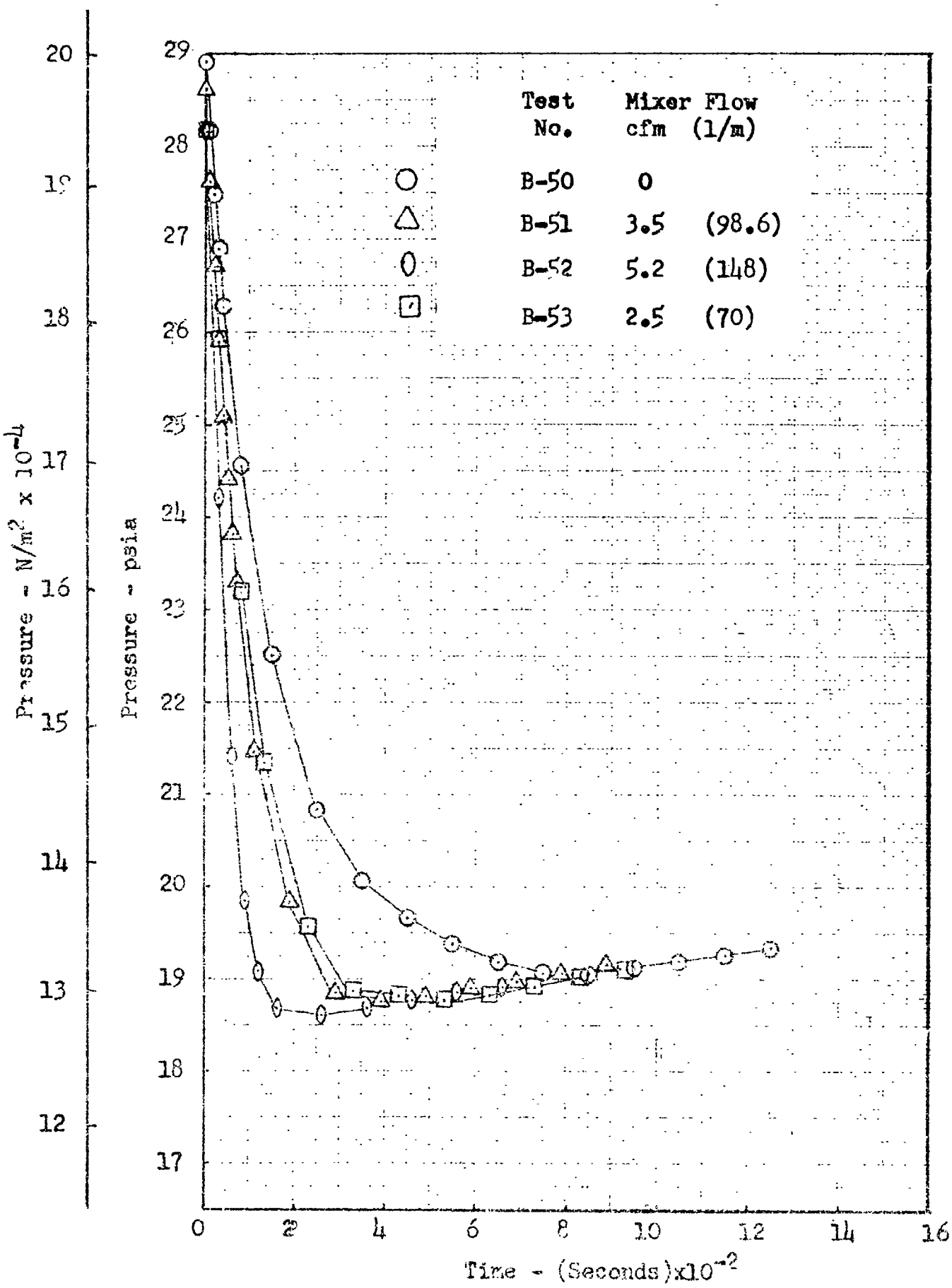

Figure 53 Comparative Effect of Mixer Flow Rate at 25 Percent Ullage - 41.5 inch(1.05m) Tank - Side Mount

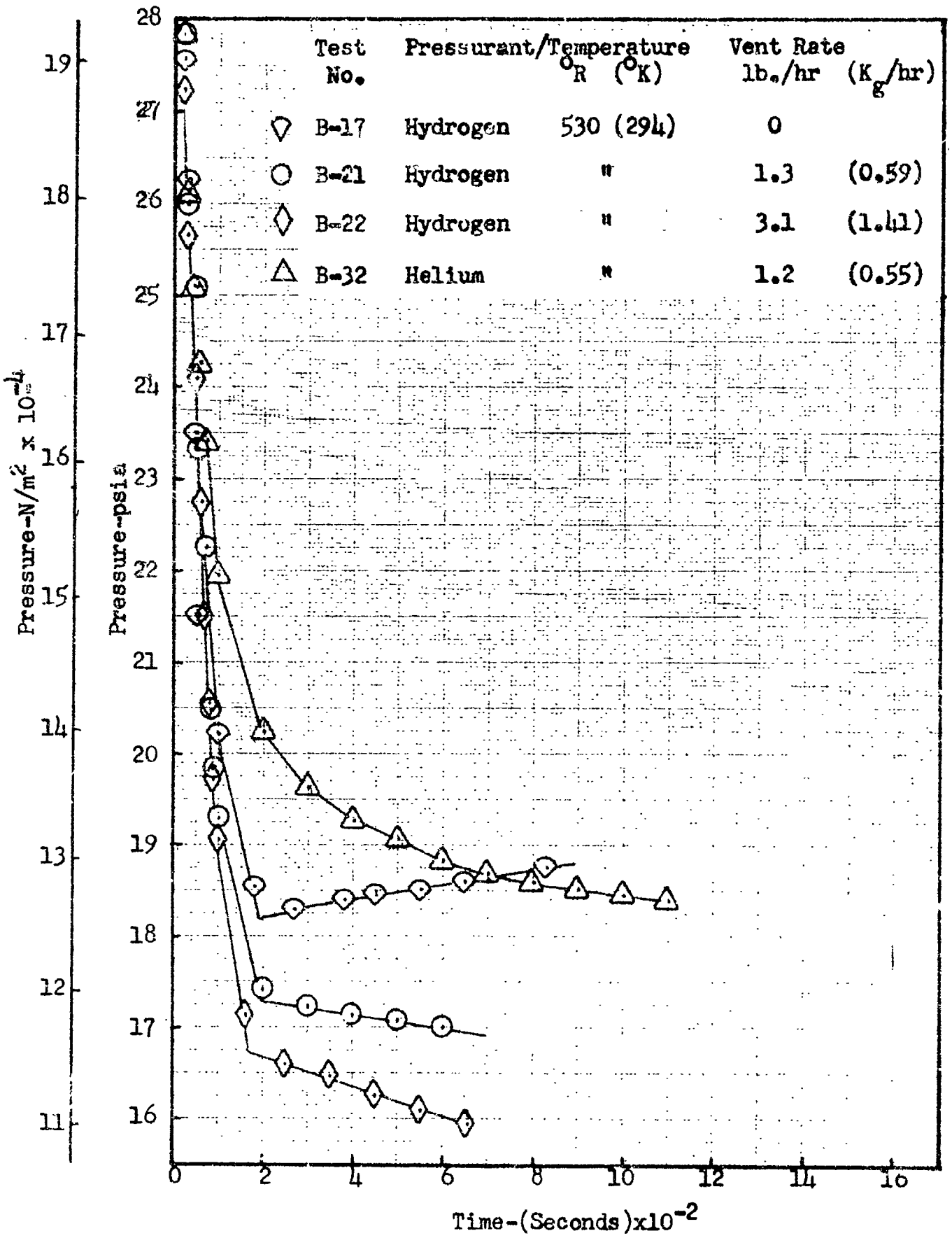

Figure 54 Effect of Vent Rate and Pressurant at 5 Percent Ullage - 41.5 inch(1.05m) Tank - Side Mount

boiloff test conducted before the side mounted test series indicated a boiloff rate of 0.9 lbs/hr (0.41 Kg/hr) which corresponds to 170 BTu/hr (50 w). For that reason, the equilibrium pressure rise rates are also higher. The influence of the various parameters was consistent with that determined from the bottom mounted tests. Figure 54 can be compared directly with Figure 44 to see that this is true for vent rate.

TEST RESULTS - 110 INCH (28M) DIAMETER TANK

The bottom mount test series covered the same parameters as for the 41.5 inch (1.05m) tank to get a direct comparison of the impact of increasing tank volume by a factor of twelve. Figures 55-57 show the influence of mixer flow rate on pressure response for different ullage ratios. Run No. 77 on Figure 56 was to be a natural pressure decay test following pressurization. However, after a very short drop, the pressure started a rapid rise, because of concentrated heating in the top of the tank. Rather than vent the tank, the mixer was turned on to the same conditions used for the subsequent test. The immediate response, and similarity to test 78 gives positive confirmation to the effectiveness of the mixer.

It can be seen from comparisons of Figures 55, 56, 57 that increasing the ullage volume from nominal five to thirty percent caused an increase in the mixing time. However, at seventy percent ullage, the time to minimum pressure was less than at thirty percent. The 41.5 inch (1.05m) tank data showed some indication of this. However, it was less conclusive by virtue of the very short response times involved for all conditions. It should be noted that the mixer jet was located approximately six inches above the liquid interface in both tanks when the ullage was seventy percent. Therefore, the liquid jet actually penetrated into the gas which would increase the interface contact area between the two phases. Camera failures prevented observation of this jet.

The relationships between vent rate and pressure control were consistent with the findings from the 41.5 (1.05m) diameter program. Figure 58 is typical, which shows that vent rate does not significantly effect the initial depres-

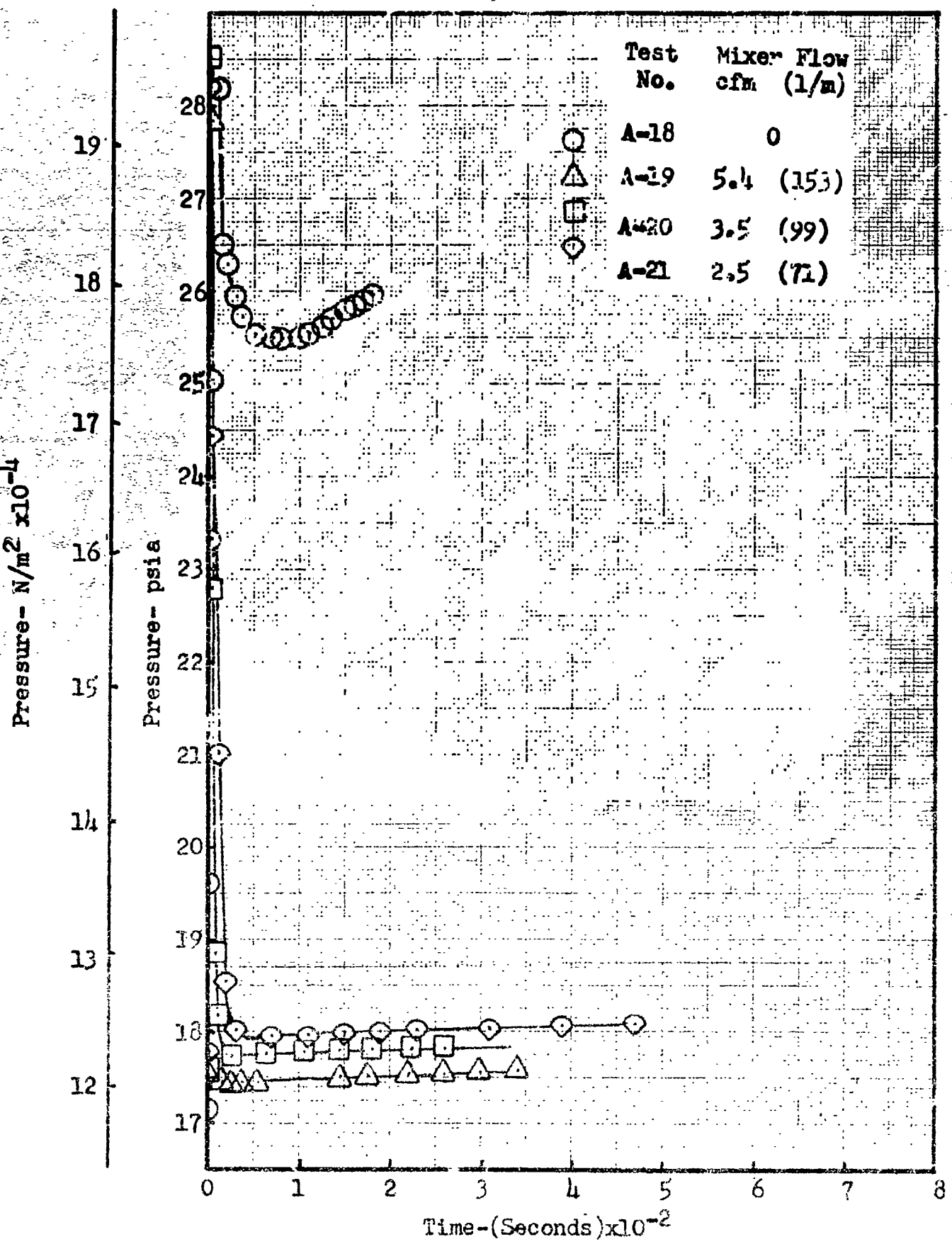

Figure 55 - Effect of Mixer Flow on Depressurization at 5 Percent Ullage - 110 inch (28m) Tank -- Bottom Mount

FOLDOUT FRAME 1

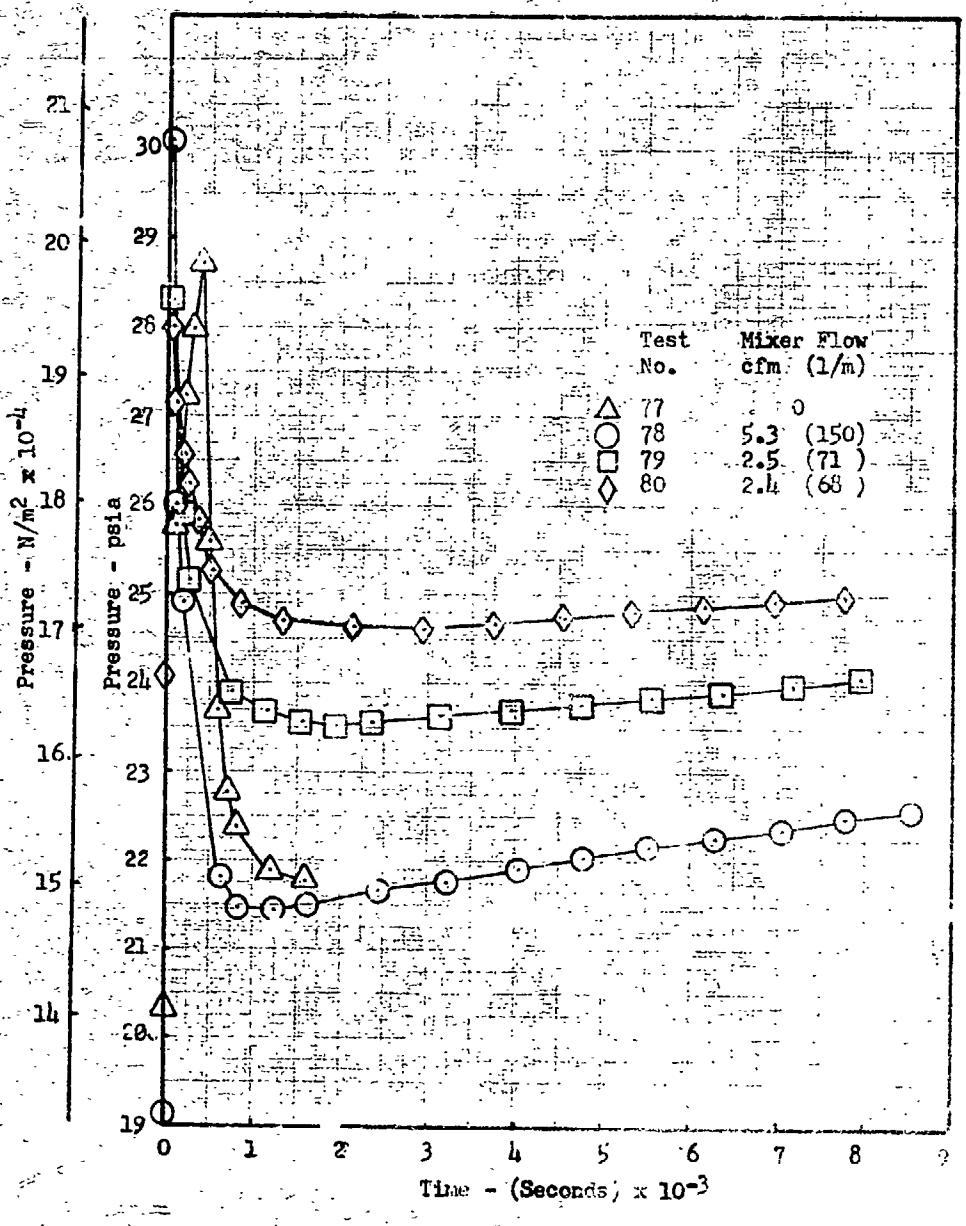

(a) Pressure Response

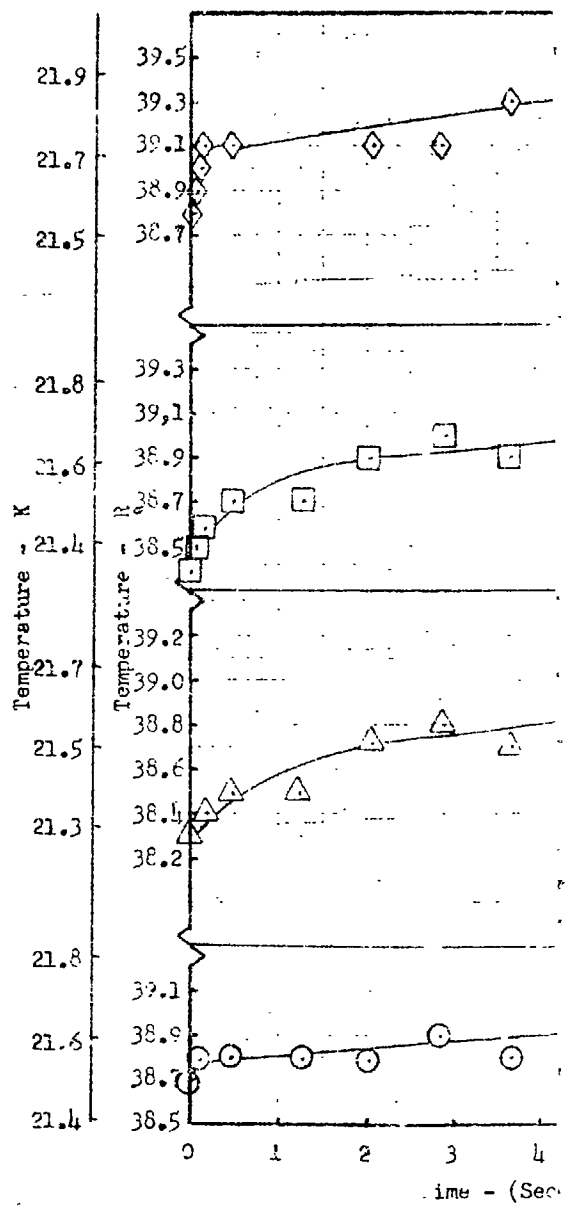

(b) Liquid Temperatures -

FOLDOUT FRAME 2

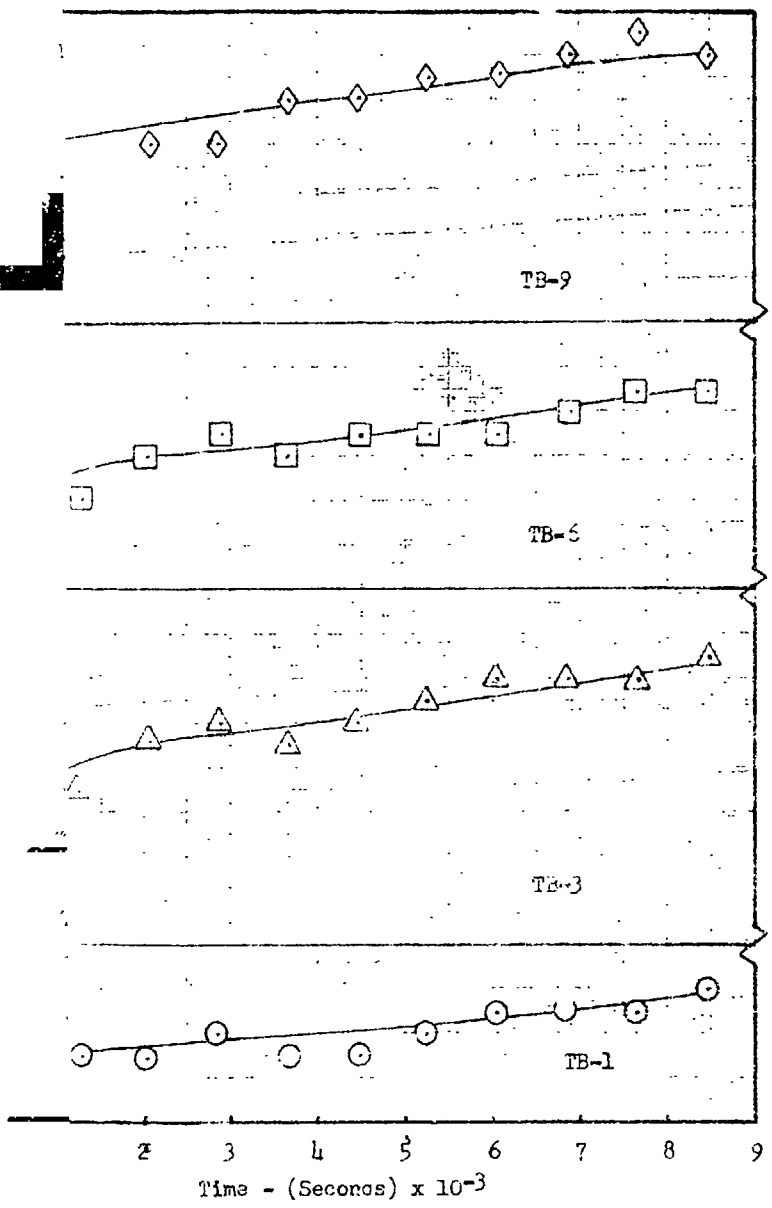

Temperatures - Test No. 78

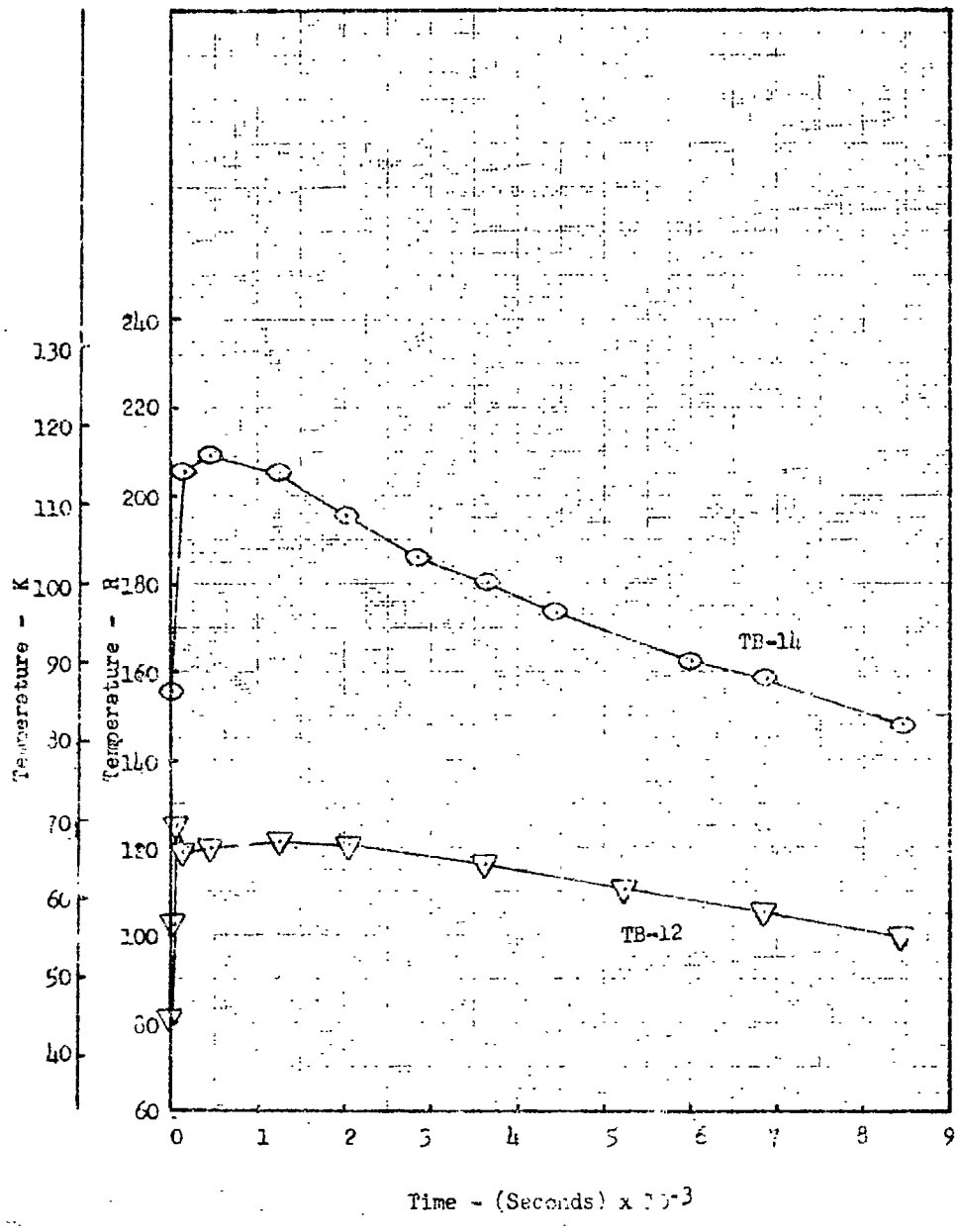

(c) Ullage Temperatures - Test No. 78

Fig. 86 — Comparative Effect of Mixer Below Rate at 29 Percent Ullage — 110 Inch (2.8M) Tank — Bottom Mount

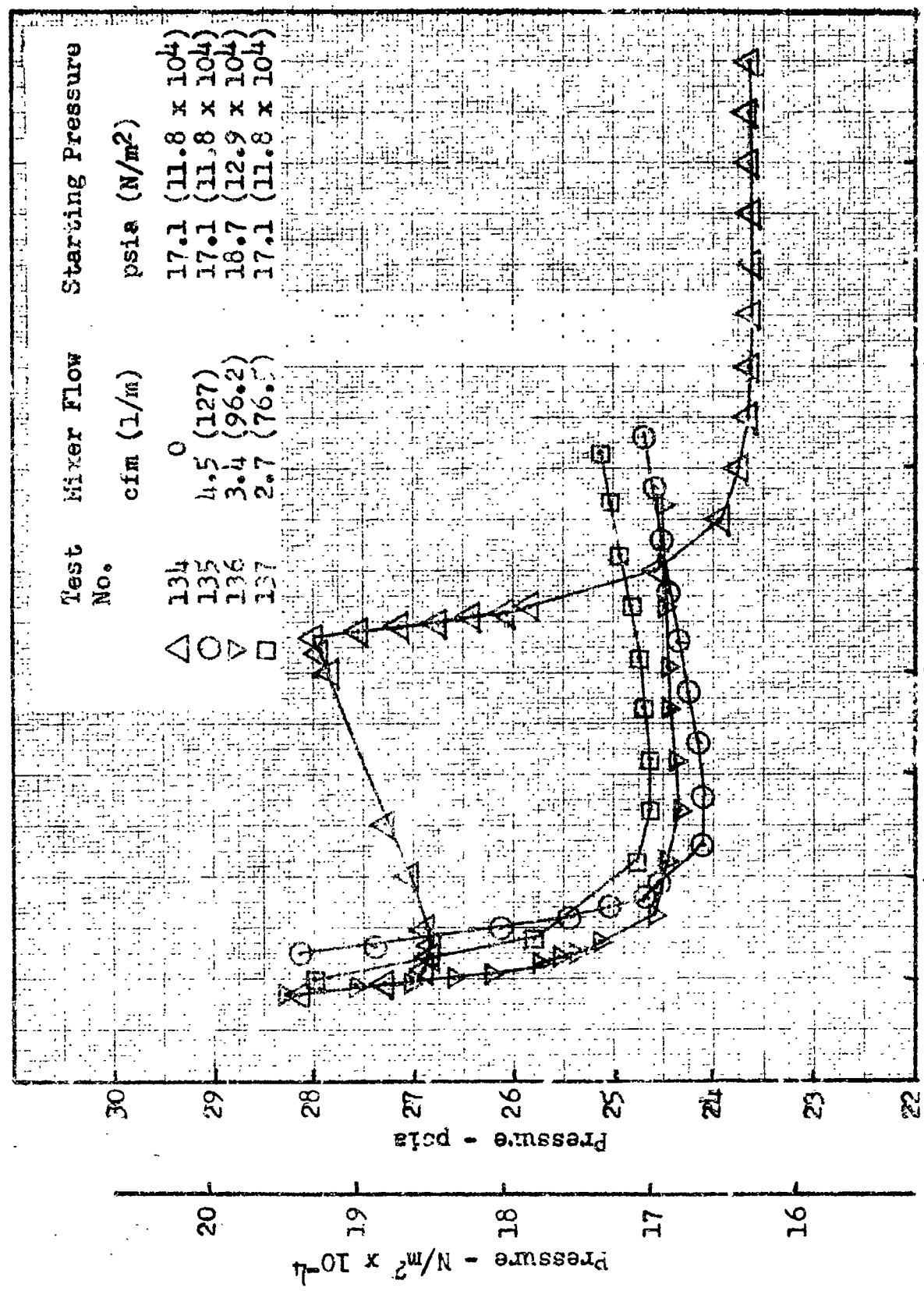

Figure 57 Comparative Effect of Mixer Flow at 70 Percent Ullage - 110 inch (2.8m) Tank - Bottom Mount

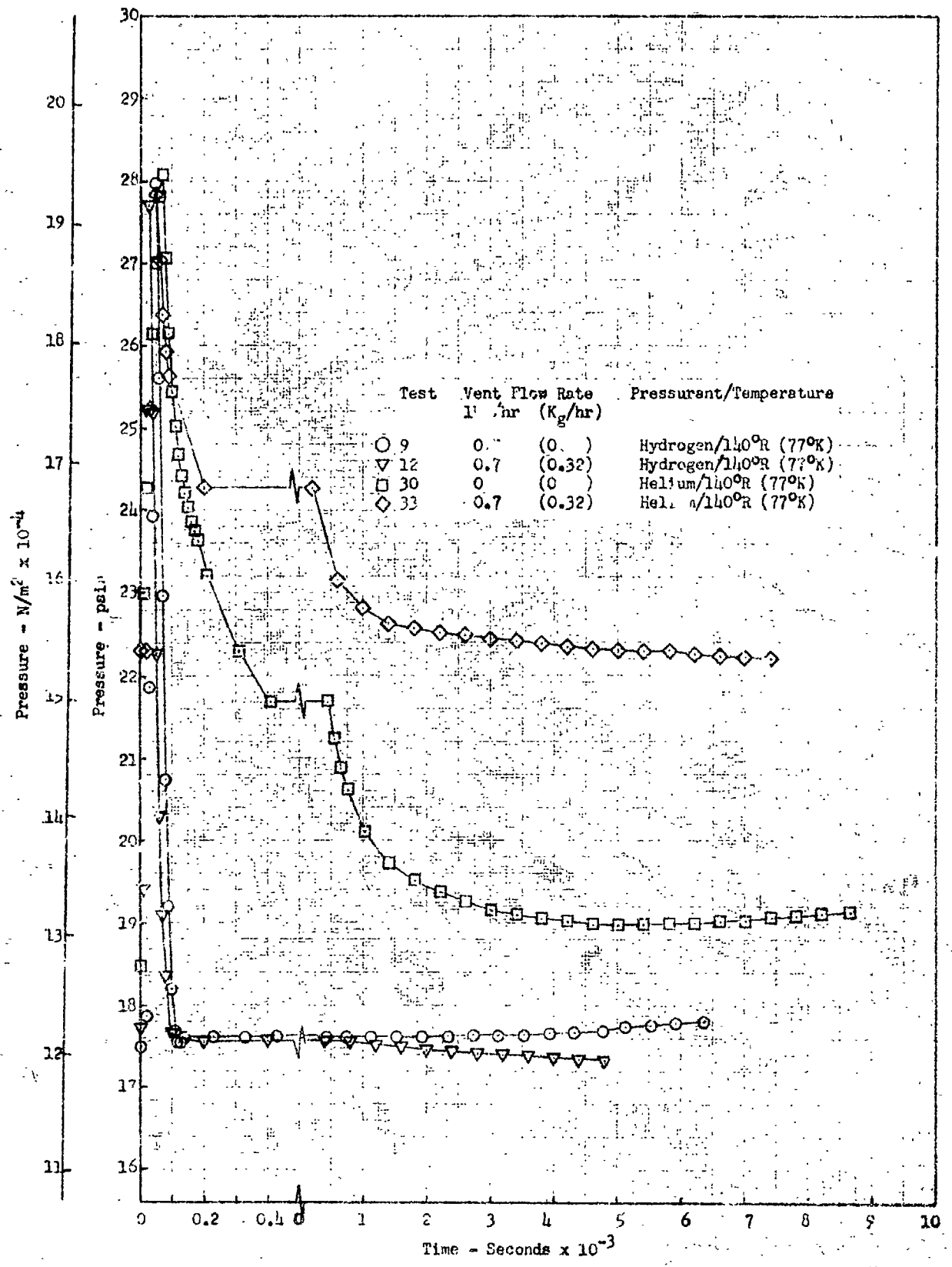

Figure 58 Comparative Effect of Vent Rate And Pressurant at 5 Percent Ullage - 110 Inch (2.8 m) Tank - Bottom Mount

surization but after equilibrium has been established, the steady state rate of change is proportional to the vent rate.

Figure 58 also presents a comparison of the response following pressurization with helium and with hydrogen. The time to achieve mixing is an order of magnitude greater with helium. However, the final equilibrium rates are the same.

Figure 59 also compares helium and hydrogen pressurant, when the ullage volume is nominally 75 percent. Here, it is noted that the two are equally responsive to mixing. This further suggests a greatly increased contact area between the two phases. As indicated previously, the transient depressurization occurs with surface evaporation (i.e., a mass transfer phenomenon). Apparently the long time constants associated with helium pressurant and low ullage volumes occur because the process is limited by mass diffusion through a helium rich gas layer near the interface. Inserting the jet directly into the ullage reduced the concentration gradient at the interface by virtue of the more widely dispersed contact and probably by increased gas convection. Therefore, if a jet is designed to penetrate the liquid-ullage interface in zero gravity, it can be expected that helium will not retard the depressurization, and the shorter time constants experienced with hydrogen will be more representative.

Figure 60 shows the pressure and temperature histories for a test wherein the tank was pressurized to 38 psi (193,000 N/m^2) with 140°R (77°K) helium and the TCU was activated to automatically control tank pressure through one complete cycle. It took approximately 33 hours to bring pressure down to the automatic cutoff value. Thereafter, cycle time was approximately one (1) hour. The long cool down time is partly due to the helium time constant but primarily due to a shift in the operating level of the pressure switch. Had the latter been operating at a nominal seventeen psi, the cool down period would have been reduced to approximately twelve hours. The automatic cycle at the end of Run 49 is shown on an expanded scale in the upper portion of Figure 60. It is compared with one cycle from test No. 28 which was an automatic control test with no pressurization. The latter is superimposed on the time scale for test No. 49. The characteristic shape and nearly identical cycle periods

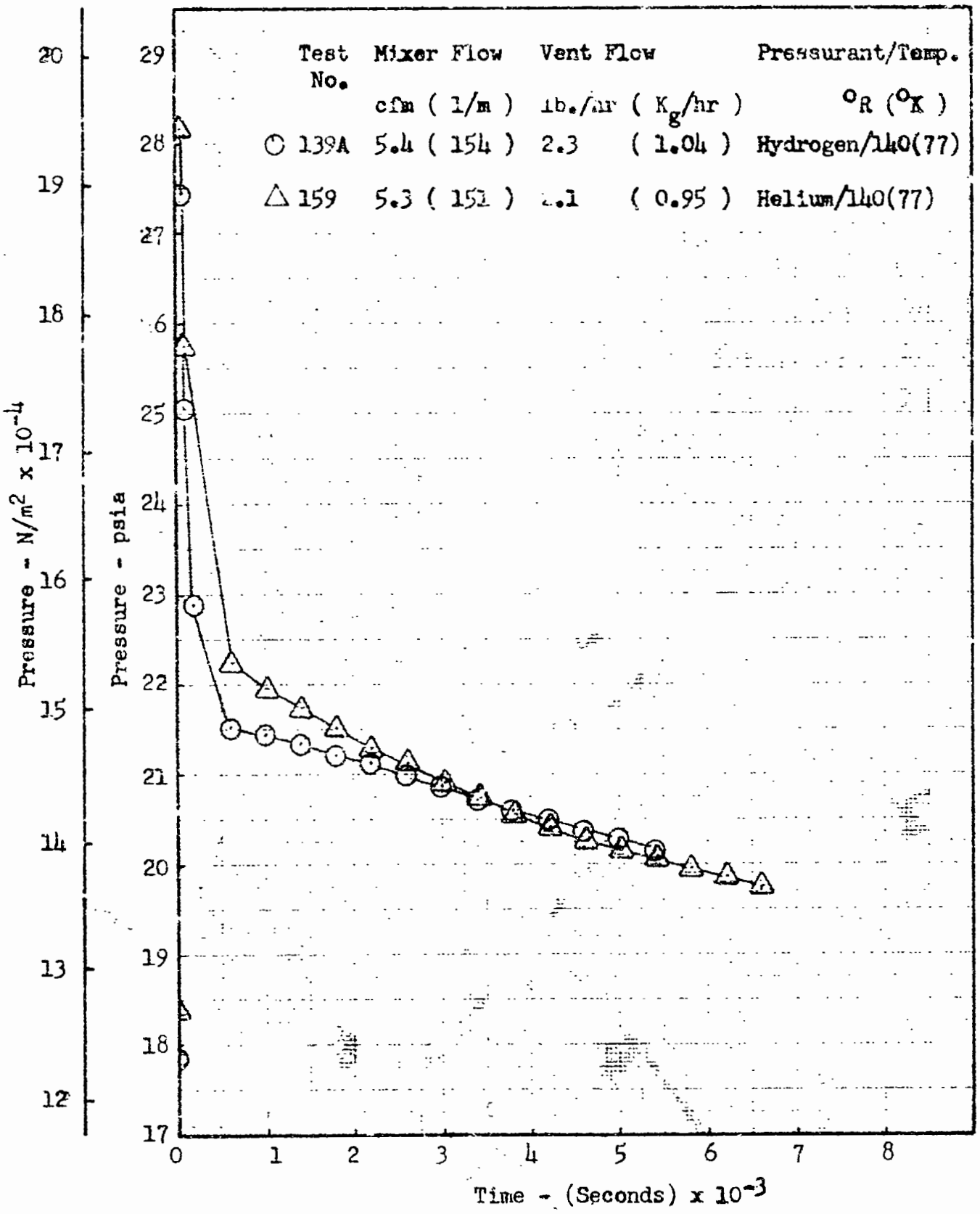

Figure 59 Comparative Effect of Helium and Hydrogen Pressurants at 70 Percent Ullage - 110 inch(2.8m) Tank - Bottom Mount

FOLDOUT FRAME /

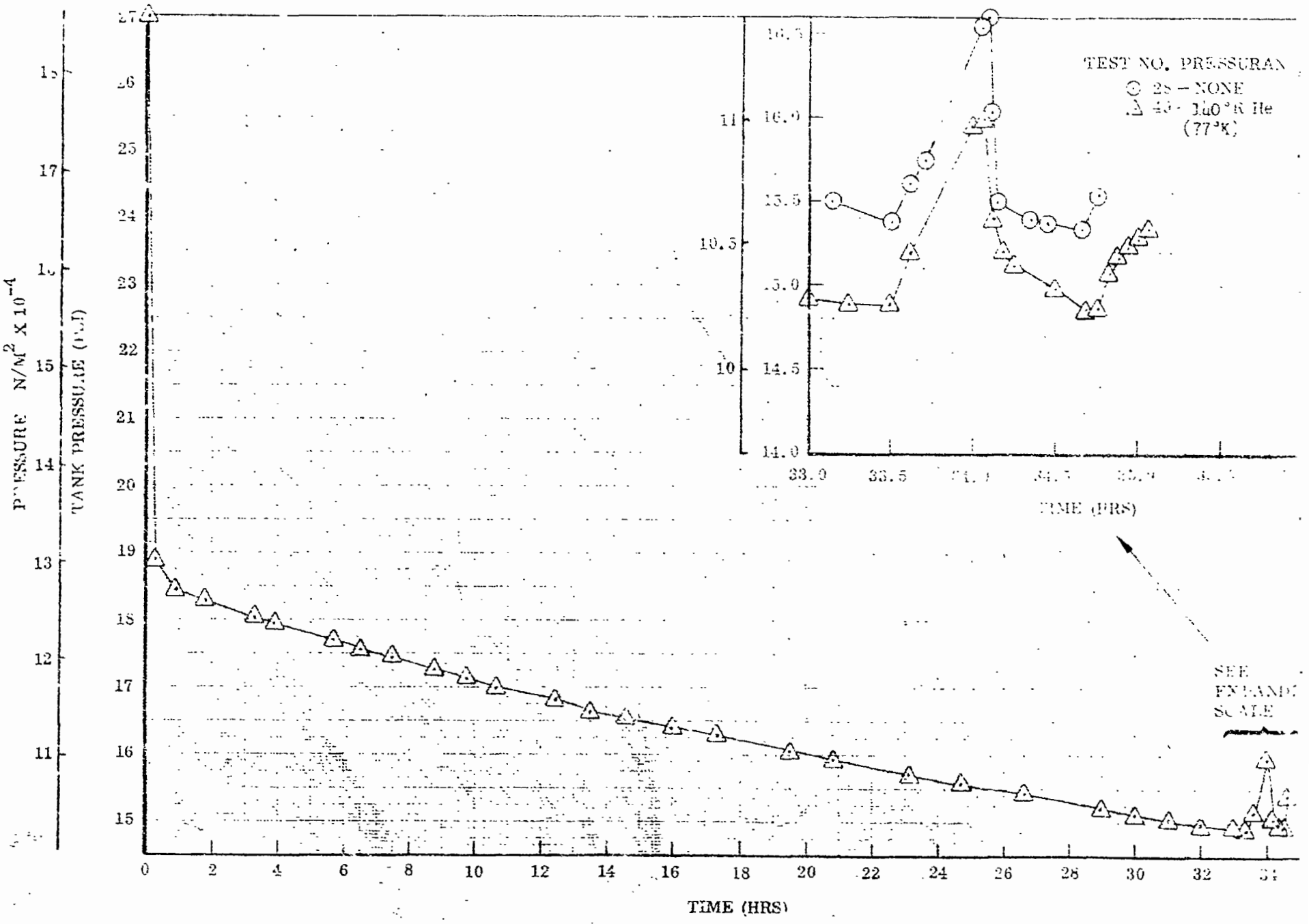

(a) Pressure Response

FOLDOUT FRAME 2

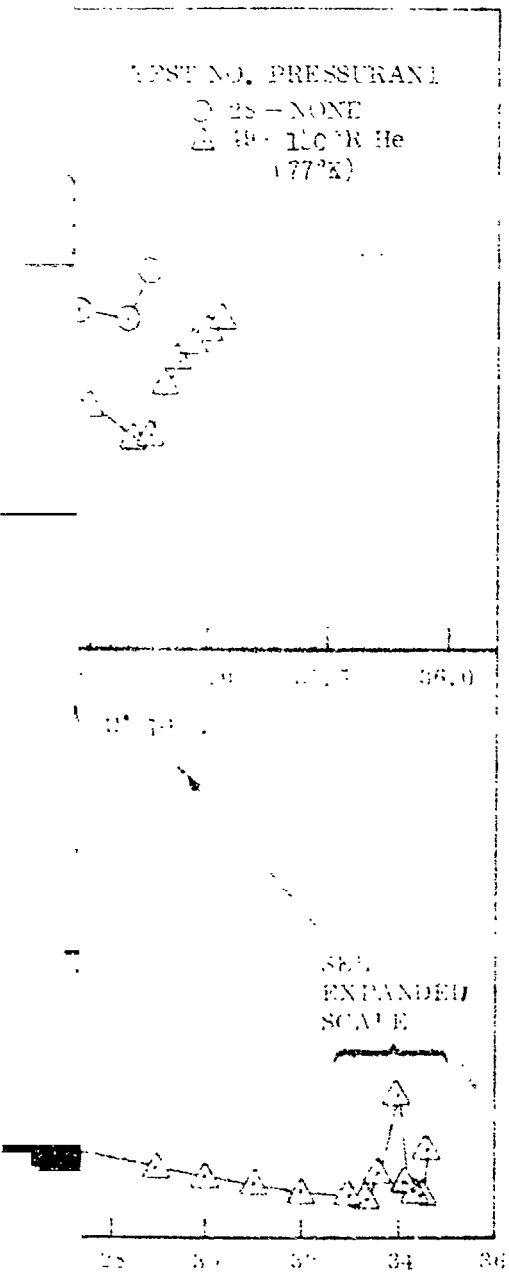

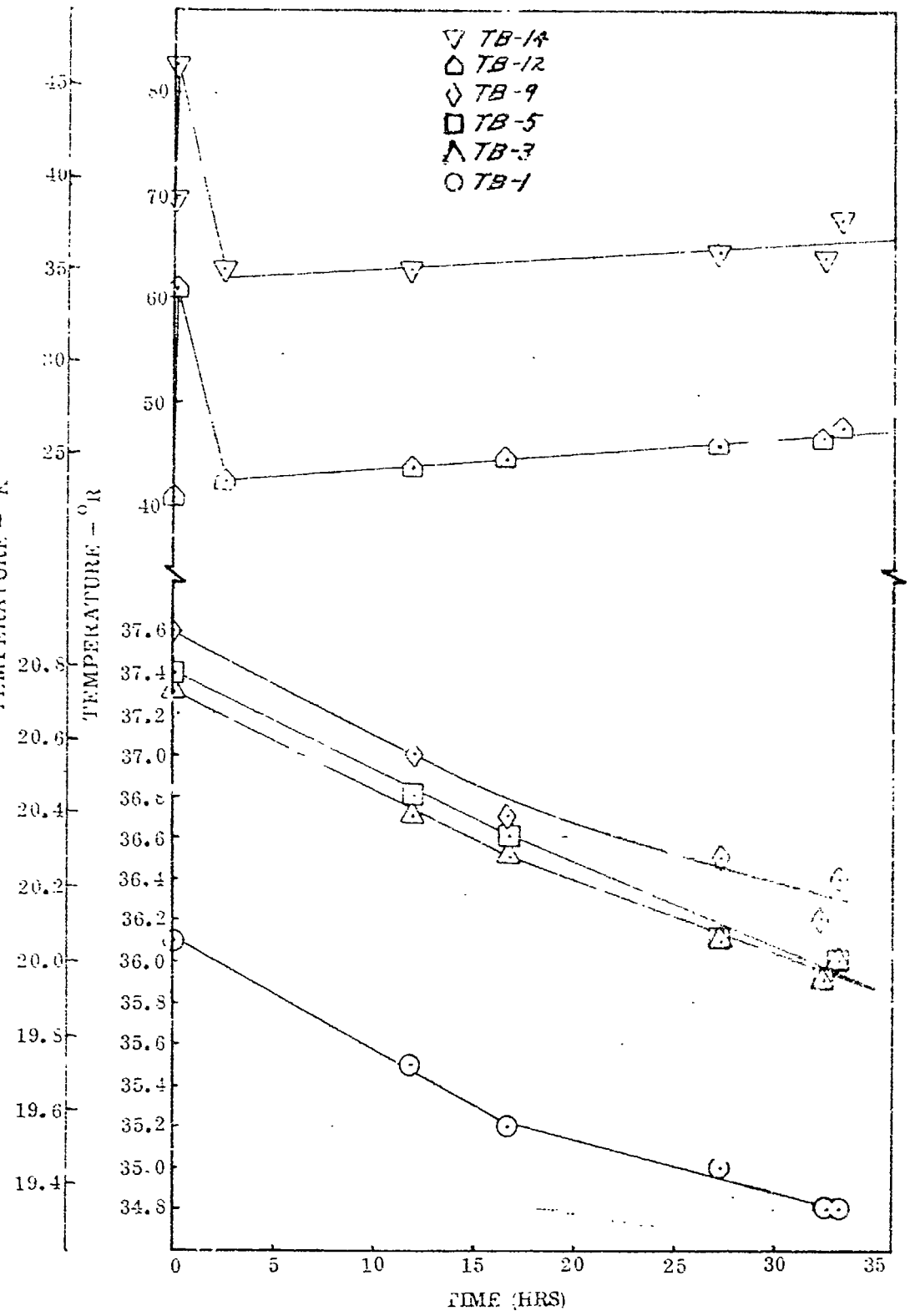

(b) Temperature Response

Fig. 60 – Pressure and Temperature Response For Automatic Control Test Following Pressurization With Helium – 110 Inch (2.8M) Tank – Bottom Mount

FOLDOUT FRAME /

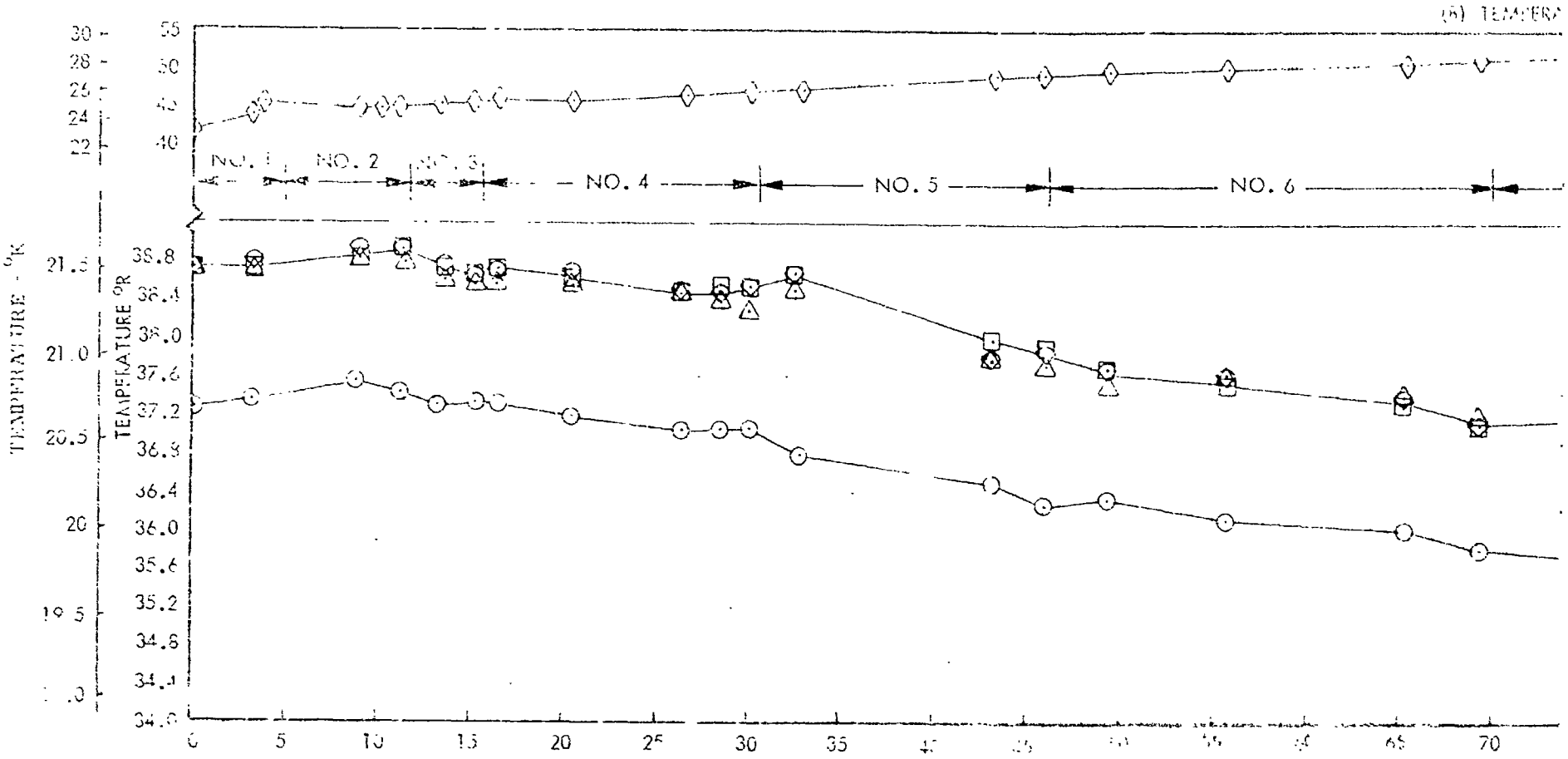

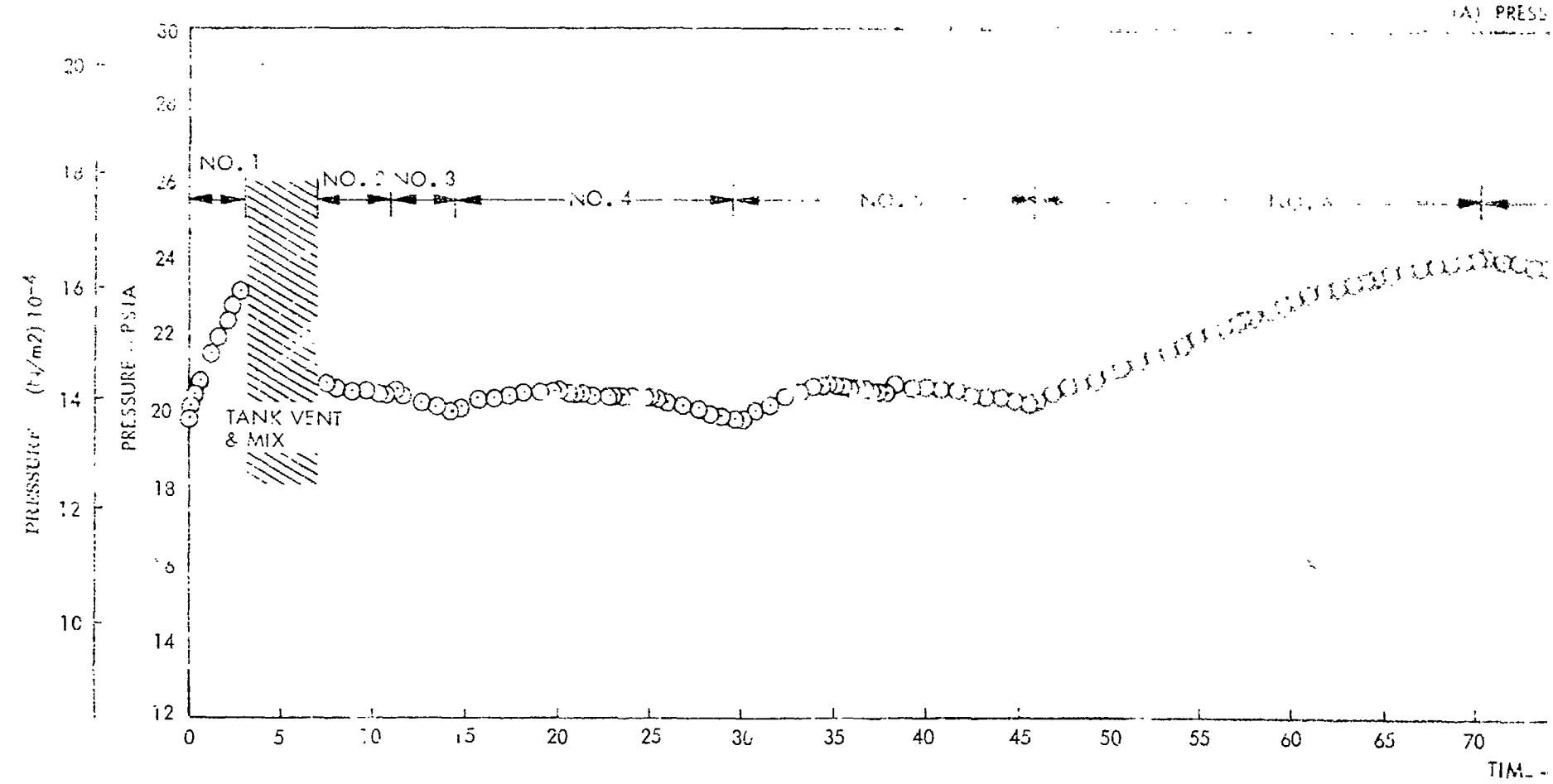

FOLDOUT FRAME 2

TURE HISTORIES

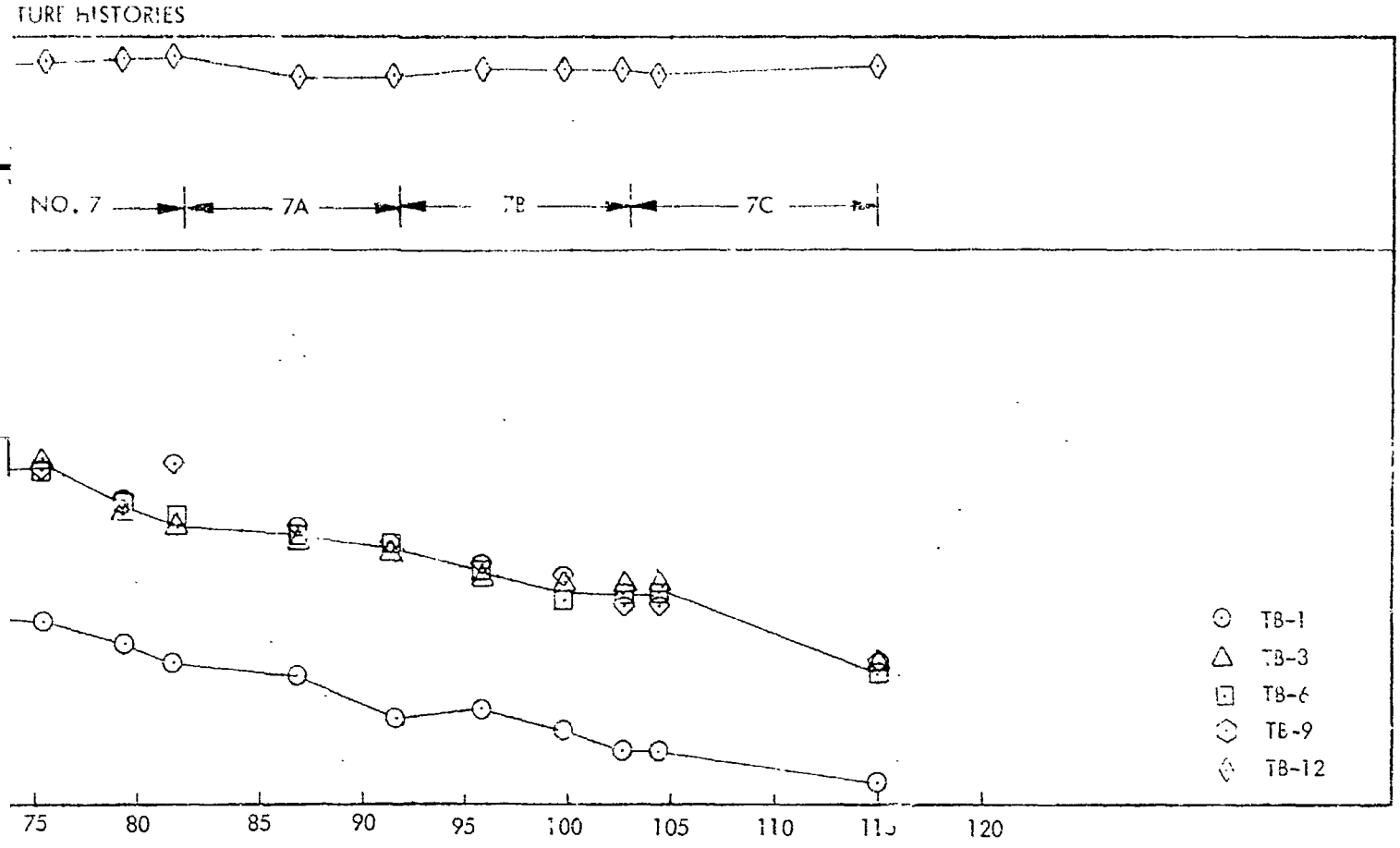

JRE HISTORIES

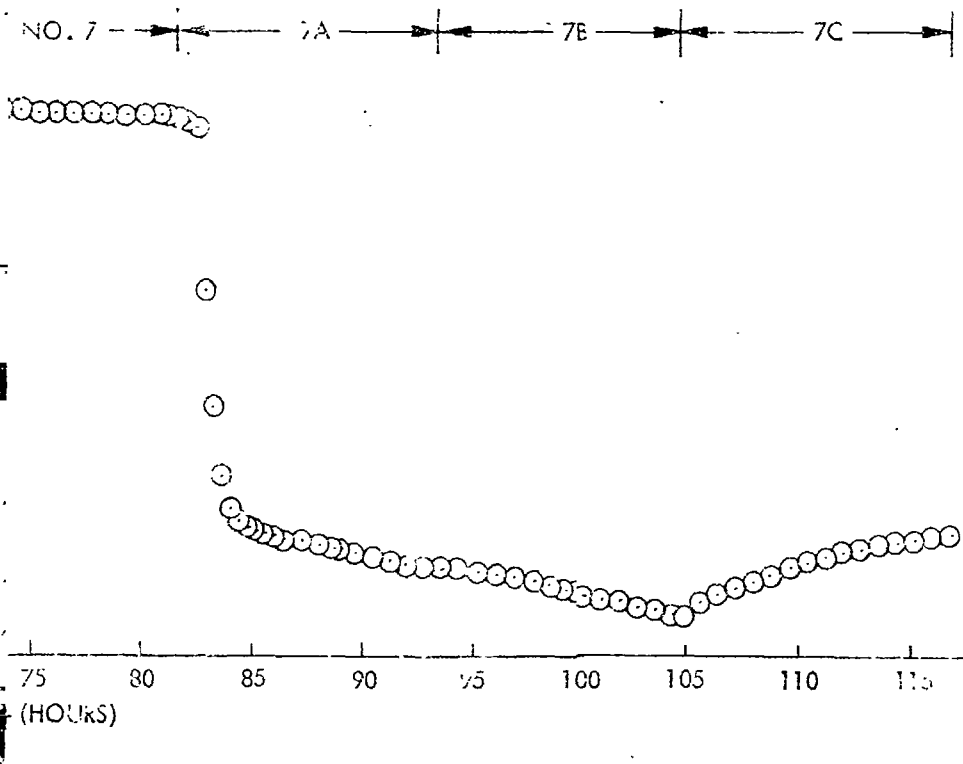

RUN NO.	VENT RATE LB/HR	KG/HR	MIXER FLOW CFM	L/M
1	0		0	0
2	2.3	1.05	5.6	158
3	3.6	1.65	5.6	158
4	2.0	0.91	3.6	102
5	3.3	1.50	3.6	102
6	2.0	0.91	2.6	73.5
7	3.1	1.41	2.7	76.5
7A	3.1		5.6	158
7B	3.0	1.36	3.6	102
7C	2.9	1.32	2.7	76.5

Fig. 61 – Temperature and Pressure Histories for Tests 1 Through 7 -- 110 Inch (2.8M) Tank -- Side Mount

confirm that the helium does not degrade the steady state performance of the system which is governed by thermal convection in the heat exchanger.

The results from the side mounted tests indicated that mixing was much less effective (when the mixer discharges below and parallel to the interface) than it was for the bottom mount installation. Figure 61 shows the pressure and temperature responses for the first seven tests in this series. These were run consecutively, with no pressurization, simply by switching to the appropriate valve or changing mixer speed.

The nominal ullage volume was approximately 5 percent for which the liquid level is 20 inches (0.5m) above the mixer. At the high mixer flows, the response rates were comparable to those from the bottom mounted tests. However, when the mixer flow was reduced (e.g., Run 4) the pressure actually reversed and it took approximately two hours before the pressure started back down, indicating that the low speed mixing was probably not sufficient to overcome stratification. When the mixer flow was further reduced (e.g., Run 6), the pressure continued to rise for seven hours. To insure that the problem was due to insufficient mixing, Runs 7A, 7B and 7C were run, varying only mixer speed. These were repeats of 3, 5, and 7 but in different sequence. When the mixer flow was increased from 2.6 to 5.6 cfm (73.6 to 158 l/m) (e.g., 7A) there was immediate response, as shown on Figure 61. This differed from the bottom mount tests wherein even the lowest mixer speed was sufficient to destratify the liquid.

Subsequent tests, wherein the tank was pressurized to 28 psi (193,000 N/m^2), substantiated the lack of good mixing. Figures 62-63 show some typical results, directly compared with similar tests from the bottom mounted series. Note that the time to achieve minimum pressure is an order of magnitude greater for the side mounted configuration, even for the highest mixer flow rate.

All of tests in this side mounted series, including those with venting, required much longer times to achieve equilibrium. However, for the tests where good mixing was obtained, the influence of vent rate, pressurant conditions, and ullage volume was consistent with the findings from the bottom mounted series in this tank and from the 41.5 inch (1.05m) diameter tank tests.

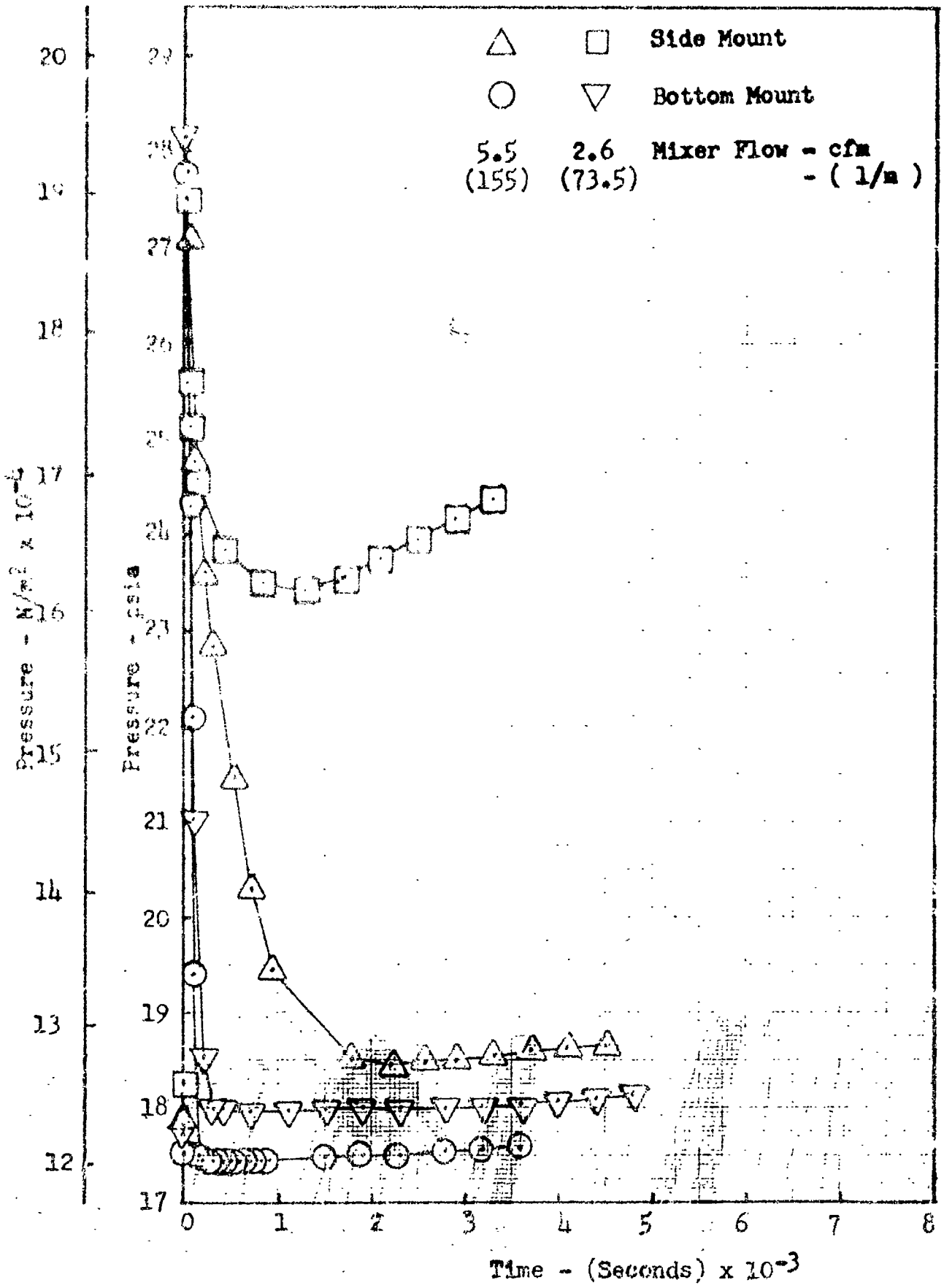

Figure 62 Comparative Pressure Response at 5 Percent Ullage - Bottom and Side Mount Configurations - 110 inch(2.8m) Tank

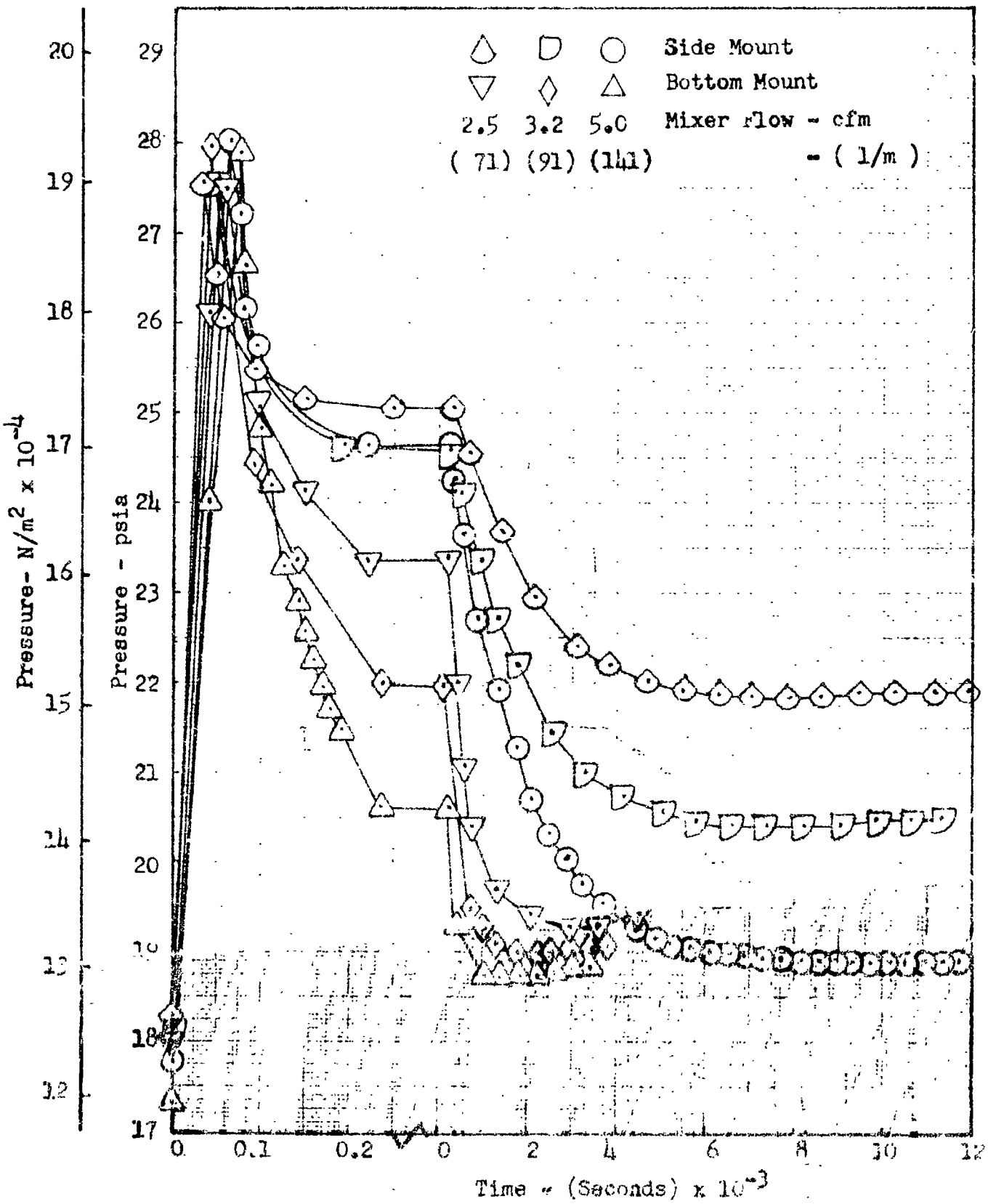

Figure 63 Comparative Pressure Response at 29 Percent Ullage - Bottom and Side Mount Configurations - 110 inch(2.8m) Tank

In the first series of tests with the extended mixer jet (configuration B), the vapor traps were charged with 140°R (77°K) gaseous hydrogen before the thermal conditioning system was activated. Figure 64 presents a comparison of the pressure responses as affected by three different mixer flow rates. The ineffectiveness of the low flow condition is indicated by the rapid rate of pressure increase. When the mixer speed was increased to the value used for test No. 3, it took approximately an hour to pull the pressure down, and come to a steady response rate. The final rate was comparable to that from test No. 3 and consistent with a mixed model prediction. Temperatures are shown at several points in the tank for these two tests on Figures 65 and 66.

Figure 66 further confirms the inadequacy of the mixer at the low speed but also indicates that the intermediate speed is not capable of depressurizing the stratified tank. However, the highest mixer flow rate is sufficient to control tank pressure but the response is comparable to those from the side mount without the extended duct. For test No. 9A shown on Figure 67, the traps were filled with 140°R (77°K) gaseous helium. The effects of the helium are similar to those noted previously, i.e., longer time constant indicating mass diffusion limitations, and higher final pressure due to the helium partial pressure. It is also interesting to note that the gas interface was always raised above the hot wire sensor when the liquid was pressurized, but with helium, it receded again when the pressure was reduced by mixing. This was not so with hydrogen, which indicates that the trapped vapor was being condensed by compression.

The effect of vent rate can be seen by comparing the responses between tests No. 4 and 5 on Figure 64. Also, note that near the end of test No. 4, the vent flow rate was increased to the value used for test No. 5 and the pressure response became parallel for the two runs.

Further illustration of the effect of vent flow rate is shown on Figure 68. A comparison of tests No. 3 on Figure 64 and test No. 13 on Figure 68 shows steady state pressure response of 0.15 psi/hr. Thus, there is no apparent effect of precirculation on final pressure response rate. Near the end of test No. 12 (Figure 68), the flow was increased from 5.4 cfm to 6.9 cfm (153 to 195 lpm) with no drop in pressure. This seems to confirm results from the previous test

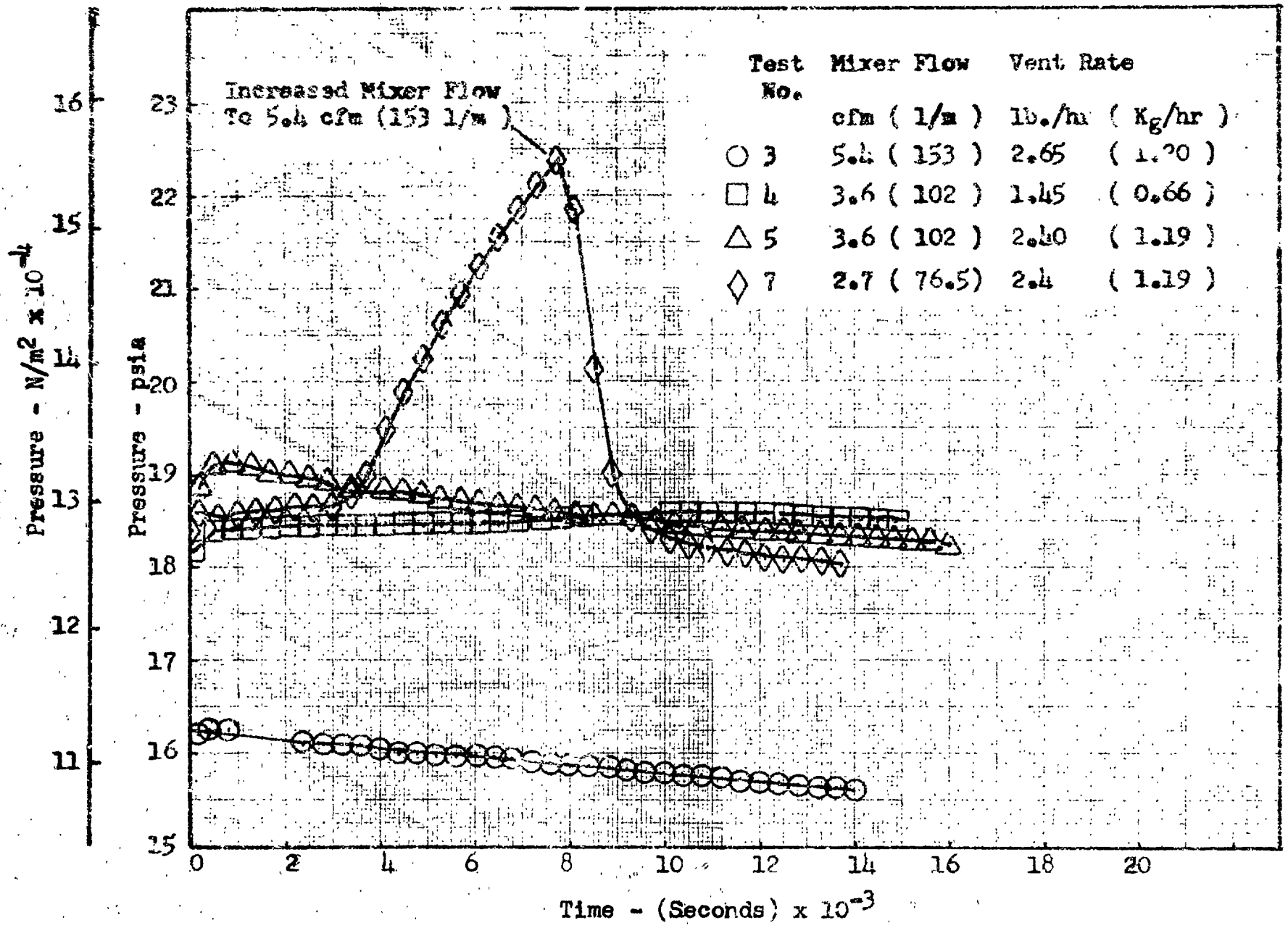

Figure 64 Effect of Mixer Flow Rate with Vapor in Trap - Configuration B

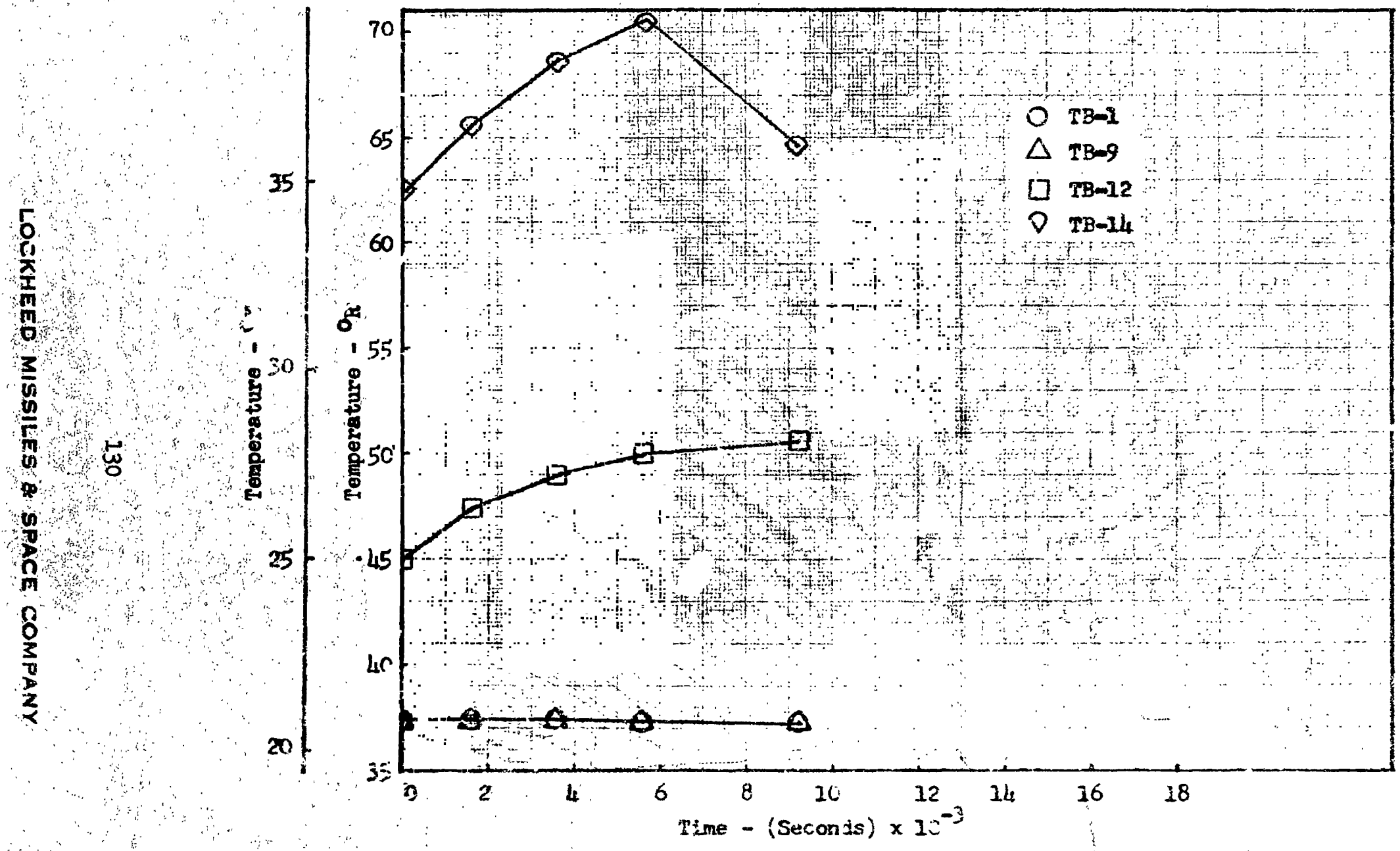

Figure 65 Temperature History for Test No. 1 - 110 inch(2.8m) Tank - Configuration B

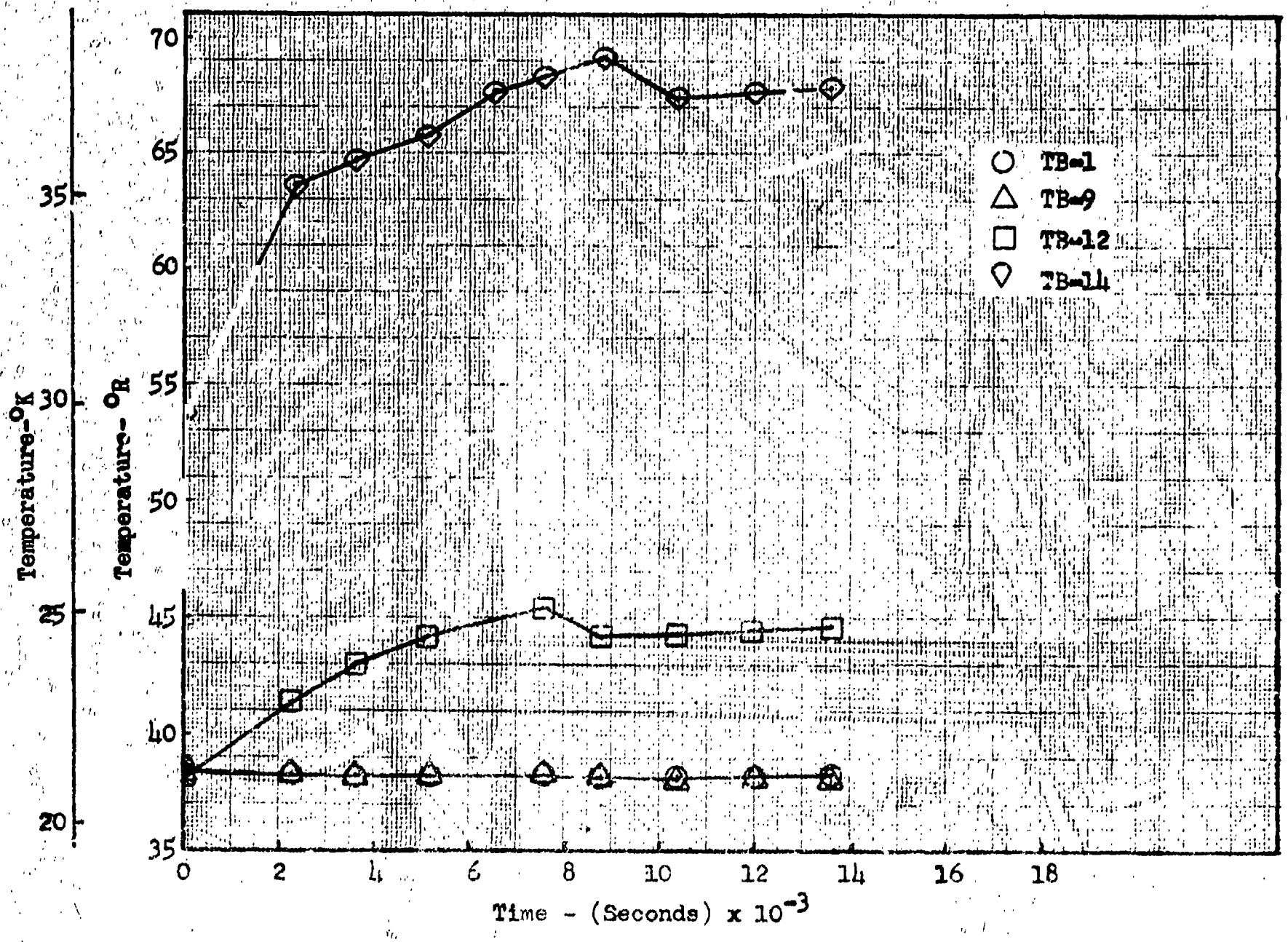

Figure 66 Temperature History for Test No. 7 - 110inch(2.8m) Tank Configuration B

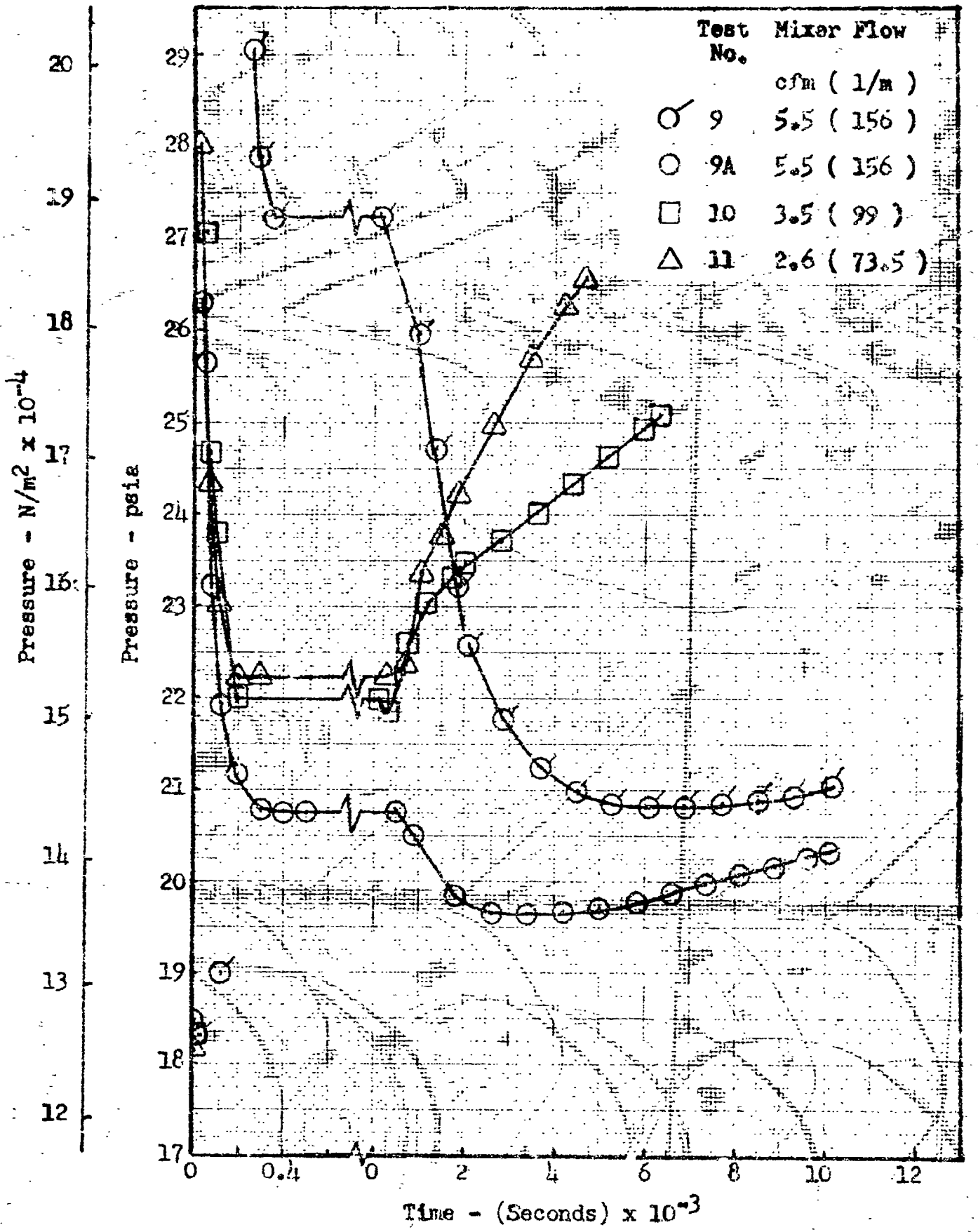

Figure 67 Effect of Mixer Flow on Tank Depressurization with Vapor in Trap - Configuration B

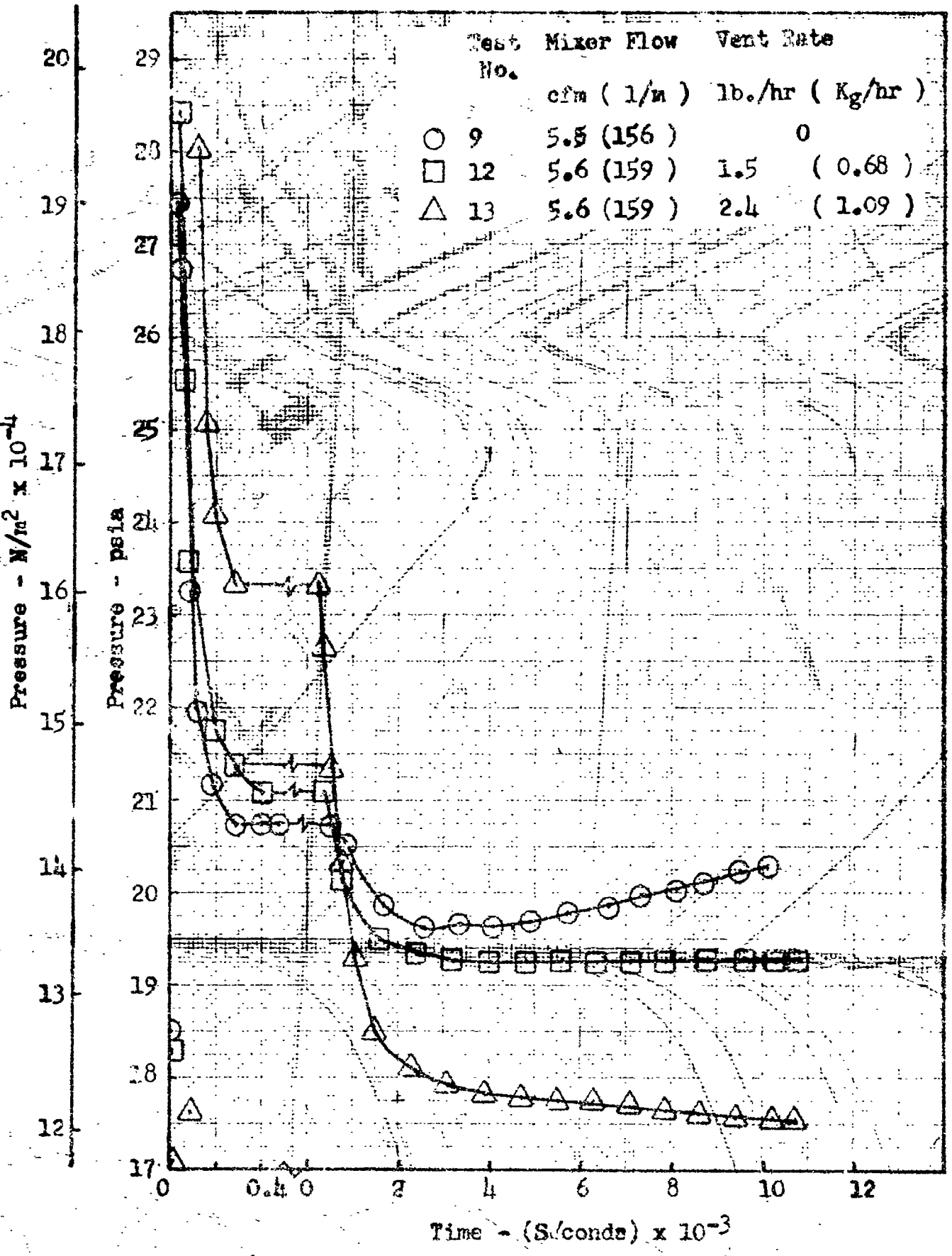

Figure 68 Effect of Vent Rate on Depressurization at 5 Percent Ullage - Configuration B

series, that indicated 5.4 cfm (153 lpm), which is near the original design value, is sufficient to mix the tank contents even in the one g environment.

The second series of tests with this configuration was conducted without the vapor in the traps. Fig. 69 is typical of the results which generally showed no discernible effect of the trapped vapor. Again, note the immediate response (test No. 23) when the mixer flow is increased from 2.7 cfm to 5.4 cfm (76.5 to 153 lpm). Fig. 70 shows the temperature histories for test No. 23.

The nozzle used for configuration 5 appears to have served the purpose for which it was intended, i.e., improving circulation. In the previous side mounted tests, with and without the crossover duct, it was found that the lower mixer flow rates were generally inadequate for controlling tank pressure. With the nozzle configuration, one run (test 11) shows a propensity for no control. This is shown on Fig. 71, which compares the pressure response for the three nominal mixer flows. The characteristics exhibited by test 11 were not found throughout the remainder of this test series (e.g., runs 23, 45, 62). Therefore, an attempt was made to duplicate the run after all other tests had been completed. This is shown on Fig. 71 as test 11A. The peak pressure is lower (because of an exhausted pressurant supply) but it is nevertheless significant that the pressure response is not sluggish as it was for test 11.

When conducting this series of tests, the procedure called for venting the tank down at the end of each test until bulk boiling occurred, as indicated by vapor generation in the traps. The drop needed to achieve this condition should provide an indication of the amount of subcooling in the bulk liquid. It can be seen from Fig. 71 that even the highest mixer flow exhibits subcooling by this criteria, although it gets progressively larger as mixer flow decreases. It is interesting to note that a straight line through the starting and ending saturation pressures indicates a rate of pressure rise approximately equal to the mixed model prediction, with the measured heat input of 235 Btu/hr (69w). It is also parallel to the measured, steady state slope of the pressure history curves; except for test 11.

Temperature histories for runs 10 and 11 are shown on Figs. 72 and 73. The following listing contains a more informative comparison of the differences

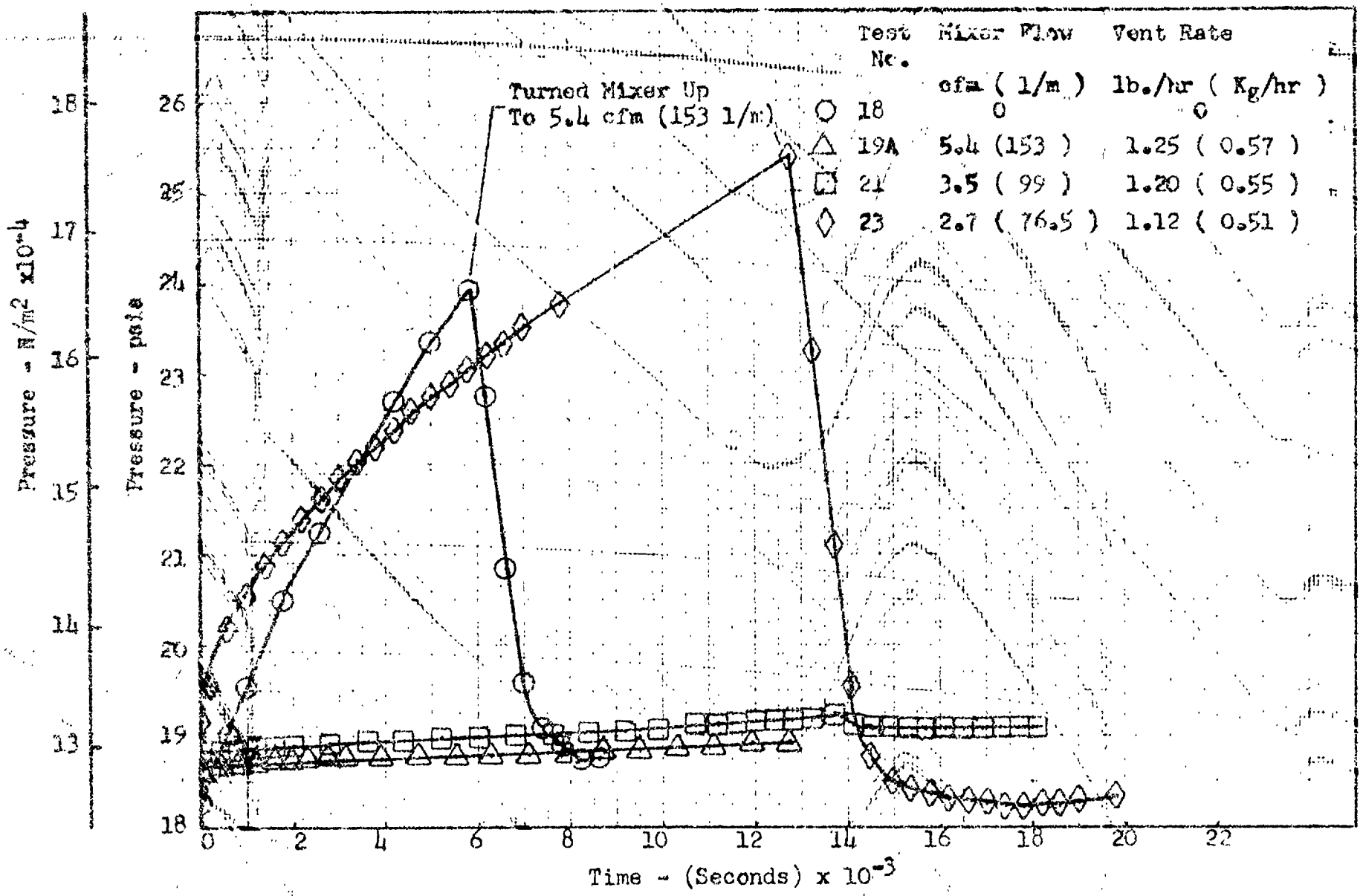

Figure 69 Effect of Mixer Speed with No Trapped Vapor - Configuration B - (Ullage Volume = 5 Percent)

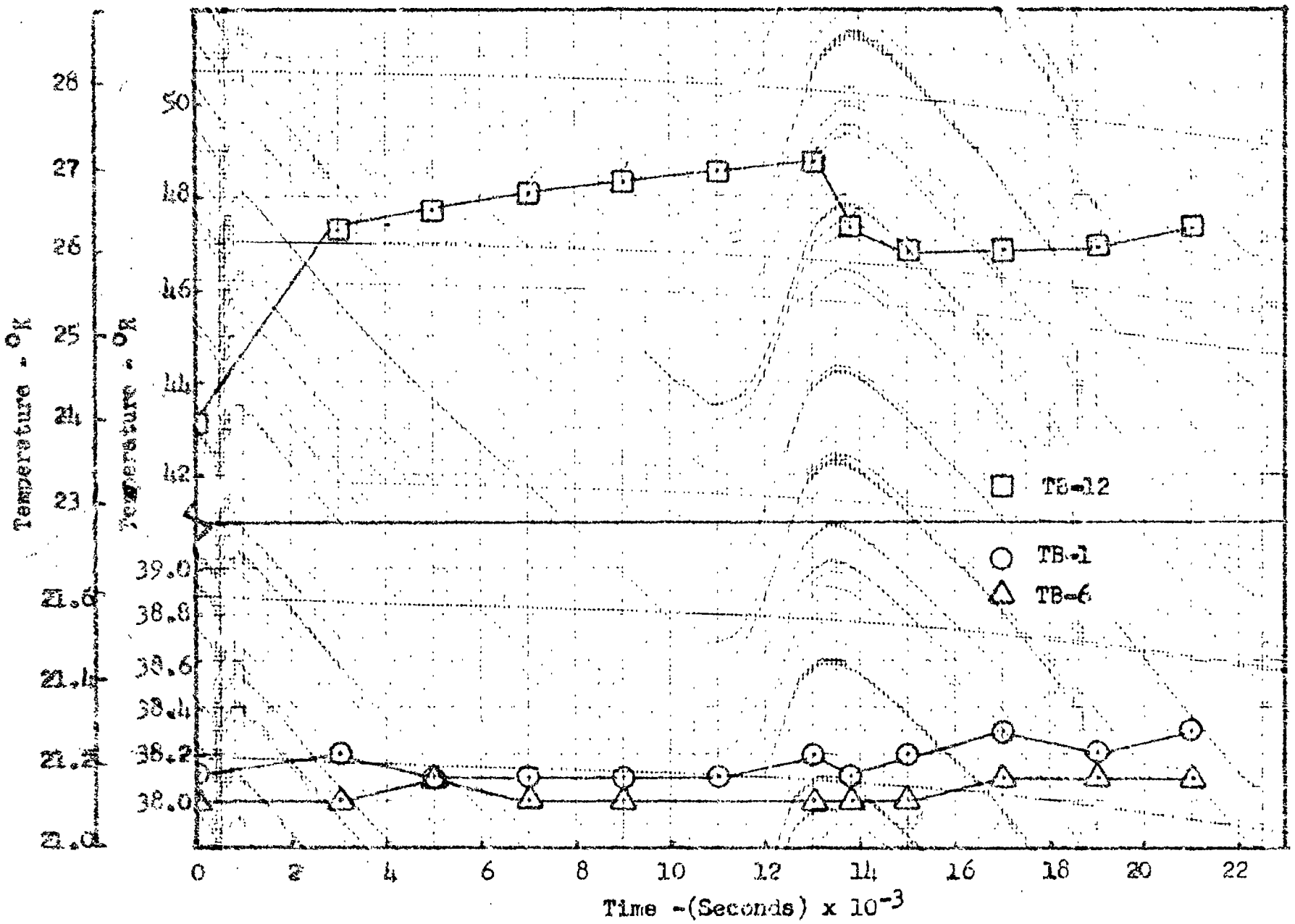

Figure 70 Temperature Histories for Test No. 23 - Configuration B

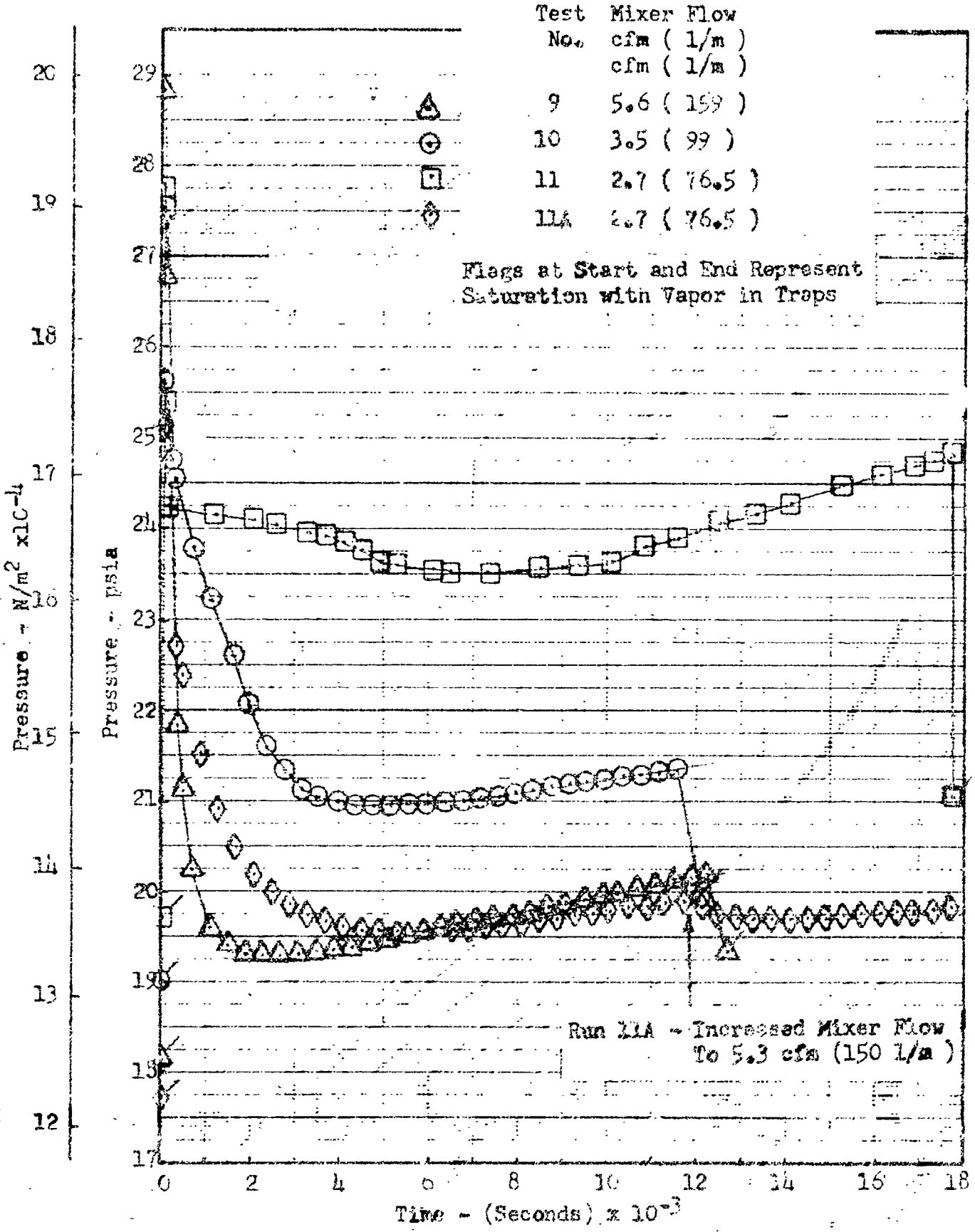

Figure 71 Effect of Mixer Flow on Pressure Response - Configuration C (Ullage Volume = 5 Percent)

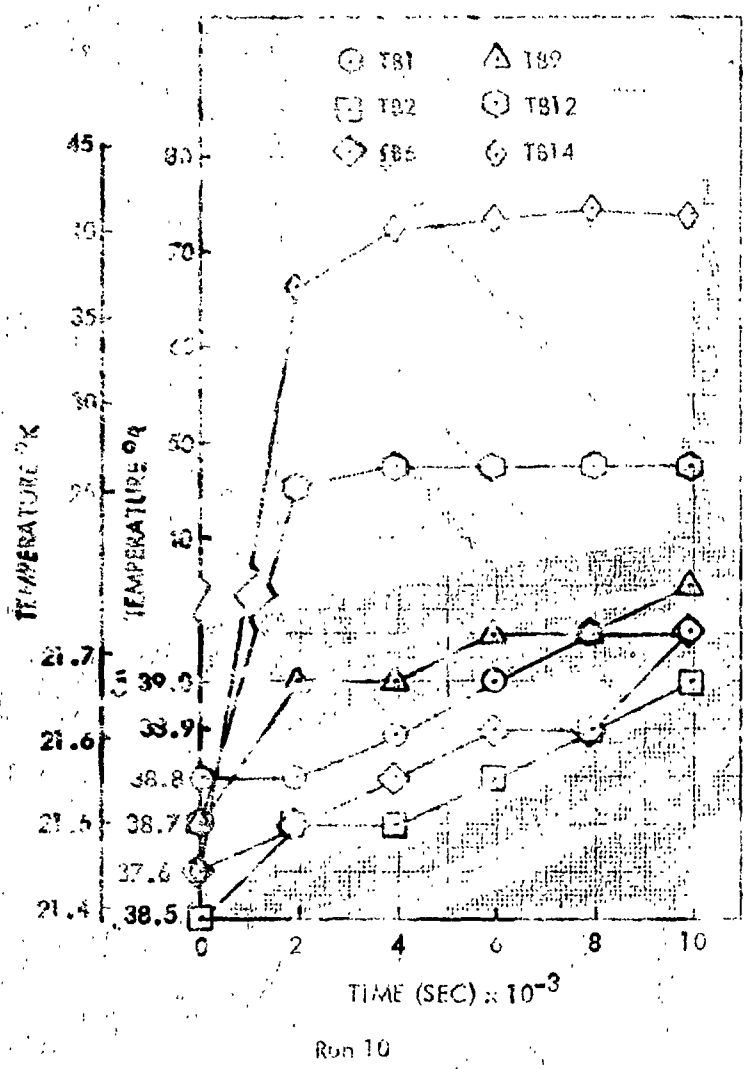

Figure 72 Temperature History - Run 10

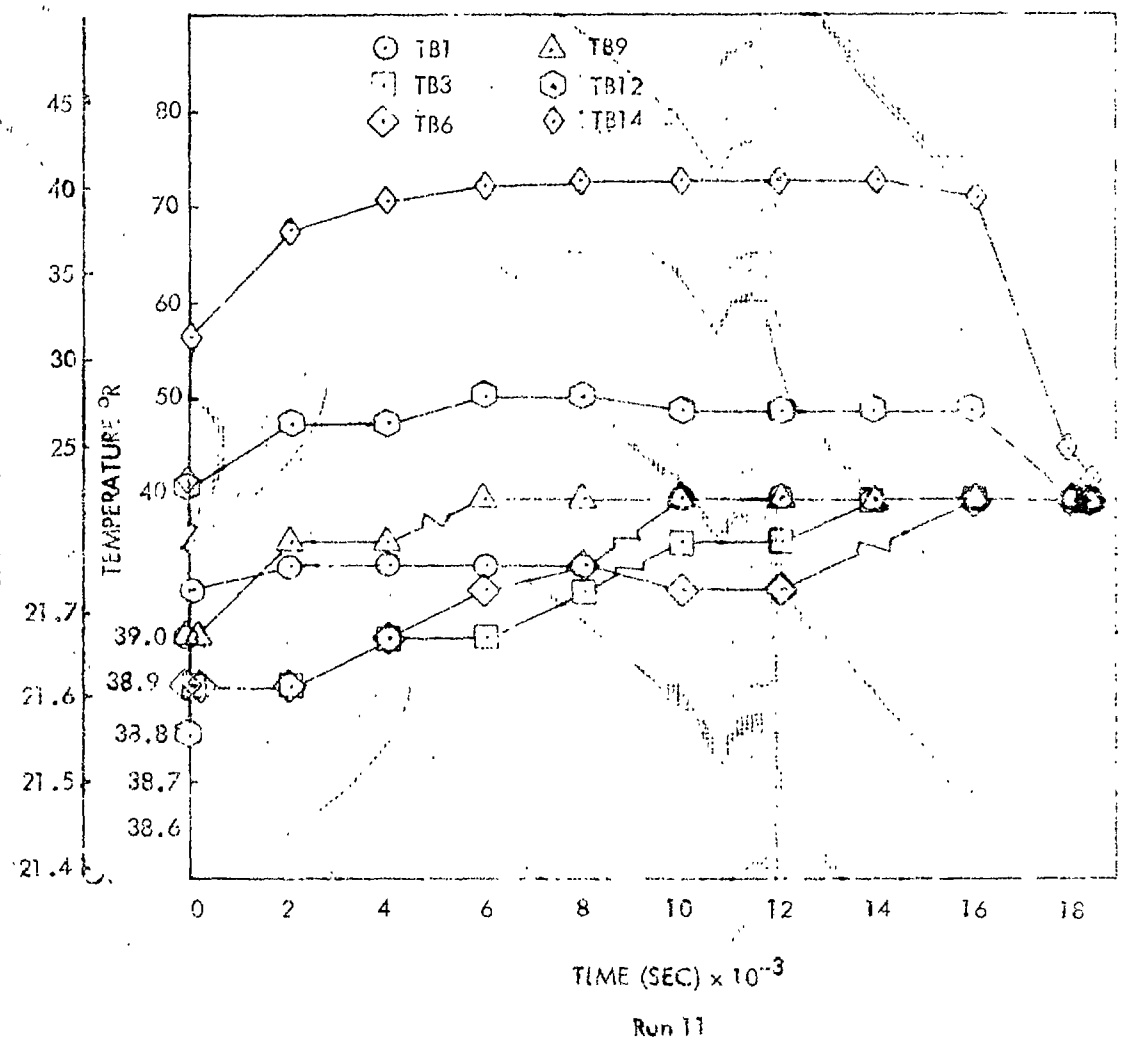

Figure 73 Temperature History - Run 11

between saturation and liquid temperatures (T_B-). Note that initially the indicated liquid temperature is slightly below saturation at the measured pressures. (These differences can be due to the combined precision limits of temperature and pressure transducers.) The liquid becomes subcooled when the tank is pressurized and approaches saturation again as mixing proceeds. The important significance is the fact that liquid subcooling was eliminated at the higher mixer speed, but still existed for run 11 at the time the run was discontinued.

COMPARATIVE TEMPERATURE HISTORIES

Time from Start (Seconds)	Run 10 Mixer Flow = 3.5		Run 11 Mixer Flow = 2.7	
	T_L* - °R	(T_S-T_L)* - °R	T_L* - °R	(T_S-T_L)* - °R
0	38.7 (21.5)	-0.5 (-0.28)	39.0 (21.6)	.3 (0.17)
50	38.8 (21.6)	+2.2 (1.2)	39.0 (21.6)	+1.7 (0.9)
2000	39.0 (21.6)	+0.2 (0.1)	39.2 (21.8)	+0.7 (0.4)
4000	39.0 (21.6)	-0.1 (-0.05)	39.2 (21.8)	+0.5 (0.28)
6000	39.1 (21.7)	-0.2 (-0.10)	39.3 (21.8)	+0.3 (0.17)
8000	39.1 (21.7)	-0.1 (-0.05)	39.3 (21.8)	+0.3 (0.17)
10000	39.2 (21.8)	-0.1 (-0.05)	39.5 (21.9)	+0.2 (0.10)
14000	-	-	39.6 (22.0)	+0.2 (0.10)

* Numbers in parenthesis are in °Kelvin

Fig. 74 compares the pressure response for different vent flow rates with a fixed mixer flow. Here, too, it is noted that a straight line through the beginning and ending saturation pressures is parallel to the steady state slope of the pressure history curve. Note, at the end of runs 12 and 13 there is a pressure recovery of 3/4 psi (5160 N/m^2) when the ullage vent is closed after generating the bulk boiling condition. This was found repeatedly throughout this test series and it is believed that most of that pressure drop previously described as possible subcooling is actually the dynamic pressure head lost through the ullage vent system.

SYSTEMS PERFORMANCE

The thermal conditioning system must be capable of controlling tank pressure efficiently. The control system has been demonstrated in both the 110 inch

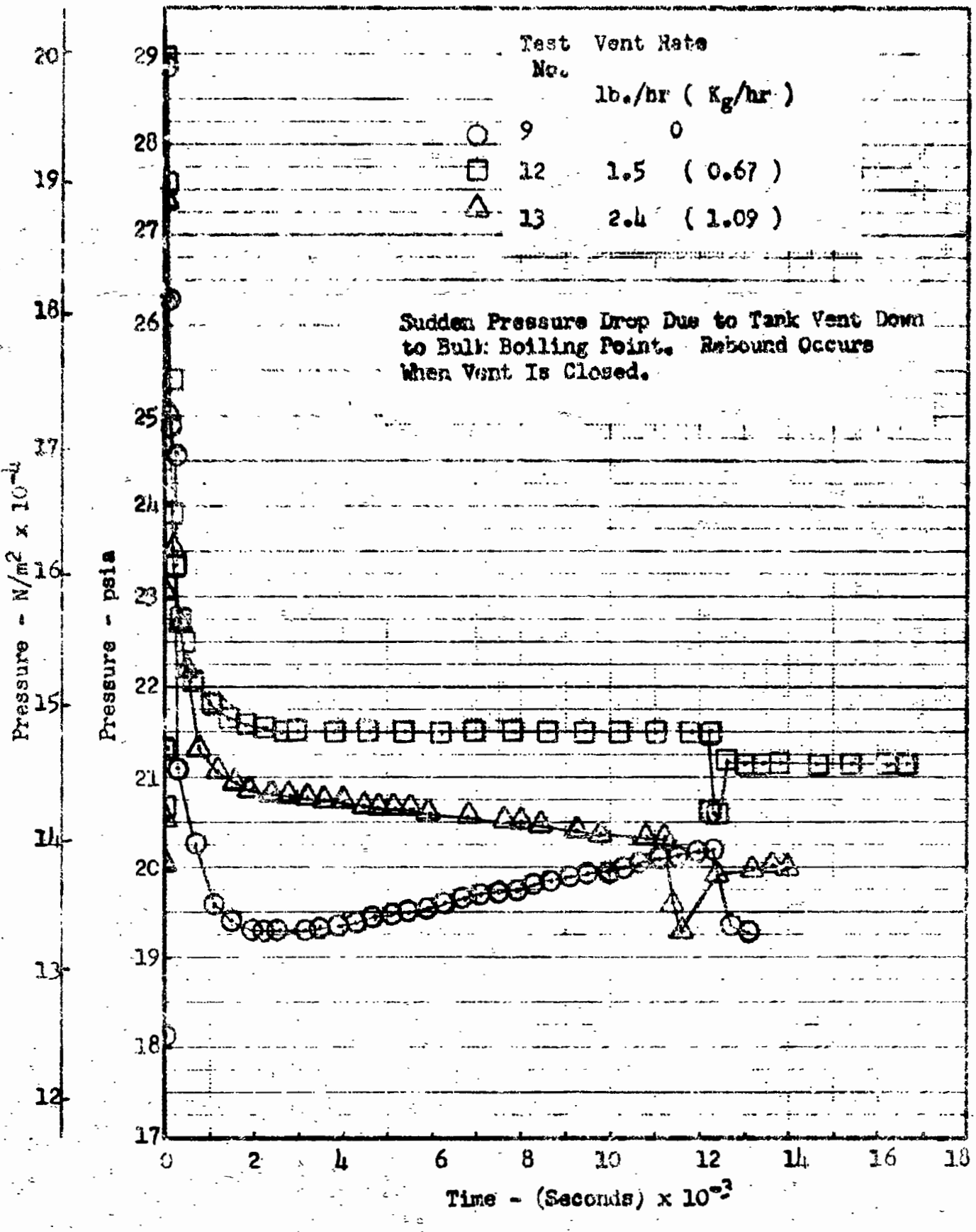

Figure 74 Effect of Vent Rate on Pressure Response - Configuration C (Mixer Flow = 5.6cfm = 158 l/m)

(2.8m) and the 41.5 inch (1.05m) tanks. The efficiency with which this control is obtained may be measured in terms of boiloff propellant.

For a tank of liquid hydrogen with no temperature gradients or stratification, the rate of pressure change is given by:

$$\frac{dP}{d\Theta} = \frac{1.25 \left[\dot{Q}_o - (M_o - 3.4P)\right]}{\rho_L V_T (1 - Vu/V_T)} \frac{1}{1 + 0.36 \frac{(Vu/V_T)}{\rho_L (1 - Vu/V_T)}} \qquad (3)$$

See Appendix B for the derivation of this equation. This thermal equilibrium model is valid if the depressurization process is limited only by the net rate of energy removed from the tank and not by mass diffusion at the liquid-vapor interface. Thus, the equation assumes the process as being limited by the rate of heat transfer within the heat exchanger only.

Fig. 75 presents a comparison between this model and the 41.5 inch (1.05m) tank data, where the pressure responses are those measured after the initial mixing transient. The ordinate is the parameter representing the net energy removal rate which is the difference between that taken out in the vented vapor and that put in by the mixer motor. The data falls basically into three groups: that on the left end is with no vent flow; the middle group is for the small flow control valve (1.2 - 1.7 lbs/hr) (0.54 - 0.77 Kg/hr) and that on the right side is for the high flow control valve (2.5 - 3.2 lbs/hr) (1.1 - 1.5 Kg/hr).

The data presented on Fig. 75 includes those from both the bottom mounted and side mounted tests. It also includes tests with both gaseous hydrogen and gaseous helium as the pressurant. It is noted that all of the data fall within the general scatter, i.e., there appears to be no distinct effect of either mixer orientation or the presence of helium in the ullage gas.

The theoretical effect of helium on the mixed model is manifested in the bracketed quantity in Eq. (3). The specific heat and gas constant in the equation are average quantities for multi specie ullage gas. This was evaluated for helium partial pressures up to 50 percent and ullage volumes up to 90 percent. The maximum calculated reduction in the pressure response was 5 percent which would not be discernible within the general data scatter.

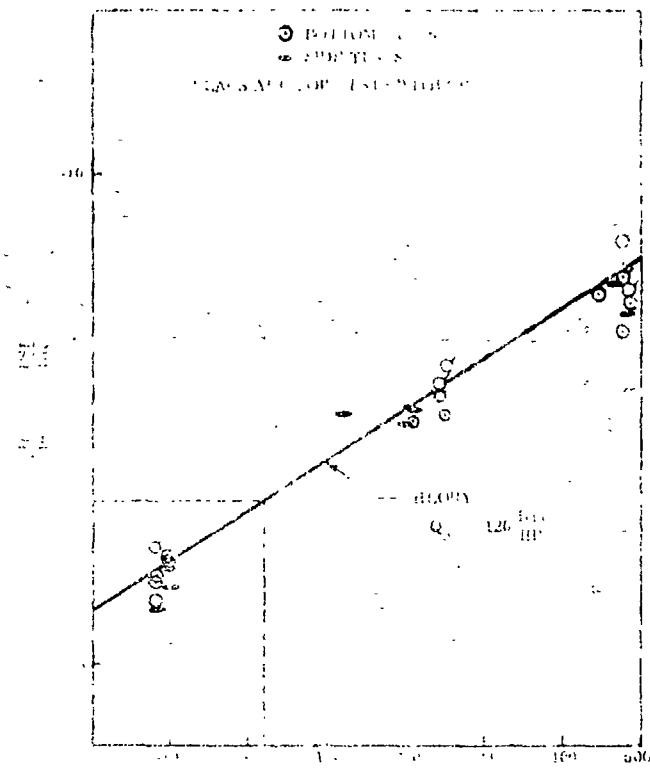

(c) 22 Percent Ullage

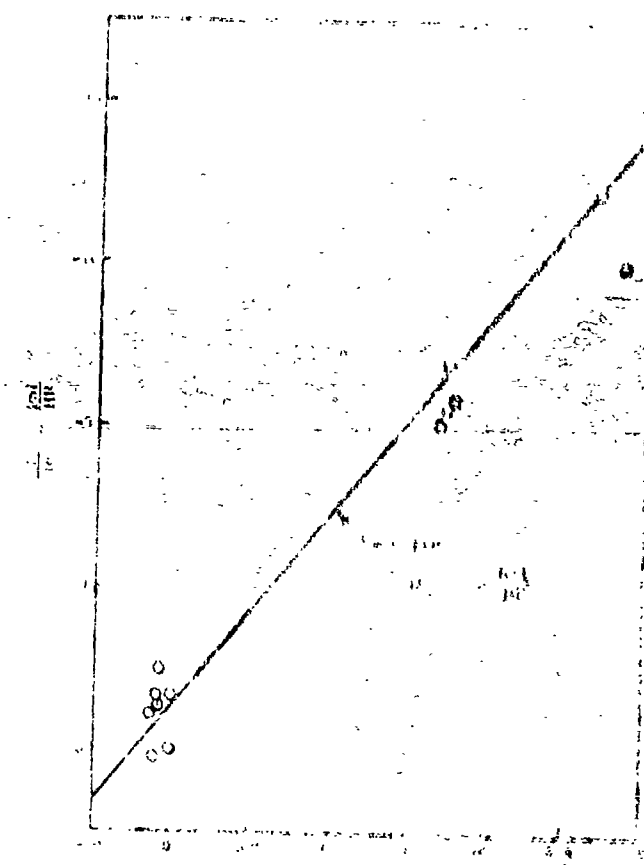

(d) 63 Percent Ullage

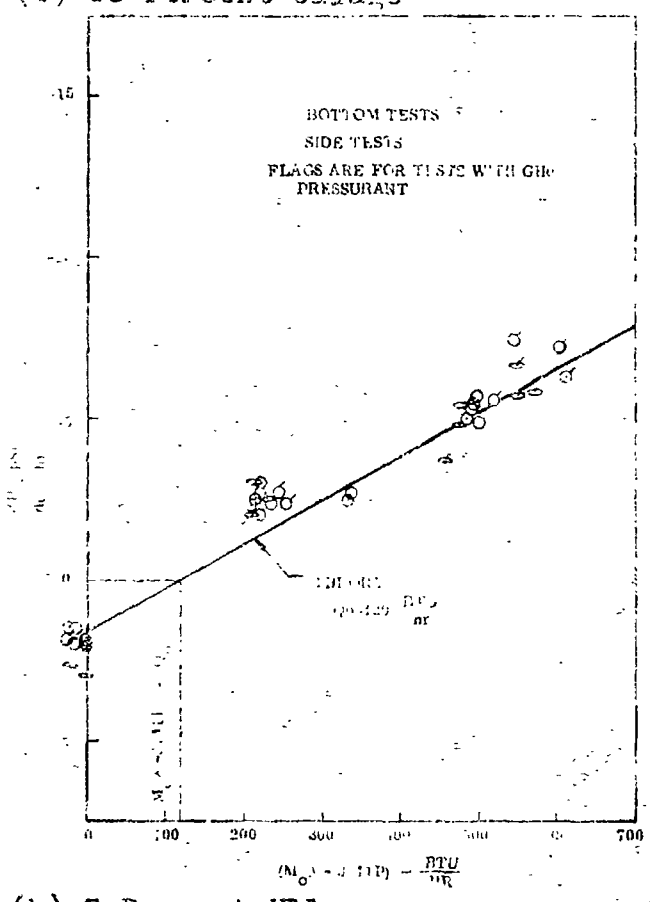

(b) 7 Percent Ullage

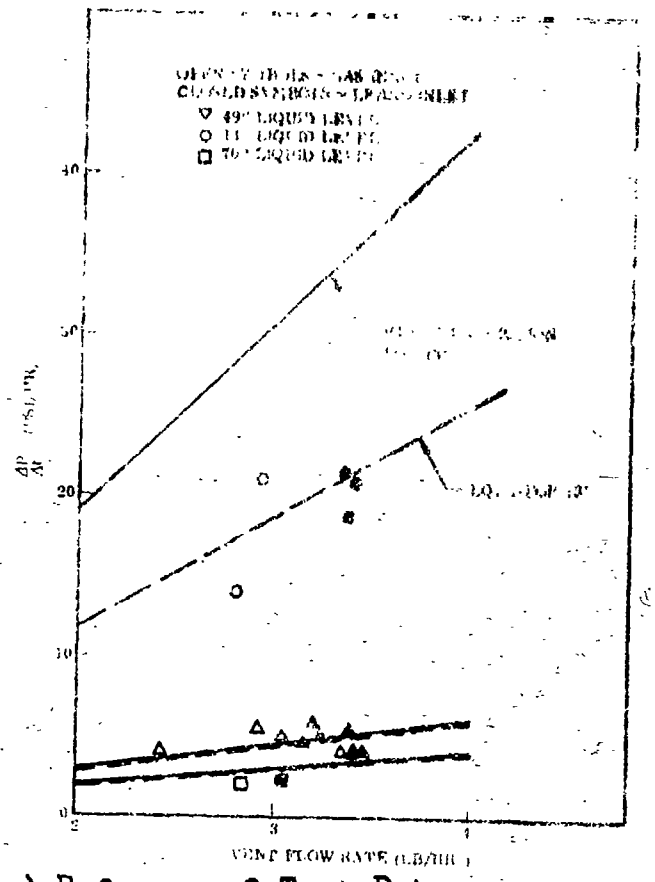

(a) Reference 2 Test Data

Figure 75 Comparison of Test Results with Mixed Model Theory

The bracketed quantity in the above expression also accounts for the thermal storage capacity of the ullage gas. It is always less than one, decreasing with increasing ullage volume, and tends to slow the response while the decreasing liquid mass tends to increase the pressure response. This thermal capacitance run was neglected in the previous work conducted under NAS 3-7942 and also in the work reported in Ref. 2. The tank used for the tests described in Ref. 2 has approximately 2.5 times the capacity as the 41.5 inch (1.05m) tank.

This mixed model was also applied to the data from Ref. 2. This is also shown in Fig. 75 and further illustrates the validity of the theory when all the storage terms are properly accounted for.

Fig. 76 presents a comparison between the mixed model and the test data from the bottom mounted test series in the 110 inch (2.8m) tank. The side mounted data is shown on Fig. 77. The theory line shown on these figures corresponds to a heat rate of 200 Btu/hr (59w). Actually, boiloff tests conducted periodically throughout the program indicated rates that varied between 185 and 218 Btu/hr (54 and 64 watts). This was due largely to the fact that the insulation was removed and reinstalled each time a change was made inside the tank. These results confirm the validity of the mixed model. When considered with the 41.5 inch (1.05m) tank, this represents verification over a twelve to one scale.

Fig. 78 shows the comparison for the extended mixer jet configuration. This illustrates again the inadequacy of the low mixer flows. However, the high flow seems to follow the trend of the theory, although slightly below it.

Finally, the data for configuration C is shown on Fig. 79. It shows very good agreement with theory at all mixing speeds. It appears that the nozzle which creates the radial jet definitely improves the circulation when compared to either of the other side mount configurations.

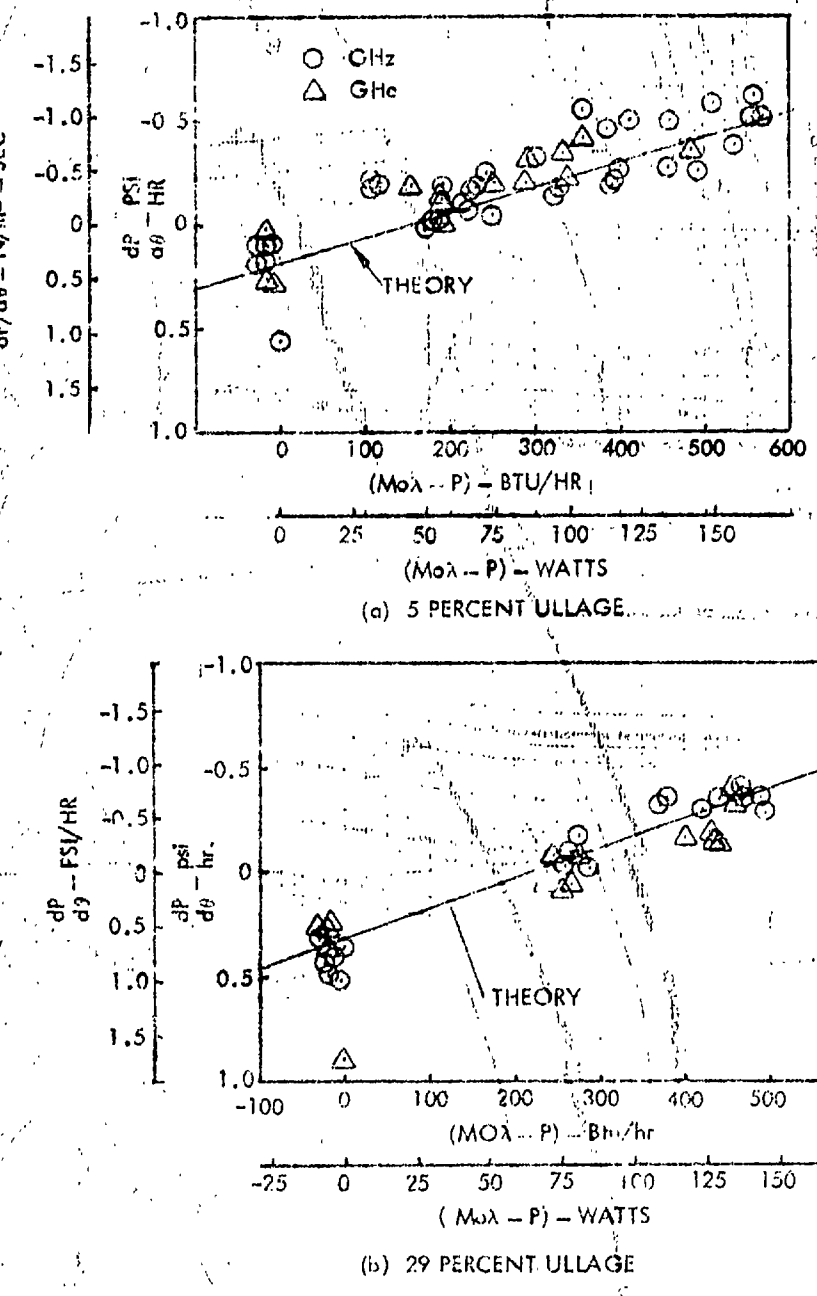

(a) 5 PERCENT ULLAGE

(b) 29 PERCENT ULLAGE

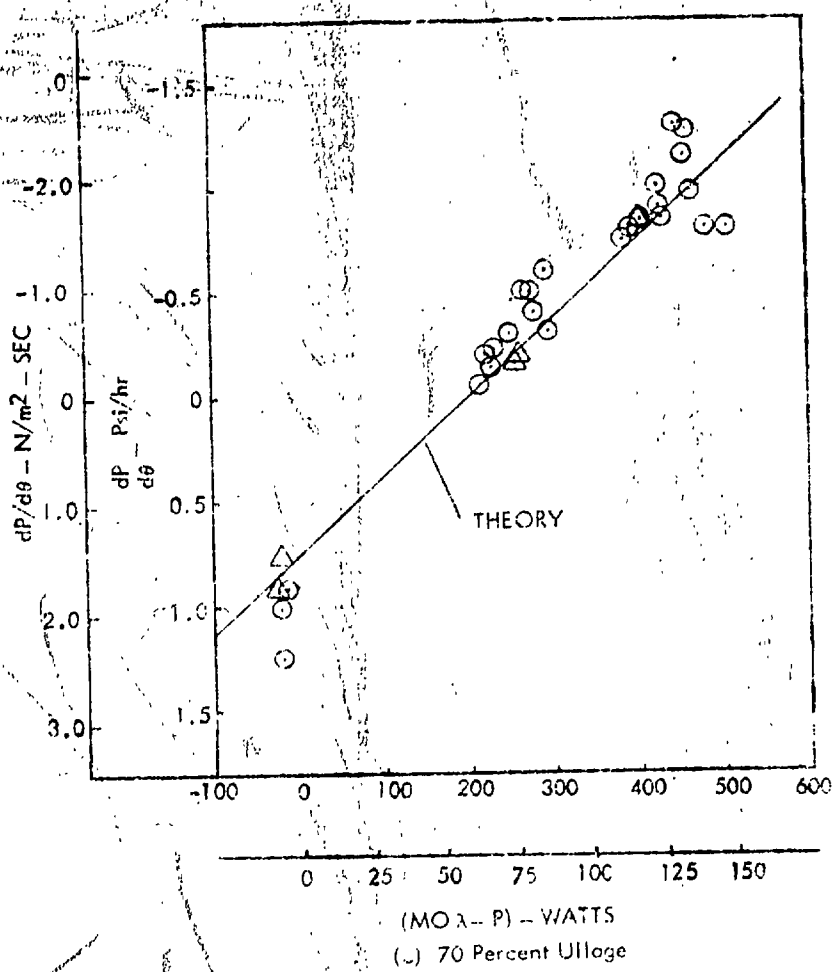

(c) 70 Percent Ullage

Figure 76 Comparison Between Mixed Model Theory and Experiment – Bottom Mount – 110 in. Dia. Tank

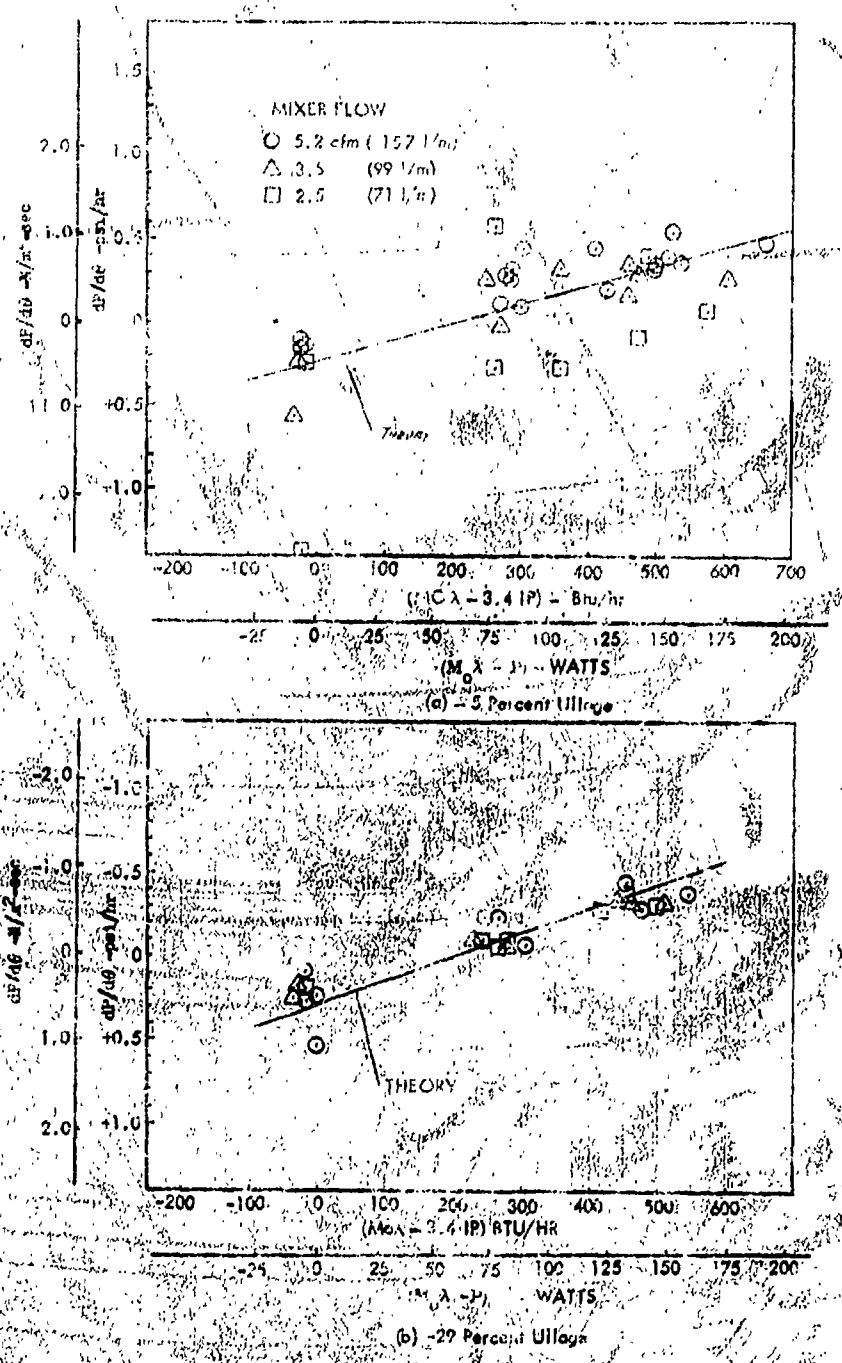

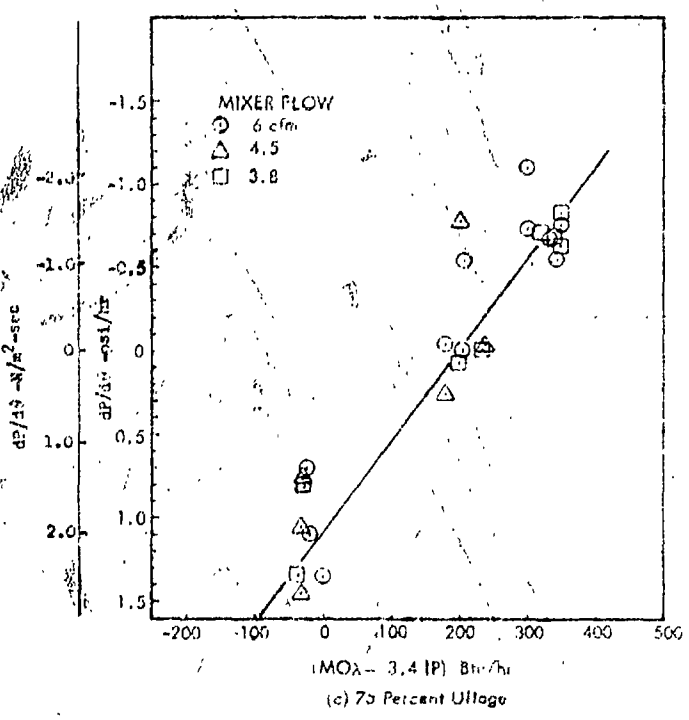

Figure 77 Comparison Between Mixed Model Theory and Experiment – Side Mount – 110 in. Dia. Tank

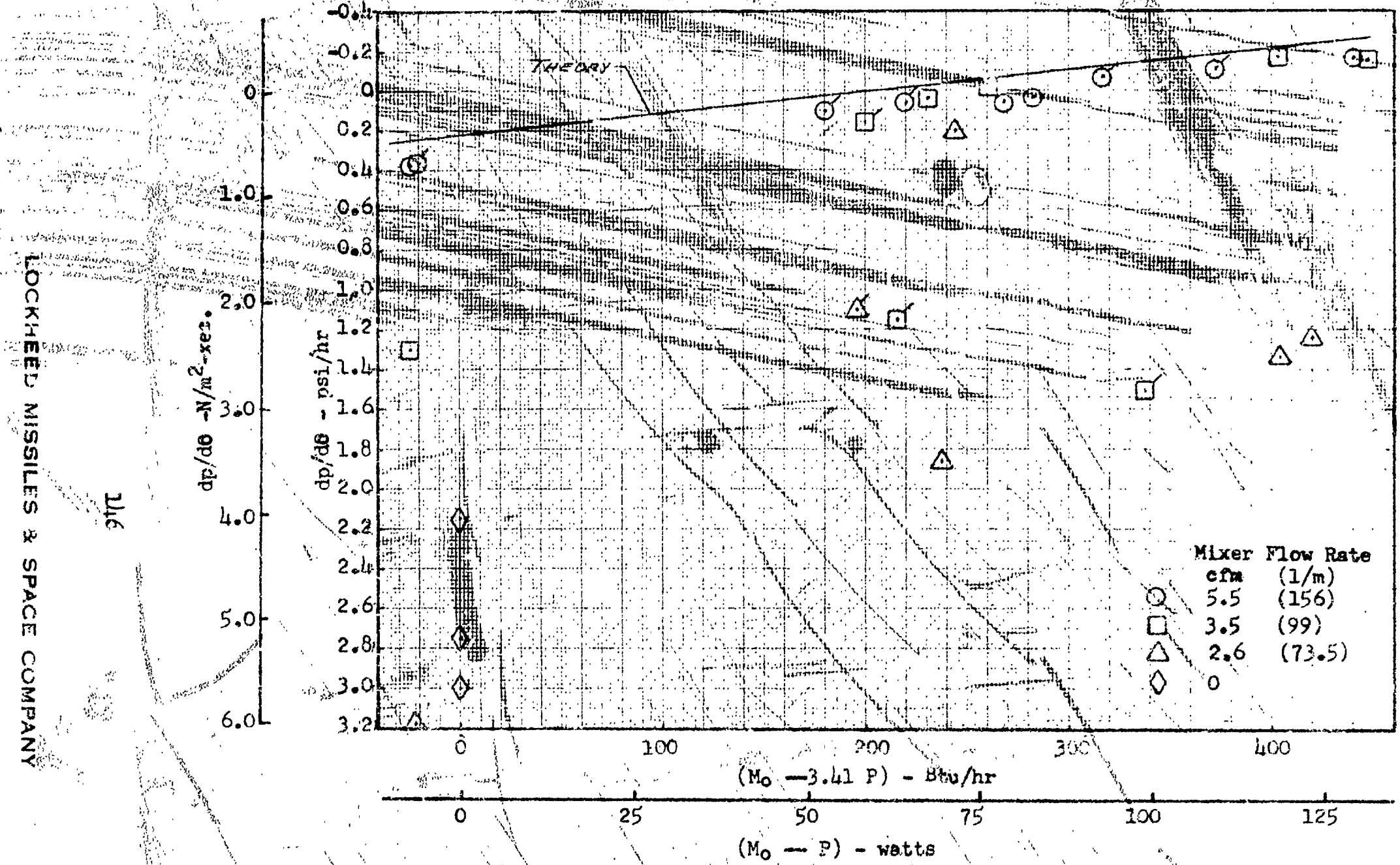

Figure 78 Comparison Between Experiment and Mixed Model Theory - Configuration B

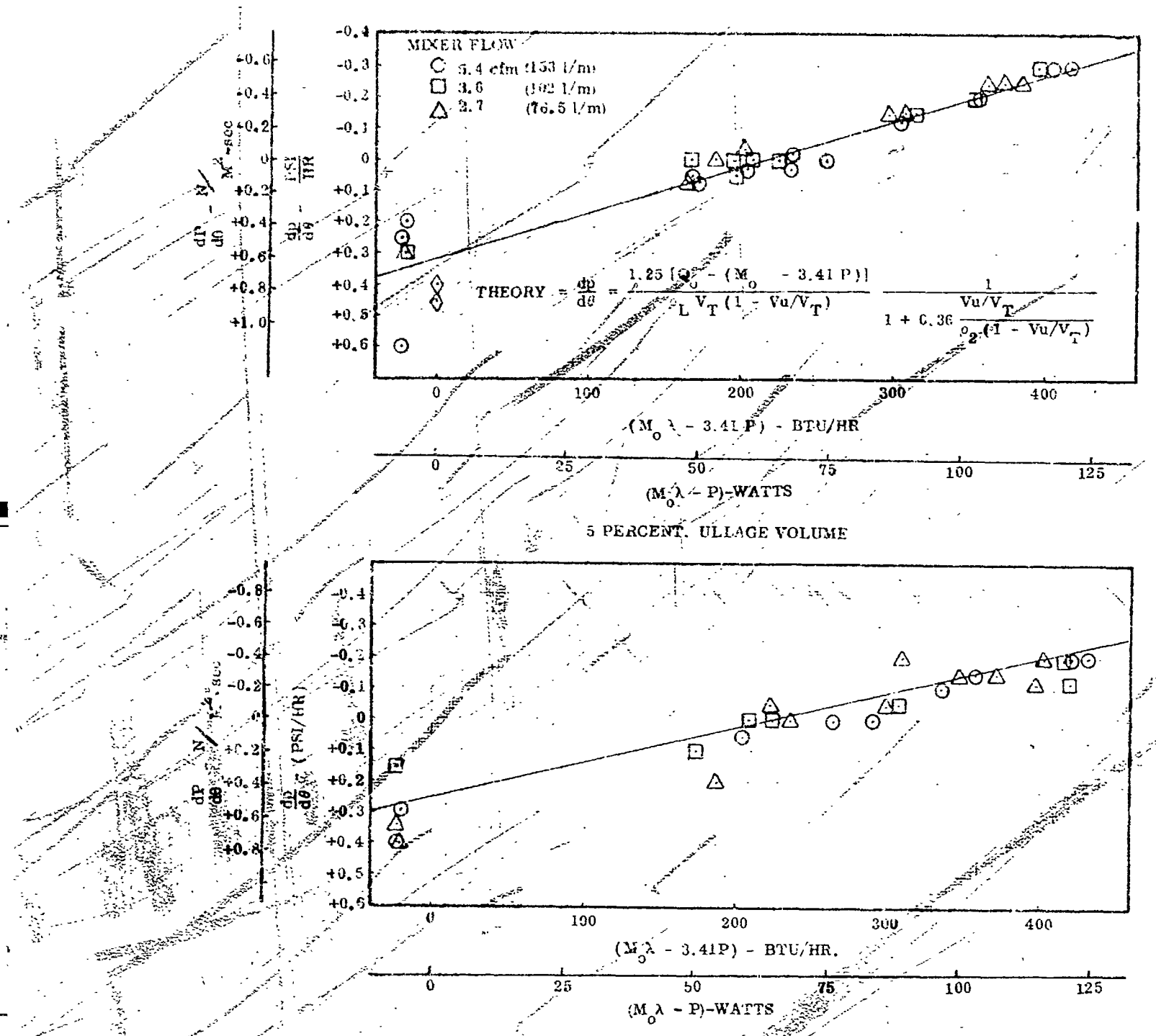

Figure 79 Comparison Between Experiment and Mixed Model Theory - Configuration C-29 Percent Ullage Volume

An analysis was made in an attempt to correlate the transient pressure response caused by mixing the tank contents after the tank has been pressurized. If a tank, initially in equilibrium at pressure, P_1, is instantaneously pressurized to a maximum pressure, P_m, then all the pressurant energy is contained in the ullage gas and the pressure rise describes the energy put into the tank, i.e.,

$$(P_m - P_1) = \frac{R}{C_v V_u} \Delta E_T \tag{4}$$

Further, if it is assumed that mixing results in a new equilibrium condition throughout and that external heating is negligible during the mixing period, the final pressure can be described by:

$$(P_2 - P_1) = (P_m - P_1) - \frac{RC_L}{C_v V_u} T_1 \left[M_{L_2} \frac{P_2}{P_1} - M_{L_1} \right] \tag{5}$$

Equations (4) and (5) can be combined to give an expression for the final equilibrium pressure of the form

$$\frac{P_2}{P_1} = \frac{P_m/P_1 + A \dfrac{1 - V_u/V_T}{V_u/V_T}}{1 + A \dfrac{1 - V_u/V_T}{V_u/V_T}} \tag{6}$$

where $A = (C_L/C_v)(\rho_L/\rho_u)$.

The thing of primary interest, however, is the time it takes to mix the tank contents. From Equation (4), the net energy to be distributed is proportional to the ullage pressurization, i.e.,

$$\Delta E_T = \frac{C_v V_u}{R} (P_m - P_1) \tag{7}$$

If the thermal capacitance of the ullage gas is neglected in the final equilibrium condition then all the added energy ends up in the liquid and the time is proportional to some average rate of mixing. Therefore,

$$E_T = \dot{m}_L t \frac{du}{dp} (P_m - P_1) \tag{8}$$

Combining (7) and (8) the expression for mixing time becomes:

$$t_m = \frac{2 C_v V_T g}{R\left(\frac{du_L}{dp}\right) \rho_L Q_m} \frac{v_u}{V_T} K \tag{9}$$

This equation was compared with test data from the bottom mount tests. It seems to provide reasonable correlation of the high ullage (70%) data where the jet exit is located in the ullage. This is shown on Figure 80. However, when the data for the lower ullage volumes were compared with the model, there appeared to be a geometrical factor separating the two sets of data. It was hypothesized that with everything else being equal, the mixing time would be inversely proportional to the interface area on which the submerged jet was acting. Therefore, the correlation for mixing time was empirically modified to read as follows:

$$t_m = K \frac{C_v V_T g (V_u/V_T)}{R\left(\frac{du_L}{dp}\right) \rho_L \left(A_s/V_u^{2/3}\right)} \times \frac{1}{Q_m}$$

This equation was rearranged in the form:

$$\frac{t_m \left(A_s/V_u^{2/3}\right)}{V_T (V_u/V_T)} = K \frac{g}{R\left(\frac{du_L}{dp}\right) \rho_L \times A_j U_j} \tag{10}$$

The experimental values of the grouping on the left is plotted against volumetric flow rate, Q_m, on Figure 81. It is noted that the best fit of the data gives a square function rather than the linear correlation as derived.

This suggests that mixing is primarily related to the jet momentum. Using the proportionality constant from Figure 81 and substituting $(AU)_j$ for Q_m, the final equation relating mixing time to jet velocity becomes:

$$t_m \frac{\left(A_s/V_u^{2/3}\right)A_j^2}{V_T(V_u/V_T)} = 0.52\, g \left(\frac{1}{U_j}\right)^2 \qquad (11)$$

where all dimensions are in units of feet and seconds. The minimum time required to completely mix the tank can be defined in terms of the critical velocity needed to give complete circulation throughout the tank.

$$t_{cR} \frac{\left(A_s/V_u^{2/3}\right)A_j^2}{V_T(V_u/V_T)} = 0.52\, g \left(\frac{1}{U_{j_{cr}}}\right)^2 \qquad (12)$$

A model is developed in Appendix C which relates the critical velocity to gravitational level. The correlating equation is:

$$\frac{U_{j_{cr}}^2}{g\, d_j} - 4\,\frac{(\sigma/\rho)}{g\, D_T^2}\left(\frac{D_T}{d_j}\right)^2 = \frac{D_T/d_j}{1 + 2\left(\frac{D_T}{d_j}\right)\tan\theta} \qquad (13)$$

The first term on the left is the jet Froude number and the second term is a modified tank Bond number. For most applications of interest the Bond number grouping is insignificant when $(g/g_o) > 10^{-3}$, and when the geometry is fixed, the Froude number, and therefore thermal mixing time is constant. For lower g levels, the critical jet velocity is nearly constant and thermal mixing time decreases with decreasing g level. Equation 9 predicts mixing times between 20 and 300 secs for the mission 2 vehicle, whereas the semi-empirical relationship (Eq. 13) results in mixing times between 1 and 15 seconds. Even allowing for an order of magnitude increase, which is representative of the poorer mixing experienced with the side mount tests, it can be seen that the transient mixing times will be insignificant in terms of boiloff propellant for the flight vehicle.

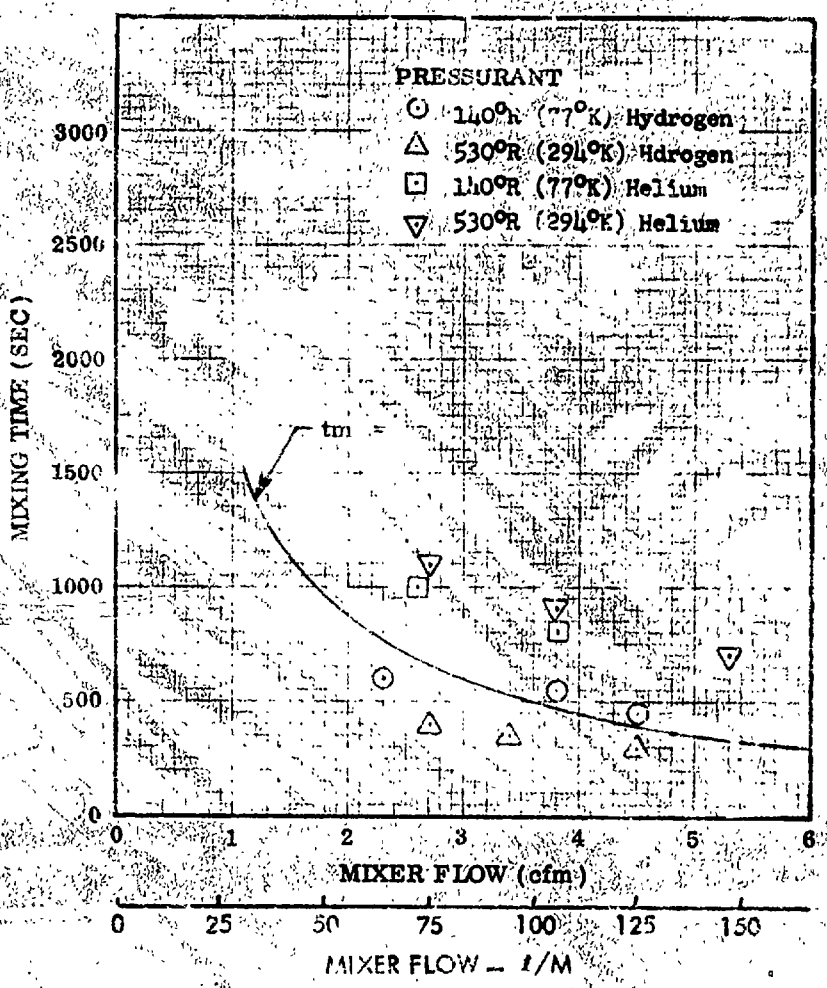

Figure 80 Effect of Mixer Flow on Mixing Time For 70 Percent Ullage

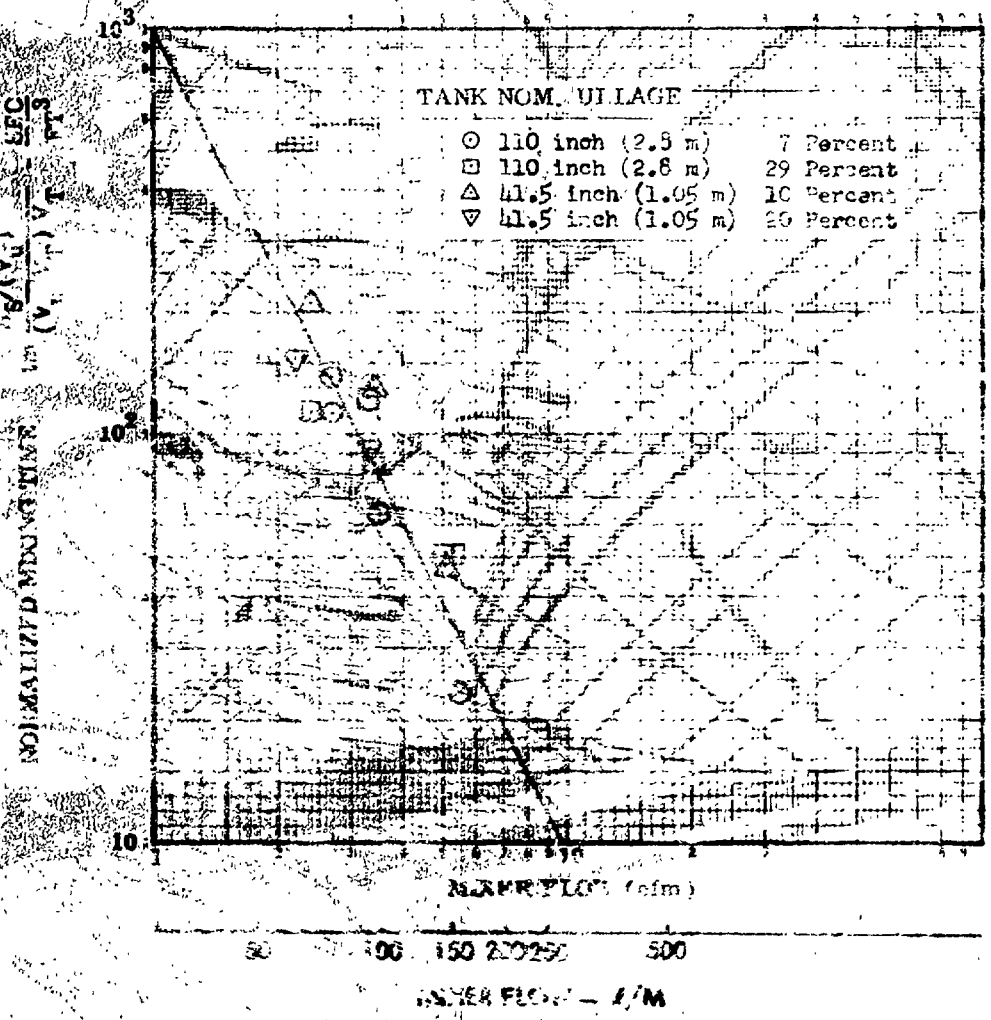

Figure 81 Effect of Mixer Flow on Mixing Time For Submerged Jet

COMPONENT PERFORMANCE

Performance data were presented for each of the components in an earlier section of this report. However, during the systems tests in the 41.5 inch (1.05 m) and 110 inch (2.8 m) tank tests, the performance of both the pressure switch and the expansion unit changed significantly. These differences are described in this section. Also, during the systems testing, data were obtained on the heat exchanger, when operating with liquid on the cold side and gas on the warm side. These data are presented and can be compared to that presented earlier for liquid-liquid operation.

Expansion Unit. One expansion unit (Part No. 393112-1-1-PB) had been used successfully for all the testing conducted under contract NAS 3-7942 as well as the component testing and the bottom tests in the 41.5 inch (1.05 m) tank. This covers approximately 300 operating hours. This unit, when received from AiResearch as an integral part of the TCU, regulated the heat exchanger pressure to a nominal 4.2 psi (28,800 N/m^2) in LH_2. However, when conducting the component calibration tests, this same unit began regulating to approximately 4 psi (27,800 N/m^2) for the bottom mounted test series. This unit failed closed at the start of the side mounted test series. It's operating history is shown in Fig. 82.

A second unit failed after 72 hours, apparently due to a flaw in the bellows. A third unit was used for the bottom mounted test series in the 110 inch (2.8 m) tank (approximately 1,000 hours). Initially, this unit regulated the heat exchanger pressure to a nominal 4.5 psi (31,000 N/m^2). However, after a month of operation, the pressure started to drop and eventually reached 1.8 psi (12,400 N/m^2) by the end of the test series.

In the interim period following the second failure, the vendor modified the bellows design (see Fig. 3) to increase the number of convolutions from 16 to 20 and to remove the internal guide. The purpose was to reduce the working stresses and to remove a possible source of stiction. One of these modified bellows was used for the remainder of the TCU tests. Fig. 83 shows

the operational history of this modified expansion unit. Each of the peaks represents a new start after the system has been shutdown for a weekend or for equipment changeover. As testing proceeds, the regulated pressure drops until the system is shut down. The sequence is repeated although each successive peak and trough is lower than the previous one. The time indicated on Fig. 83 is actual operating time and each apparent cycle represents 30-50 operating cycles. The total soak time is much longer than that indicated. It appears that the working stresses in the bellows exceeds yield and results in plastic deformation of the material. This can be eliminated by increasing the bellows diameter and/or the number of convolutes. Either solution can be undertaken as a development item for a specific application.

Pressure Switch. The pressure switch is required to sense tank pressure and actuate the solenoid valve and the mixer at a maximum pressure of 19.2 psia (132,500 N/m^2). The minimum pressure for deactivation is 16.8 psia (116,000 N/m^2). Table 16 contains a summary of the actuation and deactuation pressures obtained from the automatic control tests.

During these tests, the operational limits were consistently on the low side, and the deviation increased for the later tests. However, the total deadband was within tolerance. The actuation-deactuation points can be raised by adjusting the calibration screw (see Fig. 8) making it possible to operate within the prescribed limits.

Table 17
SUMMARY OF PRESSURE SWITCH OPERATION

Test Configuration	Test No.	Pressure - psi (N/m^2) Actuation	Deactuation	P psi (N/m^2)
41.5" - Bottom	28	16.3(1.12 x 10^5)	15.6(1.07 x 10^5)	0.7 (0.48 x 10^5)
	49	16.4(1.13 x 10^5)	15.6(1.07 x 10^5)	0.8 (0.55 x 10^5)
41.5" - Side	25	16.3(1.13 x 10^5)	15.0(1.03 x 10^5)	1.3 (0.90 x 10^5)
110" - Bottom	28	16.5(1.13 x 10^5)	15.4(1.06 x 10^5)	1.1 (0.76 x 10^5)
110" - Bottom	49	16.0(1.10 x 10^5)	14.9(1.03 x 10^5)	1.1 (0.76 x 10^5)
110" - Side	28	15.7(1.08 x 10^5)	14.6(1.00 x 10^5)	1.1 (0.76 x 10^5)
110" - Side	49	15.7(1.08 x 10^5)	14.6(1.00 x 10^5)	1.1 (0.76 x 10^5)
110" - Side - Configuration C	69	15.6(1.07 x 10^5)	14.5(1.00 x 10^5)	1.1 (0.76 x 10^5)

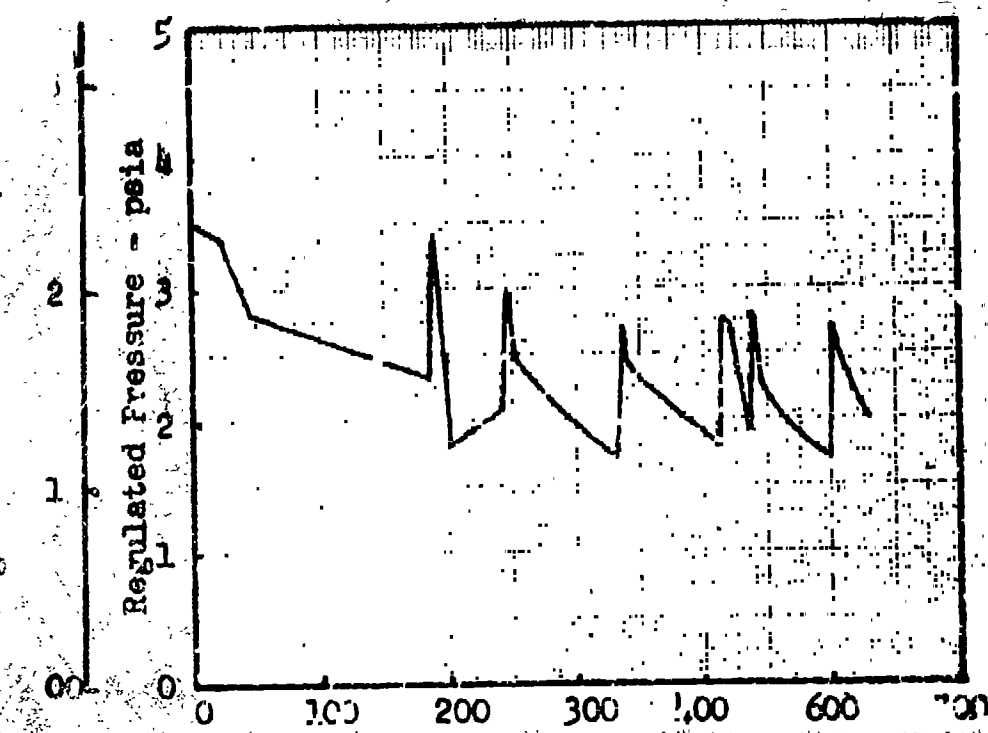

Figure 83 Expansion Unit Operating Histor, - Modified Bellows

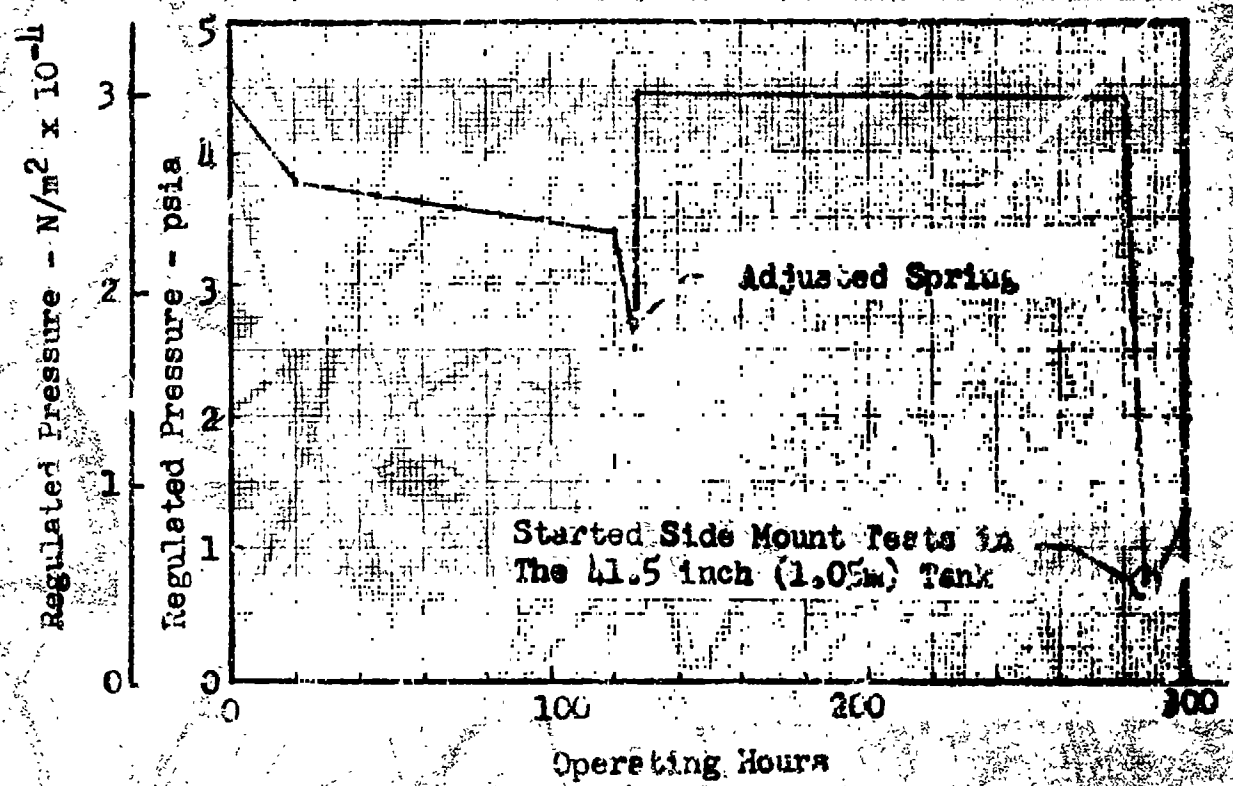

Figure 82 Operating History for Original Expansion Unit

Heat Exchanger. A series of tests was conducted in the 110 in. dia. tank wherein the regulator inlet was in liquid and the heat exchanger was in hydrogen gas. Fig. 84 shows the effectiveness as a function of the flow ratio for this condition. Although the warm side fluid is hydrogen rather than helium, the results are comparable because the forced convection heat transfer coefficients differ by only 22 percent for the two fluids (larger for hydrogen). For the flow conditions in these tests, a comparison between forced convection and condensation coefficients indicates that the convection is dominant. The design flow ratios indicated on Fig. 84 are equivalent values which give the same overall heat transfer coefficients in the superheater.

Heat transfer coefficients were calculated for the test flow conditions and, by iteration, a heat balance was obtained in the two portions of the heat exchanger. Even with gas on the warm side, the estimated boiler length constituted only ten percent of the total. In the superheater portion, the thermal resistance is controlled by the cold side flow rate, irrespective of the warm side fluid. Therefore, the experimental effectiveness values determined in these tests confirm the adequacy of this heat exchanger design.

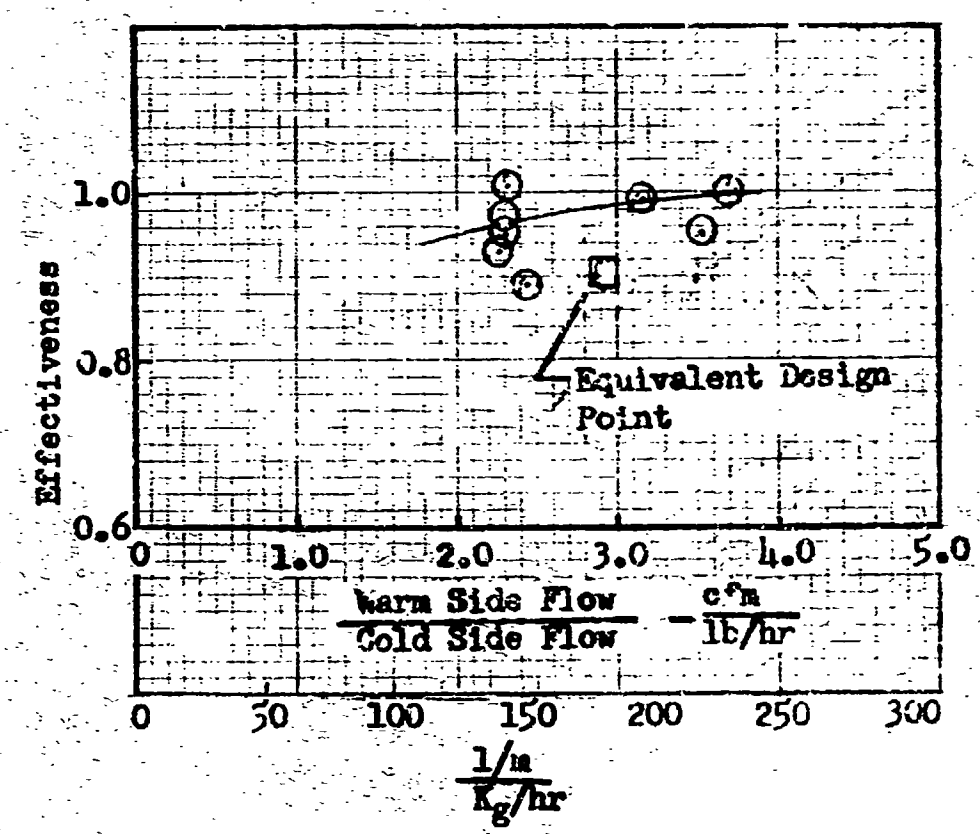

Figure 84 - Heat Exchanger Effectiveness with GH_2 on Warm Side

CONDENSATION INVESTIGATION

Propellant tank pressure is governed by the energy in the ullage gas, and pressure control is dependent upon the rate at which excess energy can be removed. Successful operation of the thermal conditioning system is predicated on the ability to transmit the energy to subcooled liquid which is cooled in the heat exchanger and circulated by the vapor. The heat transfer takes place at the interface by means of conduction and condensation, but in the absence of large temperature differentials, the condensation would normally be expected to dominate the process.

However, the thermal conditioning unit is to operate in a zero gravity environment, for which the existing theories of vapor condensation are not applicable. These classical theories deal with streamline flow where condensate is removed by gravitational forces. Therefore, a theory was developed by Sterbentz and Bullard (refs. 1, 3) which describes the condensation heat transfer coefficient in terms of the interface velocity. The non-dimensional equation is:

$$\frac{h_m L}{K} = 1.22 \left(R_e \times P_r \times N_\lambda\right)^{\frac{1}{2}}$$

However, the utility of the theory is severely limited without experimental data with which it can be compared.

The experimental program described in this section was formulated to determine, experimentally, the parameters governing condensation at a moving interface and to compare with the Sterbentz-Bullard theory.

TEST APPARATUS

The test apparatus used for other experiments is depicted in Fig. 85. The experiment is contained within a 19 inch (0.48 m) diameter cylindrical, stainless steel tank, which fits inside the 22 inch (0.56 m) diameter cryogen

FOLDOUT FRAME 1

CONDENSATION EXPERIMENT INSTRUMENTATION

Function	Instrument			
	Type	Model	Range	Accr.
Dewar Pressure	Heise gage	H-18-054 (18")	0-200 psi	0.4%
Inlet gas flow rate	Rotometer	F-P-½-25-g-5/81	0-23.45 l/m (air)	2% F.S.
Effluent flow rate	Rotometer	F-P-½-20-5	0-18.45 l/m (air)	2% F.S.
Liquid temperature	PRT	Minsco 2448 (SN 150)	30-530 °R	±0.6°R
T_1	Cu-Cu Differential	-		± 2°R
T_2	"			
T_3	"			

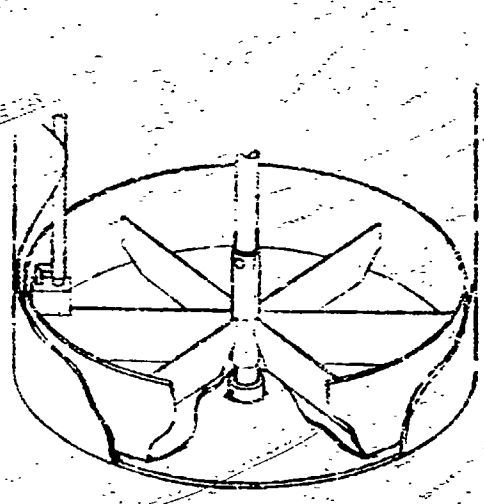

PADDLEWHEEL BUCKET ASSEMBLY

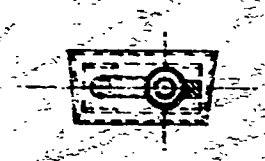

SECTION B-B

SECTION A-A

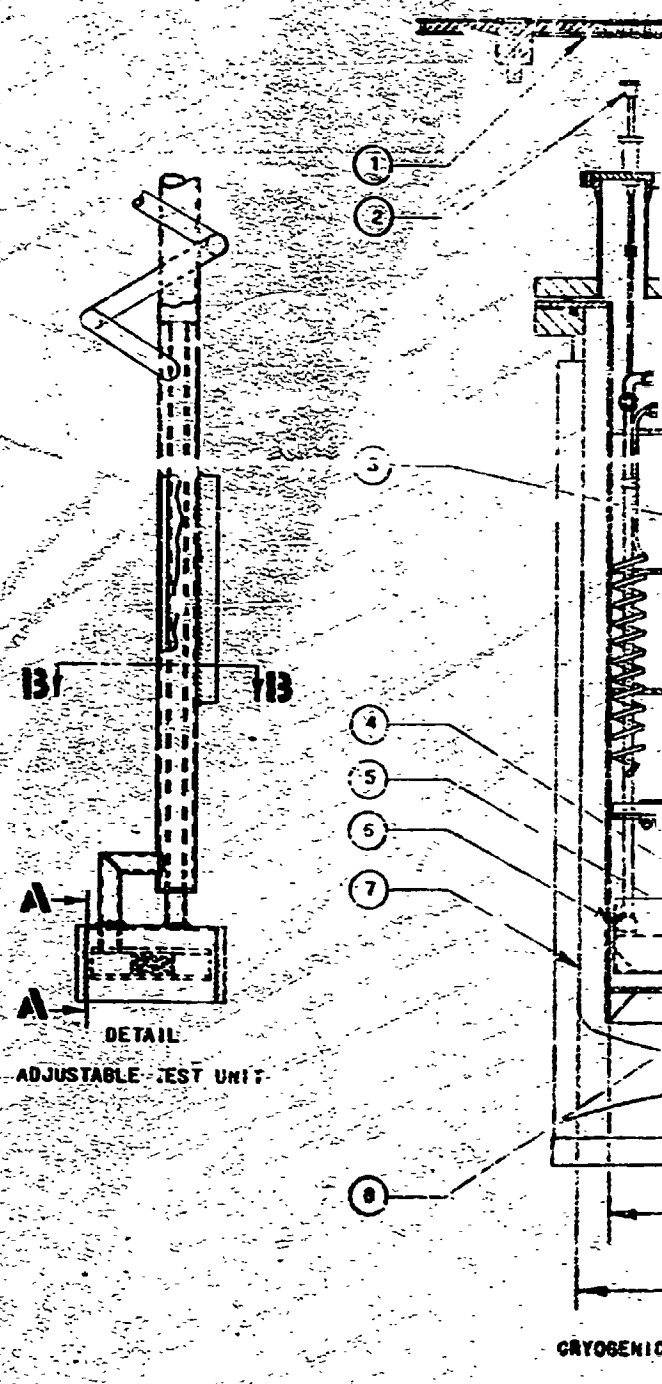

DETAIL
ADJUSTABLE TEST UNIT

CRYOGENIC

FOLDOUT FRAME 2

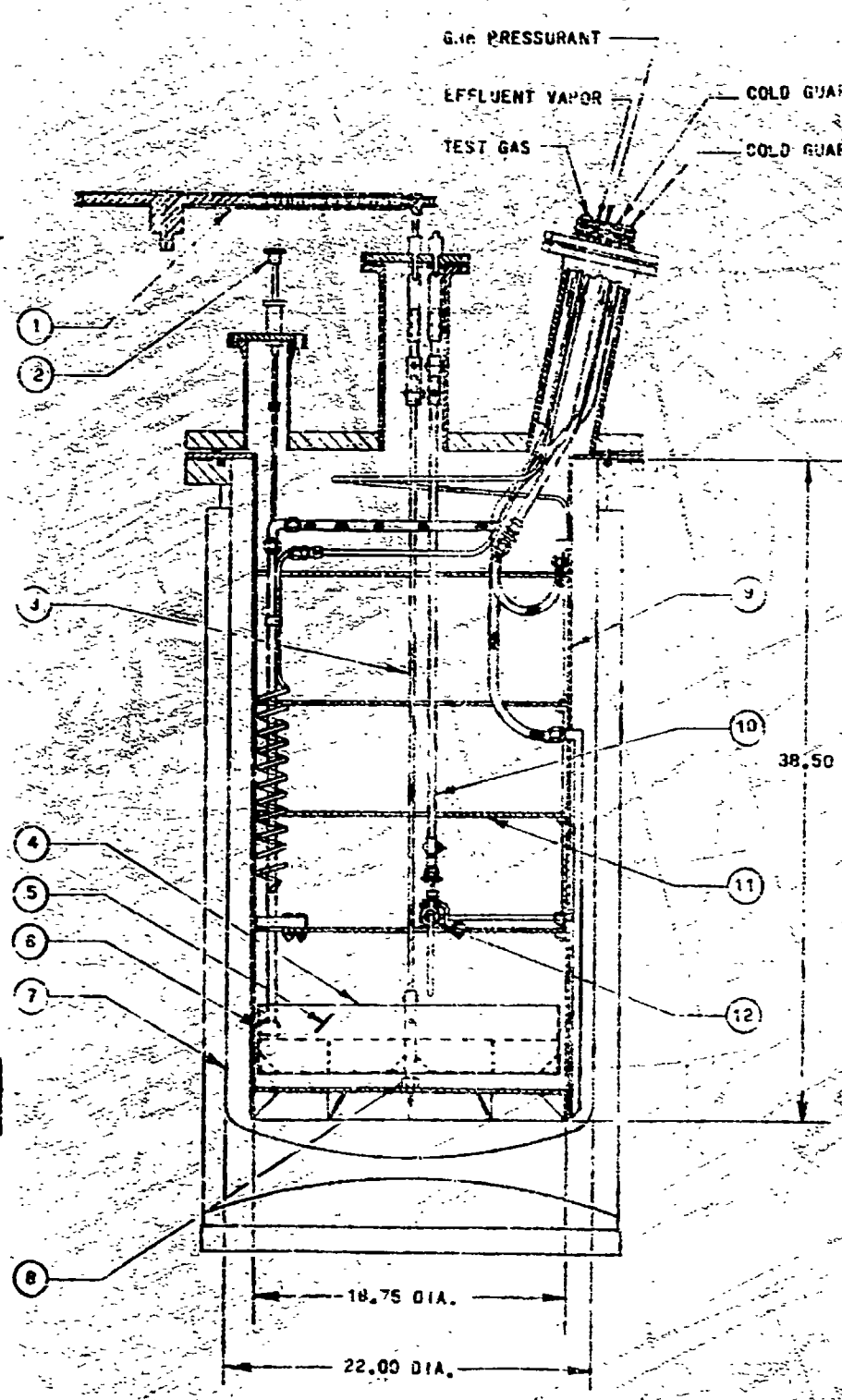

CRYOGENIC CONDENSATION TEST APPARATUS

DESCRIPTION

1. DRIVE CHAIN AND SPROCKETS
2. TEST SECTION HEIGHT ADJUST
3. FIBERGLASS DRIVE SHAFT (1 IN. O.D.)
4. PADDLEWHEEL BUCKET ASSY
5. LIQUID INTERFACE MIRROR
6. TEST SECTION
7. DEWAR
8. DRIVE SHAFT GUIDE
9. STORAGE VESSEL
10. BUCKET FILL VALVE STEM
11. COPPER RADIATION SHIELD (1/16 IN. THICK)
12. BUCKET FILL VALVE

Figure 85 Condensation Test Apparatus Desig

dewar. The tank and dewar use a common lid, which has a separate seal flange and groove for each vessel. The annulus between the two vessels serves as a cold guard when filled with the same liquid as that being used for the test.

Three copper radiation shields are placed in the ullage to intercept heat from the top of the dewar. These are thermally connected to the vessel wall. A four inch (0.1 m) diameter hole was cut in each shield to provide a view path from the observation port to the mirror which was placed to give a view of the test cell. Also, a three inch (0.076 m) diameter scallop was cut out of each shield to allow installation of the test cell assembly.

The liquid rotation is provided by the stainless steel paddle wheel-bucket assembly which is fixed on a fiberglass drive shaft, and free to rotate near the bottom of the internal vessel. This bucket, which is 4 inches (0.1 m) deep, is divided into six equal segments by 2 inch (0.05 m) deep vanes. These are welded into the bottom part of the tub. These vanes are to help create solid body rotation within the test liquid. The tub and cold guard are filled through a two way valve which is placed inside the tank and manipulated through a long fiberglass stem.

The test vapor is fed into the small test cell through a 1/4 inch (0.0064 m) line which is coiled, and thermally connected with fins, to a central efflux tube. This efflux tube is also open to the test cell and removes any vapor not being condensed in the cell, at the interface. This entire tube and test cell assembly is suspended from a screw drive which is used to raise and lower the cell over a distance of approximately 2 inches (0.05 m).

A constant speed (1 rpm) servo-motor was used to rotate the bucket assembly through a gear-chain system, as illustrated. Speed changes were accomplished by changing the chain length and the drive gear. Fig. 86 is a photograph showing the set up for a rotational speed of 5 rpm. This figure also shows other features of the apparatus. The lid was equipped with four flanged port. One of these was fitted with a quartz glass window, which was essen-

tial to the conduct of these experiments. A center port housed the fiberglass drive shaft and the stem for the two-way fill valve. All plumbing penetrations and instrument leads were brought through one of the remaining ports while the other was used for the test cell height adjustment assembly.

The instrumentation used in these experiments is given on figure 85. Volumetric flow rates of the test gas and the effluent were measured with flow raters having least count of 0.1 liters per minute. The amount of subcooling was determined from ullage pressure measurements, taken with a Heise gage, and liquid temperature measurements, obtained with a platinum resistance thermometer. The PRT was fixed to the test cell, so that the sensing element as 1/4 inch (0.0064 m) below the lower edge of the cell. Three differential thermocouples were referenced to this PRT. One of them was located even with the bottom edge of the cell, and the other two were in the test gas, at 1/2 inch (0.013 m) intervals above the lower edge.

TEST PROCEDURES

Pretest Operations

Before starting a series of tests with a cryogen, the entire test apparatus was pumped down to approximately 10 microns before initiating the fill process. The first step in the daily preparation was to fill the cold guard annulus. When this was completed, the two-way valve was switched and the bucket assembly was filled to approximately 1 inch (0.025 m) above the vanes. This was determined by setting the test cell height and visually observing the liquid interface intersection with the cell. The dewar was then allowed to stabilize with both the ullage and cold guard vented to atmospheric pressure. The test cell was then immersed in the liquid and the ullage was pressurized with helium and allowed to come to an equilibrium before testing was accomplished. When starting up with a warm dewar, the fill pressurization, and stabilization required approximately four hours. However, the heat leak was sufficiently small that liquid could be maintained overnight

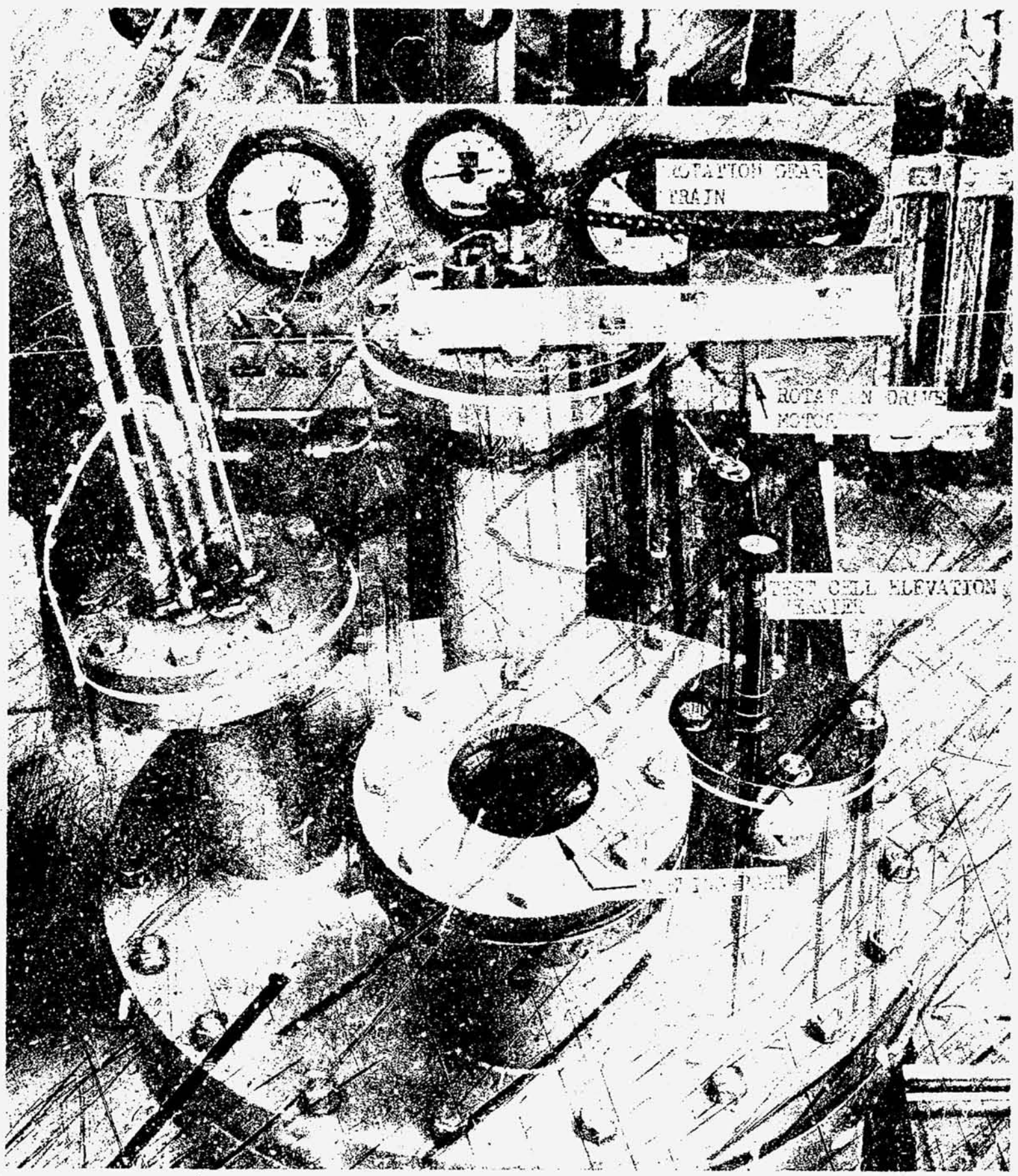

Figure 86 Photograph of Condensation Test Apparatus

even though the dewar was left vented. Consequently, only topping off was required for consecutive operating days and the normal stability period was approximately two hours.

Test Operations

After the system had come to an equilibrium condition the test cell was raised until the lower edge was barely beneath the liquid surface. The test gas inlet valve was then opened and the flow rate set. The gas would bubble from under the test cell, into the ullage. The efflux line from the test cell was then opened and the two flows balanced to the point where the bubbles would disappear. The distinction between bubbling and no bubbling was detectable with flow adjustments within half the least count of the flow meters.

When a steady state flow balance was achieved, all data was recorded. The mixer was then turned on to induce condensation. The needle valve controlling the flow rate of the effluent vapor was slowly closed down until bubbles appeared. A fine adjustment was again made from this point until the bubbles were again eliminated. All data was again recorded. The difference between flow rates with and without the mixer is the condensation induced by the velocity of the liquid as it moves by the test cell.

The mixer was then shut off and the flow rates readjusted to balance with no mixer. This was to assure repeatability. The entire sequence with and without mixer was repeated at least once for each mixer speed and for each level of helium pressure.

The drive gear was then changed and the previous sequence of events was repeated until data was obtained for four circulation speeds (1, 2, 3.5 and 5 rpm), at each nominal pressure setting.

The test program was conducted using methane (99.9 percent pure), Freon-12,

nitrogen, and hydrogen. The results and evaluations are described in the following paragraphs.

TEST RESULTS AND ANALYSIS

A total of 116 test points were obtained during this program, although many of these were deliberately duplicated to demonstrate repeatability. The majority of the tests were conducted with methane and Freon because of the relative ease with which these fluids can be handled. However, sufficient data were obtained with nitrogen and hydrogen to correlate the non-dimensional groupings of parameters.

For a given fluid, the controlled test variables were liquid rotational velocity and liquid subcooling. The dependent variable to be determined was condensation rate. Tables 18 through 21 present these quantities for the four fluids. The actual condensation rates are compared with the theoretical values in Fig. 87. The theoretical values were calculated from the Sterbentz-Bullard correlation which can be written as:

$$\dot{W}_c = 1.12\left[\frac{K_L^{\Delta}\ \rho_L^{\Delta}}{\lambda}\right]^{\frac{1}{2}} (lb^2)^{\frac{1}{2}}\ (U_o\,\Delta T)^{\frac{1}{2}} \qquad (14)$$

This direct comparison indicates that the condensation rates are considerably less than the predicted values throughout the experimental range.

Figures 88 and 89 present data with the subcooling and velocity parameters separated. It will be noted that the scatter in the test data increases markedly at the low speeds and at low values of subcooling. This is due to the fact that the condensation rates were so low that they were in the range of the least count on the volumetric flow meters. At the higher mixer speeds, the data seems to follow the general trends given by the model, even though the condensation rates are low. Visual observation revealed that the gas bubbles, which appear from under the test cell would emanate from less than

TABLE 18

CONDENSATION EXPERIMENT RESULTS - CH_4

TEST NO.	MIXER SPEED ⚠	SUBCOOLING		CONDENSATION RATE	
	rpm	°R	°K	lb/hr	gr/hr
1	5	6.8	3.8	0.090	40.9
2	5	9	5	0.121	54.9
3	5	8	4.4	0.107	48.6
4	3.5	5.4	3	0.071	32.2
5	3.5	4.4	2.4	0.069	31.3
6	1	2.7	1.5	0.019	8.6
7	1	3.7	2.1	0	0
8	1	8.7	4.8	0	0
9	1	7.4	4.1	0	0
10	1	7.8	4.3	0.045	20.4
11	3.5	8.0	4.4	0.075	34.0
12	3.5	10.4	5.8	0.080	36.3
13	3.5	11.2	6.2	0.079	35.9
14	5	8.9	4.9	0.113	51.3
15	5	8.8	4.9	0.111	50.4
16	1	8.4	4.7	0	0
17	1	6.6	3.7	0	0
18	3.5	6.3	3.5	0.069	31.3
19	3.5	5.9	3.3	0.077	35.0
20	5	5.8	3.2	0.091	41.3
21	5	4.9	2.7	0.089	40.4
22	1	4.6	2.6	0	0
23	1	7	3.9	0.015	6.8
24	1	7	3.9	0.015	6.8
25	5	6.8	3.8	0.104	47.2
26	2	6.3	3.5	0.015	6.8
27	1	4.3	2.4	0	0
28	1	2.7	1.5	0.014	6.7
29	2	3.5	1.9	0.014	6.7

⚠ Mean velocity at test cell: 5 rpm = 0.36 ft/sec = 0.11 m/sec
3.5 rpm = 0.25 ft/sec = 0.076 m/sec
2 rpm = 0.14 ft/sec = 0.043 m/sec
1 rpm = 0.07 ft/sec = 0.021 m/sec

TABLE 19

CONDENSATION TEST RESULTS - FREON-12

TEST NO.	MIXER SPEED	SUBCOOLING		CONDENSATION RATE	
	rpm	°R	°K	lb/hr	gr/hr
1	5	21.9	12.1	0.518	235
2	5	20.4	11.4	0.474	215
3	3.5	19.2	10.6	0.295	134
4	3.5	17.4	9.6	0.284	129
5	2	15.9	8.8	0.121	55.0
6	2	15.5	8.6	0.179	81.3
7	2	12.9	7.2	0.154	69.9
8	2	12.7	7.0	0.154	69.9
9	2	12.4	6.9	0.077	35.0
10	1	12.3	6.8	0.039	17.7
11	1	11.8	6.5	0.039	17.7
12	3.5	4.1	2.3	0.137	62.2
13	3.5	4.1	2.3	0.136	62.1
14	2	3.5	1.9	0.035	15.9
15	2	3.5	1.9	0.104	47.2
16	2	3.5	1.9	0.035	15.9
17	2	3.5	1.9	0.035	15.9
18	5	7.3	4.1	0.257	117
19	5	7.3	4.1	0.257	117
20	5	7.2	4.0	0.147	66.7
21	5	7.2	4.0	0.146	66.3
22	1	7.3	4.1	0.036	16.3
23	1	7.3	4.1	0.036	16.3
24	1	9.3	3.5	0.036	16.3
25	1	20.6	11.4	0.137	62.2
26	1	19.0	10.5	0.041	18.6
27	1	17.9	9.9	0.060	27.2
28	1	17.3	9.6	0.060	27.2
29	2	14.7	8.2	0.138	62.3
30	2	14.2	7.9	0.135	61.8
31	3.5	12.7	7.0	0.245	111
32	3.5	12.6	7.0	0.245	111
33	5	23.5	13.1	0.612	278
34	5	22.1	12.3	0.464	211
35	5	21.4	11.9	0.441	200
36	5	22.1	12.3	0.474	215
37	5	21.2	11.8	0.428	194
38	5	16.8	9.3	0.443	201
39	5	16.2	9.0	0.441	200
40	3.5	9.8	5.4	0.152	69.0
41	3.5	9.8	5.4	0.152	69.0
42	2	9.6	5.3	0.113	51.3
43	2	9.6	5.3	0.112	50.8
44	1	8.7	4.8	0	0
45	1	8.6	4.8	0.055	25.0
46	1	5.4	3	0	0
47	1	5.4	3	0	0
48	2	5.4	3	0.089	40.4
49	2	5.9	3.3	0.090	40.7

TABLE 20

CONDENSATION TEST RESULTS - LN_2

TEST NO	MIXER SPEED	SUBCOOLING		CONDENSATION RATE	
	rpm	°R	°K	lb/hr	gr/hr
1	3.5	5	2.8	0.180	81.7
2	3.5	5	2.8	0.180	81.7
3	5	5	2.8	0.292	133
4	5	5	2.8	0.292	133
5	2	5	2.8	0.068	30.9
6	2	5	2.8	0.045	20.4
7	1	5	2.8	0.022	10.0
8	1	5	2.8	0.045	20.4
9	1	3	1.7	0	0
10	1	3	1.7	0.021	9.5
11	2	3	1.7	0.061	27.7
12	2	2.9	1.6	0.041	18.6
13	3.5	2.9	1.6	0.081	36.8
14	3.5	2.8	1.6	0.080	36.3
15	5	2.5	1.4	0.120	54.5
16	5	2.3	1.3	0.119	54.0
17	5	1.8	1	0.076	34.5
18	5	1.8	1	0.076	34.5
19	3.5	1.7	0.9	0.066	30.0
20	3.5	1.7	0.9	0.066	30.0
21	2	1.7	0.9	0.038	17.3
22	2	1.6	0.9	0.038	17.3

TABLE 21

CONDENSATION TEST RESULTS - LH_2

NO.	MIXER SPEED	SUBCOOLING		CONDENSATION RATE	
	rpm	°R	°K	lb/hr	gr/hr
1	5	2.6	1.4	0.013	5.9
2	5	2.7	1.5	0.013	5.9
3	5	1.8	1	0.012	5.4
4	5	1.8	1	0.012	5.4
5	3.5	1.8	1	0.006	2.7
6	3.5	1.8	1	0.006	2.7
7	3.5	2.4	1.3	0.012	5.4
8	5	0.9	0.5	0	0
9	5	0.8	0.4	0	0
10	5	0.6	0.3	0	0
11	5	0.6	0.3	0	0

half the test cell perimeter. This suggests that the condensing vapor was not uniformly distributed in the test cell and condensation was occurring over a fraction of the interface area (bL).

The data for all fluids have been combined in non-dimensional form on Fig. 90. The grouping of parameters can be evolved from Eq. 15 from whence we get:

$$N_u = 1.12 \left[R_e \, P_r \, N_\lambda \right]^{\frac{1}{2}} \qquad (15)$$

where N_u is a pseudo Nusselt number used to non-dimensionalize the rate of condensation per unit area. S_B is the subcooling parameter, $(Cp\,\Delta T)/\lambda$. R_e and P_r are the Reynolds and Prandtl moduli, respectively. The low speed data has been deliberately omitted from Fig. 90 to minimize the impact of an obvic us facility inadequacy. The four fluids still give a decade variation in the parameter groupings. This non-dimensional presentation seems to confirm the parameter dependency described by the theory. However, the experimental constant is approximately twenty percent of the theoretical value which might represent the effectiveness of the test cell condensation area in these experiments.

Based upon this experimental program it can be concluded that condensation can be induced by circulation of a subcooled propellant past a liquid vapor interface. Since the process is dominated by forced convection, these results should be independent of gravity level. In the absence of further experimental data, the Sterbentz-Bullard correlation, with an empirical constant of 0.2 can be used to predict condensation rates due to fluid circulation, i.e.,

$$N_u = 0.2 \left[R_e \, P_r \, N_\lambda \right]^{\frac{1}{2}} \qquad (16)$$

However, it is suggested that further work should be accomplished to verify or improve upon this constant, and to extend the experimental range of parameters.

C 4

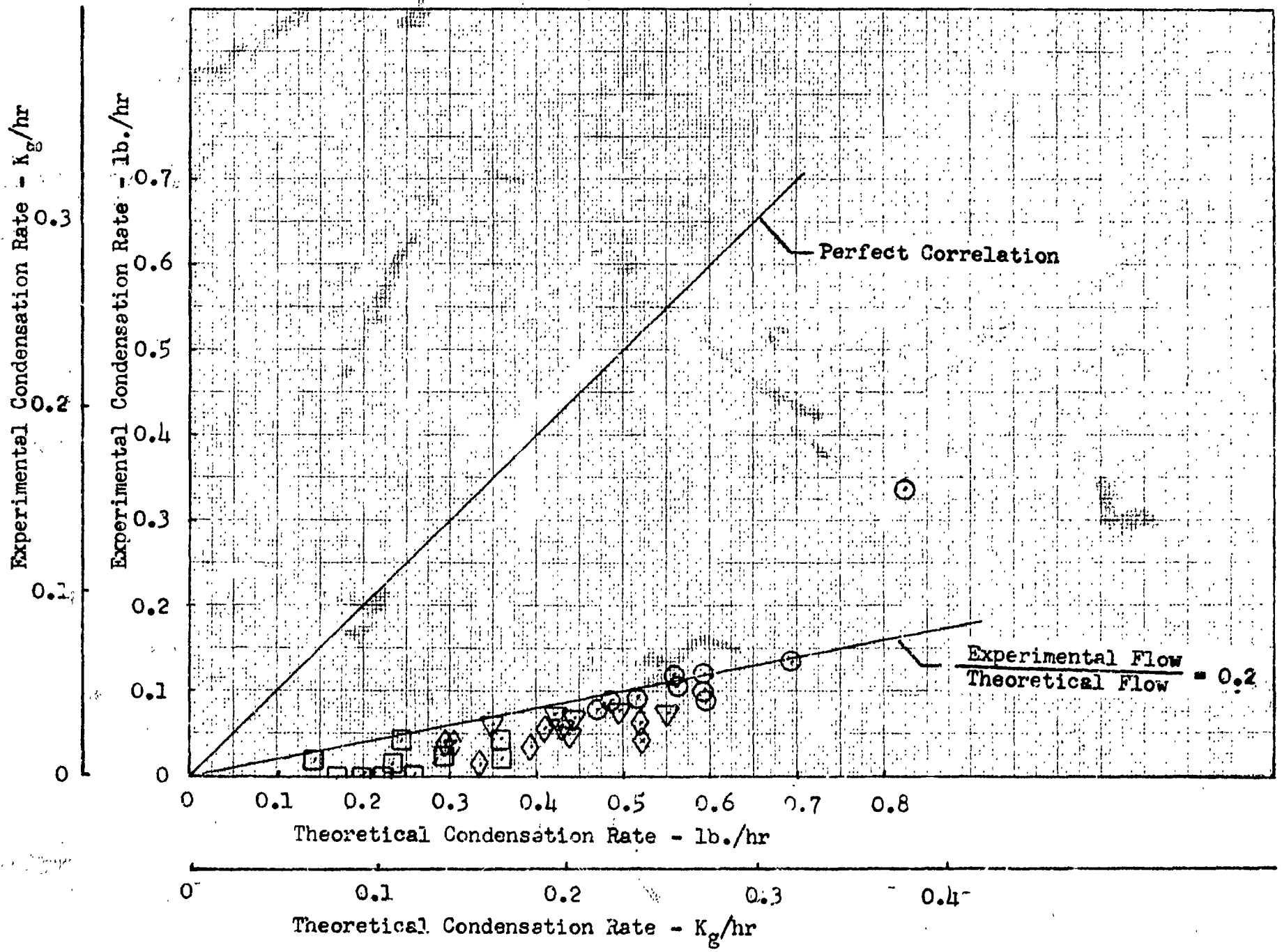

Figure 87 Direct Comparison Between Experimental and Theoretical Condensation Rate (LN_2)

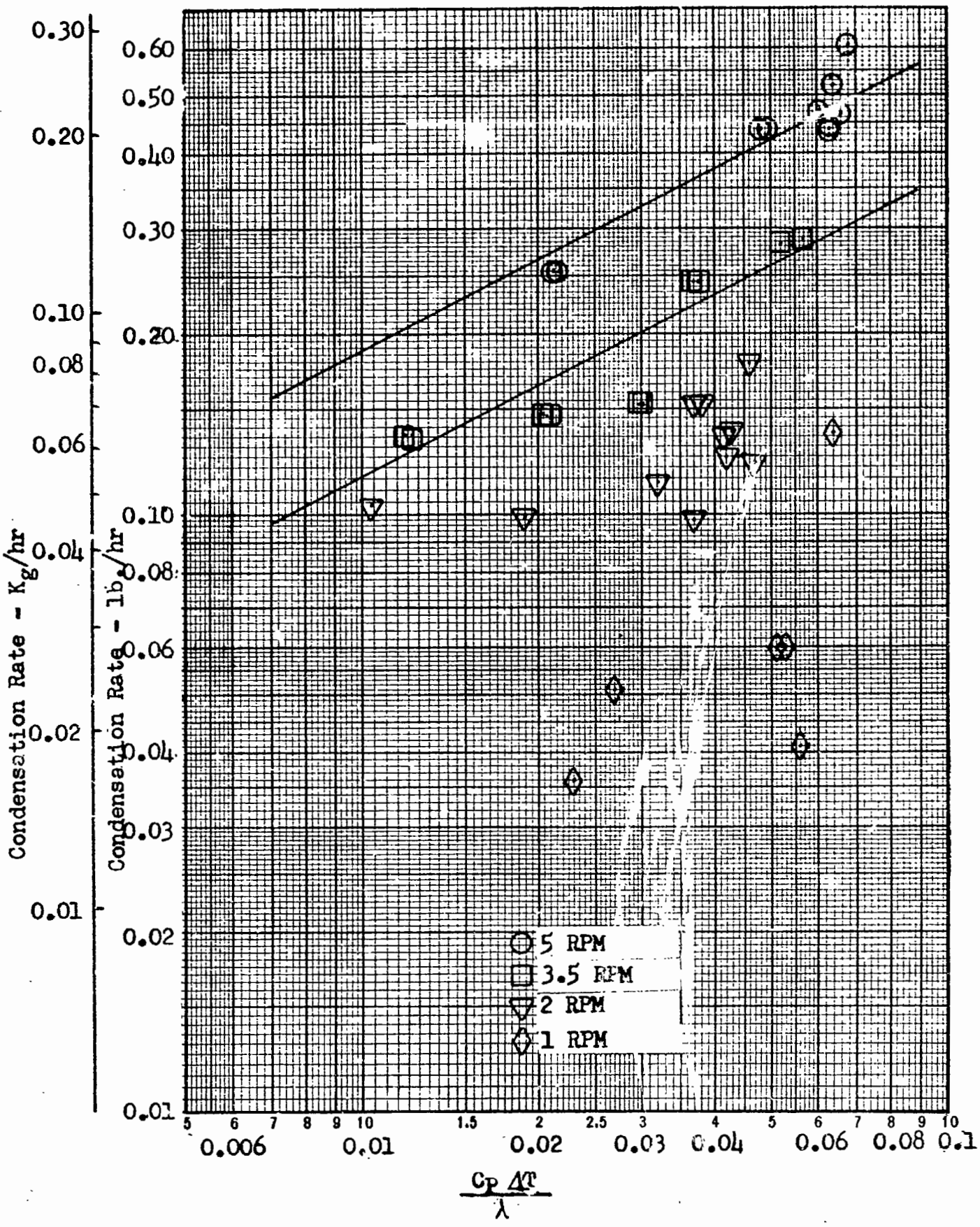

Figure 88 Experimental Correlation of Condensation Rate with Liquid Subcooling with Freon (F-12)

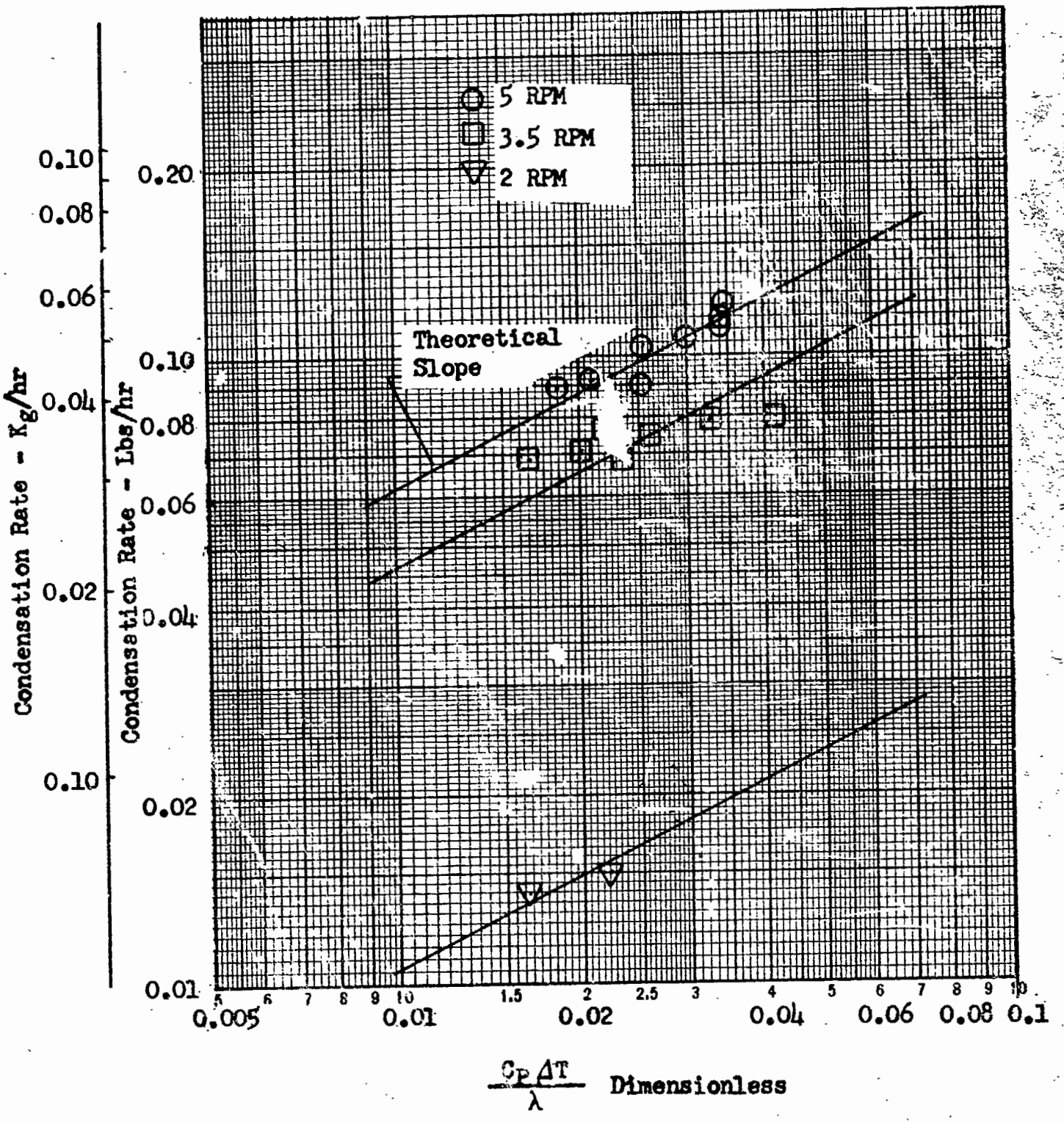

Figure 89 Experimental Correlation of Condensation Rate with Liquid Subcooling with Methane

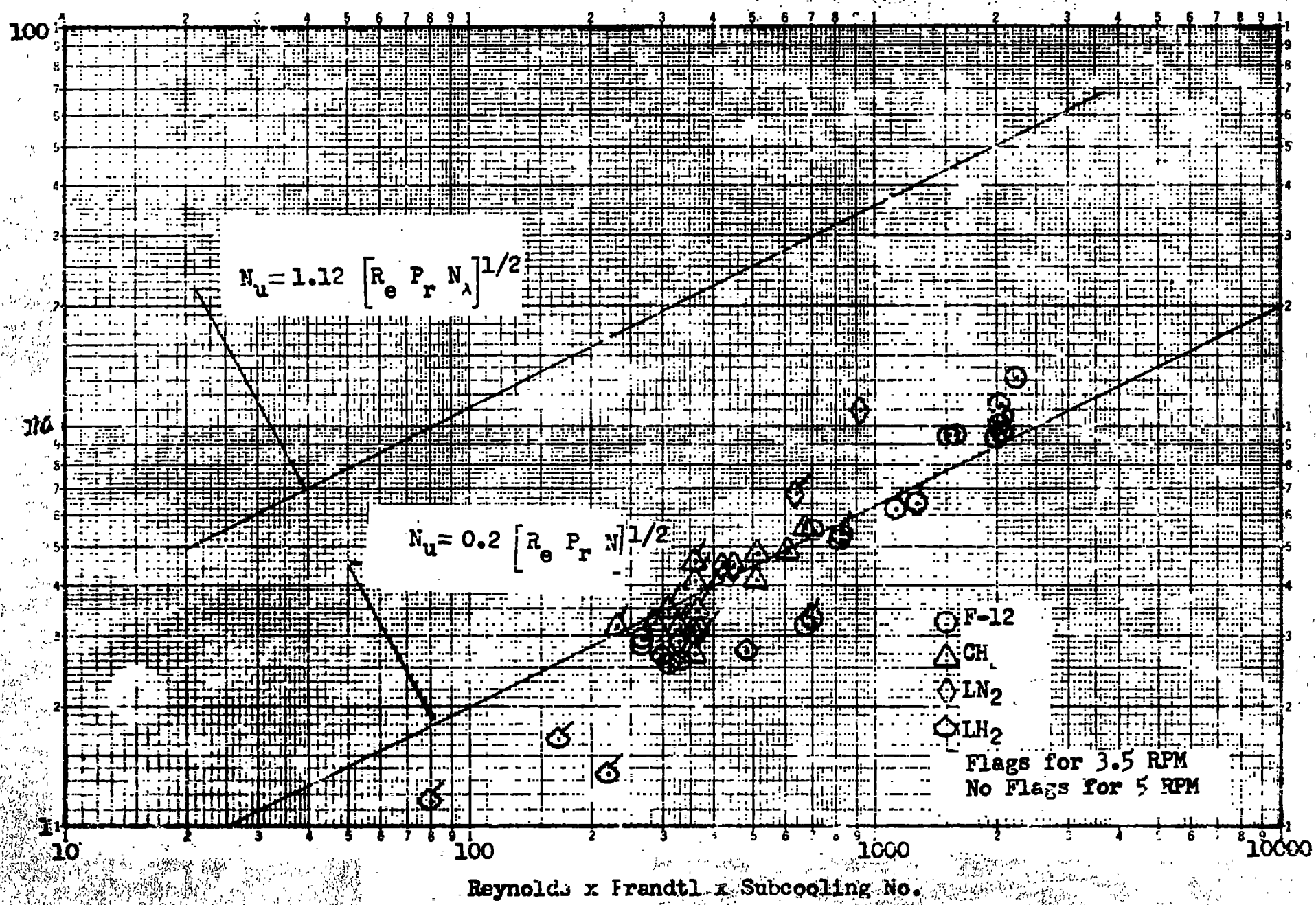

Figure 90 Comparison Between Condensation Theory and Experimental Data

VEHICLE OPERATIONAL ANALYSIS

The experimental program and the analyses, described previously in this report confirm that the thermal conditioning system will efficiently control tank pressure. This section contains a description of the flight operation of the thermal conditioning system for pressure control. Also, an integration study is presented wherein the system is used to satisfy attitude control requirements as well as provide tank pressure control. **The Earth-Mars Kickstage hydrogen tank was used for the integration. Its characteristics are:**

Dimensions	(Oblate-Spheroid)	Semi-Major Axis: 52 inch (1.32 m) Semi-Minor Axis: 42.9 inch (1.09 m)		
Pressurant	Helium for pressurization, hydrogen gas for expulsion			
Duration	220 days			
Nominal Working Pressure	28 psia (193,000 N/m^2)			
Bulk Liquid Temperature for Engine Use	37.7°R (21°K)			
Expulsion Profile	Firing Number	Weight	Firing Time (sec)	Time (days after launch)
	1	80 lb (36.3 K_g)	80	10
	2	40 lb (18.1 K_g)	40	180
	3	Remainder	Remainder 33.8 lb/sec (15.3 K_g/sec)	220
Heat Leak	Maximum = 17.2 Btu/hr (5.05 w) Minimum = 5.8 Btu/hr (1.7 w) Average = 11.5 Btu/hr (3.40 w)			

TANK PRESSURE CONTROL

The solar force acting on the vehicle in the 220 day Earth-Mars transfer trajectory is less than 10^{-7} g's. The diameter of the mission 2 vehicle is 110 inches (2.8 m) for which the critical jet velocity is calculated to be 0.63 feet per second (3 cm/sec). The thermal conditioning system mixer was designed and tested for 5 feet per second (152 cm/sec). Therefore, the complete mixing torroidal flow patterns should be achieved in the flight vehicle, and the thermodynamic equilibrium model is applicable during the coast period.

During the coast period, the fraction of time the system will be operating is given by

$$\theta^* = \frac{Q_o}{M_o\lambda - 3.41P}$$

The mixer power is 2.4 watts as determined in tests conducted at Lockheed (Ref. 8) on a brushless DC motor. Using the average heating rate, 11.5 Btu/hr (3.4 watts), the operating ratio for the mission 2 vehicle is calculated to be 0.045, i.e., the TCU will operate less than 5 percent of the time. The mixer power does represent a penalty compared to a direct ullage vent. The average energy put into the tank during the coast period is $P\theta^*$. For the 220 days this amounts to 10.2 lbs (4.6 K_g) of hydrogen boiloff.

In addition to the coast period, a penalty is associated with the transient following each of the three firings. The initial depressurization amounts to less than 15 seconds which is insignificant. However, the vehicle is assumed to use helium pressurization. When total tank pressure is the control parameter, additional boiloff occurs as a result of the noncondensible. The tests have confirmed that the helium has an insignificant effect on the rate of pressure response. However, it does raise the pressure level, which increases the length of time the TCU must operate immediately following a firing in order to return the tank to storage pressure.

For the mission 2 vehicle, nominal storage pressure i. 17 psia (117,000 N/m^2) and ambient helium is used to supply an additional 11 psi (75,800 N/m^2) for each firing. The propellant is then expelled with warm hydrogen. As the ullage volume increases, the partial pressure of helium decreases and, after mixing, comes into equilibrium with the propellant at a final partial pressure given by:

$$P_{Hef} = P_{Hei} \frac{T_f}{T_{ei}} \times \frac{V_i}{V_f}$$

where

P_{Hef} = final helium partial pressure
P_{Hei} = initial helium partial pressure (11 psi)
T_f = final tank propellant temperature
T_{ei} = mean initial ullage temperature
V_i = initial ullage volume
V_f = final ullage volume

The extra time required to reduce tank pressure an amount equal to the helium partial pressure is then

$$\Delta\theta = \frac{P_{Hef}}{(dp/d\theta)}$$

and the boiloff increment is

$$\Delta M = M_o \Delta\theta$$

For the mission 2 vehicle vent rate is 1.4 lb (0.64 K_g) per hour. Calculations were made for both the first and second firings and the results indicated that the helium which is retained in the tank adds 4.6 lb (2.1 K_g) to the mission boiloff.

TCU/ACS INTEGRATION

For the nominal flight-type thermal conditioning unit (TCU) design tested in this program, flight operation calls for dumping the cold vent hydrogen vapor overboard through a thrust nullifier nozzle during its intermittent venting cycle. Since the vented gas still has a substantial cooling capacity and potential energy content, overall vehicle weight penalties could be reduced by utilizing the vented gas for other vehicle functions.

Two major areas suggest themselves: (1) cooling of tank penetrations or equipment to reduce tank heat leaks or maintain equipment operational temperatures, and (2) expulsion of the gas through thruster nozzles to provide desired vehicle orientation or maneuvering capability. The first application was covered in Ref. 1. In the current program, the feasibility and desirability of integrating the thermal conditioning and attitude control systems was evaluated for an Earth-Mars mission where continuous payload to the sun orientation is required.

The ground rules which were used in this study are given in Table 22. These were taken from a previous NASA study (Ref. 5) to determine Earth-Mars mission requirements. In that program six different ACS propellant combinations were investigated for payload-to-sun orientation. Consequently, this study provides an ideal reference against which monopropellant GH_2 ACS applications can be compared, when the monopropellant is vented hydrogen gas.

The primary continuous disturbing solar torques in Earth-Mars transit shown in Table 22 are estimates based on Earth-Moon space and thus are conservative for the Earth-Mars mission (since solar pressure varies as the inverse square of distance from the sun).

Solar torques may be augmented in orbital cruise modes by gravity gradient torques. Gravity gradient torques depend on the spacecraft moment of inertia sensor, together with spacecraft orientation relative to the local vertical.

TABLE 22
STUDY GROUND RULES

1. Vehicle Configuration:.....Figure 91

2. Vehicle Mass Distribution as a Function of Time:.....Table 23

3. Vehicle Weight and Moments of Inertia:.....

		Earth Departure	Mars Arrival	Mars Orbit
Weight - lbs. (K_g)		9700 (13140)	5880 (7950)	4900 (6140)
Moments of Inertia	I_{xx} -slug-ft^2 (K_g-m^2)	3079 (4160)	1999 (2700)	1753 (2370)
	I_{yy} -slug-ft^2 (K_g-m^2)	2885 (3910)	1739 (2355)	1250 (1690)
	I_{zz} -slug-ft^2 (K_g-m^2)	3580 (4850)	1789 (2420)	1268 (1713)

4. Separation of Thrusters:..... 10 ft. (3.05m)

5. Vehicle Deadband Sun Orientation:.....± 1 degree

6. Disturbing Torques:.....

Transit (Solar Pressure	Orbit (Solar Pressure Plus Gravity Gradient)
$M_x = 0.2 \times 10^{-5}$ ft.-lb (0.27×10^{-5} N-m)	$M_x = 1.0 \times 10^{-5}$ ft-lb (1.35×10^{-5} N-m)
$M_y = 1.0 \times 10^{-5}$ ft-lb (1.35×10^{-5} N-m)	$M_y = 5.0 \times 10^{-5}$ ft-lb (6.8×10^{-5} N-m)
$M_z = 1.0 \times 10^{-5}$ ft-lb (1.35×10^{-5} N-m)	$M_z = 5.0 \times 10^{-5}$ ft-lb (6.8×10^{-5} N-m)

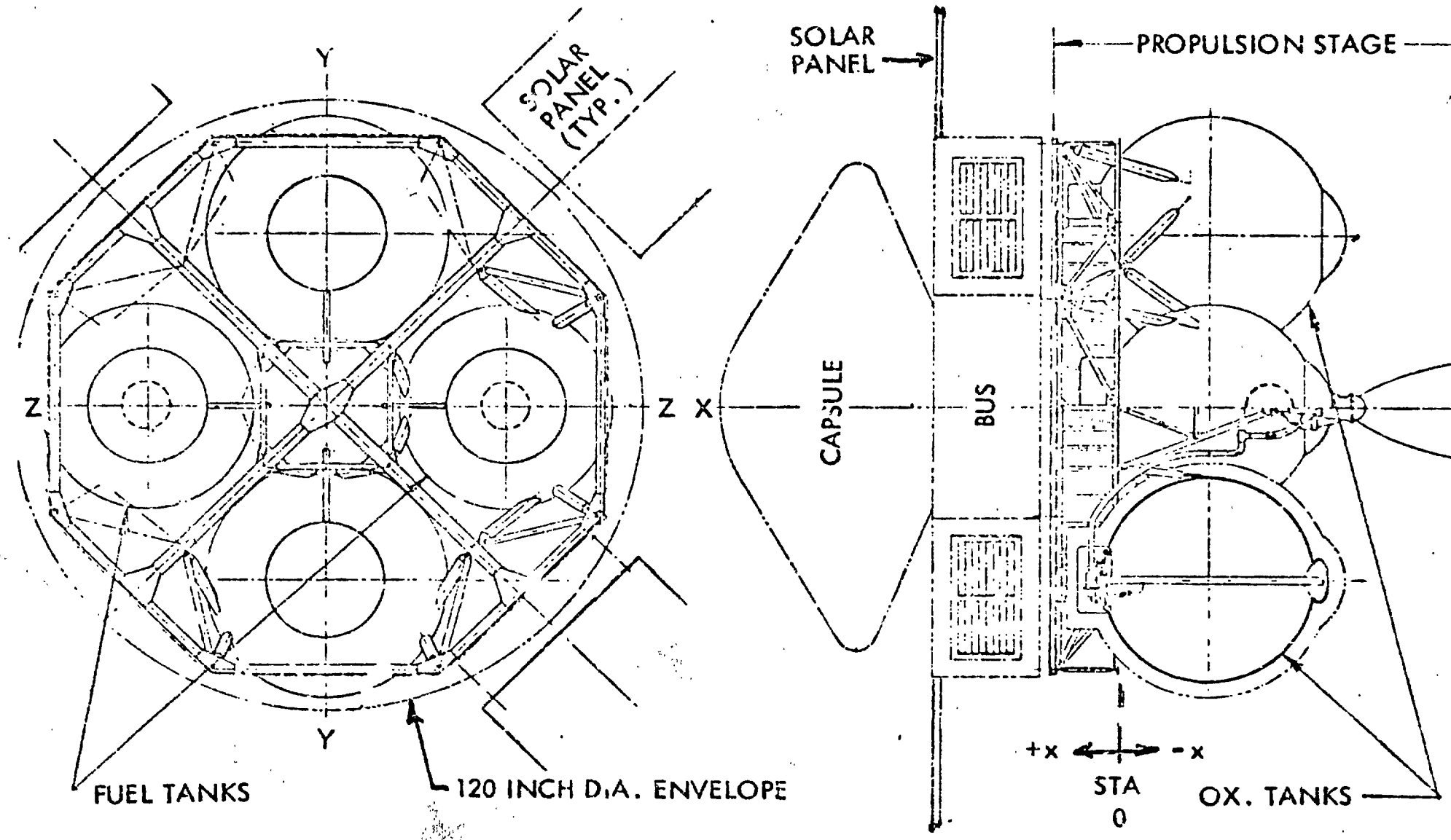

Figure 91. Typical Spacecraft at Start of Cruise

Since the spacecraft remains sun oriented while cruising in orbit, the relative orientation has large magnitude, periodic variations so that many of the cyclical motions induced by these torques may be within deadbands and thus not induce control response. Nevertheless, the combined solar and gravity gradient torque envelopes were increased for orbital cruise to account for an estimated secular effect.

Disturbing torques generally exist about all body axes during periods of main engine burn. It is assumed the main engine has a thrust vector control system to compensate for pitch and yaw disturbance torques. It is further assumed that the pitch and yaw attitude control thrusters are normally disabled during main engine burns to prevent channel response with attendant expenditure of attitude control propellant. The roll channel of the attitude control system must counteract engine-generated roll disturbance torques, however. Values for these swirl torques are based on mariner data scaled by engine thrust level, resulting in 3.0 ft-lb (4.05 N-m) for a 5,000 lb (22,200 N) engine.

Operating Modes

The attitude control system operating modes which significantly affect GH_2 propellant expenditure are listed below:

(1) Tipoff Rate Removal

The removal of spacecraft tipoff rates about all three control axes following separation from the launch vehicle.

(2) Acquisition Transients and Searches

The starting and stopping of spacecraft roll, pitch, and yaw rates in sun/Canopus acquisition processes.

TABLE 23

VEHICLE WEIGHT DISTRIBUTION AS A FUNCTION OF FLIGHT EVENTS

Item No. and Name	Mass (lb)	X (in.)	Radius From X-X (in.)	Assumed Mass Distribution
EARTH DEPARTURE				
1. Engine	98	-50	0	Point mass
2. Engine Support	10	-10	0	Point mass
3. Stage Frame	43	6	51 to 53	12 in. thick ring perpendicular to XX axis
4. Beams	34	6	0 to 52	Cruciform with two 2 × 12 × 104 in. beams ⊥ to XX
5. Insulation	18	13	0 to 52	Disc of uniform mass ⊥ to XX axis
6. Bus	3981	27	15 to 52	21 in. thick disc of uniform mass ⊥ to XX
7. Solar Panels	100	39	68 to 155	Four 25 lb panels, 42 × 87 in., from r = 68 to r = 155
8. Fuel System	270	-17	34	Two 135 lb point masses in opposite quadrants
9. Oxid. Syst.	346	-17	34	Two 173 lb point masses in opposite quadrants
10. Fuel (usable)	640	-17	34	In two spherical masses of 34 in. dia., centered on ZZ
11. Oxid. (usable)	3360	-17	34	In two spherical masses of 40 in. dia., centered on YY
12. Capsule	800	64	0 to 48	36 in. thick disc of uniform mass ⊥ to XX
MARS ARRIVAL				
1. through 9.	4900	(Same as Earth Departure)		
10. Fuel (usable)	30	-17	34	In two point masses of 15 lb ea.
11. Oxid. (usable)	158	-17	34	In two point masses of 79 lb ea.
12. Capsule	(Same as Mars 1)			
MARS ORBIT				
1. through 9.	4900	(Same as Earth Departure)		
10. Fuel (usable)	0	—	—	
11. Oxid. (usable	0	—	—	
12. Capsule	0	—	—	

(3) Commanded Turns

The maneuvers generated by sequential turn commands at prescribed rates. A roll-pitch-roll sequence was taken as the standard with unwinding accomplished in reverse order.

(4) Transit Cruise

Limit cycle expenditures based on the most likely maximum solar torque levels about each axis.

(5) Orbital Cruise

Limit cycle expenditures based on the most likely maximum sum of solar and gravity gradient torque levels about each axis.

(6) Main Engine Burns

The counteracting of main engine swirl (roll) torques during escape, midcourse, orbit insertion, and orbit trim engine burns.

Propellant expenditures are minimized for operating modes 2, 4 and 5 by minimizing thrust levels and impulse bits. Higher thrust levels are required for operating modes 1, 3 and 6. Details on the reasoning behind the above two statements are provided in Ref. 5.

Candidate Integrated TCU/ACS Systems

Based on the study ground rules and proposed operating modes, three representative system schematics were laid out as shown in Fig. 92.

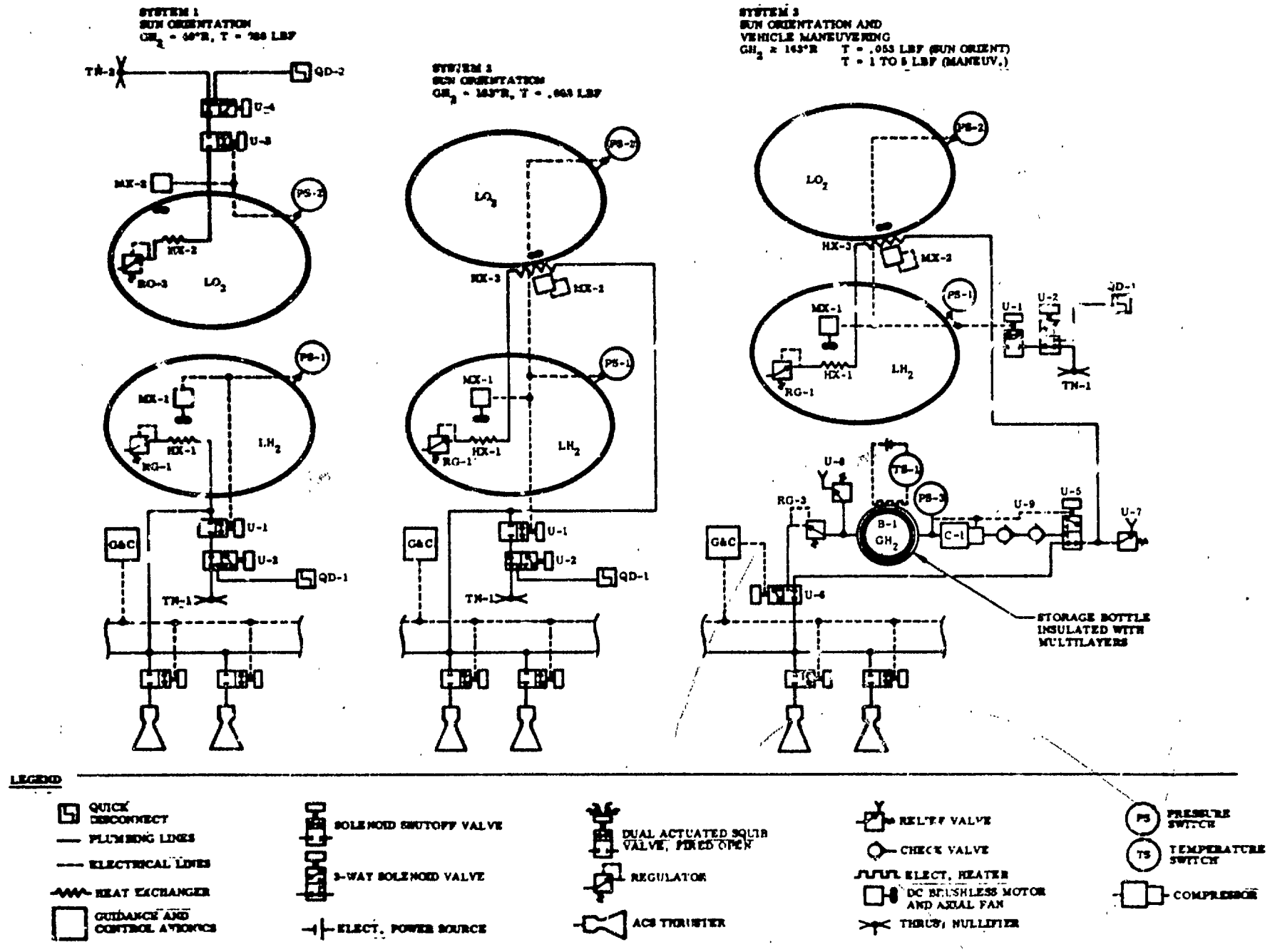

Figure 92 Candidate Integral TCU/ACS Systems

Systems 1 and 2 have a low thrust level suitable for operating modes 2, 4 and 5 described above. System 3 has both a low and high level thrust capability and thus can cover all six operating modes.

System 1

Both the hydrogen and oxygen tanks use separate TCU's to maintain tank pressure control. The vent hydrogen at 40°R (22.2°K) can either be dumped overboard through a thrust nullifier nozzle or passed through the ACS thrusters to maintain the desired sun orientation. Twelve thrusters, plus associated plumbing and controls, are the only additional hardware required to provide sun orientation.

System 2

Hydrogen vapor at 40°R (22.2°K) is passed through an external heat exchanger located on the liquid oxygen tank access cover to cool the 163°R (90.5°K) oxygen and maintain a nonvented oxidizer tank. This series venting and cooling arrangement was found to be competitive with a bypass system as described in Ref. 6. For the series system, the total oxygen tank heat input is adjusted (by adjusting the oxygen tank insulation thickness) to match the total hydrogen boiloff. However, oxygen tank temperatures and pressures will vary somewhat throughout the mission based on the changing ratio of heat inputs to the oxygen and hydrogen tanks. (A somewhat more complicated parallel, bypass system can be used that will hold the oxygen tank pressure relatively constant; excess coolant hydrogen gas bypasses the oxygen tank heat exchanger based on pressure switch operation. The 163°R (90.5°K) hydrogen can either be dumped overboard through a thrust nullifier or passed through the ACS thrusters to maintain sum orientation. Additional hardware required for attitude control are the 12 thrusters, associated plumbing and controls and the oxygen tank heat exchanger.

System 3

Systems 1 and 2 are designed to handle the low thrust requirements associated with sun orientation. If higher thrust levels are needed for vehicle maneuvering, a vane or piston type compressor with a 1.2 HP electric motor drive, plus storage bottle and associated plumbing, are added. An electrical heater and temperature switch are used to maintain the storage bottle about 163°R (90.5°K).

The lightest weight ACS developed in Ref. 5 was used as a base reference against which the hydrogen systems were compared. This reference system stores cold N_2H_4 gas for the low thrust requirements and liquid N_2H_4 for the high thrust requirements.

Other techniques for providing attitude control or vehicle maneuvering capability were not examined since the intent of the study was only to investigate the use of vent hydrogen. These other techniques should be reviewed, however, when ACS selections are made for a mission 2 type vehicle.

ACS Requirements

Analyses were performed to establish the following ACS requirements: thrust levels, pulse cycle widths, impulse requirements, propellant quantities and thruster cycles. From these requirements, total system weights can be calculated and recommendations made on system selection.

Prior to beginning the analyses, data were obtained on the specific impulse values to be expected using hydrogen monopropellant as a function of gas temperature and nozzle divergence area ratio as shown in Fig. 93. For the remaining calculations, a nozzle divergence area ratio of 20 was used.

Low level thrust as a function of hydrogen gas temperature was also calculated for a vent flow rate of 1.4 lb/hr (0.64 K_g/hr) as shown in Fig. 94.

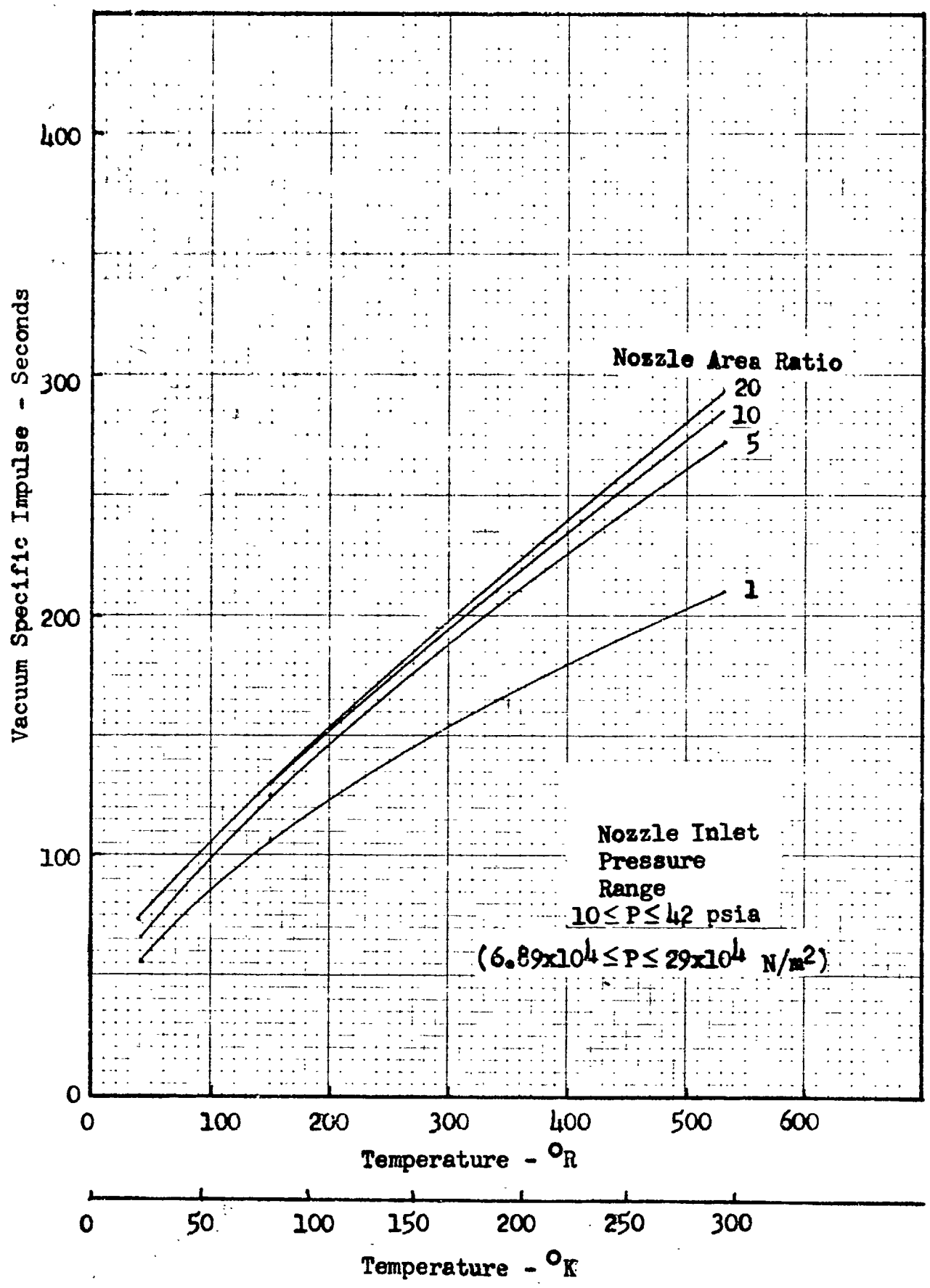

Figure 93 Specific Impusle as A Function of Temperature And Nozzle Area Ratio for Gaseous Hydrogen Monopropellant

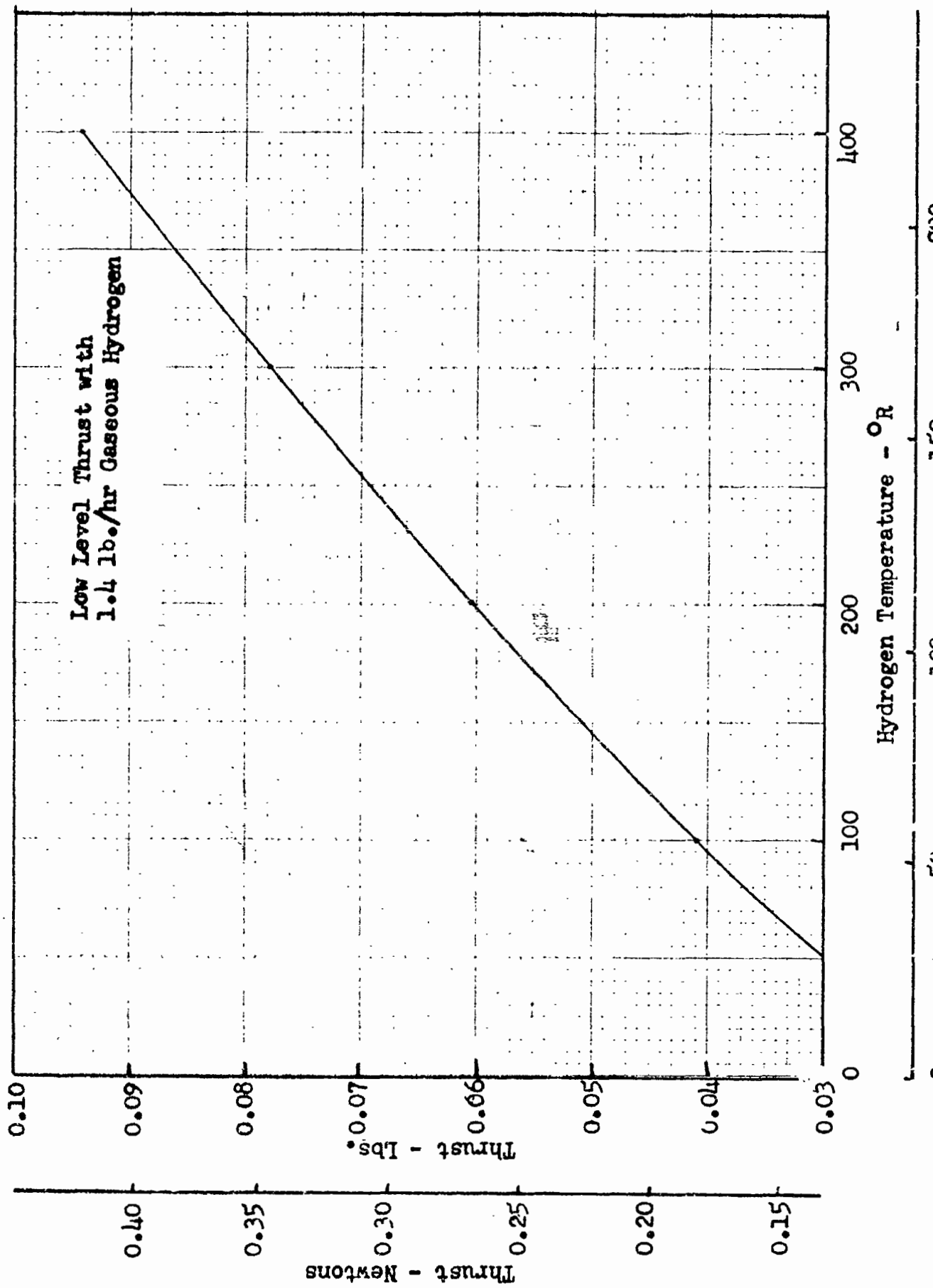

Figure 94 Low Level Thrust Variation with Temperature

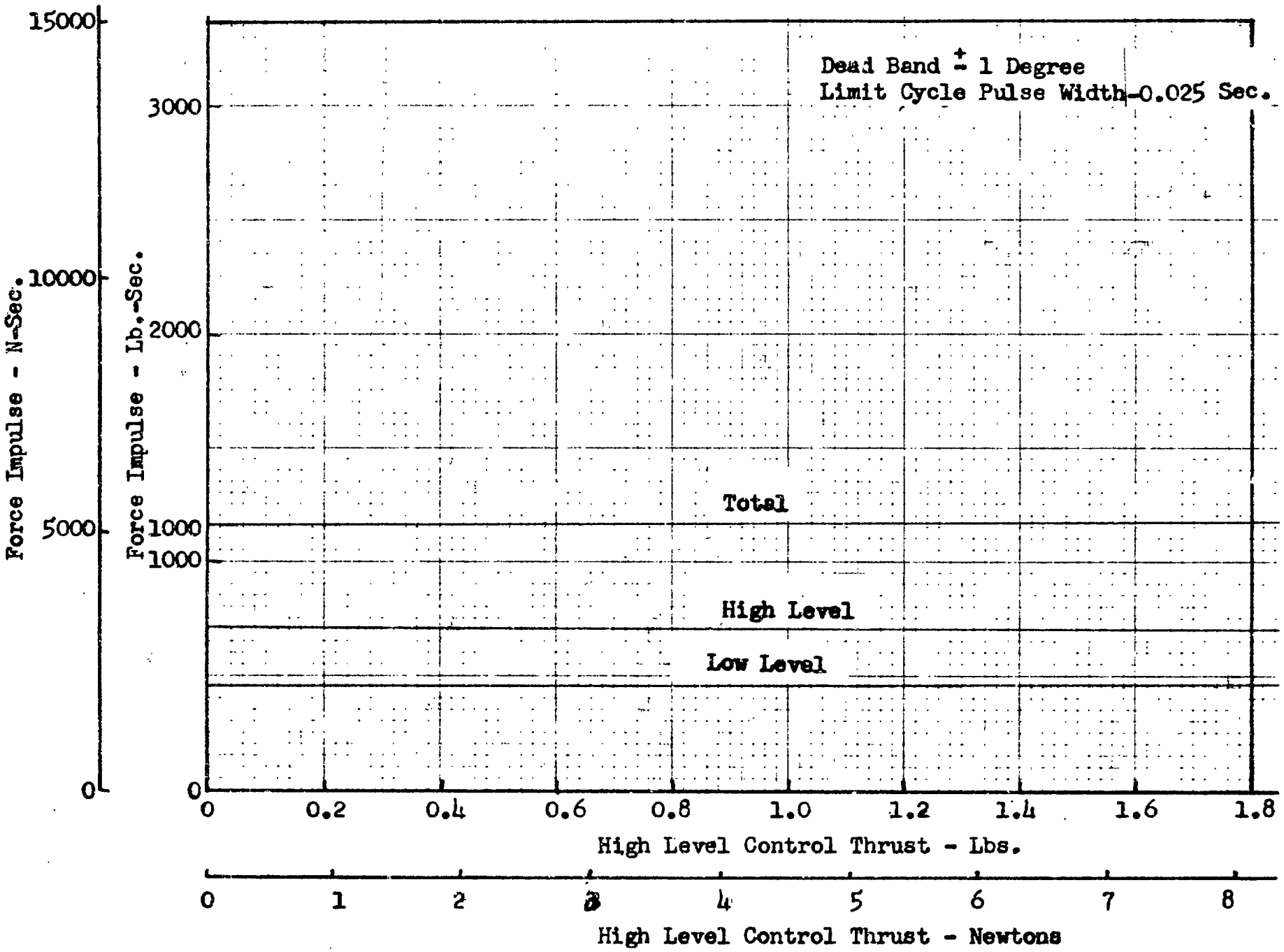

Figure 95 ACS Thruster Requirements (0.025 Second Pulse Width)

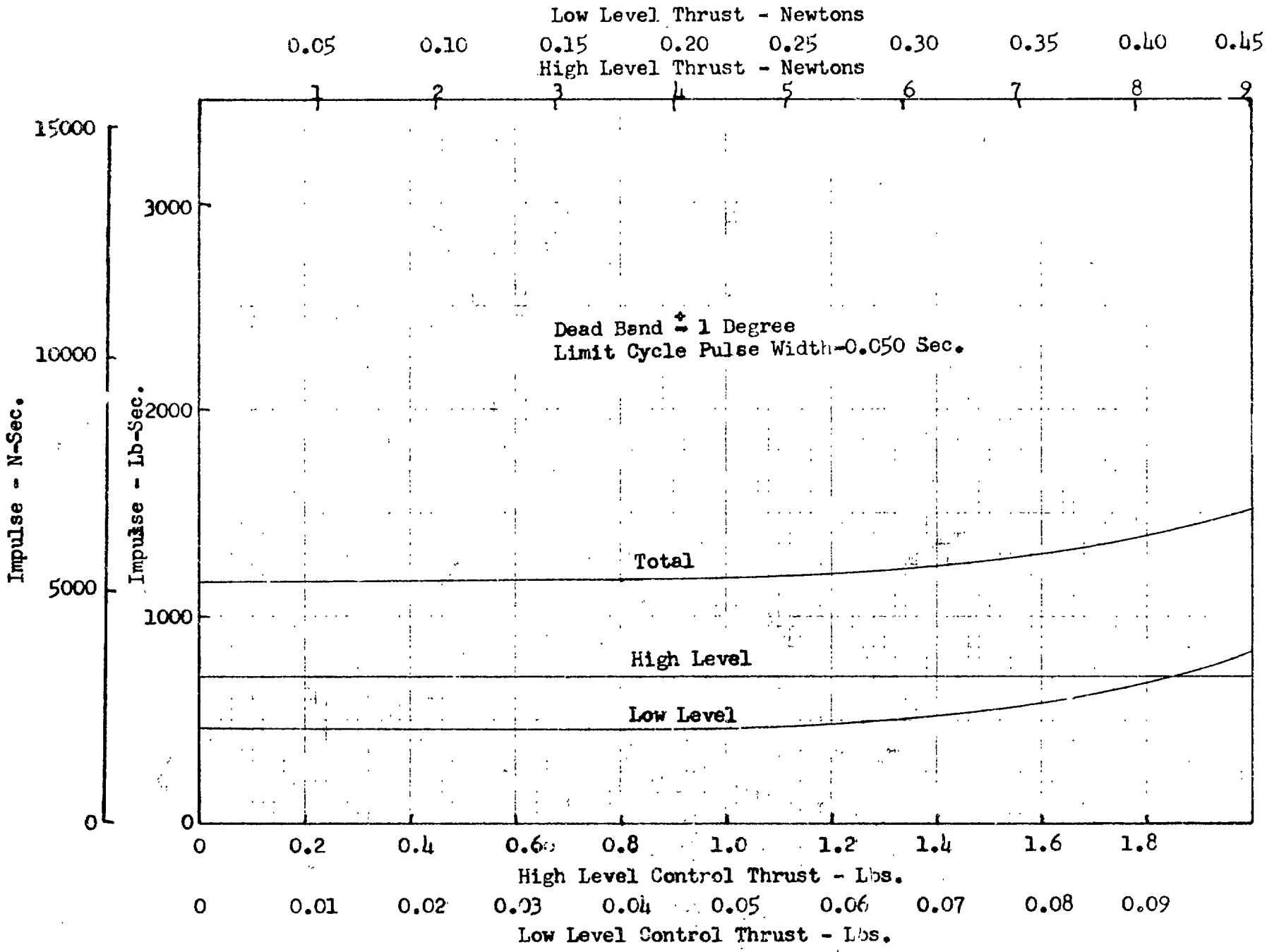

Figure 96 ACS Thruster Requirements (0.050 Second Pulse Width)

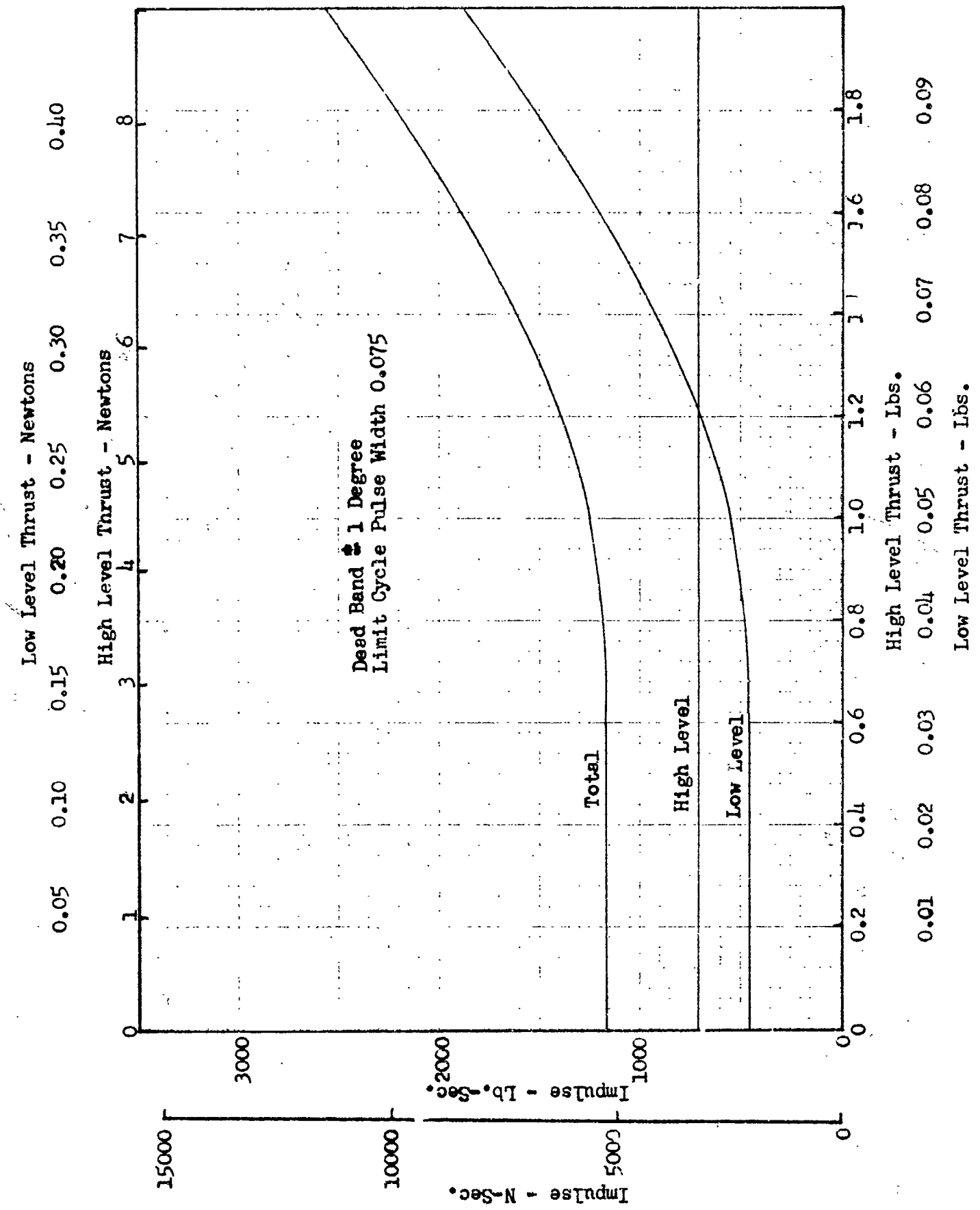

Figure 97 ACS Thruster Requirements (0.075 Second Pulse Width)

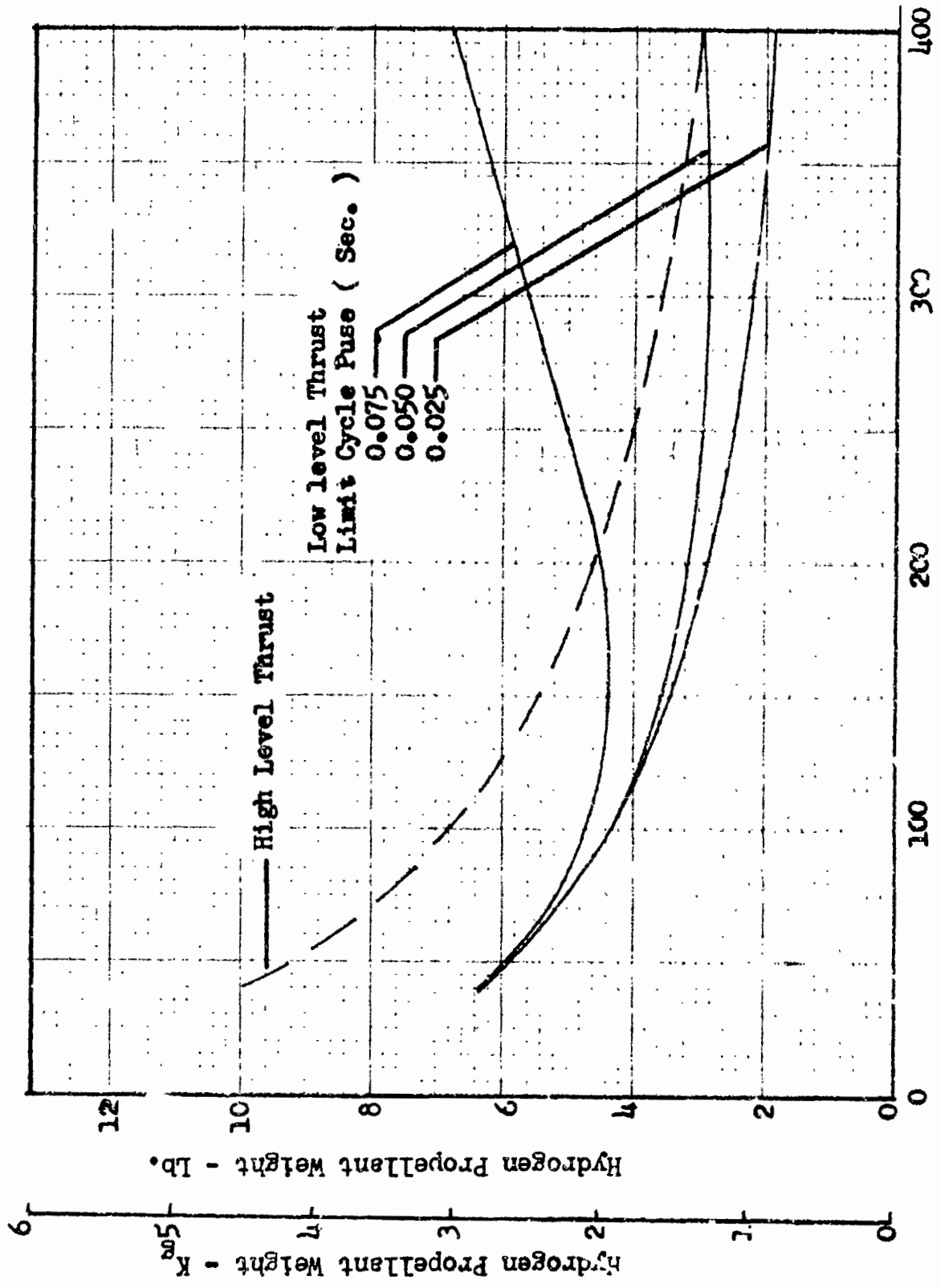

Figure 98 Gaseous Hydrogen Requirements for Low and High Level Thrust

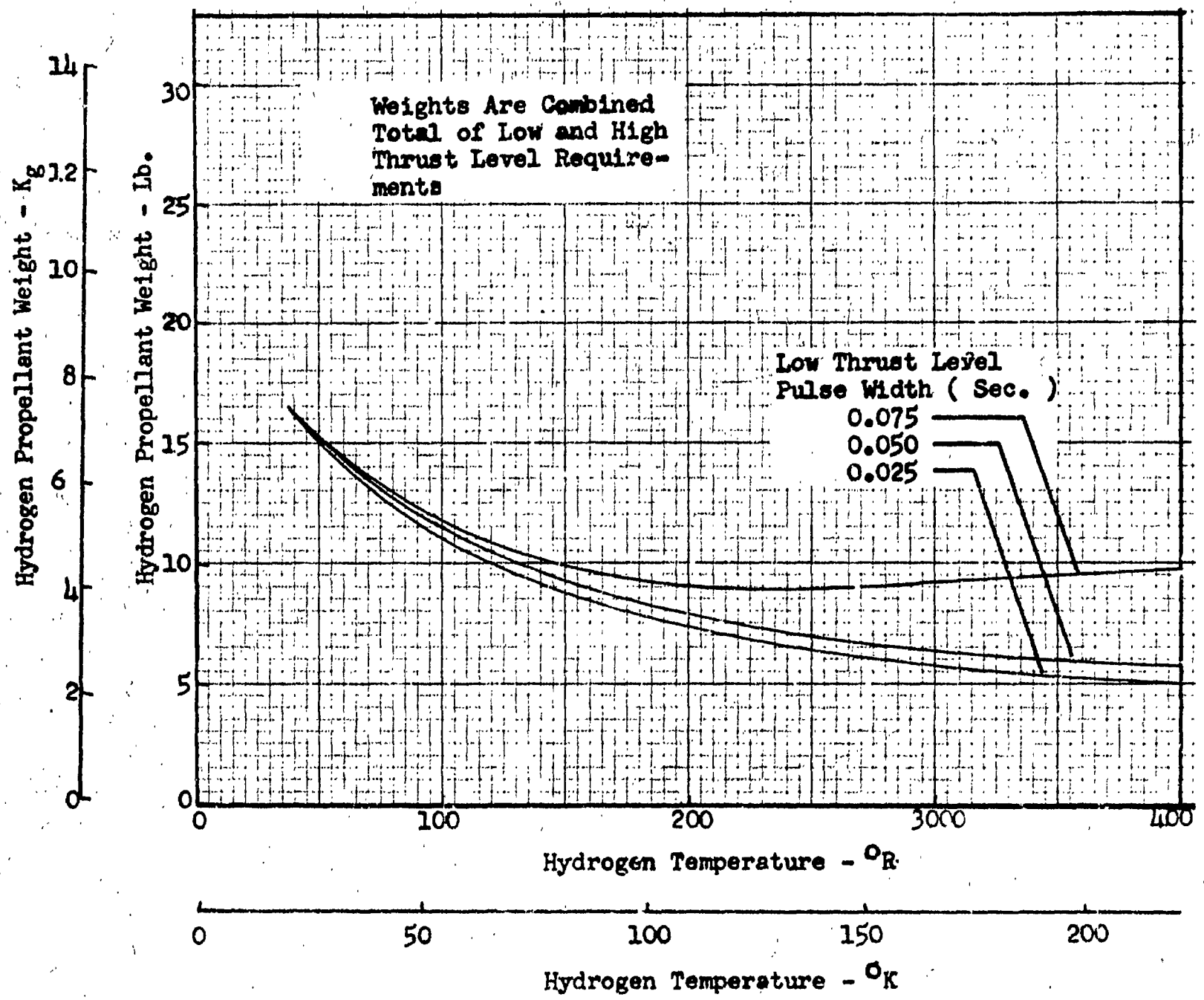

Figure 99 Total Gaseous Hydrogen Requirements

This flow rate, selected previously on the basis of minimizing overall thermal conditioning system weight penalties, is also, by coincidence, near the optimum flow rate for the low level thrust ACS operation (as shown by later calculations). Therefore, the 1.4 lb/hr (0.64 K_g/hr) vent rate was held constant for all the low level thrust calculations.

Total force impulse requirements were taken from the analyses performed in Ref. 5. These data are plotted in Figs. 95, 96, and 97 as a function of thrust level and pulse width. The pulse widths selected, 0.025, 0.050, and 0.075 sec for the low level thrust requirement, were based on current state-of-the-art fast-acting valves. The lower pulse width of 0.025 sec is felt to be readily achievable.

As can be seen from the figures, the force impulse requirements for high level thrust are constant over the thrust range 0 to 2 lbf (8.9 N).

The low level force impulse requirements are constant between 0 and 0.1 lbs (0.45 N) thrust for a limit cycle pulse width of 0.025 sec. For 0.050 and 0.075 sec, the impulse force requirement starts to rise at ≈0.05 lbf (0.023 N) and 0.03 lbf (0.13 N), respectively. This trend shows the desirability of using minimum impulse bits to reduce propellant expenditures.

The flat portion of the low level thrust curves represents one-sided ACS operation. External solar torques return the vehicle before it reaches the other side of the deadband. The force impulse requirements start to rise when two-sided ACS operation occurs at higher thrust levels.

From the data presented in Figs. 95 through 97, gaseous hydrogen propellant requirements were calculated for both the high and low level thrust requirements as a function of hydrogen gas temperature as shown in Fig. 98. The sum of the high and low level propellant requirements is given in Fig. 99. From these two figures, it can be readily seen that the quantity of hydrogen required for vehicle orientation or maneuvering is considerably below the

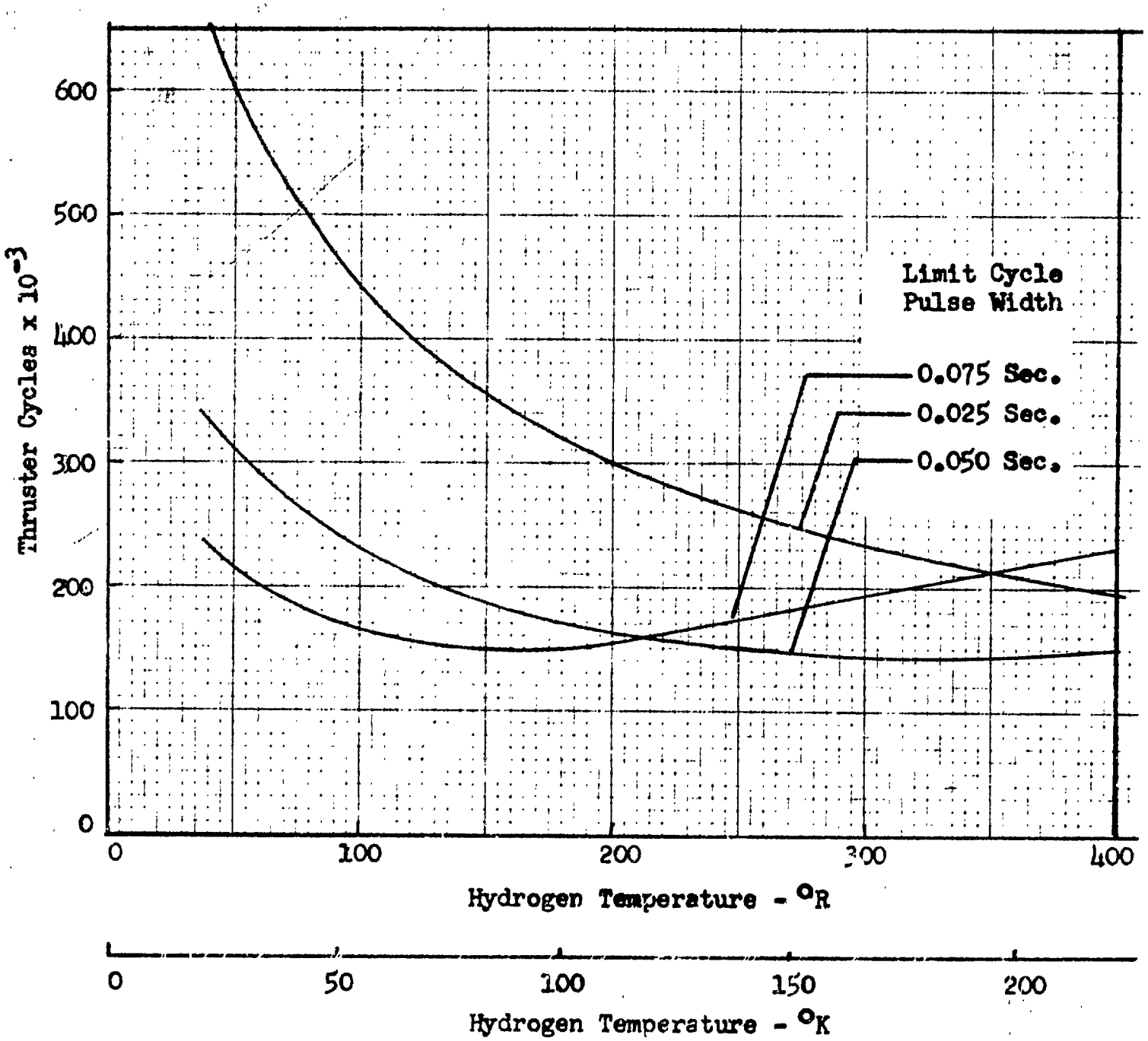

Figure 100 Thruster Cycles for Low and High Level Thrust

quantity vented overboard during the Earth-Mars transit [316 lb (141 Kg)] based on an average heat rate of 11.5 Btu/hr (3.4 w). Consequently, most of the hydrogen is dumped overboard through the thrust nullifier nozzles and less than 5 percent of the total is used for vehicle orientation and maneuvering. Unless the vented hydrogen is used for other functions, or the tanks are designed to go non-vented, minimizing the quantity required for ACS operation is relatively unimportant.

Other considerations enter in, then, in selecting one system over another. Due to the extended operational life required (of the low level thrust system to maintain sun orientation for 220 days), the valves on the thrusters require high cycle life capability as shown in Fig. 100. Since it is desirable to minimize cycle requirements in order to maximize system reliability, it is desirable to use a 0.075 sec pulse width for expulsion temperatures between 40 and 210°R (22 and 116°K) and a 0.050 sec pulse width between 210 and 400°R (116 and 222°K) as shown in Fig. 100. Longer pulse widths at the lower end of the temperature curve may reduce the cycle requirement even further.

ACS Performance Comparison

Using the ACS requirements described in the previous section, performance data were tabulated for 4 hydrogen expulsion temperatures as shown in Table 24. The four temperatures were chosen for the following reasons: 40°R (22°K) represents direct venting of the liquid hydrogen tank while 163°R (90.5°K) is achievable by passing hydrogen gas through a heat exchanger on the liquid oxygen tank. (The hydrogen maintains the oxygen tank in a non-vented condition.) A typical mean vehicle temperature for the Earth-Mars transit is represented by the 220°R (122°K) temperature; 400°R (222°K) is an arbitrary temperature used to investigate the effects of higher temperature expulsion.

The recommended limit cycle pulse widths shown in Table 24 are based on minimizing thruster cycles rather than minimizing gaseous hydrogen propellant

TABLE 24

ACS PERFORMANCE DATA AS A FUNCTION OF GH_2 TEMPERATURE

PERFORMANCE DATA	GH_2 TEMPERATURE			
	40°R (22°K) (System 1)	163°R(90.5°K) (Systems 2&3)	220°R(122°K)	400°R(222°K)
Nominal Limit Cycle Deadband ± deg	1.0	1.0	1.0	1.0
+ Nominal Thruster Separation Distance Assumed - ft (m)	10 (2.54)	10 (2.54)	10 (2.54)	10 (2.54)
Recommended Limit Cycle Pulse Width for Low Level Thrust - sec	.075	.075	.050	.050
Low Level Thrust - lbf (N)	.028 (0.13)	.053 (0.24)	.064 (0.29)	.094 (0.44)
Recommended High-Level Thrust-lbf(N)	1 (4.5) to 5 (22.6)	1 (4.5) to 5 (22.6)	1 (4.5) to 5 (22.6)	1 (4.5) to 5 (22.6)
Low Level Impulse Required - lb-sec (N-sec)	454 (2020)	580 (2640)	500 (2270)	720 (3270)
High Level Impulse Required at 2 lbf - lb-sec (N-sec)	717 (3250)	717 (3250)	717 (3250)	717 (3250)
Sum of Low & High-Level Impulse - lb-sec (N-sec)	1171(5320)	1297(5890)	1217(5520)	1437(6510)
* Low Level Propellant-lb (K_g)	6.3 (2.9)	4.3 (1.9)	3.0 (1.4)	3.0 (1.4)
* High Level Propellant-lb (K_g)	10.0 (4.5)	5.2 (2.4)	4.3 (1.9)	3.0 (1.4)
Total Propellant-lb (K_g)	16.3 (7.4)	9.5 (4.3)	7.3 (3.3)	6.0 (2.7)
Number of Thruster Cycles (1000)	230	150	160	150
No. of Thruster Cycles/Hr, Mean (220 day mission)	44	28	30	28

• Impulse propellant with no redundancy.

+ Thruster separation of 20 to 25 ft (5.1 to 6.3 m), easily achievable with spacecraft using solar panels for power, would reduce thrust levels and impulse requirements in direct proportion to the increased separation distance.

requirements (as discussed previously in the requirements section). The low level thrusts shown are based on the vent rate of 1.4 lb/hr (0.64 K_g/hr) of hydrogen; the high level thrust recommendation was taken from Ref. 5.

Table 25 presents a weight statement for the three integrated systems. The weights attributable to the ACS function are specifically identified. The remaining elements are attributable to the TCU and are independent of the ACS selection.

A summary of the weight comparison for the low level thrust systems is given below, where each is compared with a cold hydrazine system, which was the lightest of those studied in Ref. 5.

VEHICLE ORIENTATION, LOW LEVEL THRUST, (OPERATING MODES 2,4&5)	ACS RELATED		TCU RELATED		TOTAL		WT SAVINGS AS COMPARED TO COLD N_2H_4	
	lb	(K_g)	lb	(K_g)	lb	(K_g)	lb	(K_g)
System 1 (40°R) (22°K)	4.6	(2.1)	32.1	(14.6)	36.7	(16.7)	6.4	(2.9)
Cold N_2H_4	11.0	(5.0)	32.1	(14.6)	43.1	(19.6)	0	(0)
System 2 (163°R)(90.5°K)	5.3	(2.4)	20.2	(9.2)	25.5	(11.6)	5.7	(2.6)
Cold N_2H_4	11.0	(5.0)	20.2*	(9.2)	31.2	(14.2)	0	(0)

* TCU system is required, independent of ACS selection

For system 1, 6.4 lb (2.9 K_g) can be saved over the N_2H_4 system; system 2 saves 5.7 lb (2.6 K_g). However, when comparing absolute total weights of systems 1 and 2, system 2 is 11.2 lbs (5.1 K_g) lighter. In addition, system 2 has 3 fewer operating components than system 1 with an attendant increase in reliability. (System 2 also has fewer operating components than the N_2H_4 system.) Consequently, on the basis of lower weight and higher reliability, system 2 is the optimum selection.

TABLE 25

TCU/ACS COMPONENT WEIGHTS

ITEM	WEIGHTS - LB (K_g) System 1	System 2	System 3
Valves (All Types)			
U-1	0.65 (0.3)	0.65	0.65
U-2	0.85 (0.39)	0.85	0.85
U-3	0.2 (0.09)	-	-
U-4	0.85 (0.39)	-	-
U-5	-	-	0.85 *
U-6	-	-	0.85 *
U-7	-	-	1.1 *
U-8	-	-	1.1 *
U-9	-	-	0.4 *
Regulators			
RG-1	1.0 (0.45)	1.0	1.0
RG-2	1.0 (0.45	-	-
RG-3	-	-	2.3 *
Heat Exchangers			
HX-1	7.2 (3.3)	7.2	7.2
HX-2	7.2 (3.3)	-	-
HX-3	-	0.7 (0.32)	0.7 *
Pressure Switches			
PS-1 (R)	1.0 (0.45)	1.0	1.0
PS-2 (R)	1.0 (0.45)	1.0	1.0
PS-3 (R)	-	-	1.0 *
Temperature Switch	-	-	0.1 * (0.05)
Mixers			
MX-1	2.0 (0.90)	2.0	2.0
MX-2	2.75 (1.25)	2.75	2.75
Quick Disconnects			
QD-1	0.1 (0.05)	0.1	0.1
QD-2	0.1 (0.05)	-	-
Accumulator Bottle	-	-	35.6 * (16.2)
Compressor	-	-	10.0 * (4.5)
Thrust Nullifier Nozzles			
TN-1	0.5 (0.23)	0.5	0.5
TN-2	0.5 (0.23)	-	0.5
ACS Thruster Assys (Low Level)	3.6 * (1.6)	3.6	3.6 *
ACS Thruster Assys (High Level)	-	-	6.0 * (2.7)
Plumbing & Misc. Fittings	1.0 * (0.45) 5.2 (2.4)	1.0 * 3.2 (1.45)	2.6 * (1.2) 3.2

* Related only to ACS function. Other weights relate to TCU function.

A summary of the weight comparison for the combined low and high thrust level system is shown below.

VEHICLE ORIENTATION & MANEUVERING, LOW & HIGH LEVEL THRUST (OPERATING MODES 1 THROUGH 6)	ACS RELATED		TCU RELATED		TOTAL		WT SAVINGS AS COMPARED TO COLD N_2H_4/N_2H_4	
	lb	(K_g)	lb	(K_g)	lb	(K_g)	lb	(K_g)
System 3 (163°R)(90.5°K)	66.2	(30)	20.2	(9.2)	86.4	(38.4)	-31.8	(-14.5)
Cold N_2H_4/N_2H_4	34.4	(15.7)	20.2*	(9.2)	54.6	(24.8)	0	(0)

* TCU system is required, independent of ACS selection

In this case, the hydrazine system is 31.8 lb (14.5 K_g) lighter than the hydrogen expulsion system. In addition, the hydrazine system has three less operating components than system 3, improving system reliability. Therefore, on both a weight and reliability basis, the hydrazine system is preferable to system 3 for the high level thrust applications.

ORBITAL FLIGHT TEST PLAN

As an extension to the ground test program performed on the thermal conditioning unit (TCU), an orbital flight test program was laid out that demonstrates positive hydrogen tank pressure control in a low-g environment. (An alternate flight test experiment is proposed at the end of this section that expands the subsystem tests into a complete propulsion system orbital flight test.)

The orbital flight test designs and sequences shown in this plan were selected so direct correlations could be made between the ground test results obtained on this program and the orbital flight data. The flight test provides the final operational demonstration of the TCU system; the feasibility of the design and acquired operational engineering data were obtained on the ground test program.

A Titan IIIB/Agena launch vehicle is used as a reference for the study. The Agena remains attached to the experiment for the two weeks test duration. Other launch vehicle combinations can be used for shorter test durations.

EXPERIMENT SELECTION

Due to the cost of an orbital flight test, it is desirable on a cost effectiveness basis to obtain data on other critical vehicle subsystems at the same time. For this reason, the state of development of vehicle subsystems applicable to future space systems were reviewed as shown in Table 26.

The table is subdivided into two groups. The first group includes those subsystems in which a flight test is the only way to obtain required performance data. The second group covers subsystems whose feasibility can be demonstrated and performance data can be obtained in ground-based simulation tests. The TCU falls into this second category. The divisions shown were

TABLE 26

NECESSITY OF AN ORBITAL FLIGHT TEST TO OBTAIN SUBSYSTEM PERFORMANCE DATA

Engineering data or subsystem data that can be obtained only:		Flight test provides demonstration of subsystem operation within design limits (verification of ground-based test data)
During Ascent	In Long Duration Low-G Environment	
o Multilayer Insulation pressure history above 50,000 ft (to orbit)	o Low-G Mass gaging system (for use in reusable space vehicles or propellant depots) o Propellant transfer between tanks (i.e. propellant depot to space vehicle) o Multilayer insulation thermal performance after experiencing combined ascent environments	o Thermal conditioning unit (TCU) operation o Tank pressure response o Stratification/destratification o Thrust nullifier perturbations o Use of vent GH_2 from TCU for limit cycle sun orientation (ACS) o Fiberglass tank supports o Sub-cooled propellant orientation system o Thermal control coating o Pressurization system o Propellant tank dynamics o Slosh supression o Suction dip suppression o Propellant settling time and bubble growth dynamics

based on prior program results and engineering judgment made by people working in that particular specialty or field.

With this list as a basis, the following subsystems were selected for a flight test experiment:

1. Thermal Conditioning Unit (TCU)
2. ACS for vehicle orientation using the vented hydrogen from the TCU for mass expulsion.
3. Gaseous hydrogen pressurization system.
4. Fiberglass strut tank supports.
5. Multilayer insulation system.
6. Teflon/Silver Thermal Control Coating.
7. Zero-g propellant gaging system (RF or nuclear detectors).

The above listed subsystems were selected based on the following criterion:

- o Certain performance data can be obtained in no other manner. (Subsystems 5 & 7). Propellant transfer shown in Table 26 was not included because of the additional complexity of the experiment design.
- o Operation of the subsystem is critical to potential cryogenic space vehicle applications. (Subsystems 1 through 6)
- o The subsystem is required to perform desirable test sequences. (Subsystem 3)
- o The subsystem is required on a majority of potential space system applications as shown in Table 27. (Subsystems 1 through 7)

The subcooled propellant orientation system listed in Table 26 was not included because the use of autogenous pressurization systems does not require single phase, subcooled liquid for engine startup, i.e., for most of the foreseeable multi-start mission applications in the future, a tank head idle, pump idle mode engine start with autogenous pressurization appears to be the least complex engine start mode (when all aspects of vehicle design are considered).

Propellant tank dynamics were felt to be more suitable for a research type experiment or for a complete propulsion module demonstration, similar to the

TABLE 27

APPLICABILITY OF FLIGHT

TEST DATA TO POTENTIAL SPACE SYSTEMS

Potential Space Systems	Propellants	FLIGHT EXPERIMENTS						
		TCU (LH_2)	ACS Orientation	Low-G Mass Sensing	Pressurization	Insulation	Fiberglass Tank Supports	Thermal Control Coating (low α_s/ϵ)
o Space Shuttle Orbiter	LO_2/LH_2	x	x	x	x	x	x	-
o Space Tug	LO_2/LH_2	x	x	x	x	x	x	x
o Orbit to Orbit Shuttle	LO_2/LH_2	x	x	x (Reusable Mode)	x	x	x	x
o Versatile Upper Stage	LO_2/LH_2	x	x	-	x	x	x	x
o Earth and Lunar Space Stations	LO_2/LH_2	x	x	x	-	x	x	-
o Nuclear Shuttle and Mars Excursion Module	LH_2	x	x	x (Reusable Mode)	x	x	x	x
o Propellant Depots	LO_2/LH_2	x	x	x	x	x	x	x

alternate flight experiment proposed at the end of this section; consequently, the dynamic tests were not included in the proposed program.

STUDY GROUND RULES

In order to take the seven selected subsystems described previously and combine them into a meaningful orbital flight experiment, it is desirable to select a future mission application and model the experiment on these mission requirements. The mission selected for the orbital experiment is specified in the contract as an Earth-Mars transfer using oxygen and hydrogen as propellants. Other mission requirements of interest are summarized in Table 28.

Using these mission requirements, plus applicable vehicle study results from other programs, a set of unmanned experiment requirements were developed as shown in Table 29. The tank pressures shown are representative for this type of vehicle; electrical heaters are used on the liquid hydrogen tank so heat input could be a controlled experiment variable for the TCU tests; the acceleration levels provide both oriented and nonoriented propellants for the mass gaging test. The data acquisition, data transmission and experiment command requirements resulted from the flight test plan selected and described later.

EXPERIMENT DESIGN

Using the experiment selection criteria, reference mission 2 vehicle data and experiment requirements discussed previously, an experiment design was laid out as shown in Figure 101. The 110-inch (2.8 m) major diameter $\sqrt{2}$ ellipsoidal hydrogen tank selected duplicates both the ground test tank shape and volume and the mission 2 vehicle tank volume. Full scale testing eliminates any uncertainties in scaling test results, particularly those associated with LH_2 mixing patterns in the tank and accuracies of the zero-g propellant gaging system. Due to the low density of liquid hydrogen, the the total experiment package weight is kept under 2000 lb (908 Kg) and thus can be flown on a number of booster systems as described later.

The flight experiment design can be sub-divided, for convenience of dis-

cussion, into the following categories:

- Tankage and test fluid
- Structure
- Subsystems being testing
  - TCU
  - ACS
  - Gaseous hydrogen pressurization system
  - Thermal protection system (multilayers, fiberglass tank supports, plumbing penetrations and thermal control coating)
  - Zero-g propellant gaging system
- Experiment plumbing
- Instrumentation
- Experiment dimensions, weight, power and energy requirements

Each of these categories is discussed in turn.

Tankage and Test Fluid

The 110-inch (2.8 m) $\sqrt{2}$ ellipsoidal tank is constructed of 2219-T87 aluminum alloy, fabricated in three parts; two one-piece, double-action draw-formed domes and a machined Y-ring. The domes are welded to the Y-ring; the tank is supported off the Y-ring by 8 filament-wound fiberglass struts, with 0.035-inch (0.0009 m) walls, 1.5-inch (0.038 m) in diameter and 26-inch (0.66 m) long. A 19-inch (0.48 m) access cover using a conoseal closure is centrally located on top of the tank. Plumbing penetrations and the TV viewing system are located on the cover. The tank working pressure is 50 psia (344,000 N/m^2) and the yield limit pressure is 1.10 times the operating pressure. Room temperature material allowables are used in the design. Liquid hydrogen was chosen as the test fluid to provide direct correlation with the ground test results and allow direct projections to be made for the mission 2 vehicle performance.

Structure

The hydrogen tank is mounted within a tubular 7075-T6 aluminum frame. The frame is supported off the Agena by a tubular truss arrangement. The frame

acts as a convenient mounting structure for the gaseous hydrogen pressurization bottle, plumbing lines, ACS and instrumentation such as the TV camera system. The external surface of the frame is covered with the Teflon/silver thermal control coating to lower this boundary temperature in orbit.

Subsystems Being Tested

Each of the subsystems discussed here was selected from many competing designs based on extensive screening analyses and tests performed on this program and other related in-house programs or government contracts. Thus, they represent a reasonable design choice in each area based on the current state-of-the art. This choice of systems should be again reviewed at the initiation of the flight test program.

Thermal Conditioning Unit, TCU. The TCU developed for this program provides positive liquid hydrogen tank pressure control under low acceleration in the space environment. The TCU consists of an expansion regulator, compact counter-flow heat exchanger, A.C. induction motor* with an axial flow fan, a control valve, redundant pressure switches, a thrust nullifier nozzle for venting hydrogen gas overboard and a 3-way valve for ground evacuation and back purging of the lines. Details of the system operation are provided in another section of this report.

Hydrogen ACS. Use of vent hydrogen gas from the TCU to provide vehicle orientation has been shown to be the lightest design of competing ACS propellant combinations. The only hardware addition required to provide this capability are the thruster nozzles with associated shut-off valves and a line teed off downstream of the TCU heat exchanger.

---

* The optimum design described in Ref. 1 uses a DC brushless motor, but all ground based testing of the TCU has been with the AC induction motor. However, NASA LeRC is sponsoring development of a DC brushless motor under contract NAS 3-11208. This unit would be substituted into the flight test package, providing the development has progressed to the point where it has been incorporated into, and ground tested as an integral part of the TCU.

TABLE 28

POTENTIAL VEHICLE APPLICATION
ON WHICH THE FLIGHT EXPERIMENT IS MODELED

1. Mission 2 Vehicle
2. Mission: Earth-Mars transfer
3. Duration: 220 Days
4. Propellants: LO_2/LH_2
5. Vented LH_2 Tank; Non-vented LO_2 Tank
6. Engine Mixture Ratio: 5/1
7. Engine Start Sequence: Tank idle head, pump idle mode start.
8. Propellant Weights: lbs (Kg)

	LO_2	LH_2	TOTAL
Usable	3740 (1695)	748 (339)	4488 (2015)
Loaded	3794 (1700)	1150 (316 lb. vented) (143 Kg vented)	4944 (2240)

9. Ignition Weight: 9700 lb (including 4100 lb payload)
10. Mass Fraction 0.80
11. Vehicle Orientation: Payload to Sun
12. Vehicle Deadband: ±1°
13. Expulsion Profile:

Firing No.	Time after Launch (days)	Duration (sec)	Flow Rate (lb/sec) Kg/sec	Weight (lb)/Kg) LO_2	Weight (lb)/Kg) LH_2
1	10	80	6 ((2.72))	400 (181)	80 (36.3)
2	180	40	6 (2.72)	200 (90.5)	40 (18.2)
3	220	112	33.8 (15.4)	3140 (1425)	628 (285)

14. Pressurization System: Autogenous
15. LH_2 Tank Characteristics:
    - o 2 oblate spheroid, 104 inch (2.64 m) major diameter
    - o 282 ft^3 (8.02 m^3) volume
    - o 28 psia (19.3 x 104 N/m^2) working pressure
    - o Bulk LH_2 temperature 37.7°R (20.8°K) corresponding to 17 psia (11.7 x 10^4 N/m^2)
    - o Heat Leak (Btu/hr) (watts)

Max..	17.2	(5.05)
Min.	5.8	(1.7)
Ave.	11.5	(3.37)

TABLE 29

UNMANNED EXPERIMENT REQUIREMENTS

1.	Test Fluid:	LH_2
2.	Test Tank Configuration:	Sphere to 2 oblate spheroid, 109.8 inch (2.78 m) major dia.
3.	Tank Pressure: (psia)	

	Psia	$(N/m^2) \times 10^{-4}$
Max:	50	34.4 x
Operating:	28 to 30	19.3 to 20.6
Vent:	23 to 25	15.8 to 10.2

4.	Pressurant Gas, Autogenous System:	GH_2
5.	Heat Rate to Test Tank:	
	o Ambient Heak Leak:	to 50 BTU/Hr (14.6 watts)
	o Controlled Heat Leak (electrical heaters):	to 300 BTU/Hr (89 watts)
6.	Drain Rate:	5.6 lb/sec (2.54 Kg/sec)
7.	Intermittent Vent Rate:	1.4 lb/hr (0.64 Kg/hr)
8.	Acceleration Levels:	10^{-6} g_o, 10^{-3} g_o
9.	Weight:	Consistent with booster capability
10.	Duration:	To 14 days (possible extension to 220 days)
11.	Data Acquisition:	Visual average of LH_2, temperature, pressure, acceleration, mass flow, LH_2 quantity, mixer RPM, current, voltage
12.	Data Transmission:	Telemetry, real time and delayed (taped)
13.	Experiment Command:	Preprogrammed with reprogram commands from ground possible.
14.	Support Hardware:	Electrical Power
		Tape Recorder
		TV Tape Recorder
		Rate Gyros
		Command Receiver
		Decoder
		Programmer
		ACS
		Signal Conditioning
		Commutation
		Telemetry
		Umbilicals, Electrial and Fluid Servicing (GN_2, CHe and LH_2)

FOLDOUT FRAME 1

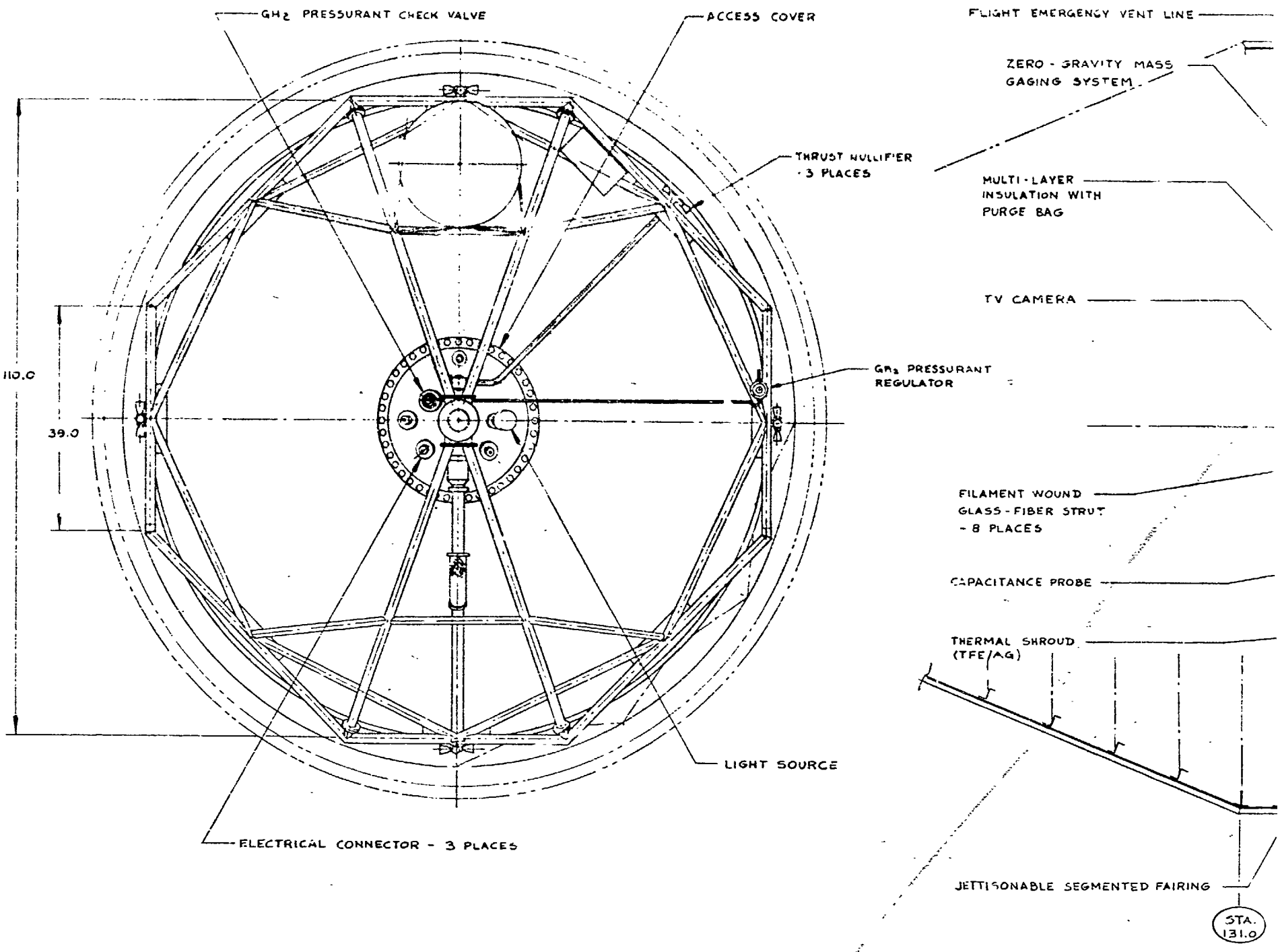

FOLDOUT FRAME 2

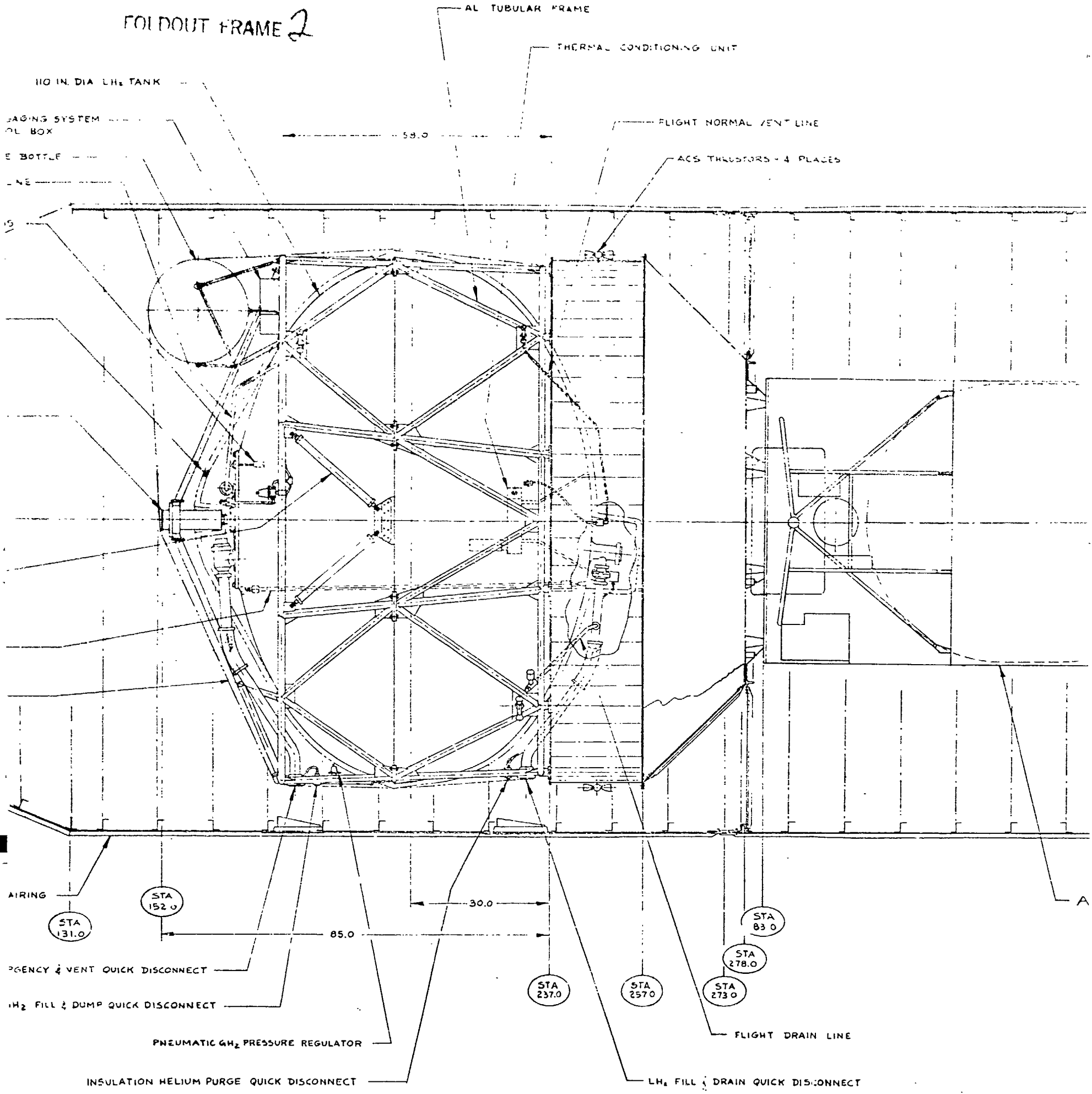

LH₂ TANK FLIGHT TEST EXPERIMENT

NOT TO SCALE

Fig. 101 – Liquid
ment D

FOLDOUT FRAME 2

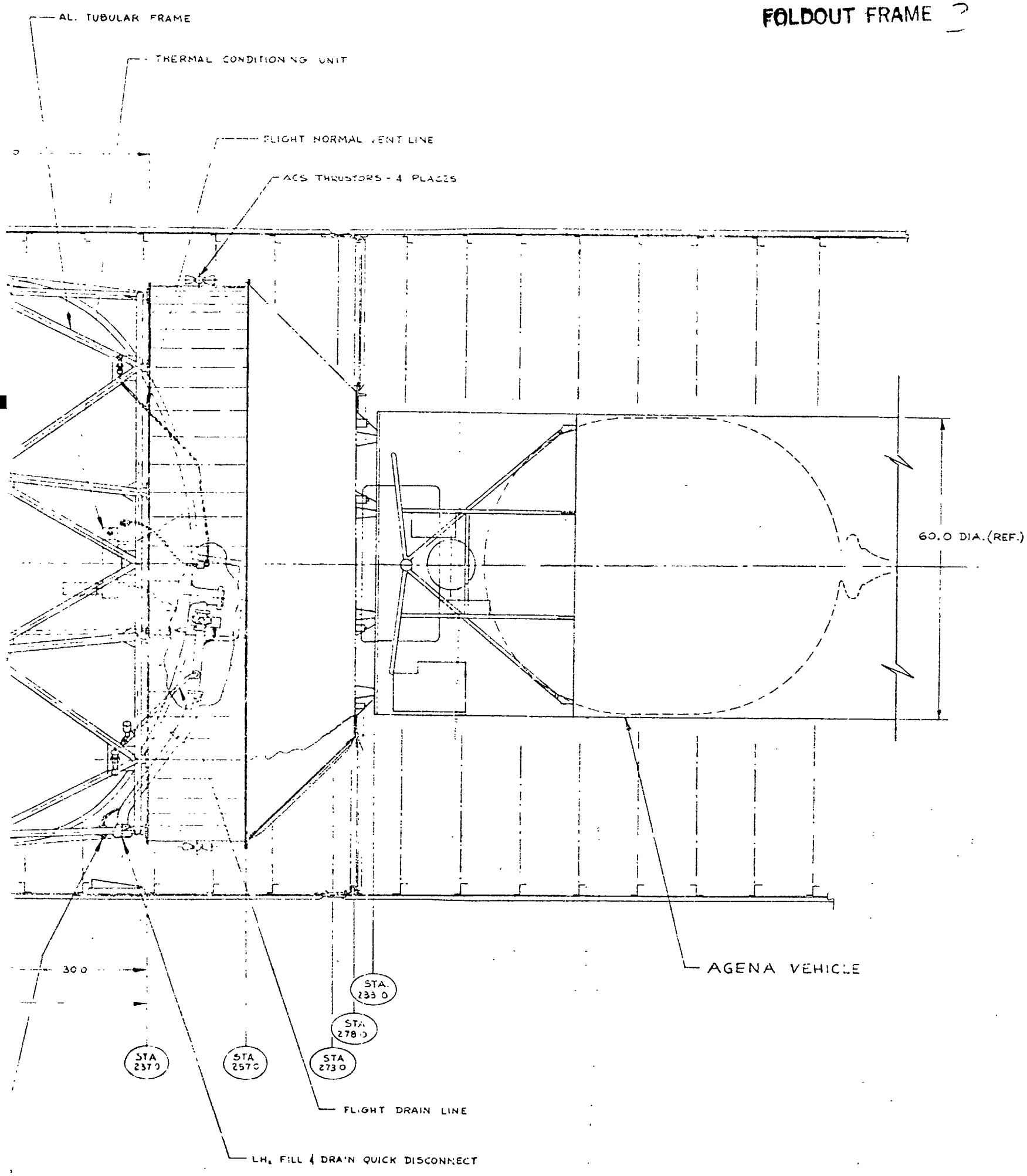

LIGHT TEST EXPERIMENT

NOT TO SCALE

Fig. 101 – Liquid Hydrogen Flight Tank Experiment Design

Thermal Protection System. The thermal protection system consists of the multilayer insulation system on the liquid hydrogen tank, the tank supports, the plumbing lines and the thermal control coating. Each of the separate items are designed to reduce the heat leak into the tank. The multilayer system selected consists of double gold-coated Mylar film separated by silk net spacers. The layers are combined into three separate blankets by inserting molded FEP Teflon thread/button designs through the layers on 12-inch (0.3 m) centers. TFE Teflon buttons are installed on the opposite end of the thread. The butt joints from one blanket to another are staggered to reduce radiation tunneling.

A 4-mil Mylar purge bag is used for a helium purge of the multilayers during ground hold. Nichrome wires, 4-mil in diameter, are attached to the Mylar bag over the multilayer butt-joints with heat-sealed Mylar tape. A short electrical pulse (<0.1 sec) through the wires just prior to lift-off cuts (melts) the bag and allows the helium to vent out during ascent. Screening analyses and test results (which resulted in selection of the helium purge method and nichrome wire opening technique) are given in Ref. 6 .

Selection of filament wound fiberglass struts with integral end fittings as the optimum tank support method is the result of screening analyses and test performed on 12 candidate designs (Ref. 7). These struts have been fabricated and tested thermally; cryogenic structural tests are currently underway on contract NAS 3-12037.

Heat leaks through plumbing lines are kept low by using thin-walled stainless steel tubing. If further reductions in heat leak are desired, short sections of filament wound glass-fiber stainless steel composite lines can be used. Selection of either stainless steel or composite lines will depend on the development status of the composites at the initiation of the flight test program.

Use of thermal control coatings on a vehicle external surface (with a low α_s/ϵ ratio) drops the outer shell temperature in space and, consequently, the heat load to the tank. Screening analyses performed in Ref. 6 show that

a 3-mil FEP Teflon film with a silver back-side coating (and tungsten protective over-coating) has an $\alpha_s/\epsilon = 0.071$ and is stable under ultra violet exposure up to 100 days (tests were run for periods up to 100 days).

The tape, up to 36-inches (0.91 m) in width, is attached using a contact silicone adhesive in a manner similar to applying scotch tape. Advantages of this system over conventional white paints are lower α_s/ϵ, stability in ultraviolet and fewer problems with contamination (finger prints can be removed with a solvent wipe).

Pressurization System. The pressurization system selected for the experiment consists of a high pressure, ambient gaseous hydrogen storage bottle, a two-stage pressure regulator, and shut-off valve. This system is used to simulate an engine bleed pressurization system contemplated as the most likely candidate for future multi-burn space vehicle systems.

Zero-G Propellant Gaging System. Zero-g propellant mass gaging on expendable vehicle systems has never been a requirement. (Propellant quantities could be determined during an engine firing when the propellants are settled.) However, with the advent of reusable Earth-Orbit-Shuttles, Space Tugs, Orbit-to-Orbit Shuttles and Propellant Depots, the ability to determine quantities of propellant remaining (without resorting to settling of the propellants) becomes desirable; that is, the decision can be made whether to refuel a vehicle (in orbit) prior to flying a specified mission. Of the various methods proposed to accomplish this requirement, two systems are the leading candidates - an RF volume sensing system and a nuclear detector mass gaging system. It is not clear at this time which of these two systems is preferable, on the basis of accuracy, weight and power requirements. However, for purposes of discussion, the RF system is used in this section for defining experiment parameters. Choice of one system over another will have to be made at the time the flight program is initiated based on the latest data available. The RF system consists of a small sensor head located in the tank, a power supply and associated electronics.

Plumbing

A schematic of the experiment plumbing system is shown in Figure 102. Items of special interest are described below. Redundant pressure switches on the TCU are used for reliability reasons. A two stage regulator is provided for the 4000 psia (2.75×10^7 N/m^2), 2.2 ft (0.67 m) diameter gaseous hydrogen pressurization bottle. All valves shown are solenoid actuated. Use of pneumatic valves for the ground vent, liquid hydrogen fill line and for the drain line should be considered when more indepth analyses are conducted.

Instrumentation

A list of minimum instrumentation recommended for the experiment is given in Table 30; the locations of the experiment measurements are shown in Fig. 103. Measurements requiring further clarification are discussed below.

Insulation pressure history during ascent in the 25 to 10^{-6} torr range is of interest since it cannot be simulated in ground tests. One type of gage cannot cover this whole range; however, the lower end of the range is of more interest since the curve is flattening out there as shown in Fig. 104. Therefore, an alphatron gage that covers only the 10^{-3} to 10^{-6} torr pressure range is felt to be adequate. Capillary sampling tubes are used with the transducers to sample pressure at the tank surface and mid-way through the blanket layers centrally located between the edges of the blanket gore section (the vent path length is equidistant in either direction and represents the maximum pressure location at that insulation layer).

Acceleration levels are inferred from the rate gyros on the Agena. Acceleration is of interest as related to TCU performance and mixing patterns in the tank. The TV coverage is provided to qualitatively examine mixing patterns in the tank during TCU operation. An Image Isocon TV camera was selected because light levels, on the order of 2 watts, can be used and consequently heat rates into the tank can be kept at an extremely low level. The shaped capacitance probe is used as a reference measurement of mass propellant quantities in the tank (when the propellants are settled) against which the RF measurements can be compared (when the propellants are not

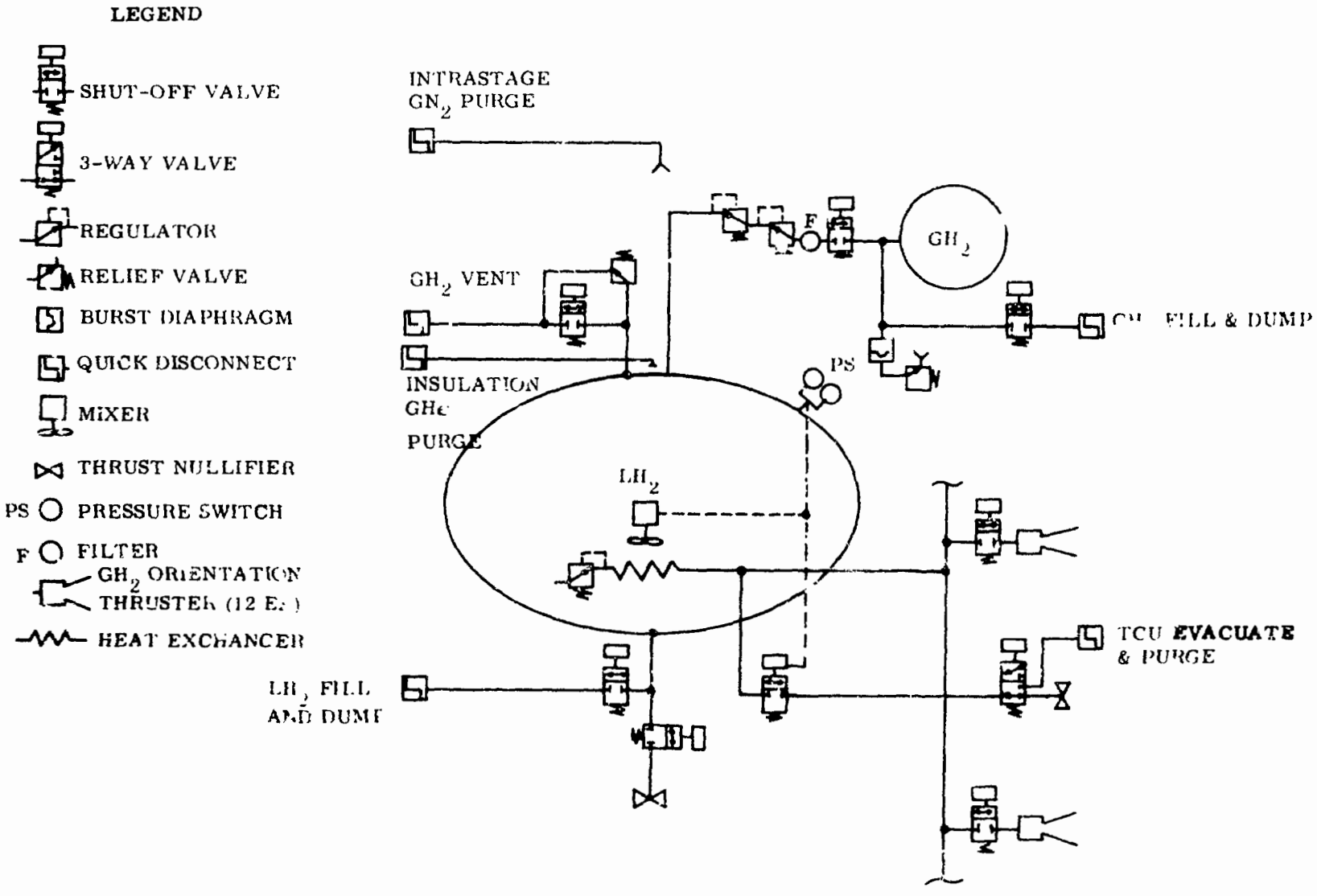

Figure 102 Plumbing Schematic For A Liquid Hydrogen Tank Flight Experiment

TABLE 30

INSTRUMENTATION LIST FOR THE FLIGHT DEMONSTRATION TEST

MEASUREMENT	TYPE	RANGE*	NO.
THERMAL PROTECTION SYSTEM			
Insulation Temperature Profile -	Cu-Cn	40-300°R (22.2-167°K)	4
2 places	Cu-Cn	100-460°R (55.6-256°K)	4
	Cu-Cn	300-700°R (167-382°K)	4
Insulation Surface	Cu-Cn	300-700°R (167-382°K)	12
Tank Surface	Cu-Cn	40-300°R (22.2-167°K)	12
Support Structure	Diff. Cu-Cn	100-400°R (55.6-222°K)	5
Plumbing Surfaces	Diff. Cu-Cn	40-460°R (22.2-256°K)	16
Insulation Pressures	Alphatron	10^{-3} - 10^{-6} torr	5
PROPELLANT CONDITIONING SYSTEM			
Thermal Condition System Temperatures	GRT	25-100°R (13.9-55.6°K)	4
Thermal Condition System Pressures	Strain Gage	0 - 20 psia (138,000)	2
Propellant Temperatures	PRT	25-100°R (13.9-55.6)	4
Propellant Temperatures	Diff. Au-Co	25-100°R (13.9-55.6)	18
Tank Pressure	Strain Gage	C - 50 psia (344,000)	2
Acceleration Level (Available from Agena)	Inferred from Rate Gyros	10^{-5} to 10^{-7} g/g_o	3
Vent Flow Rate	Thermal Mass Meter	C - 3 lb/hr (1.36)	1
Mixer Speed	Magnetic Speed Sensor	0 - 1800 RPM	1
Mixer Current	D.C. Ammeter	0 - 0.2 amps	1
Mixer Voltage	D.C. Voltmeter	0 - 30 volts	1
TV Camera, Lights	Secondary Electron Conduction (SEC)	-	1
ZERO-GRAVITY MASS GAGING SYSTEM			
Liquid Level Sensor	Capacitance Probe	95% to 0	1
Mass Sensor (Volume sensing & temperature measurements)	RF	95% to 0	1
PRESSURIZATION SYSTEM			
GH_2 Bottle Pressure	Strain Gage	0 to 4000 psia (2.75×10^7)	2
GH_2 Bottle Temperature	Cu-Cn	300 to 600°R (167-333)	1
GH_2 Flow Rate	Turbine Flow Meter	0 to 0.1 lb/sec (.045)	1
GH_2 ACS			
Thruster Chamber Pressure	Strain Gage	0 to 5 psia (34,400)	12
Thruster Chamber Temperature	PRT	20 to 100°R (11.1-55.6)	12
Vehicle Attitude	IR Horizon Sensors	± 0.4 deg	3

* Numbers in parenthesis are in SI units: Temperature - °K
Pressure - N/m^2
Flow Rate - k_2/hr

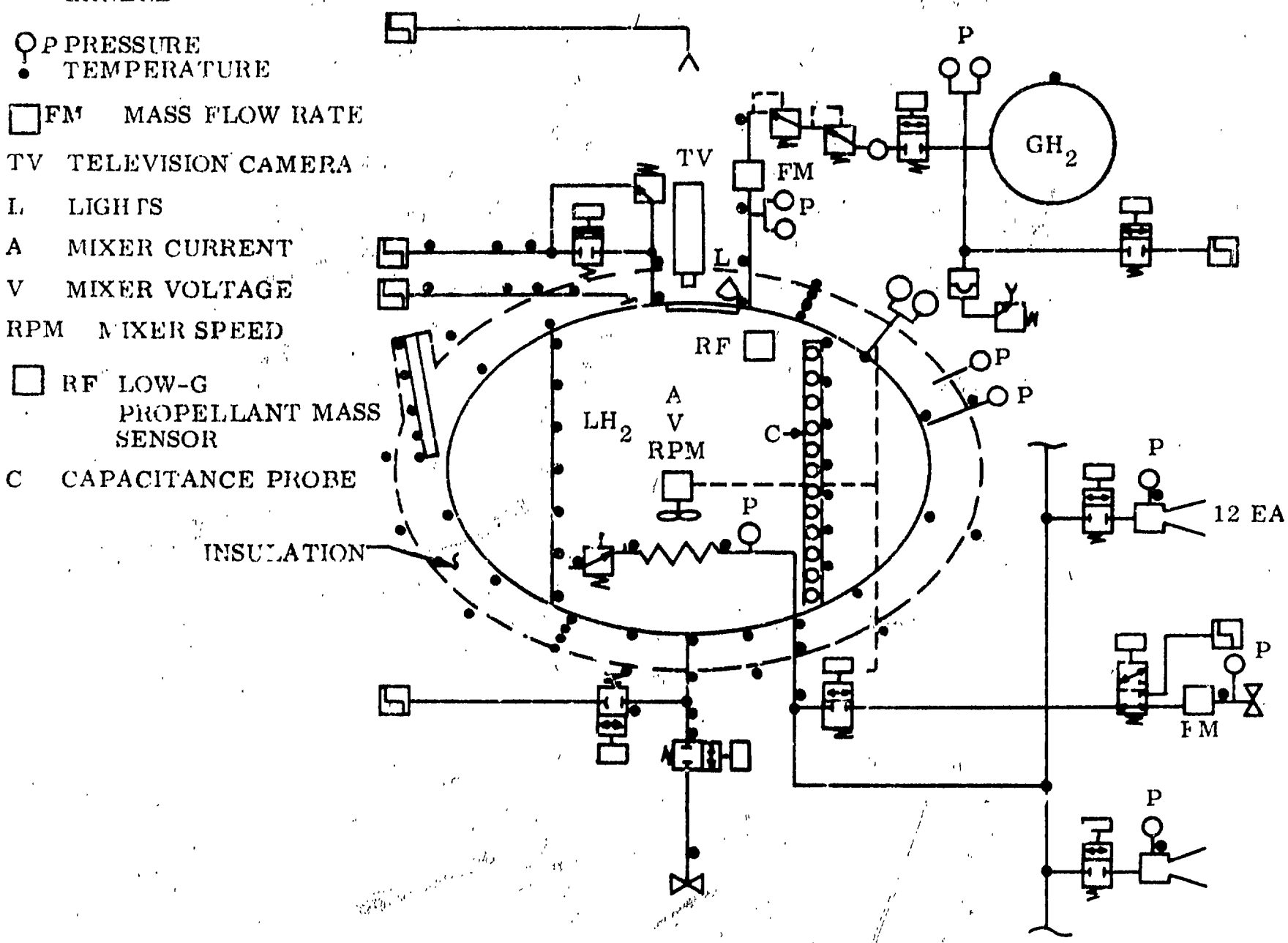

Figure 103 Instrumentation Locations for the Hydrogen Experiment

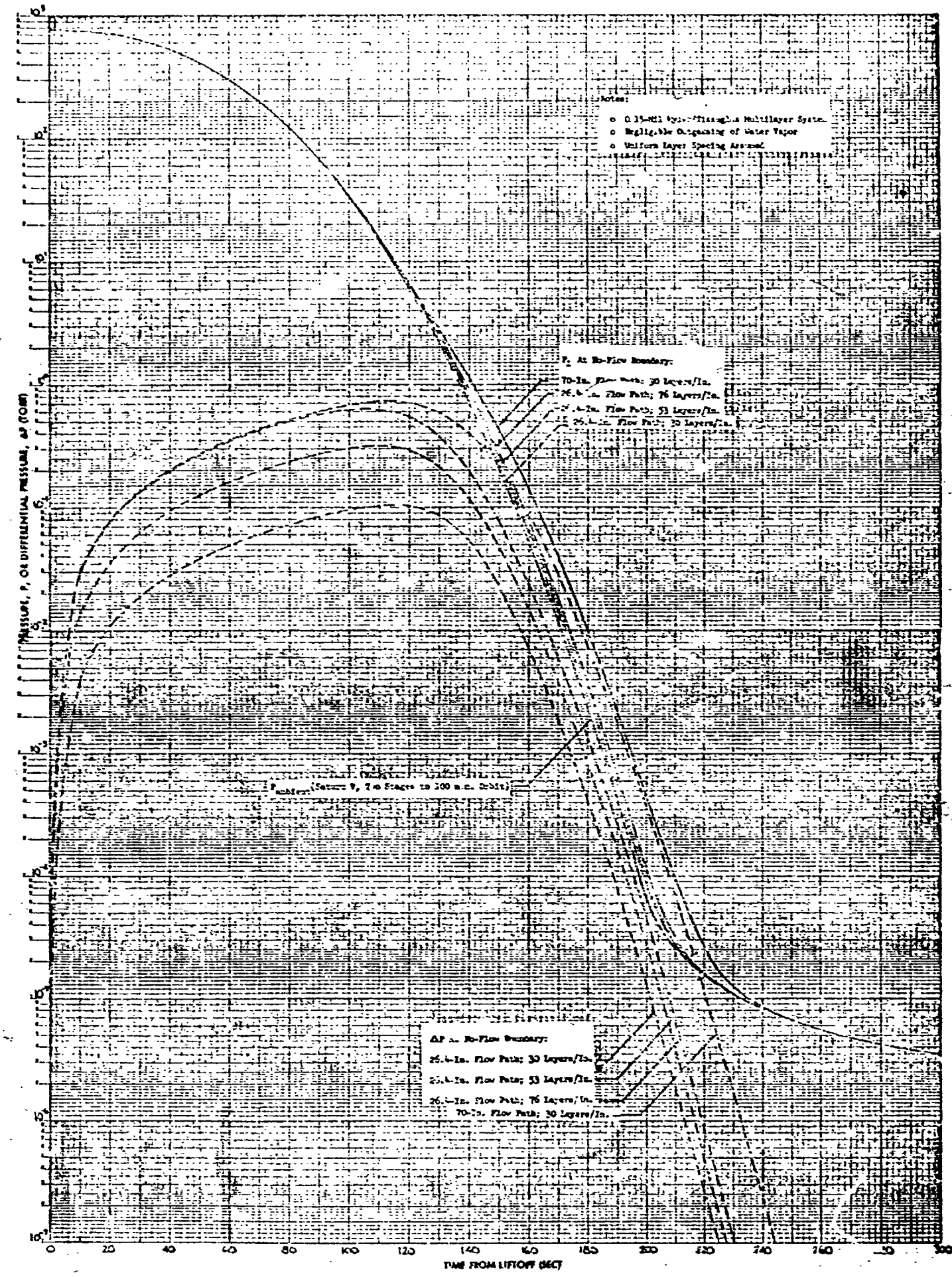

Fig. 104 Typical Predicted Pressure-Time Histories for Flight Evacuation of Helium-Purged Multilayer Insulation

oriented). Vehicle attitude measurements are made using IR horizon sensors located on the Agena. Performance of the hydrogen gas ACS in holding the vehicle attitude to ± 1 degree (to an axis passing through the Earth's center) can be determined by this measurement.

Time sequencing of the measurements is shown in the Flight Test section.

EXPERIMENT FLIGHT TEST SEQUENCE

Background Information

To provide a background on why the flight test sequence was laid out in the manner shown at the end of this section, a discussion is provided of critical test parameters associated with each subsystem followed by a description of the recommended flight sequence and experiment control.

Thermal Conditioning Unit (TCU). The primary objective of this flight experiment is to evaluate the performance of a thermal conditioning unit for venting a hydrogen tank in a low-g environment, and collect engineering data that can be compared with that previously obtained in ground tests. A secondary objective is to obtain data on the rates of stratification, pressure rise, etc., during low-g coast, then to evaluate the effectiveness of mechanical mixing in controlling pressure and bringing about uniform conditions in the propellant tank.

The pressure control in a propellant tank is affected both by the energy distribution within the propellant and by the net rate at which energy enters or leaves the tank. The net heat rate is primarily a function of the thermal protection and tankage system designs which can be made independent of gravity level. The energy distribution is, however, affected by the propellant circulation, which has been shown to be very dependent upon the gravity condition. Low-gravity fluid mixing can be simulated in drop tower tests. However, the test articles and test durations are too small to permit quantitative measurement of the thermal mixing (destratification) and pressure response. On the other hand, pressure control with a thermal conditioning system has been demonstrated in a one gravity environment, in a full scale

tank, but with less than complete circulation as shown in a previous section. Complete circulation, and pressure control can only be demonstrated in a flight experiment.

Vent hydrogen gas for ACS. Constant orientation of the reference Mission 2 Earth-Mars vehicle is desirable for two reasons: vehicle communication and reduction of the heat rate into the propellant tanks. Since the propellant orientation requirements are rather modest to counteract solar torques, use of vented hydrogen vapor for this function suggests itself (rather than just dumping the hydrogen overboard). An analyses was conducted under the current program which shows that this system minimizes vehicle system weight, is simple and should prove to be highly reliable. Consequently, flight demonstration of this TCU-related system is highly desirable.

Thermal Protection System. The major item of interest is a multilayer insulation system (MLI) although the entire thermal protection system also includes low heat leak tank supports, plumbing lines and a thermal control coating.

The thermal performance of MLI can be adequately evaluated in thermal simulation chambers in ground based tests although its performance might improve in a low-g environment. Structural integrity due to rapid depressurization down to approximately 0.5 psi (3440 N/m^2), and due to individual effects of vibration, g-loading, acoustics, etc. can also be assessed in ground based facilities. However, the combined structural environments can only be obtained with an actual flight.

A major limitation of ground based tests is the inability to simulate the rapidly changing environmental pressure in the range from 25 torr to 10^{-5} torr, with representative size test articles. With this limitation, there is no way to demonstrate the self evacuating capabilities of MLI except with a flight test.

Analytical predictions are inconclusive and widely variant in the estimated self evacuation rates and associated propellant losses. In some cases, the

estimated heat input due to the pressure lag, is the same order as that calculated for an entire space mission with the insulation evacuated. Thus, this area of uncertainty must be resolved with engineering data from a flight development test inasmuch as it can seriously affect the practical application of multilayer insulation systems.

Pressurization System. Pressurization system tests using gaseous hydrogen pressurant were included since tests on other systems require different fill levels and tank draining is necessary. Ground tests will provide the major engineering data such as collapse factors, flow rate, optimum expulsion temperature, etc., required to design the system. The flight demonstration test will provide a verification of these ground test data and provide additional data on low-g start transients which can't be simulated accurately in ground-based tests.

Zero-Gravity Mass Gaging System. Mass gaging systems (i.e., capacitance probes) currently in use require that the propellant be in a settled condition at the time of measurement. This requirement can be eliminated with the use of RF or nuclear sensor systems. The technology has been developed and preliminary accuracies of these instruments verified in ground-based tests. However, a flight demonstration test is needed to verify that the technique does indeed work when the liquid and vapor phases are randomly dispersed in the tank.

To evaluate the sensor in zero-gravity coast flight, it will be necessary to provide a reference against which the sensor could be checked. Thus, this experiment will require the ability to settle the propellant and measure the mass with a conventional technique such as a calibrated capacitance probe; simultaneously, a measurement would be made with the sensor. The zero-g coast condition would then be established and a second measurement made with the sensor. A minimum of three liquid fill levels should be evaluated, which will require draining the tank at some time during the extended test duration.

Flight Test Sequence

The recommended flight test sequence is shown in Fig. 105. The periods of

FOLDOUT FRAME /

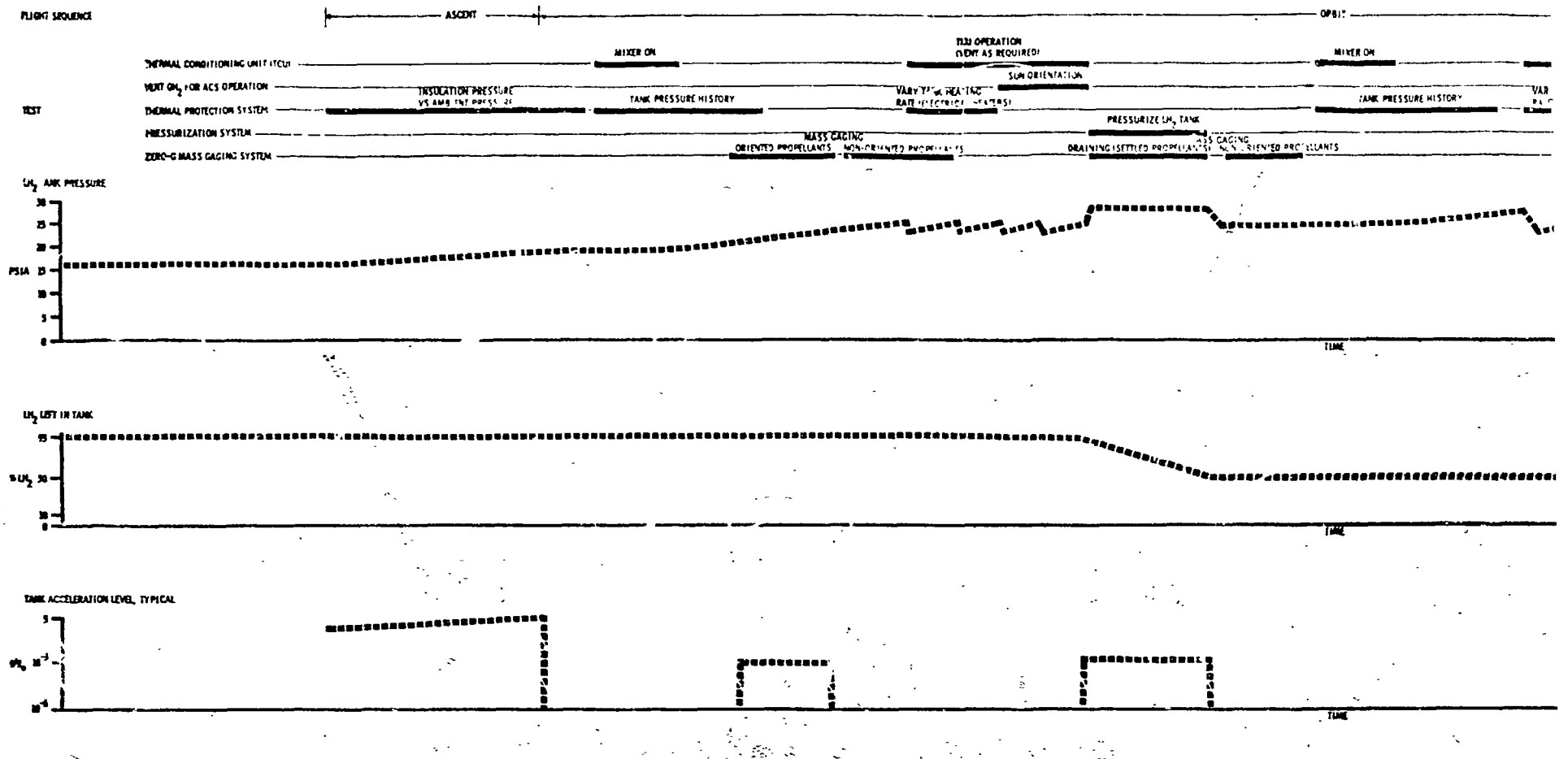

FOLDOUT FRAME 2

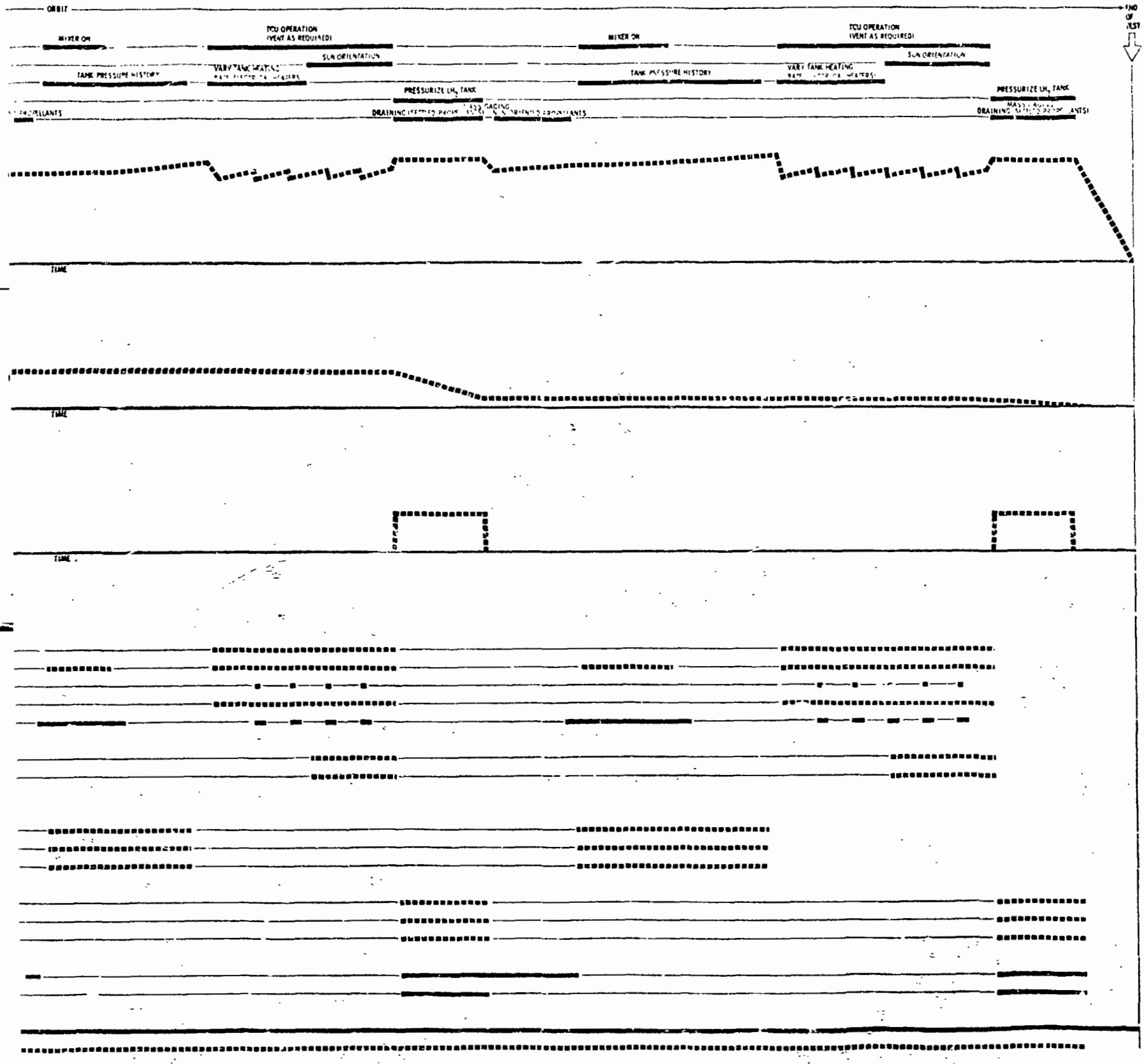

Fig. 105 -- Flight Test Sequence

time when each subsystem is being tested is shown by solid bars at the top of the chart. For ease of visualizing the tests being performed, the liquid hydrogen tank pressure, liquid hydrogen quantity left in the tank and vehicle acceleration level were plotted. At the bottom of the chart, experiment measurements required as a function of time are shown.

The sequence for flight tests starting with launch pad events is as follows: The tank insulation and plumbing are purged with gaseous helium and the volume between the shroud and experiment is purged with gaseous nitrogen. The tank is filled to 95 percent of capacity with 16 psia (110,000 N/m^2) liquid hydrogen. Just prior to liftoff, the purge bag is opened (using the nichrome wires). Insulation pressure is monitored during ascent and into orbit until the pressure reaches 10^{-6} torr. The orbital altitude is not critical as long as it is > 100 nm and sufficiently high to reduce drag and prevent atmospheric reentry during the test period. The mixer is turned on (it is wired so it can be turned on independently of the TCU operation) and tank pressure is monitored until a steady state pressure is reached. The pressure rise is then measured as a function of time with the mixer on (since pressure rise in an isothermal tank is a direct measurement of heat input) and then with the mixer off (to note stratification effects).

The Agena SPS is fired to settle propellants and a mass propellant reading is obtained from the capacitance probe. The RF system is also sensing propellant quantities during the thrusting period. Following shutdown of the SPS, the RF system continues to sense propellant quantities to determine the effect of propellant location on the quantity reading.

Electrical power is then supplied to the TCU system to investigate its operation and ability to hold the tank pressure between 23 and 25 psia (158,600 - 172,500 N/m^2). Tank heat rates are varied using electrical heaters to investigate this effect on TCU tank pressure control. During the latter part of the test, the ACS system is activated and the Agena/Experiment combination is oriented with respect to the Earth.

The SPS system is again fired, the tank is pressurized to 28 to 30 psia

(193,200 to 206,500 N/m^2) and the liquid hydrogen is drained to the 50 percent level. The capacitance and RF systems are operational during this time period.

This sequence of experiments is repeated at the 50 percent level and at the 10 percent level before the tank is finally drained and the pressure reduced to 0 psia. The total time over which this sequence occurs is estimated to be 14 days (to provide sufficient time for measurable pressure rises and to exercise the TCU system for a reasonable period of time).

DATA ANALYSIS AND INTERPRETATION

Flight test data will be available for analysis and interpretation based on the recommended instrumentation types and quantities and the recommended flight sequence discussed previously. For each subsystem under test, flight performance data will be available on a point design. These data will be used to check (or if required, modify) generalized analytical performance models developed for each subsystem (by previous extensive analyses and ground test programs).

A discussion of some of the more pertinent analytical models and computer programs is given below for each subsystem with a discussion on how the flight data will be analyzed.

Thermal Conditioning Unit (TCU)

The fundamental criteria for evaluating the performance of the TCU is the pressure response obtained with different mixer and vent flowrates. The initial transient response, following a pressurization has been found to be primarily dependent upon the mixing, ullage volume, and pressure level. This initial transient is followed by a steady pressure decay rate which can be described by the thermodynamic equilibrium model for which the expression is:

$$\frac{dP}{d\theta} = \frac{1.25\ (Q_o - M_o\lambda + 3.41\ P)}{\rho_L V_T\ (1 - V_u/V_T)} \left[\frac{1}{1 + 0.363\ \dfrac{(V_u/V_T)}{\rho_L(1 - V_u/V_T)}} \right]$$

The measured response rates will be compared directly with similar measurements from the ground based tests. Also, the temperature profile throughout the propellant tank will be measured as a function of time, and correlated with pressure response rates. In addition, the TCU component parameters will be monitored and the performance of each one evaluated to verify that each one functioned as it does in ground tests.

Vent Hydrogen for ACS

Ground based analyses and tests will establish vacuum thrust levels and gaseous hydrogen flowrates as a function of thruster chamber pressure and temperature. Flight data on thruster chamber temperature and pressure will then allow thrust levels and flowrates to be calculated. Width of the vehicle dead band (plus vehicle orientation information) will be inferred from output of the Agena's rate gyros and horizon sensors.

Thermal Protection System

Thermal performance calculations, using an existing complete system thermal model computer program will be made on the thermal protection system for a typical ascent and orbit flight profile. Input data to the program will include (1) the insulation outgassing rate and specific mass flow conductance, (2) multilayer insulation heat flux as a function of layer density, pressure and hot boundary temperature, (3) thermal conductivity of the fiberglass struts, and (4) thermal conductivity and emittance of the plumbing lines.

Semi-empirical equations developed under different government contracts that provide these relations are shown below.

Insulation Pressure History. The insulation pressure history is given by:

$$\frac{\partial P}{\partial t} = \frac{R_o T Q}{M y_o} + \left(\frac{R_o T C_M}{M}\right) + \left(\frac{\partial^2 P}{\partial X^2}\right) + \left(\frac{y^2_o}{3\mu}\right)\left(\frac{\partial P^2}{\partial X}\right)$$

where

P	=	local pressure of insulation being measured
t	=	time, sec
R_c	=	universal gas constant, $in^2/sec^2\ °R$
T	=	absolute temperature, °R
Q	=	local outgassing rate per unit area as a function of time, pressure and temperature, lbm/sec in^2 (experimental data)
M	=	gas molecular weight, dimensionless

y_o = distance between shield and spacer, in.

C_M = specific mass flow conductance, sec (experimental data)

X = distance along flow channel measured from no-flow boundary, in.

μ = viscosity of flow gas, lbm/in sec

The above listed pressure equation accounts for both the venting of purge gas and any outgassing that occurs. The outgassing rates and the specific mass flow conductance values need to be obtained from ground-based experiments. These data are used as input for a computer program based on the above listed equation to predict insulation pressure histories.

Gold Coated Mylar/Silk Net Thermal Performance. The heat rate through the insulation is given by:

$$q = \frac{4.37 \times 10^{-11}(\bar{N})^{3.27} T_M}{N_S + 1}\left(T_H - T_C\right) + \frac{6.70 \times 10^{-13}}{N_S}\left(T_H^{4.51} - T_C^{4.51}\right)$$

where

q = heat flux, Btu/hr-ft^2

$\bar{N}$ = number of radiation shields/in.

N_S = number of radiation shields

T_H = hot boundary temperature, ^oR

T_C = cold boundary temperature, ^oR

Empirical data on heat flux versus gas pressure are used to modify the heat flux values obtained from the above listed equation during ascent.

Fiberglass Tank Support Struts. The thermal conductivity of the fiberglass tank support struts is given by:

$$K_e = 0.050 + 6.35 \times 10^{-4} T$$

C5

where

K_e = thermal conductivity of fiberglass filament wound struts, Btu/hr-ft^{o}R

T = absolute temperature, ^{o}R

Radiation tunneling inside the struts is reduced to negligible values using chopped Dexiglas paper.

Plumbing. The heat rates through the plumbing lines is given by:

$$Q_T = Q_{\text{solid conduction}} + Q_{\text{radiation tunneling}}$$

A radial, three dimensional insulation penetration computer program has been developed to handle all the insulation penetrations, including the effect of thermal degradation in the multilayers surrounding the penetrations.

Data Evaluation. As a check on the experiment-point-design orbit thermal performance, the experiment is tested in a vacuum chamber and the empirical constants in the equations are modified, if required, to match the test data for both a vented tank (hydrogen boiloff) and non-vented, isothermal tank (mixed model, pressure rise test). The hot boundary temperature is changed for individual tests over a range consistent with expected orbital temperatures. Temperature profiles through the insulation, over the liquid hydrogen tank and along the penetrations provide additional test data (besides the boiloff rate and tank pressure rise rate) needed to check (or modify) the thermal performance equations.

For the ascent portion of the mission, the predicted and measured insulation pressure profile is compared. If differences are noted, the specific mass flow conductance values, C_M, and distance between radiation shields, $2y_o$, (due to ballooning effects) would be adjusted till a better fit occurs.

Total heat deposited in the tank during ascent would be obtained from the minimum pressure value obtained on the first mixed model pressure rise test (and compared to the analytical predictions); thermal performance of the thermal protection system in orbit would be obtained from the three mixed model pressure rise tests and compared to the vacuum chamber test results for different thermal control boundary temperatures and the three fill levels. Values of empirical constants would then be adjusted, if required, so the CSTM computer program can predict thermal performance for the total flight profile.

Ability to accurately predict stratified (non-mixed) tank pressure histories as a function of heat rate and percent of liquid hydrogen left in the tank is currently not available. Highly sophisticated differential equations and computer program needs to be developed to handle this problem. The flight test experiment would act as a point design check on the ability of this program to predict tank pressure rise in low gravity.

Pressurization System

A pressurization computer program, e.g., FORTRAN Program for the Analysis of a Single-Propellant Tank Pressurization System, will be used to predict the gaseous hydrogen quantities required for each drain cycle (burn) for the temperatures, pressures and drain rates contemplated. The ground-based tests will provide experimental data required to modify the pressurant collapse factors if required. The orbital flight test data will then be compared with the modified predictions based on the ground test results. Gaseous hydrogen quantity used in orbit will be determined from temperature and pressure measurements of the storage bottle. An integrated value of the gaseous hydrogen flow rate obtained from the flow meter located on the pressurization line will provide a cross reference check on this quantity. Temperature probes located throughout the tank will aid in analyzing energy exchange in the liquid, ullage, at liquid/ullage interfaces and to the tank wall.

Zero-G Propellant Gaging System

The basic property measurement desired from the orbital flight test is the change in frequency output (precision) of the radio frequency system with propellant location in the tank (settled to non-oriented). The percent change indicates the effect of propellant location on system accuracy. It is also desirable, but not absolutely necessary, to know the accuracy of the measurement. The following ground-based tests assumes both precision and accuracy of the measurement are required.

The tank volume is volumetrically calibrated with triple-distilled water, with the tank immersed to remove the hydrostatic loads. Changes in volume due to temperature are computed using expansion coefficients for the aluminum alloy 2219-T87. The tank is assembled into the experiment and the experiment is mounted on a load cell weighing system located in a vacuum chamber. The chamber is pumped down and the tank is filled with liquid hydrogen; the RF system frequency and capacitance probe system output are calibrated against the weight measurements. Temperature measurements are required to convert the RF outputs from volume measurements to mass measurements. The shaped capacitance probe measures mass directly (total of liquid and gas).

In orbit, the capacitance probe is used as the primary mass standard when the propellants are settled during a thrusting period. The RF output should correspond to the capacitance probe output at this time based on the ground calibration tests. The change in RF frequency output when the thrust is terminated is indicative of the effect of different propellant locations on system accuracy for the 95, 50 and 10 percent levels of liquid hydrogen tested. The TV picture provides qualitative information on the liquid location when the tests are conducted.

Experiment Dimensions, Weight, Power and Energy

The experiment dimensions are approximately 9.2 feet (2.8m) in diameter by 8.6 feet (2.6m) long (not including the adapter truss to the Agena). The experiment weight is 1954.5 lb (886 Kg), as summarized in Table 31. The Agena provides the electrical power, telemetry, tracking and command link, SPS for periodic thrusting periods and astrionic equipment required for vehicle attitude stabilization. The experiment electrical requirements are 300 watts maximum power at any one time with a 1355 watt-hr maximum electrical energy requirement as shown in Table 32. Twenty lb (9.1 Kg) of Ag-Zn batteries added to the Agena will handle these requirements.

TABLE 31

PRELIMINARY LH_2 TANK EXPERIMENT WEIGHT STATEMENT

	LBS	(Kg)	LBS	(Kg)
TANKAGE				
LH_2 Tank (2.19Al)	220	(99.8)	350	(158.9)
GH_2 High Pressure Bottle	130	(59.0)		
FLUIDS				
LH_2	1150	(522)	1159	(572)
GH_2	9	(4.5)		
STRUCTURE				
8 Fiberglass Tank Supports	7	(3.4)		
Al Tubular Frame	110	(50)		
Multilayer Insulation (36 rad shields)	55	(25)	192	(87.2)
Purge Bag	9	(4.5)		
Therm Control Coating	11	(5.0)		
PLUMBING				
Pressure Switches (2)	2	(0.9)		
Expansion Regulator	1	(0.45)		
Mixer	2	(0.9)		
Compact Heat Exchanger	5.8	(2.7)		
Control Valve	0.8	(0.2)		
3-Way Valve (TCU evacuate)	0.8	(0.2)		
Thrust Nullifiers (2)	2	(0.9)		
LH_2 Fill Valve	11	(5.0)		
LH2 Flight Drain Valve	5	(2.3)		
Ground Vent Valve	4	(1.8)	74	(33.6)
GH_2 Fill Valve	1.3	(0.6)		
GH_2 Relief Valve & Burst Disc	1.1	(0.7)		
GH_2 Shutoff Valve	1.4	(0.6)		
GH_2 Regulator (2)	6	(2.7)		
Quick Disconnects (6)	2.8	(1.3)		
Thrusters (12)	6	(2.7)		
Lines	21	(9.5)		
INSTRUMENTATION				
Mixer Parameters (E, I, RPM)	2	(0.9)		
Pressure Transducers	5	(2.3)		
Temperature Transducers	6	(2.7)		
Flow Meters	2.5	(1.1)	82.5	(47.5)
TV System	25	(11.0)		
RF System	22	(10.0)		
Capacitance System	20	(9.1)		
ELECTRICAL *				
Relays	5	(2.3)		
TV Tape Recorder	32	(14.5)		
Tape Recorder	25	(11.0)		
Programmer/Controller (Solid State)	10	(4.6)	97	(44.0)
Signal Conditioning	5	(2.3)		
Wire	10	(4.6)		
Buffer Box (Solid State)	10	(4.6)		
TOTAL			1954.5	(943)

* Remainder of astronic equipment is assumed to be provided by the Agena.

TABLE 32

PRELIMINARY LH_2 TANK EXPERIMENT ELECTRICAL REQUIREMENTS

ITEM	OPERATING VOLTAGE	CURRENT (AMPS)	POWER (WATT)	MAX ENERGY (WATT-HR)
Gaseous Hydrogen Shutoff Valve	26 to 30 VDC	2	60	4
ACS Valves (6 ea)	26 to 30 VDC	1	30	Neg
TCU Control Valve	26 to 30 VDC	1	30	Neg
LH_2 Drain Valve	26 to 30 VDC	4	120	8
Mixer	26 to 30 VDC	0.02	0.6	18
RF Sensor	26 to 30 VDC	0.2	5	5
Capacitance Probe	110 VAC, 400	0.1	14	14
Image Isocon TV Camera	26 to 30 VDC	1.3	40	40
Lights	26 to 30 VDC	0.2	6	6
Mass Flow Meter (2)	10 VDC	0.1	2 (Total)	60
Temperature Transducers (96)	26 to 30 VDC	up to .02 (ea)	20 Total	20
Pressure Transducers (20)	10 VDC	.03 (ea)	6 Total	200
TV Tape Recorder	26 to 30 VDC	2.0	60	60
Tape Recorder	26 to 30 VDC	2.0	60	600
Electrical Heaters	26 to 30 VDC	3.0	90 (Max)	270
Programmer/Controller	26 to 30 VDC (through buffer box)	0.3	10	50
			Max power at one time ~ 300	1355

EXPERIMENT TELEMETRY TRACKING AND CONTROL (TT&C)

Subsystem Functions

The experiment instrumentation sensor data listed in Table 30 will be collected, conditioned and transmitted to the ground station when the vehicle is within operational ranges. The experiment sequence and the corresponding vehicle attitudes and movements will be programmed. Ground controlled override of the program based upon the interpretation of the telemetered data and the equipment performance is desired. The detail functions identifiable within the stated subsystem function such as signal conditicning, data storage, data transmission and vehicle control are discussed below and a concept for implementation of the functions is described.

Signal Conditioning. The signals from the instrumentation sensors will be shaped and amplified to achieve a uniform signal format suitable for multiplexing and digitizing. A PCM (NRZ) format is desired in order to be compatible with existing ground station capabilities. The data from the TV sensor will be of analog type in order to conserve bandwidth and minimize program cost.

Data Storage. The orbital vehicle will be within transmitting range of the ground station for a very limited time only. Consequently, an on-board data storage is required for the sensor data. Since the data will be in digital form, a digital storage device is desired. Capability to store data at low rate and dump at a fast rate is desired. The effective dump time available is illustrated in Fig.106. A record to dump time ratio of 10-20 is desired.

Transmission. The stored data will be dumped into a telemetry transmission link and transmitted to the ground station whenever a favorable station pass is accomplished. This process will require an RF system with adequate power for the intended ranges and the data bandwidth.

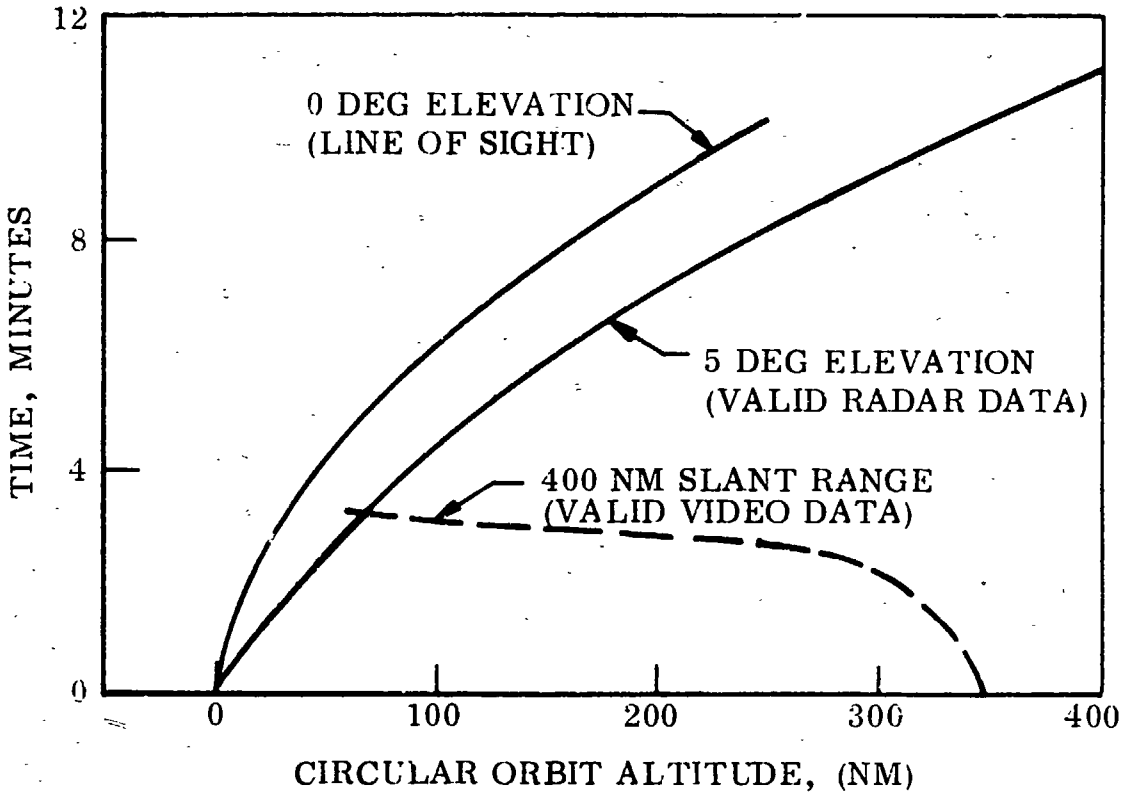

Figure 106 Maximum Aquisition Time Over A Tracking Station, 10 Watt Transmitter

Vehicle and Payload Control. The experiment equipment sequence will be reprogrammed and executed on-board the vehicle. Capability to reprogram the sequence and to interrupt or bypass the program may be needed and will be executed by ground command. Vehicle attitude and movement, associated with the experiment must also be controllable from the ground in order to fully utilize the flight time and optimize the returned data. These functions will require a vehicle to ground command capability and a reprogrammable decoder on-board the vehicle. Compatibility with existing ground station equipment is required for both the telemetry and the control functions.

System Concept. The functions described in the previous section can best be implemented by the use of the standardized space-ground link system (SGLS) presently used in most spacecraft. This system will provide vehicle tracking, ranging and command capability in addition to the telemetry transmission capability needed for the experiment.

The SGLS performs the requisite tracking, telemetry, and command functions through the use of a coherent radio link, i.e., by multiplexing the command analog, and tracking data onto a single ground-to-vehicle carrier in the 1760- to 1840-mc band and, similarly, by multiplexing the telemetry and tracking data onto a coherently offset vehicle-to-ground carrier in the 2200- to 2300-mc band. The high-rate PCM data (128 kbps or greater) are modulated on a second noncoherent vehicle-to-ground carrier 5.0 mc below the coherent transmission. A simplified block diagram of the system is shown in Fig. 107.

The ground-to-vehicle carrier is generated in the ground transmitter and, after modulation by the command, voice, and ranging data, is passed through the diplexer to the antenna for radiation to the vehicle. This carrier is received at the vehicle and passed through the multiplexer to the vehicle phase-lock receiver which demodulates the carrier. The composite data are then passed on to the various recipients such as the command decoder.

The vehicle receiver also serves to generate coherent drive for vehicle transmitter 1 at a rational fraction of the received frequency (8/205). This signal

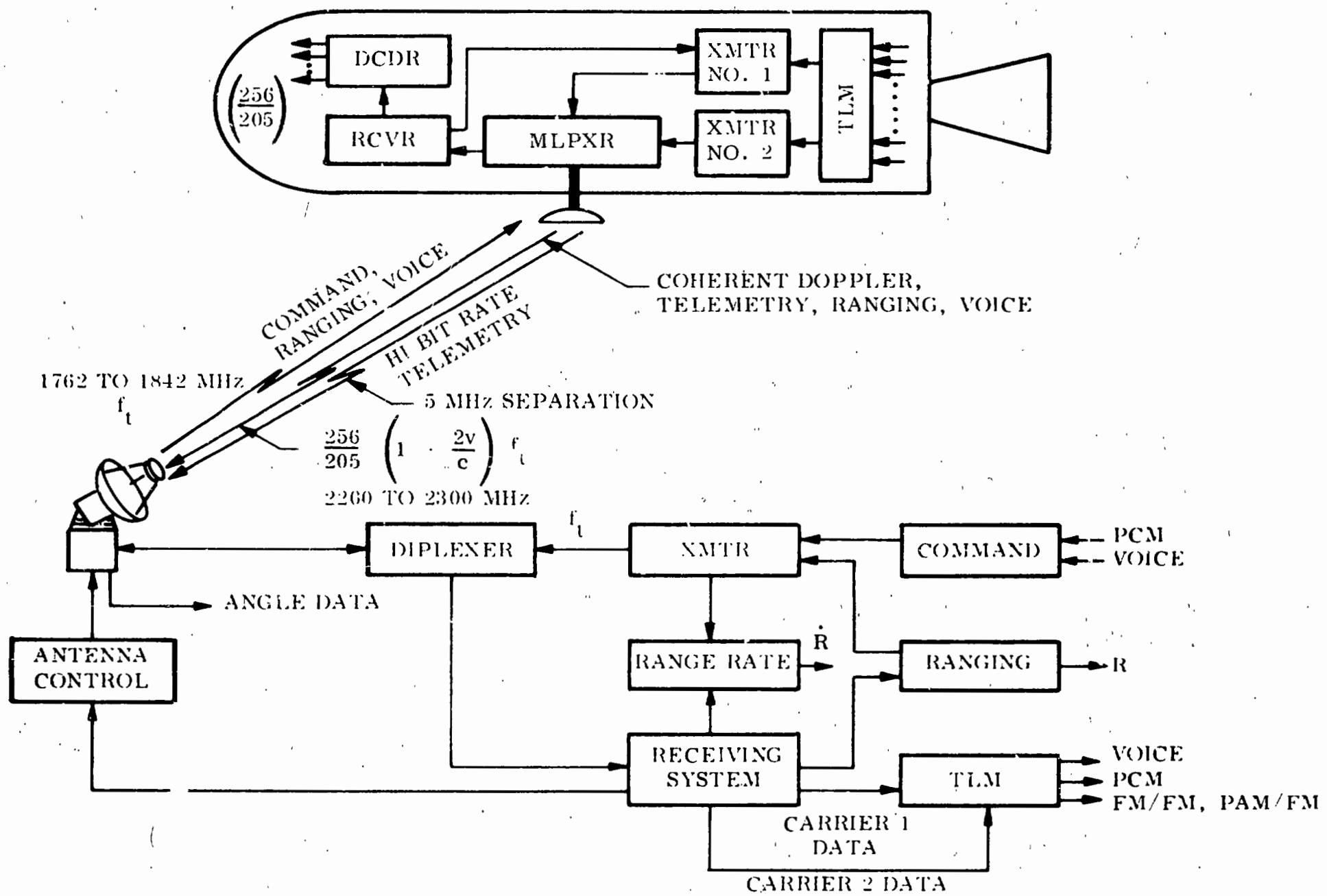

Figure 107 Simplified SGLS Block Diagram

is subsequently amplified and multiplied by 32 in the transmitter to form vehicle-to-ground Carrier No. 1, coherently related to the received carrier by the rational fraction 256/205. This carrier is modulated by the medium bit-rate PCM, voice, PAM/FM, FM/FM, and ranging signals. This signal is passed through the multiplexer to a common antenna for radiation to the ground station. A second carrier, 5.0 mc below the first, is generated in transmitter 2, and, after modulation by the high bit-rate PCM, is passed through the multiplexer to the antenna.

The received signals at the ground station are fed through the diplexer to the receiving subsystem which demodulates both carriers and routes the data to the telemetry and ranging subsystems as appropriate.

The use of the high bit rate PCM channel for the TV-sensor data will permit use of the SGLS subsystem with only minor modifications. A modified transmitter allowing direct modulation of the subcarrier by the TV-data will be added and a corresponding receiver capability will be added in the ground stations. The effective bandwidth of the SGLS high rate PCM channel is approximately 1 MH_2. This bandwidth is lower than the normally used bandwidth for TV-sensors.

TV-Sensor. Currently available low light level TV cameras are designed for the standard frame rate of 30 frames per second required for real time viewing. This results in a bandwidth requirement for transmission in excess of 5 MH_2. To modify the SGLS system to accommodate this sensor will be a major development effort and is not recommended. Instead, a camera designed to fit within the current SGLS capability is advocated. A slow frame rate will accomplish this without degradation of sensitivity or resolution. Work performed at LMSC under contract to the Air Force Test Laboratory at Eglin Air Force Base, Florida, has resulted in a camera design capable of imaging at an input light level of 5.6×10^{-4} foot-candles-seconds at a rate of 2 frames per second using an exposure time of 1 millisec. The limiting resolution is 800 TV-lines at a signal to noise ratio of 35 db. The camera utilizes the RCA C 21095 ISOCON tube which is commercially available. A camera of this type will provide adequate coverage

since real time viewing is not contemplated. The data storage requirements will be modest and can readily be filled by a magnetic tape recorder such as the one listed in Table 33.

In the case of fluid dynamic type investigations such as flow patterns or velocity measurements, this camera will be inadequate. It is still possible, however, to perform these measurements by using a second camera. This camera will image at the faster frame rate (30 frames/sec) and the data will be recorded on tape. Subsequent playback of the tape at lower speed will enable transmission of the data by the modified SGLS. This option will involve addition of a wide band recorder with slow playback. A moderate development effort is anticipated to provide this piece of equipment.

The functional arrangement of the SGLS vehicle equipment using the slow scan type of TV camera is shown in Fig.108. Most of the experiment instrumentation sensors will be served by the No. 1 digital telemetry unit. The data will be conditioned, multiplexed and digitized in this unit and passed on to the base band assembly unit where range information will be added. The resulting data stream will be applied to transmitter No. 1. The TV data from the video recorder or direct from the camera will be used to modulate transmitter No. 2 directly. This arrangement will require modification of this transmitter to accept analog data in lieu of PCM data. Commands received by the SGLS receivers will be processed to assure validity and address and forwarded to the vehicle decoder. This unit (or units) is capable of executing a total of 32 commands each seven of which can be reprogrammed via the command link. An eleven bit code is used as input to each command. If extensive ground programming capability is desired (more than seven commands) several units may be employed.

The ground station configuration needed to match the vehicle installation is illustrated in Fig. 109. The only modification needed in the existing ground station arrangement will be the addition of a wide band recorder and display for the TV-data.

Equipment Status. The described Space to Ground Link consists of a number of standard components designed in such a way that a subsystem can be built to fit the individual flight profile but still be compatible with the fixed

TABLE 33

MAGNETIC TAPE RECORDER

LMSC TYPE 23

Recording Mode	Direct Analog
Number of channels	2
Record/Reproduce Time	5.5 minutes
Bandwidth	1 KH_z - 1 MH_z
Start/Stop Time	Less than 5 sec
Input signal amplitude	0.3 volt peak-to-peak
Rise Time	Less than 0.55 μsec
Cross talk	30 db down
Flutter	Less than 2%
Power	25 watts 28 vdc
Weight	12 lb

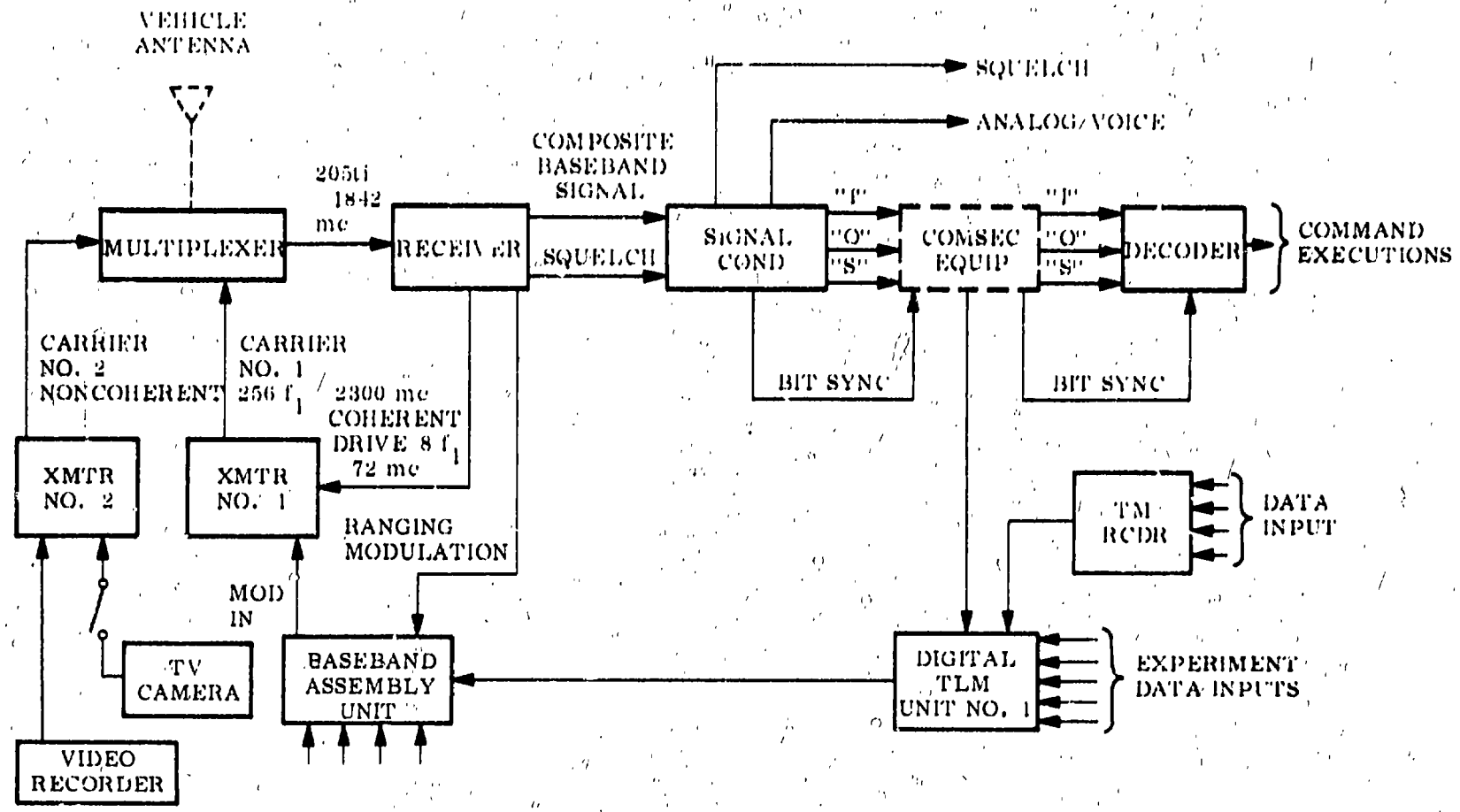

Figure 108 SGLS Vehicle Equipment Functional Block Diagram

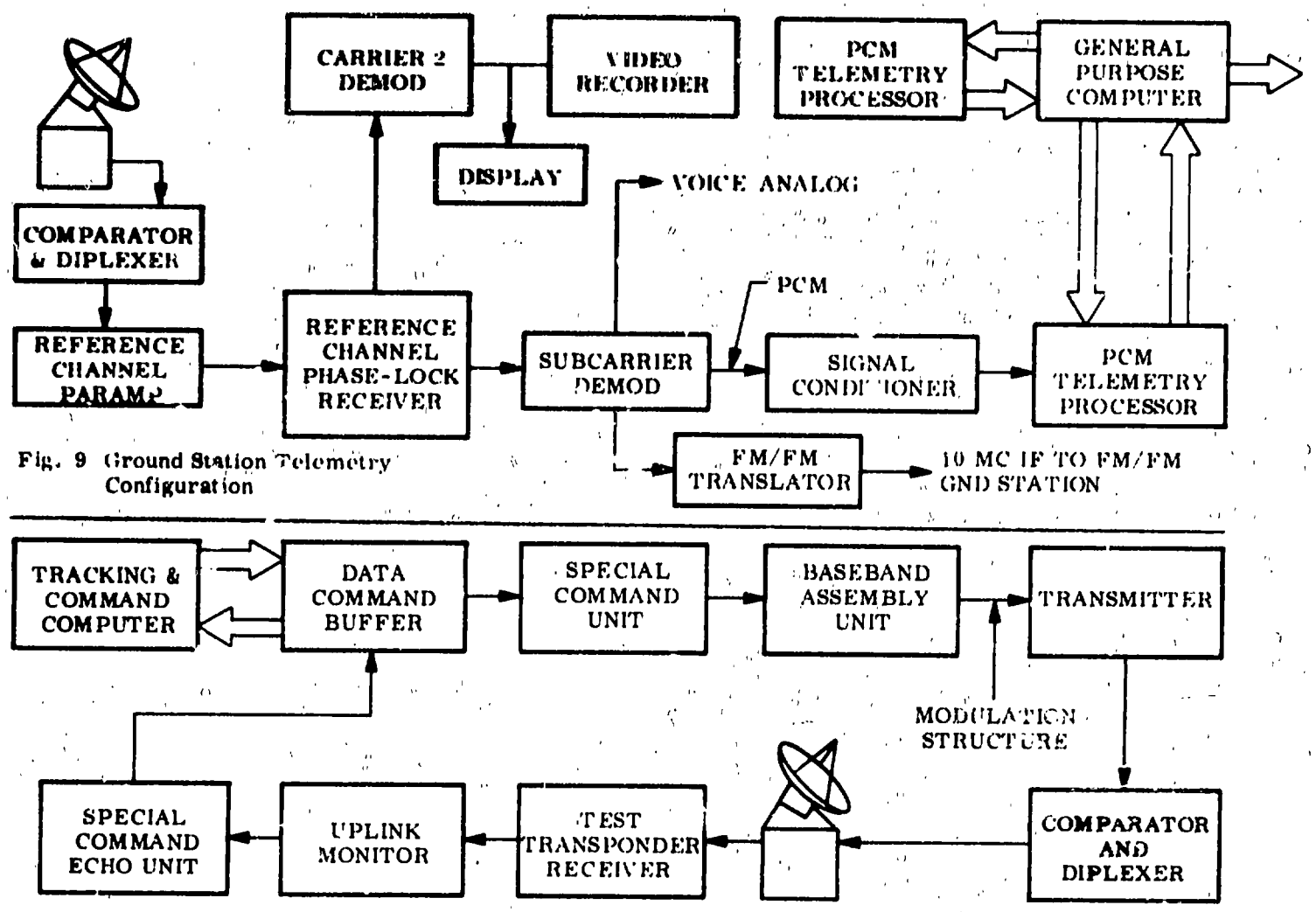

Fig. 9 Ground Station Telemetry Configuration

Figure 109 Ground Station Command Configuration

ground installation. It appears likely at this point that only minor modifications of the existing equipment will be needed both in the vehicle and in the ground station. Previous flight history of the equipment and the relatively simple additions-modifications will assure a high probability of trouble-free operation during the experiment period.

LAUNCH VEHICLE SELECTION

As previously indicated, the cryogenic experiment requires an extended stay time in space. The necessary stationkeeping ability, along with the extensive communication capability and associated power can be provided as a part of the experimental package. In this case, the only requirement of the launch vehicle is the capability to insert the experiment into orbit. A second approach is to use a launch vehicle system with an orbiting upper stage that has the necessary power, guidance and control, and communications. The test module would stay attached to the orbiting stage and use its facilities for controlling, monitoring, and transmitting data from the experiment.

Several launch vehicle systems are capable of boosting the 1955 lb (877 Kg) experiment into a 100 nm circular earth orbit. A few of these are shown in Table 34 for a due east launch from ETR.

TABLE 34

LAUNCH VEHICLE CAPABILITIES

BOOSTER	2ND STAGE	PAYLOAD CAPABILITY	
		LBS	(Kg)
Thor	Delta		
Atlas E,F	-	2500	(1135)
Atlas	Centaur		
Atlas SLV-3	-	4200	(1907)
Titan III C	Transtage		
Titan III B	Agena		

The Thor-Delta is the least expensive vehicle with sufficient payload capability. However, it has no GC&C capability. The test module must then, in effect, be a non-propulsive spacecraft, and this will be reflected in relatively high development costs. The Centaur and Transtage have GC&C but are limited to a few hours on orbit.

The Agena is the only currently available orbiting stage that has the necessary capabilities for conducting a meaningful cryogenic experiment (exclusive of Saturn Stages). It should be noted that decreasing the size and weight of the test module does not significantly alter the requirements for extended stay time, test control, and communications. Consequently, it would not result in a significant weight savings.

DEVELOPMENT PLAN

A development program plan and experiment costs were defined in the study.

Assumptions used in the analyses are as follows:

- The booster system is a Titan III-B/Agena. Other first stage boosters such as Thorad (3-bottle), Atlas E and F and Atlas SLV-3 could be substituted for the Titan III-B if desired (based on payload capability).

- The Agena spacecraft remains attached to the experiment module in orbit and provides the communications and command link, electrical power, positive acceleration at specified times and astrionic equipment required for vehicle attitude stabilization. Vent hydrogen from the TCU plus 6 thrusters provide vehicle attitude stabilization for desired test sequences in the mission. (The Agena is the only spacecraft qualified for mission durations of two weeks or longer contemplated for the orbital test.)

- The fairing used is qualified and encloses both the experiment module and Agena. Fairing dimensions are 10 ft (3.04 m) diameter by 43 ft (13.1 m) long.

- The launch site is the WTR based on availability of launch support equipment; the launch profile uses a dog leg to an inclined orbit. ETR launches are also acceptable from a mission standpoint.

- Two identical experiment modules are built but only one is flown.

- No additional ground testing is required for the thermal conditioning system.

- Additional development testing is required for the cold hydrogen gas ACS thruster system, flight type RF system and flight type TV viewing system.

The development plan schedule is shown in Fig. 110. An orderly development schedule shows a 34 month span is adequate from program go-ahead to the submission of the flight test report. The plan given in Fig. 110 shows fabrication of two identical experiment modules. The primary purpose of the second module is to serve as an investigative aid. It will be used to duplicate the flight test profile on the ground, permitting reference data to be obtained without inducing an unknown amount of wear in the components of the first (flight test) module. Also, the second module acts as an investigative apparatus in post flight ground testing in case of gross malfunction during the flight of the first module. On the other hand, data obtained during a successful orbital flight of the first module may suggest additional useful ground testing which could be accomplished by the second module (with modifications are desired).

ALTERNATE EXPERIMENT DESIGN

An alternate (or follow-on) experiment was laid out that represents a complete propulsion system consisting of liquid hydrogen and liquid fluorine

FOLDOUT FRAME 1

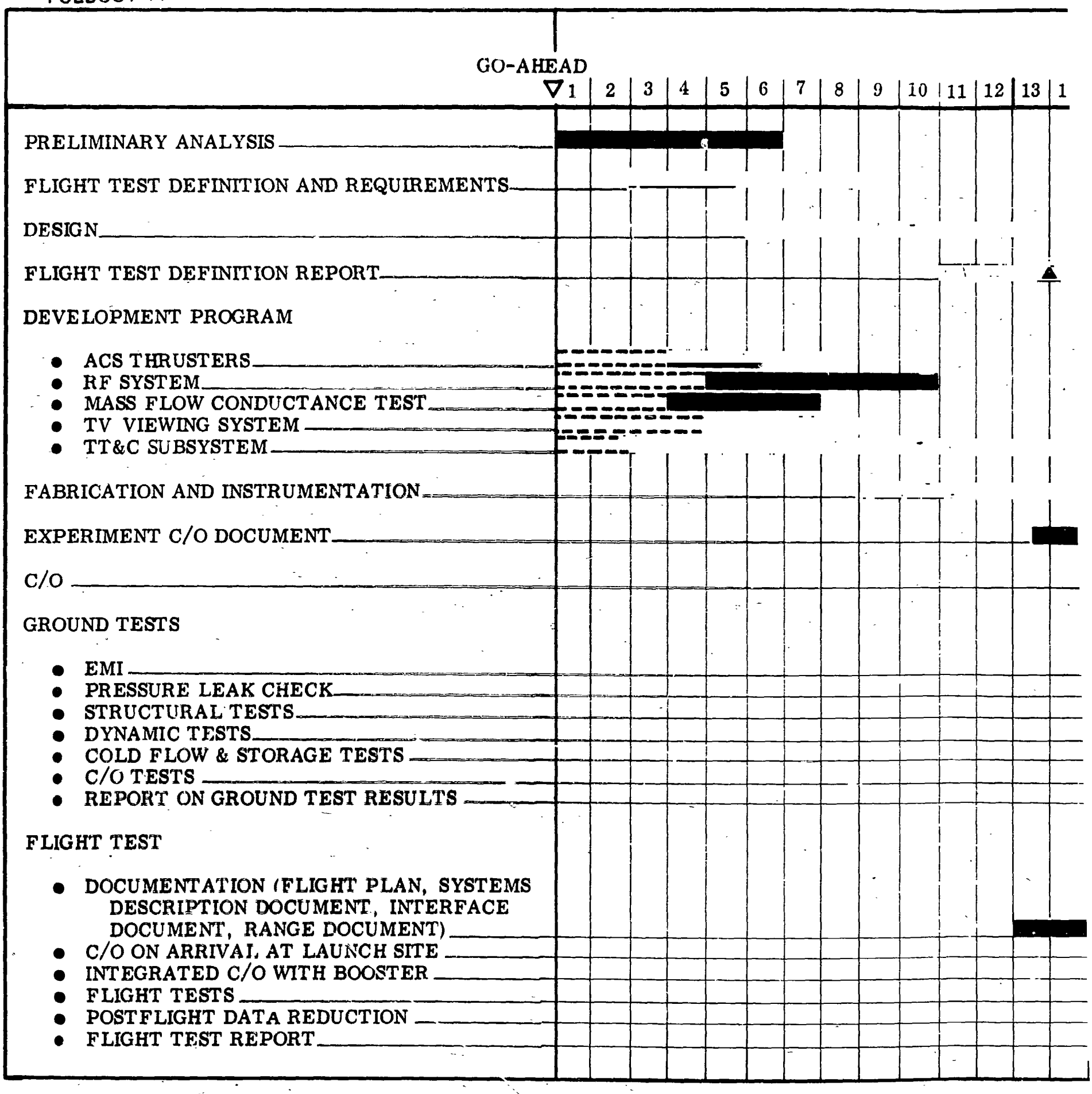

FOLDOUT FRAME 2

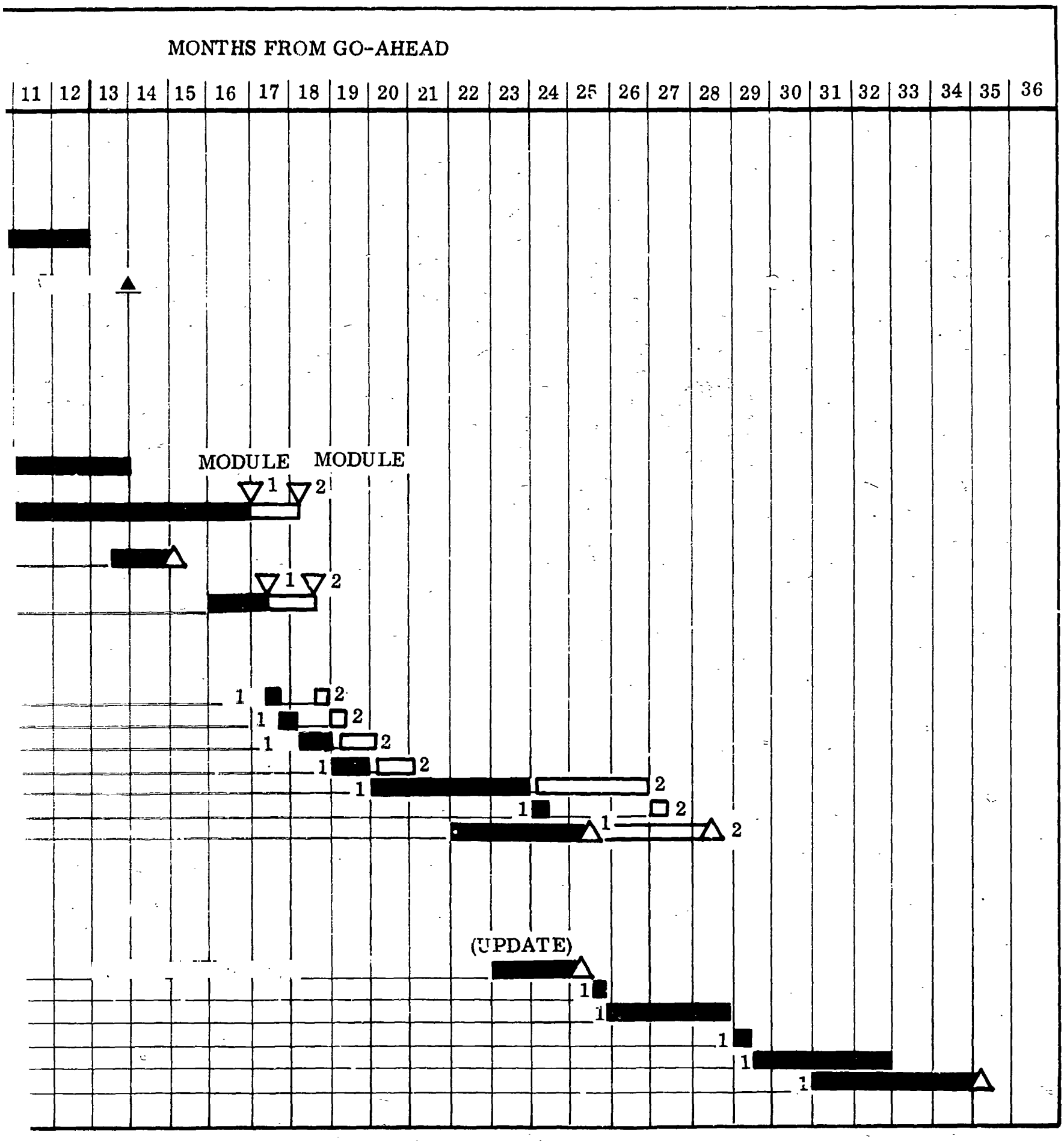

Fig. 110 – Development Plan For The Liquid Hydrogen Tank Flight Test Module

tankage integrated with a 5000 lb-force (22,240 N) thrust bell nozzle main engine. This high energy upper stage design, currently being pursued by Lockheed on in-house funds as shown in Fig. 111, has applications for many high velocity missions such as planetary orbit insertion. The experiment represents the next logical step in experiment sophistication (from the single liquid hydrogen tank experiment described previously) in that all propulsion subsystems can be tested independently or concurrently.

The size of the propulsion stage is 5.0 feet (1.52 m) in diameter by 10.0 feet (3.04 m) long. The dry weight of the stage (for a pressure fed engine) is 535 lbs (243 Kg). Propellant weight adds another 1745 lbs (792 Kg), for a loaded vehicle weight of 2280 lbs (1035 Kg), as shown in Table 35. Weight for experiment instrumentation shown in Fig. 112 are not included in this total. A typical plumbing schematic for the experiment is shown in Fig. 113. The liquid hydrogen tanks are pressurized with bleed hydrogen gas from the engine; heated helium is used for the fluorine tanks. The subsystems that would be tested include the TCU, the gaseous hydrogen ACS, the thermal protection system, the pressurization system, the zero-g propellant gaging system and the engine, as shown in Fig. 113. Instrumentation is similar to the liquid hydrogen tank experiment, with additional temperature and pressure measurements required for the liquid fluorine tanks and the main engine.

The flight sequence would include a boost into orbit (without an experiment engine burn) and a series of tests on the subsystems similar to those described previously with the exception that engine firings would be substituted for the liquid hydrogen drain cycles. This flight sequence is recommended since many subsystem tests could be conducted even if engine malfunction occurred. Again, it is recommended that two flight experiments be fabricated for the same reason given previously in the Development Plan.

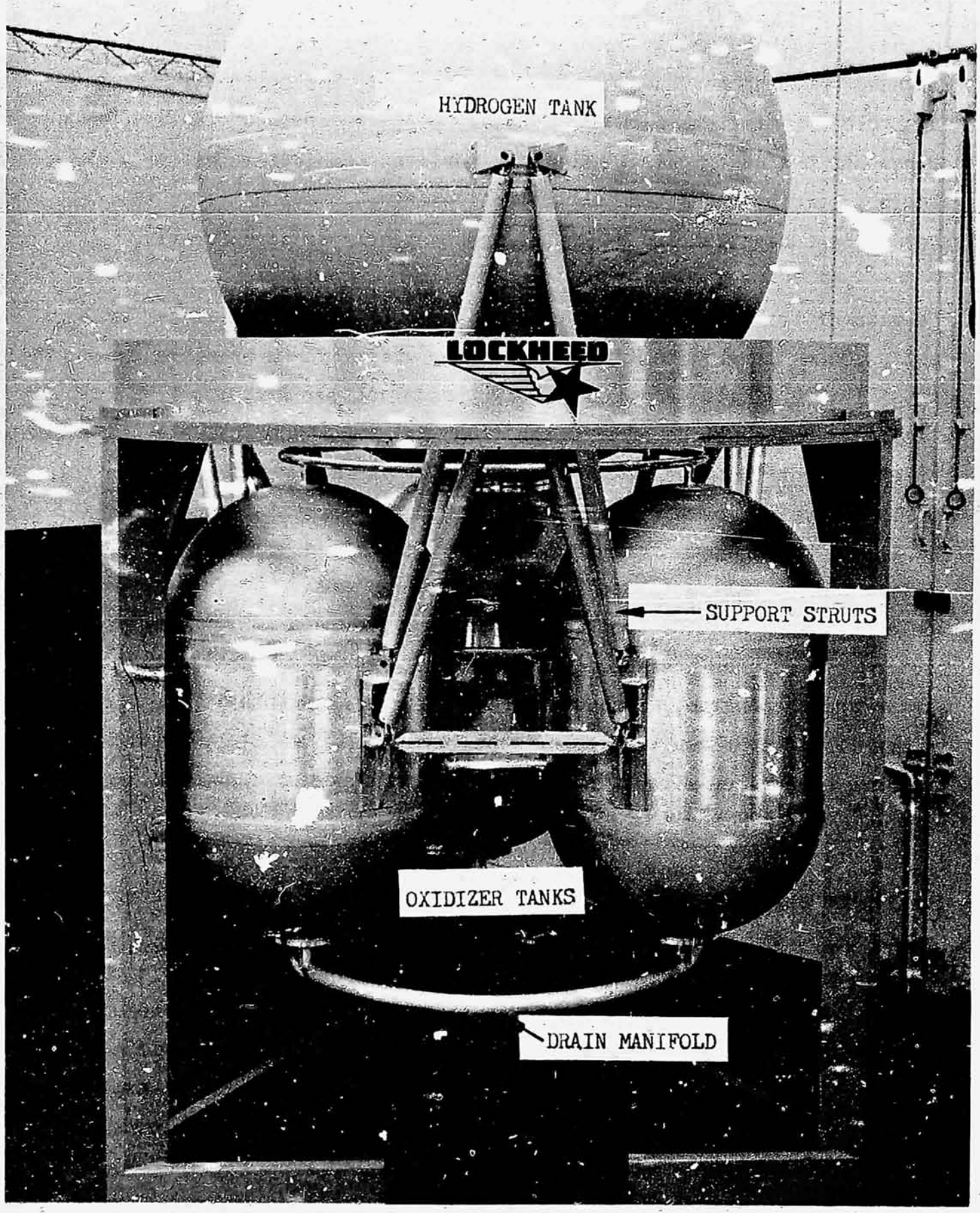

Figure 111 High Energy Upper Stage - Propulsion Test Module

Table 35

SUMMARY WEIGHT STATEMENT FOR AS-BUILT
PROTOTYPE HIGH VELOCITY STAGE

	(lbs)	(Kg)
LH_2 Tank	36.28	(16.45)
LF_2 Tank Assembly	83.13	(37.70)
Support Structure	56.52	(25.65)
Insulation	59.49	(27.00)
Plumbing	17.36	(7.88)
Electrical Power	48.50	(22.00)
Guidance & Control	101.50	(46.02)
Engine Installation	95.80	(43.50)
Pressurization System	5.50	(2.51)
Pyrotechnics	9.00	(4.09)
Communications & Control	10.70	(4.86)
Hdwe, Nuts, Bolts, etc.	11.22	(5.11)
Dry Weight	535.0	(242.8)
Propellant Residuals	5.0	(2.27)
Burn Out Weight	540.0	(245.1)
LH_2	124.0	(56.4)
LF_2	1616.0	
Usable Propellant	1740.0	(734.0)
Launch Weight	2280.0	(1035.5)

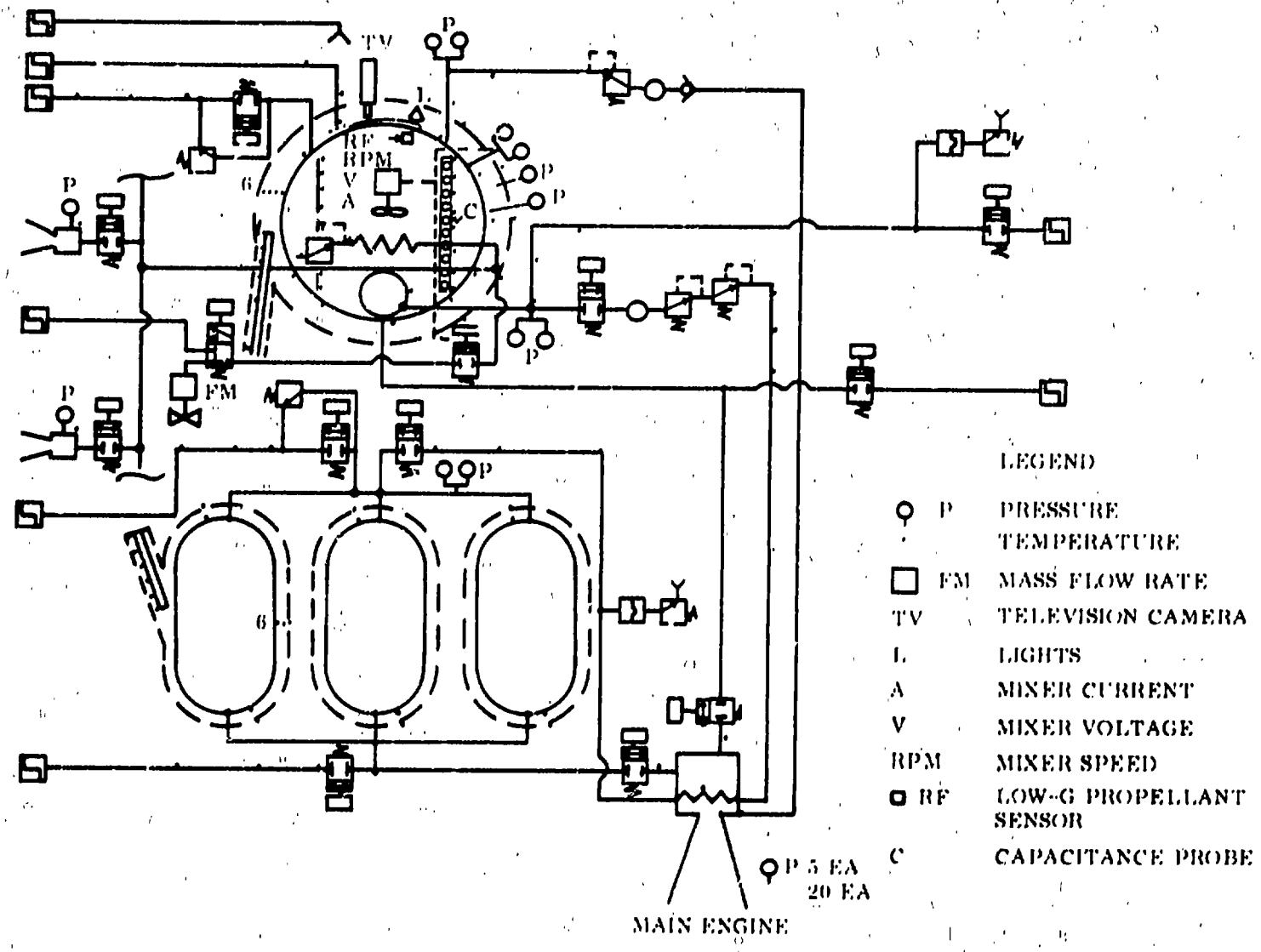

Figure 112 Instrumentation Locations for the Propulsion System Flight Experiment

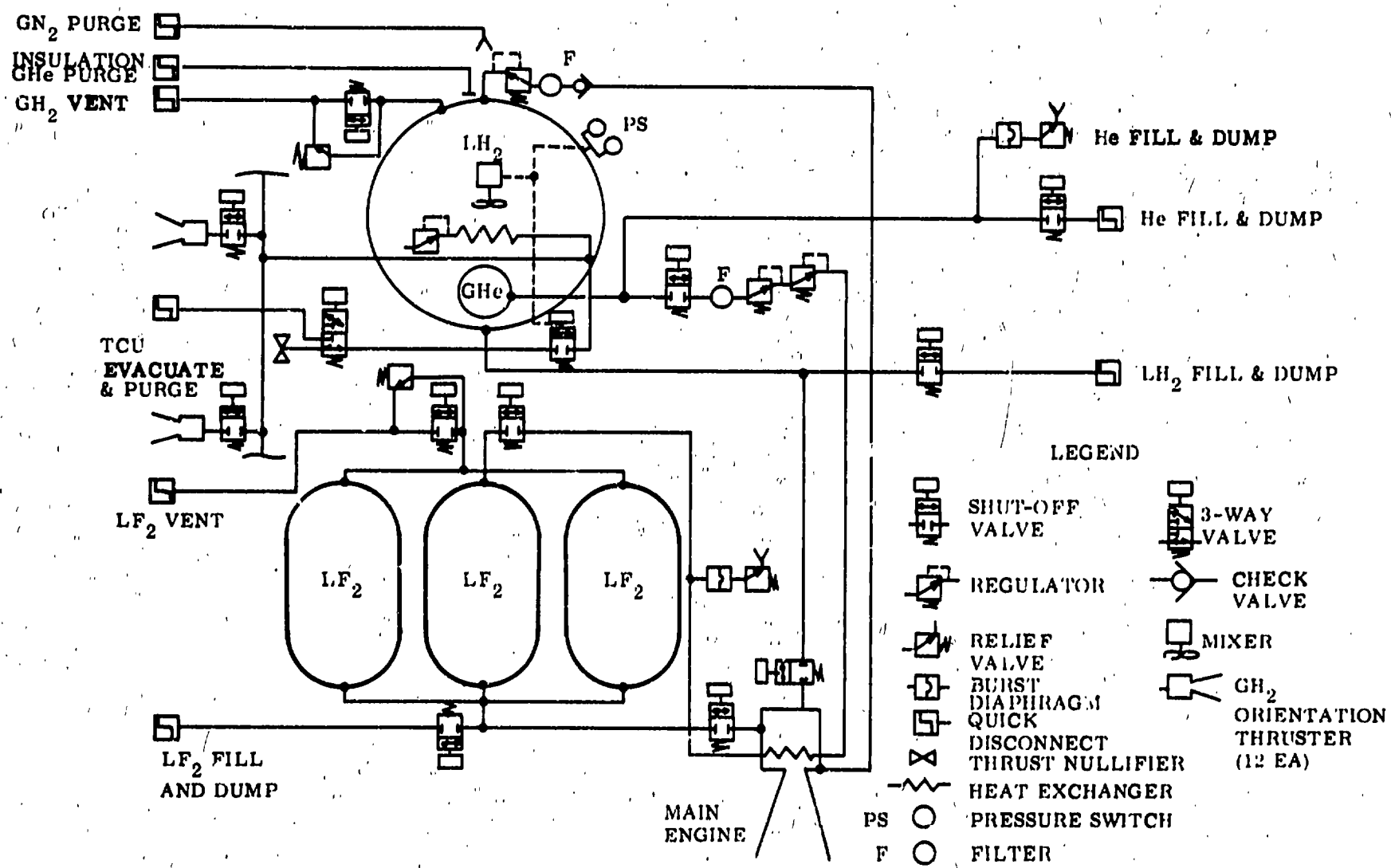

Figure 113 Plumbing Schematic for the Propulsion System Flight Experiment

CONCLUDING REMARKS

A number of very significant conclusions can be drawn from the work accomplished on this program. The most important of these may be summarized as follows:

(1) The thermal conditioning system, as designed, and built, will control the pressure in a full scale liquid hydrogen tank, efficiently, and is equally effective whether the unit is submerged in liquid or gas.

(2) The mixer design flow rate is sufficient to mix the tank contents, even in the severe one-g environment, as contrasted to the low-g environment of a flight system. This result was obtained at all orientations and with all test configurations.

(3) Tank fluid mixing and liquid-ullage coupling are necessary for efficient pressure control. In a gravity dominated regime, this is best achieved with the mixer jet directed at the interface.

(4) Using similarity relationships, and experimental data, the mixing time was found to be inversely related to the jet momentum, and is predicted to be directly proportional to gravity level. Positive confirmation of this will require additional testing and ultimately a flight demonstration test.

(5) Depressurization rates that result from mixing, are significantly reduced when helium is present in the ullage, and the mixer jet is submerged. The effect is much less severe when the jet penetrates into the ullage. This suggests that the helium may be of little consequence when the jet velocity exceeds the critical value.

(6) The overall performance of the TCU, in terms of its ability to control tank pressure, can be predicted with a thermodynamic equilibrium model. Conformance with this model indicates that tank pressure response is basically governed by the heat transfer rates within the heat exchanger. Since the heat exchanger is forced convection dominated, the system should perform in zero gravity as it did in

the one-gravity tests for the design mixer flow. Positive verification of this conclusion can only come from a flight test.

(7) In general, the individual components, comprising the thermal conditioning unit, met or exceeded their design performance. However, the expansion unit design must be changed to increase reliability and lifetime before it can be incorporated into a flight system.

(8) The theory previously developed for induced condensation at a moving liquid-vapor interface appears to have included the proper variables and parameter groupings. However, additional experimental work is needed to firmly establish the proper value of the constants to be used in the correlation.

REFERENCES

1. Lockheed Missiles & Space Company, Liquid Propellant Thermal Conditioning System, Interim Report, NASA CR-72113, LMSC-A839783, Contract NAS 3-7942, Sunnyvale, Calif., 20 April 1967

2. General Dynamics, Convair Division, Cryogenic Zero-Gravity Prototype Vent System, DCN 1-6-52-01144, GDC-DDB67-006, Contract NAS 8-20146, San Diego, Calif., October 1967

3. Lockheed Missiles & Space Company, Liquid Propellant Thermal Conditioning System, Final Report, NASA CR-72365, LMSC K-07-68-2, Contract NAS 3-7942, Sunnyvale, Calif., 15 August 1968

4. National Aeronautics and Space Administration, Lewis Research Center, An Experimental Investigation of the Effect of Gravity on a Forced Circulation Pattern for Spherical Tanks, by S. G. Berenyi, R. C. Nussle, and K. L. Abdalla, NASA TN D 4409, 6 February 1968

5. Lockheed Missiles & Space Company, Propellant Selection for Unmanned Spacecraft Propulsion Systems, Contract NASw-1644, Final Report, Phase II, Vol. III, NASA CR105203, pp. 115-207, 15 September 1969

6. Lockheed Missiles & Space Company, Advanced Maneuvering Propulsion System, LMSC-A960593, 31 January 1970

7. Lockheed Missiles & Space Company, Cryogenic Tank Support Evaluation, Final Report, NASA CR-72546, Contract NAS 3-7979, Sunnyvale, Calif., 1 December 1969

SYMBOLS AND ABBREVIATIONS

C_v	=	specific heat	Btu/lb-°R (cal/gr-°K)
E_m	=	energy input to mixer	Btu/hr (cal/hr)
h_v	=	enthalpy of vented vapor	Btu/lb (cal/gr)
M_o	=	vent flow rate	lb/hr (gr/hr)
p	=	pressure	psi (n/m^2)
Q_o	=	external heat leak into the tank	Btu/hr (cal/hr)
R	=	gas constant	ft-lb/lb-°R (cm-gr/gr-°K)
T	=	temperature	°R (°K)
u	=	internal energy	Btu/lb (cal/gr)
V	=	volume	ft^3 (ℓ)
W	=	weight of fluid in the tank	lb (gr)
θ	=	time	hr
ρ	=	propellant density	lb/ft^3 (gr/cm^3)
λ	=	latent heat of vaporization	Btu/lb (cal/gr)

Subscripts

L	=	liquid
g	=	gas
T	=	total

Appendix A

PRESSURE DECAY WITH MIXING ONLY

Consider a propellant tank in a non-equilibrium condition without mass addition or extraction, but subjected to environmental heating rate Q_o. The total energy contained in the tank at any time is given by:

$$E_t = W_L \bar{u}_L + W_g \bar{u}_g \qquad \text{(A-1)}$$

and the rate of change is:

$$\dot{E}_t = Q_o = W_L \dot{\bar{u}}_L + \bar{u}_L \dot{W}_L + W_g \dot{\bar{u}}_g + \bar{u}_g \dot{W}_g \qquad \text{(A-2)}$$

Also, an energy balance on the ullage, combined with the perfect gas law, gives:

$$\frac{V_g C_v}{R} \dot{p} = W_g \dot{\bar{u}}_g + \bar{u}_g \dot{W}_g \qquad \text{(A-3)}$$

From a mass balance on the closed container, we get:

$$\dot{W}_g = - \dot{W}_L \qquad \text{(A-4)}$$

Combining (A-3) and (A-4), and substituting for $\bar{u}_g$, gives:

$$\frac{V_g C_v}{R} \dot{p} = (WC_v)_g \dot{\bar{T}}_g - \bar{u}_g \dot{W}_L \qquad \text{(A-5)}$$

If a stratified propellant is being depressurized by mixing only, the pressure must decay to some minimum value and then increase. The condition at the minimum pressure is given by (A-5), i.e.,

$$(WC_v)_g \dot{\bar{T}}_g - \bar{u}_g \dot{W}_L = 0 \qquad \text{(A-6)}$$

Since $\dot{\bar{T}}_g \leq 0$, the depressurization process is one of evaporative cooling.

The conditions that must prevail in the liquid at minimum pressure can be derived by substituting (A-3) into (A-2), which gives:

$$Q_o = W_L \dot{\bar{u}}_L + \bar{u}_L \dot{W}_L + \frac{V_g C_v}{R} \dot{p} \qquad \text{(A-7)}$$

At minimum pressure, $\dot{p} = 0$. Combining (C-6) and C-7), and substituting for u_L, we get:

$$Q_o = (WC_v)_L \dot{T}_L + \frac{u_L}{u_g} (WC_v) \dot{T}_g \qquad \text{(A-8)}$$

One criteria that is necessary, but perhaps not sufficient for having minimum pressure occur simultaneously with attainment of a completely mixed condition, is that $\dot{\bar{T}}_g = 0$, in which case, we know:

$$Q_o = W_L C_{vL} \dot{\bar{T}}_L \qquad \text{(A-9)}$$

During the decay period

$$Q_o < W_L C_{vL} \dot{\bar{T}}_L$$

and after minimum pressure has passed

$$Q_o > W_L C_{vL} \dot{T}_L$$

SYMBOLS AND ABBREVIATIONS

C_v	=	specific heat	Btu/lb-°R (cal/gr-°K)
E_t	=	internal energy of tank contents	Btu/lb (cal/gr)
p	=	tank pressure	psi (n/m^2)
Q_o	=	external heat rate to tank contents	Btu/hr (cal/hr)
R	=	gas constant for the ullage	ft-lb/lb-°R (cm-gr/gr-°K)
$\bar{T}$	=	average temperature	°R (°K)
u	=	specific internal energy	Btu/lb (cal/gr)
W	=	weight contained in the tank	lb (gr)
V	=	volume	ft^3(liters)

Subscripts

g	=	gas
L	=	liquid

NOTE: Dots above a symbol indicate rate of change with time

Appendix B

PRESSURE DECAY WITH CONTINUOUS EQUILIBRIUM

Venting from a tank of LH_2 while in thermodynamic equilibrium can be described as follows in terms of the rate of tank pressure decay, $\frac{dp}{d\theta}$.

The total energy content of the liquid and gas may be expressed as

$$Q = W_L u_L + W_g u_g \qquad \text{(B-1)}$$

The rate of change of Q is, therefore

$$\frac{dQ}{d\theta} = \frac{d}{d\theta}(W_L u_L) + \frac{d}{d\theta}(W_g u_g) \qquad \text{(B-2)}$$

Also,

$$\frac{dQ}{d\theta} = Q_o + E_m - M_o h_v \qquad \text{(B-3)}$$

If the perfect gas low is applied to the ullage, we get

$$\frac{d}{d\theta}(pv)_g = \frac{d}{d\theta}(WRT)_g \qquad \text{(B-4)}$$

Also, note that for the relevant range of conditions over which $\frac{R}{C_{v_g}} \approx$ constant, we get

$$\frac{d}{d\theta}(WRT)_g \doteq \frac{R}{C_{v_g}} \frac{d}{d\theta}(W_g u_g) \qquad \text{(B-5)}$$

Therefore, Eqs. (B-2), (B-4) and (B-5) can be combined with (B-3) to give

$$Q_o + E_m - M_o h_v = u_L \frac{dW_L}{d\theta} + M_L \frac{du_L}{d\theta} + \frac{C_{v_g}}{R} \frac{d}{d\theta}(pv)_g \qquad \text{(B-6)}$$

For small changes in equilibrium conditions, the following assumptions are valid

$$\frac{dM_L}{d\theta} \doteq -M_o; \quad \frac{dV_g}{d\theta} \doteq 0; \quad \frac{du_L}{d\theta} \frac{du_L}{dp} \frac{dp}{d\theta}$$

Incorporating these assumptions into (B-6), we get for the equilibrium rate of pressure change

$$\frac{dp}{d\theta} = \frac{Q_o + E_m - M_o\lambda}{W_L \; du_L/dp} \left[\frac{1}{1 + \frac{(C_v/R)V_g}{W_L \; du_L/dp}} \right] \qquad \text{(B-7)}$$

For liquid hydrogen, the pressure response in psi/hr reduces to the following equation, when other parameters are evaluated in English units

$$\frac{dp}{d\theta} = \frac{1.25(Q_o + E_m - M_o\lambda)}{\rho_L V_T (1-V_g/V_T)} \left[\frac{1}{1 + 0.36 \frac{(V_g/V_T)}{\rho_L(1-V_g/V_T)}} \right] \qquad \text{(B-8)}$$

Equation (B-8) is applicable with helium in the ullage providing the distribution is uniform. This is so because the ratio of specific heat and gas constants are nearly equal for hydrogen and helium.

Appendix C

COMPLETE MIXING THECRY

Previous analytical models (ref. 1) have considered critical velocities that will create forced circulation throughout a tank in a zero-gravity (i.e., Weber number criteria). The experimental work at LeRC (ref. 4) provided a correlation against gravity level but no analytical model to extend the application beyond the test variables. A model is developed herein which attempts to bridge this gap.

The essential features of the model are illustrated in the sketch. A radial nozzle is located in liquid at one end of a tank. This nozzle emits a steady jet of liquid which attaches to the wall and travels towards a vapor pocket located near the opposite end of the tank. By definition, complete circulation occurs when the liquid jet penetrates the vapor bubble and returns down a center core to the nozzle intake. The corresponding jet velocity is defined as the critical velocity. If the jet velocity is less than this critical value, it will either be deflected by the interface or the liquid may collect behind the bubble.

The jet inertial forces causing jet penetration of the bubble is given by

$$F_I = A_x \rho U_x^2 \qquad \text{(C-1)}$$

The opposing surface tension force is given by

$$F_\sigma = \pi x \sigma \qquad \text{(C-2)}$$

If viscous, forces are neglected, conservation of jet momentum gives

$$\rho A_x U_x^2 = \rho_j A_j U_j^2 - \rho g D_T A_x \qquad \text{(C-3)}$$

For bubble breakthrough by the jet, the following condition must be satisfied

$$\frac{\rho A_j U_j^2 - \rho g D_T A_x}{\pi \sigma x} \geq 1 \qquad \text{(C-4)}$$

where the equality holds at critical conditions. If it is assumed that the downcomer column of liquid is of uniform cross section then (C-4) can be rearranged to give

$$\left(\frac{U_{j_{CR}} \delta_j}{\sigma/\rho}\right) \frac{d_j}{x} - \frac{1}{4}\left(\frac{g D_T^2}{\sigma/\rho}\right) \frac{x}{D_T} = 1 \qquad \text{(C-5)}$$

The left side of (C-5) consists of a jet Weber number and tank Bond number, each modified by a different geometry factor.

However, by rearranging the geometrical factors one can get a more useful form of the equation which can be compared directly with the NASA LeRC experimental data.

If eq. (C-5) is multiplied by (σ/ρ) and divided by $(D_T/2)$ it becomes

$$\frac{U_{j_{CR}}^2}{(R_T/\delta_j)} \frac{d_j}{x} - g_o\left(\frac{g}{g_o}\right)\frac{x}{2} = 2\frac{\sigma/\rho}{D_T} \qquad \text{(C-6)}$$

Finally, eq. (C-6) can be rearranged to give

$$\frac{U_{j_{CR}}}{(R_T/\delta_j)^{1/2}} = \left(\frac{1}{2}\frac{x}{d_j}\right)^{1/2}\left[\frac{4\sigma/\rho}{D_T} + \left(\frac{g}{g_o}\right) g_o x\right]^{1/2} \qquad \text{(C-7)}$$

This equation is compared with the LeRC data for ethanol on Fig. C-1. The horizontal portion of the curve is in the capillary dominated regime, corresponding to the surface tension term in Eq. (C-7) while the sloped portion of the curve is gravity dominated. It is noted that the theory predicts the shape of the correlation very well throughout the range from 10^{-5} to 1 g, but the absolute values are low by approximately a factor of four. This may be due to viscous effects which were not included in the analysis. A second important point to note is that there is an individual effect of the tank size and the jet dimension, which is not revealed by the experimental data possibly because combinations of dimensions fall within the range of experimental scatter. It appears, however, that the analysis does incorporate the proper parameters and can be used with correction factors from the experimental data to predict critical velocities for other tanks throughout the gravity regime.

The same analytical approach was used to predict the critical velocity requirements for a central jet. The resulting expression is:

$$\frac{U_j}{(D_T/d)^{1/2}} = \left[1 + \frac{D_T}{d}\tan\theta\right]\left[dg_o\left(\frac{g}{g_o}\right) + \frac{4\,\sigma/\rho}{D_T\left(1 + \frac{D_T}{d}\tan\theta\right)}\right]^{1/2} \qquad \text{(C-8)}$$

It can be seen that in zero-gravity, Eq. (C-8) reduces to

$$\frac{U_j^2 d_j}{\sigma/\rho} = 4\left(1 + \frac{D_T}{d_j}\tan\theta\right) \qquad \text{(C-9)}$$

which is the same expression developed in ref. 2.

Eq. C-8 was used to calculate the critical velocities in the 41.5" and 110" tanks. The results are shown in Fig. C-2. It is noted that in 1-gravity the theoretical critical velocity is approximately 6 times the maximum test velocity for the small tank and 50 times for the 110" tank. Also note on Fig. C-2 that for these tank sizes, the circulation is primarily gravity dominated above 10^{-5} g's, whereas in the smaller LeRC tanks surface tension domirates below 10^{-3} g's. However, the test velocities are at least 5 times those required for complete circulation at 10^{-5} g's, which is approximately the marginal factor between test results from LeRC and the theory.

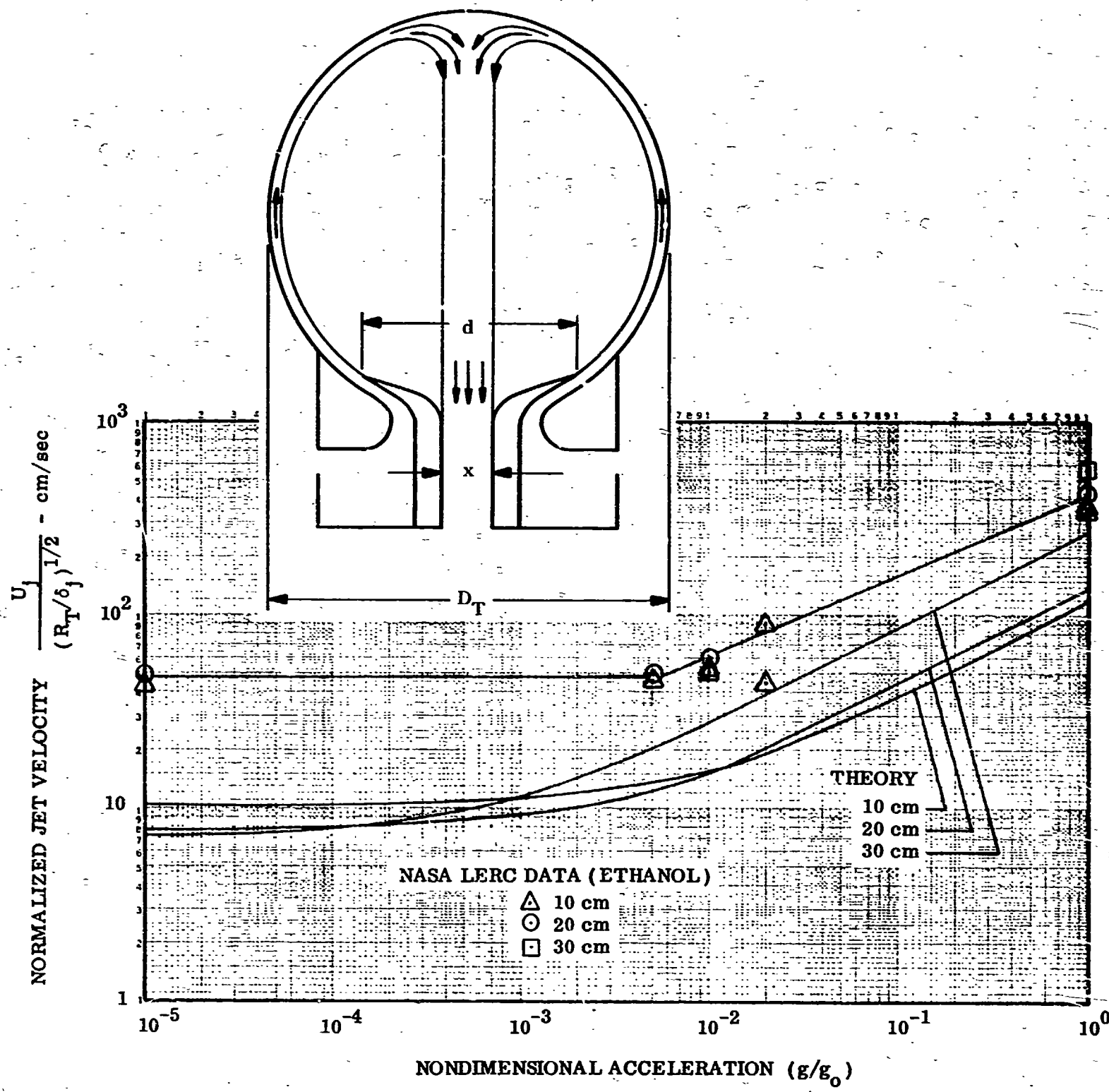

Figure C-1 Effect of Gravity On Critical Velocity Requirements - Experiment And Theory

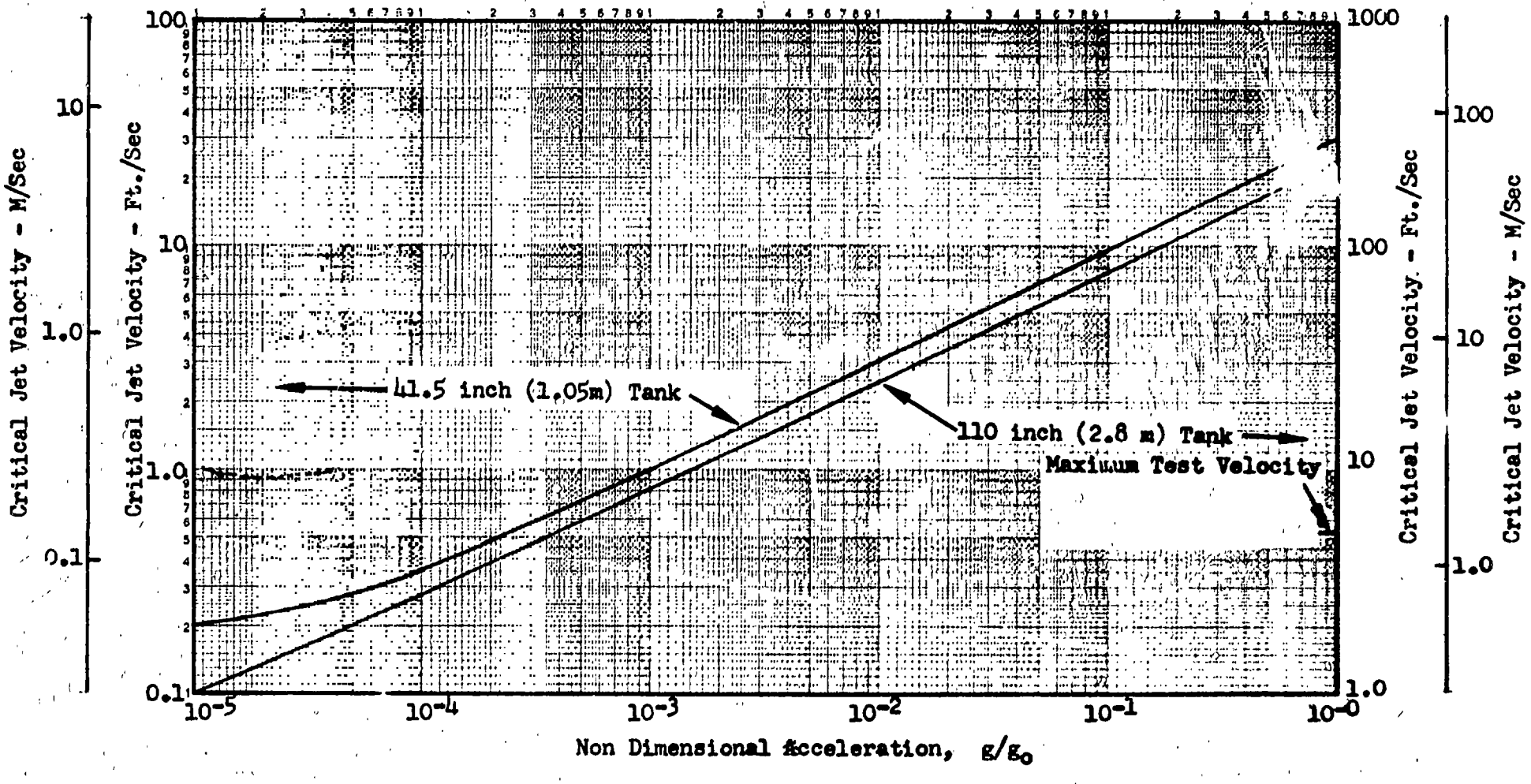

Figure C-2 Theoretical Jet Velocities For Complete Circulation In The Test Tanks